

Copyright is owned by the Author of the thesis. Permission is given for a copy to be downloaded by an individual for the purpose of research and private study only. The thesis may not be reproduced elsewhere without the permission of the Author.

**An investigation of the Rapanui and Ngarino marine terraces  
in South Taranaki: covered stratigraphy, distribution and  
tectonics.**

A thesis presented in partial fulfillment of the requirements  
for the degree Masterate of Science in Quaternary Science  
at Massey University, Palmerston North, New Zealand.

Andrew James Wards

1996



**Frontispiece.** Rapanui wave-cut surface exposed on S.H.3 *c.* 0.3 km south of the Manawapou River.

## Acknowledgements

I would like to thank the following:

My supervisors, Assoc. Prof. V.E. Neall and Dr. A.S. Palmer for their help during the early stages of field work and their encouragement and constructive criticism during the preparation and presentation of this thesis.

Also fellow students from the Department of Soil Science, Massey University; in particular Shane Cronin and Andrew Hammond for assistance in the field during some rather unpleasant Taranaki weather and Scott Keeling for use of his computer and many informal meetings and discussions. Thanks also to Mike Elliot for his review and discussions regarding interpretation of palynological information.

Thanks are due to the Geological Society of New Zealand for the presentation of the 1991 Student Research Award and to the Taranaki Regional Council for kindly supplying borehole data and information on gravel extraction in Taranaki.

Thanks to the numerous landowners who gladly allowed access to their properties and in particular for access to the many recent farm track and oxidation pond cuttings that provided excellent exposures.

My parents Diane and Ian, to whom I am very grateful for their assistance and moral support during this project.

## Abstract

Uplifted marine terraces, formed by successive marine onlap during interglacial and interstadial sea level maxima are preserved parallel to the South Taranaki coastline between Kakaramea in the southeast, and Hawera to the northwest.

The objective of this research was to investigate the formation, deformation and subsequent landscape evolution of the Ngarino and Rapanui Terraces in the area between Hawera and Kakaramea. The northwestern part of the study area occupies the southeastern margin of the Egmont ringplain where terraces that extend from the southeast sector are progressively buried by volcanoclastic sediments west of the Tangahoe River. Ages of the wave-cut platforms have been inferred from the covered stratigraphy and subsequent correlation to sea-level and oxygen isotope curves. Mapping the height of wave-cut platforms also allowed calculation of marine terrace deformation rates and patterns in this area.

In the past, studies have tentatively concluded that between Kakaramea and Hawera the younger 120 ka Rapanui Terrace is cut out at the coast along with the 100 ka Inaha Terrace, and that to the west only the Ngarino Terrace is preserved. Examination of covered stratigraphy has established that both the Ngarino and Rapanui Terraces (210 and 120 ka respectively) are present in the study area. The terrace covered stratigraphy presented here indicates that next to the coast the terrace is younger than 210 ka. On this terrace loess units, corresponding to oxygen isotope stages 2,3,4 and 5 are found and gives a maximum age of 120 ka. Inland, the terrace stratigraphy reveals loess units corresponding to stages 2,3,4,5, and 6, providing a maximum age of 210 ka.

Structural interpretation has demonstrated that underlying tectonics associated

with the Taranaki Fault Zone has subsequently deformed the wave-cut platforms from their shallow angled seaward-dipping profiles. Southeast of the Tangahoe River, uplift rates between 0.3 - 0.55 mm/yr have formed well-defined terraces. The doming of the terrace surfaces is the surface expression of the Patea-Tongaporutu High, which is east of and parallels the Taranaki Fault Zone. The Tangahoe River is interpreted to overlie the Taranaki Fault Zone. This Zone marks the eastern boundary of the Taranaki Basin where uplift rates decrease to below 0.3 mm/yr. Stern *et al.*, (1990) suggest that at this point broad bending of the lithosphere is induced by west-moving thrust sheets within the Taranaki Fault Zone and this is thought to be responsible for the increased uplift rates in this area. The uplift pattern displays the differential between the Patea-Tongaporutu High to the southeast and the Taranaki Basin to the west.

## Contents

|                       |  | <b>Page</b> |
|-----------------------|--|-------------|
| -                     | Frontispiece   | i           |
| -                     | Acknowledgements                                     | ii          |
| -                     | Abstract   | iii         |
| -                     | Contents   | v           |
| -                     | List of figures                                      | viii        |
| -                     | List of tables                                       | xi          |
| -                     | List of plates                                       | xii         |
| <b>Chapter One:</b>   | <b>Introduction</b>                                  | <b>1</b>    |
|                       | 1.0 Objective of study                               |             |
|                       | 1.1 Introduction                                     |             |
|                       | 1.2 Study area                                       |             |
|                       | 1.3 Geologic setting                                 |             |
|                       | 1.3.1 Subsurface geology                             |             |
|                       | 1.3.2 Surface geology                                |             |
|                       | 1.4 Present climate                                  |             |
|                       | 1.5 Past and present vegetation                      |             |
|                       | 1.6 Soils  |             |
|                       | 1.7 Landuse  |             |
| <b>Chapter Two:</b>   | <b>Previous work and terminology</b>                 | <b>16</b>   |
|                       | 2.1 Previous work                                    |             |
|                       | 2.2 Marine terrace terminology                       |             |
|                       | 2.3 Lahar and debris-avalanche deposits              |             |
| <b>Chapter Three:</b> | <b>Terrace covered stratigraphy and physiography</b> | <b>25</b>   |
|                       | 3.1 Introduction                                     |             |
|                       | 3.1.1 Southeast sector                               |             |
|                       | 3.1.2 Northwest sector                               |             |

|       |  |  |
|-------|--|--|
| 3.1.3 | Method of study                                |  |
| 3.2   | Holocene deposits                              |  |
| 3.2.1 | Patea Dunesand                                 |  |
| 3.2.2 | Egmont Ash                                     |  |
| 3.3   | Ohakean substage deposits                      |  |
| 3.3.1 | Loess 1 (L1)                                   |  |
| 3.3.2 | Wereroa sand                                   |  |
| 3.3.3 | Landscape erosion during the Ohakean substage  |  |
| 3.3.4 | Interbedded andesitic tephra                   |  |
| 3.4   | Ratan substage deposits                        |  |
| 3.4.1 | Loess 2 (L2)                                   |  |
| 3.4.2 | Ratan lignite and Huxley sand                  |  |
| 3.4.3 | Opunake Formation                              |  |
| 3.5   | Porewan substage deposits                      |  |
| 3.5.1 | Loess 3 (L3)                                   |  |
| 3.5.2 | Stratford Formation                            |  |
| 3.6   | Oxygen isotope stage five terrestrial deposits |  |
| 3.6.1 | Auburn dunesand                                |  |
| 3.6.2 | Loess 4 (L4)                                   |  |
| 3.6.3 | Whakamara dunesand                             |  |
| 3.6.4 | Loess 5 (L5)                                   |  |
| 3.6.5 | Kaihuahua dunesand                             |  |
| 3.7   | Oxygen isotope stage five marine deposits      |  |
| 3.7.1 | Kaikura formation                              |  |
| 3.8   | Oxygen isotopoe stage six deposits             |  |
| 3.8.1 | Loess 6 (L6)                                   |  |
| 3.9   | Oxygen isotope stage 7 deposits                |  |
| 3.9.1 | Ingahape formation                             |  |
| 3.10  | Chapter Three conclusions                      |  |

**Chapter Four: Palynological interpretation and correlation of the Ohawe Waterfall and Ohawe East Sections to the Inaha and Ararata Road sections**

149

|     |   |  |
|-----|---|--|
| 4.0 | Introduction                            |  |
| 4.1 | Ohawe Waterfall and Ohawe East Sections |  |
| 4.2 | Inaha Section                           |  |
| 4.3 | Ararata Road Section                    |  |

|                      | <b>Page</b>   |            |
|----------------------|---|------------|
| 4.4                  | Correlation   |            |
| 4.5                  | Chapter Four conclusions                            |            |
| <b>Chapter Five:</b> | <b>Terrace uplift, deformation and preservation</b> | <b>175</b> |
| 5.1.1                | Introduction  |            |
| 5.1.2                | Methodolgy  |            |
| 5.2.1                | Structural contours                                 |            |
| 5.2.2                | Shore-normal terrace gradients                      |            |
| 5.2.3                | Positioning of the terrace risers                   |            |
| 5.3.1                | Uplift rates  |            |
| 5.4                  | Uplift rates of time                                |            |
| 5.4.1                | Results   |            |
| 5.5                  | Shore-parallel terrace deformation                  |            |
| 5.5.1                | Results   |            |
| 5.5.2                | Shore-parallel deformation over time                |            |
| 5.5.3                | Results   |            |
| 5.5.4                | Shore-parallel tilting                              |            |
| 5.5.5                | Results   |            |
| 5.6                  | Interpretation                                      |            |
| 5.7                  | Terrace preservation                                |            |
| 5.7.1                | Introduction  |            |
| 5.7.2                | Results   |            |
| <b>Chapter Six:</b>  | <b>Summary</b>                                      | <b>202</b> |
| 6.1                  | Summary   |            |
| 6.2                  | Future research                                     |            |
| <b>Appendix</b>      |   |            |
| A                    | Section locations                                   |            |
| <b>References</b>    |   |            |

## List of figures

### Chapter One

- 1.1 (a) Location map of study area in relation to Wanganui Basin and Taupo Volcanic Zone. (b) Positions of terrace strandlines between Wanganui and Hawera (after Pillans, 1983). (c) Terrace distribution in study area with northwest and southeast sectors shown.
- 1.2 Regional geology and study area location in relation to South Wanganui Basin, Patea-Tongaporutu High and South Taranaki Basin (after Pillans, 1990).
- 1.3 Southeastwards then south-southwestwards migration of South Wanganui Basin depocentre from Early Pliocene to Late Pleistocene and the southward younging of uplifted marine sediments to the north.
- 1.4 SSE-NNW cross section of South Wanganui Basin showing depocentre migration progressing as a lithospheric downwarp with subsidence occurring in the south and uplift in the north (after Stern *et al.*, 1993).
- 1.5 Climatic regions of the Taranaki-Manawatu region.

### Chapter Two

- 2.1 South Taranaki-Wanganui Pleistocene marine terrace chronology and correlation to the marine isotope record (after Pillans, 1990).
- 2.2 The five stages of marine terrace development as expressed by the relationship between rate of sea level rise and fall and terrace uplift rate (after Pillans, 1981).
- 2.3 Sea level and oxygen isotope curves to which marine terrace coverbeds are correlated. (a) Sea level 340-160 ka (after Chappell, 1983). (b) Sea level 160 ka-present (after Pillans, 1983). (c) Oxygen isotope curve (after Martinson *et al.*, 1987).
- 2.4 Marine terrace chronology and oxygen isotope stage correlation (after Pillans, 1990) with paleosea level data used in this study.
- 2.5 Generalised marine terrace cross section and nomenclature (after Pillans, 1990).

### Chapter Three

- 3.1 Location of type and reference sections.

- 3.2 Composite stratigraphic columns of aeolian and marine coverbeds overlying the Rapanui and Ngarino Terraces in the southeast sector.
- 3.3 Distribution of Patea Dunesand, Egmont Ash, Wereroa sand and the Mokoia erosion surface.
- 3.4 Toko Tephra Sub-group: likely contributors to the Egmont Ash in the study area.
- 3.5 Paleovalleys in the northwest sector and distribution of Opunake and Stratford Formations.
- 3.6 Northwest sector correlation diagrams.
- 3.7 Generalised stratigraphy of L1 and Wereroa sand.
- 3.8 Southwest sector correlation diagrams showing extensive unconformity beneath Egmont Ash.
- 3.9 Stratigraphy of Tuna Group tephtras (after Alloway, 1989).
- 3.10 Distribution of Tuna Group tephtras in study area.
- 3.11 Distribution of Auburn dunesand and L4.
- 3.12 Distribution of Whakamara dunesand and L5.
- 3.13 Distribution of Kaihuahua dunesand.
- 3.14 Generalized stratigraphy and depositional environments of the Kaikura formation, Rapanui Terrace.
- 3.15 High stand systems tract showing depositional environments, dominant processes and lithofacies (after Vail *et al.*, 1991).
- 3.16 Inferred distribution of the Denby shell bed, Kaikura fine sand and Kaikura silt and fine sand sub-members.
- 3.17 Correlation diagram showing marine sediment facies changes from SE to NW.
- 3.18 Distribution of L6.

- 3.19 South Taranaki marine terrace covered units and their correlation to the oxygen isotope curve.

#### **Chapter Four**

- 4.1 Combined covered stratigraphy, pollen zones and inferred age of the Ohawe waterfall and Ararata sections (after Bussell, 1988) and Inaha section (after McGlone *et al.*, 1983).
- 4.2 Ohawe waterfall, Ararata Road and Inaha section pollen diagrams.
- 4.3 Summary diagram and correlation of the Ohawe waterfall section.
- 4.4 Proposed correlation of Ohawe waterfall, Ararata Road and Inaha pollen zones to the oxygen isotope curve.

#### **Chapter Five**

- 5.1 Structural contours of the Inaha, Rapanui, Ngarino and Brunswick marine terrace WCS's and location of transects A-A' to D-D'.
- 5.2 Terrace cross sections A-D showing inferred position of terrace strandlines and heights of risers.
- 5.3 Shore normal terrace gradients along transects A-A' to D-D'.
- 5.4 Contoured mean uplift rates and inferred position of the Taranaki Fault Zone.
- 5.5 Shore normal uplift rates for transects A-A' and D-D'. Shore parallel uplift rates along transect E-E'.
- 5.6 Average increase in terrace gradient per 100 ka for transects A-A' to D-D'.
- 5.7 Shore parallel terrace strandline heights between Hawera and Kakaramea.
- 5.8 Calculated average shore parallel uplift rates for the periods 310-210 ka, 210-120 ka, and 120 ka to present.
- 5.9 Height of Rapanui WCS between the Manawapou River and Ohawe Beach showing faults offsetting the Tangahoe Formation.

## List of Tables

### Chapter Two

- 2.1 Marine terrace chronology and oxygen isotope stage correlation.

### Chapter Five

- 5.1 Terrace gradients along transects A-A' to D-D'.
- 5.2 Summary of terrace gradients at 310, 210, 120, 100 ka and present, including rates of change of uplift.
- 5.3 Relative strandline heights at sections A-A' to D-D'.
- 5.4 Inferred strandline heights and shore parallel uplift rates for transects A-A' to D-D' for the period 210ka to present.
- 5.5 Uplift rates required to preserve 240 ka terrace from 210 ka sea level highstand.
- 5.6 Uplift rates, paleosea level and preservation of terraces formed at 210, 120, and 100 ka.

## List of Plates

### - Frontpiece

### Chapter Three

- 3.1 Wind erosion of the Patea Dunesand
- 3.2 Egmont Ash profile (partially stripped L1). Section 21.
- 3.3 Egmont Ash profile overlying fluviually reworked andesitic sands and gravels. Section 32.
- 3.4 Over thickened L1 with prominent Kawakawa Tephra at Q21/274774.
- 3.5 Kawakawa Tephra within sandy L1 above thick Wereroa sand. Section 48.
- 3.6 Ripple-bedded sands above L1 and overlying Wereroa sand in the northwest sector.
- 3.7 Wereroa sand interbedded with L1 and overlying L2 in the southeast sector. Section 13.
- 3.8 Angular unconformity with L1 overlying L4 and Whakamara dunesand. Section 16.
- 3.9 Mokoia erosion surface with reworked andesitic gravels and sands underlying Egmont Ash at Q21/273774.
- 3.10 Fluvial andesitic sands and gravels on Mokoia erosion surface thickening towards existing stream at Q21/274748.
- 3.11 Kaihouri, Paetahi and Poto tephra overlying Kawakawa Tephra. Section 47.
- 3.12 Pocketed grey/black sandy lapilli of Poto Tephra overlying Kawakawa Tephra with fine grey lapilli of Tuikonga Tephra below.
- 3.13 Mangapotoa Tephra within L2 below L1 and Wereroa sand at Q21/314717, in the southeast sector.
- 3.14 1-2m thick lignite containing Mangapotoa Tephra. Section 30, in the northwest sector.

- 3.15** Type section of the Rapanui Terrace showing strong chocolate paleosol on L3 and covered stratigraphy. Thin dunesand unit separating intertidal deposits from the loess units (L1-L4). Section 24.
- 3.16** Ohawe waterfall section (Q21/ 144785). Stratford Formation unconformably overlying lignite.
- 3.17** Fallen debris avalanche block showing basal contact with silts. Note rip-up clasts. Coastal cliffs, southeast of Ohawe Beach.
- 3.18** Stratford Formation debris avalanche, valley fill facies.
- 3.19** Andesitic boulder 2 m in diameter derived from the Stratford Formation, found *c.* 45 km from source (Q21/244740).
- 3.20** Large megaclast within the Stratford Formation exposed in coastal cliffs, southeast of Ohawe Beach.
- 3.21** Distinctive fine bedding in Stratford Formation debris avalanche revealed by wave action removing fine material.
- 3.22** Section through Auburn dunesand overlain by L3 at Q21/313717.
- 3.23** L4 below Auburn dunesand and above Whakamara dunesand
- 3.24** Whakamara dunesand with thin interbedded Epiha Tephra overlying L5. Section 17.
- 3.25** Whakamara and Auburn dunes near outer margin of the Ngarino Terrace.
- 3.26** L5 showing the contact with the Kaihuahua dunesand below and the Whakamara dunesand above. Section 17.
- 3.27** L5 showing bright colours, tephric nature and paleosol which is truncated by an unconformity below the Wereroa sand. Section 15.
- 3.28** Interbedded lignite and andesitic lapilli within the Kaihuahua dunesand and below L5. Section 1.
- 3.29** Steeply dipping beds of the Kaihuahua dunesand and top contact with L5. Section 1.
- 3.30** Rapanui WCS truncating fine micaceous sands of the Tangahoe Formation muddy sandstones. Section 37.

- 3.31 Planar cross bedding in marine sands on Rapanui marine terrace. Flow directions parallel to section. Section 24.
- 3.32 Trough cross bedding in marine sands on Rapanui marine terrace. Flow direction normal to the section away from observer. Section 24.
- 3.33 L6 near front of Ngarino Terrace showing pale colours and interbedded lapilli. Section 3
- 3.34 L6 towards the back of the Ngarino Terrace showing less visible lapilli bedding and greyer colours below Kaihuahua dunesand. Section 15.
- 3.35 Contact between L6 at base and the overlying Kaihuahua dunesand above. Section 3.
- 3.36 Rounded andesitic gravels (Ingahape sands and gravels) towards back of Ngarino marine terrace. Note clay coatings infilling voids. At Q21/280780.
- 3.37 Small rounded iron stained andesitic gravels at rear of Ngarino marine terrace. Section 27.

## Chapter Five

- 5.1 Southwestward dipping sandstones and mudstones of the Tangahoe Formation exposed along the coastline *c.* 0.5 km west of the Tangahoe River.

## **Chapter One          Introduction**

### **1.0      Objective of study**

The objectives of this study were to elucidate the distribution of the Rapanui and Ngarino marine terraces in the area between Kakaramea and Hawera in South Taranaki, New Zealand (Figure 1.1a) by:

- investigating terrace covered accumulation history and mapping the distribution of important stratigraphic units,
- correlating these stratigraphic units to established sea level and oxygen isotope curves in order to establish age constraints on individual stratigraphic units, and
- determining rates of shore normal and shore parallel terrace deformation by mapping heights of wave-cut platforms and strandlines.

### **1.1      Introduction**

West of Kakaramea the risers separating the Rapanui and Ngarino Terraces become difficult to locate. This may have resulted from factors such as low uplift rates resulting in little relief between terrace treads or covered dunesands ramping up against terrace risers and obscuring them.

Erosion of cover beds between the Tangahoe and Manawapou Rivers has made mapping of the strandline between the two terraces difficult. Recent studies by Pillans (1991) and Bussell (1988) have suggested that the Rapanui Terrace northwest of Manutahi is cut out at the coast (Figure 1.1a) and that the younger Inaha Terrace intersects the present coastline *c.* 1.5 km southeast of the Manawapou River.

In this study mapping of the terrace surfaces was achieved using structural interpretation of the wave-cut surfaces (WCS) and covered stratigraphy to explain the history of terrace formation, deformation and uplift in the area. Discussed are the effects of near source volcanoclastics and low uplift rates on depositional environments west of the Tangahoe River, and erosion of the terrace coverbeds between the Tangahoe and Manawapou Rivers.

The coverbeds mapped in this study are correlated with the sea level curves of Chappell (1983) and Pillans (1987) and the oxygen isotope curve of Martinson *et al.*, (1987) to ascertain more directly the age of the marine terraces. Correlation of units to the Wanganui region (Pillans, 1981; Wilde, 1978) and to North Taranaki (Alloway, 1989) is presented.

## 1.2 Study area

The study area is located in South Taranaki, North Island, New Zealand (Figure 1.1a). It covers a northwest-southeast trending coastal strip approximately 30 km in length, with the northwestern boundary at Inaha Stream, west of Hawera and the southeastern boundary being Kakaramea township. The major rivers draining the study area are, from the north: the Waingongoro River which is sourced from Egmont Volcano and which in the past has been the conduit for a number of lahars, and the Tangahoe and Manawapou Rivers in the centre of the study area which drain the Tertiary mudstone hill country inland of the study area (Figure 1.1a). The larger water courses are deeply incised and have small floodplains. Smaller streams such as the Waikaikai and Mangaroa Streams drain the coastal parts of the study area, rising on the Inaha and Rapanui Terraces. Unlike the Tangahoe and Manawapou Rivers these

streams have not entrenched deeply into the terrace surfaces, which is probably an indication of their youthfulness. In the past these streams have had their courses impeded by advancing sand dunes, forming swamps and dune-impounded lakes. The study area is bounded by coastal cliffs up to 70 m in height which are currently eroding at approximately 0.7 m/yr (Gibb, 1978). The Waingongoro, Tangahoe and Manawapou Rivers are the only features within the study area that have cut the coastal cliff down to sea level. The smaller streams, yet to incise, plunge over the cliffs as waterfalls, usually in a series of steps formed by resistant lithologic units within the coverbeds.

Holocene sand dunes extend inland up to four kilometres between the Manawapou and Wanganui Rivers (Fleming, 1953), but within the study area reach a maximum of 2 km inland (Figure 1.2).

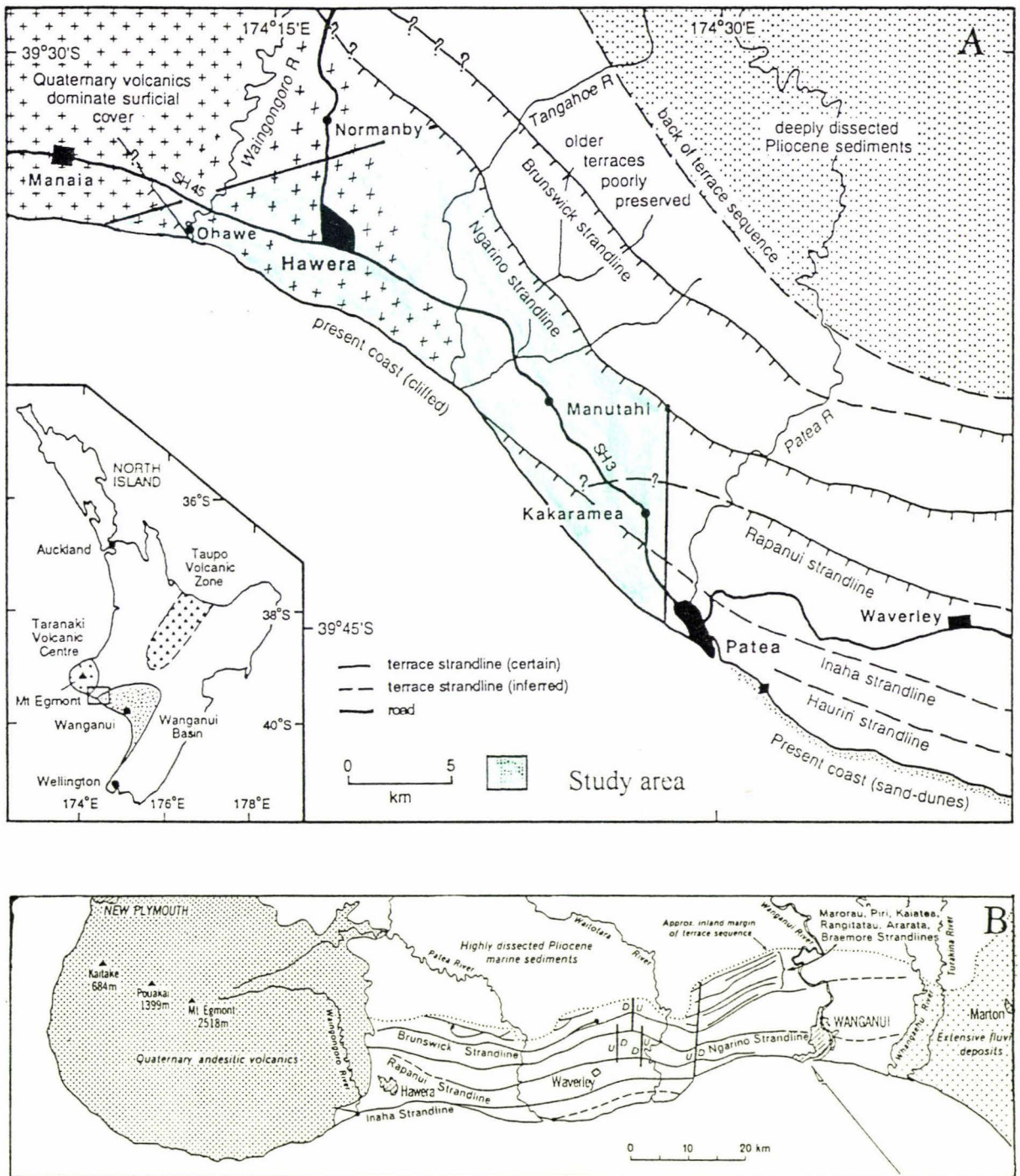


**Figure 1.1** (A) Location of the study area in relation to the Wanganui and Taranaki Basins and the Taupo Volcanic Zone. Uplifted marine terraces in the southeast sector of the study area become progressively buried west of the Tangahoe River beneath Quaternary volcanics of the Egmont ringplain. West of Kakaramea the distribution of the Rapanui and Ngarino Terraces is uncertain but it is believed that the Rapanui Terrace either cuts out west of Kakaramea (after Bussell, 1993), or as shown in (b) widens towards the west. (B) Distribution of Quaternary marine terraces between Wanganui and Hawera (after Pillans, 1983).

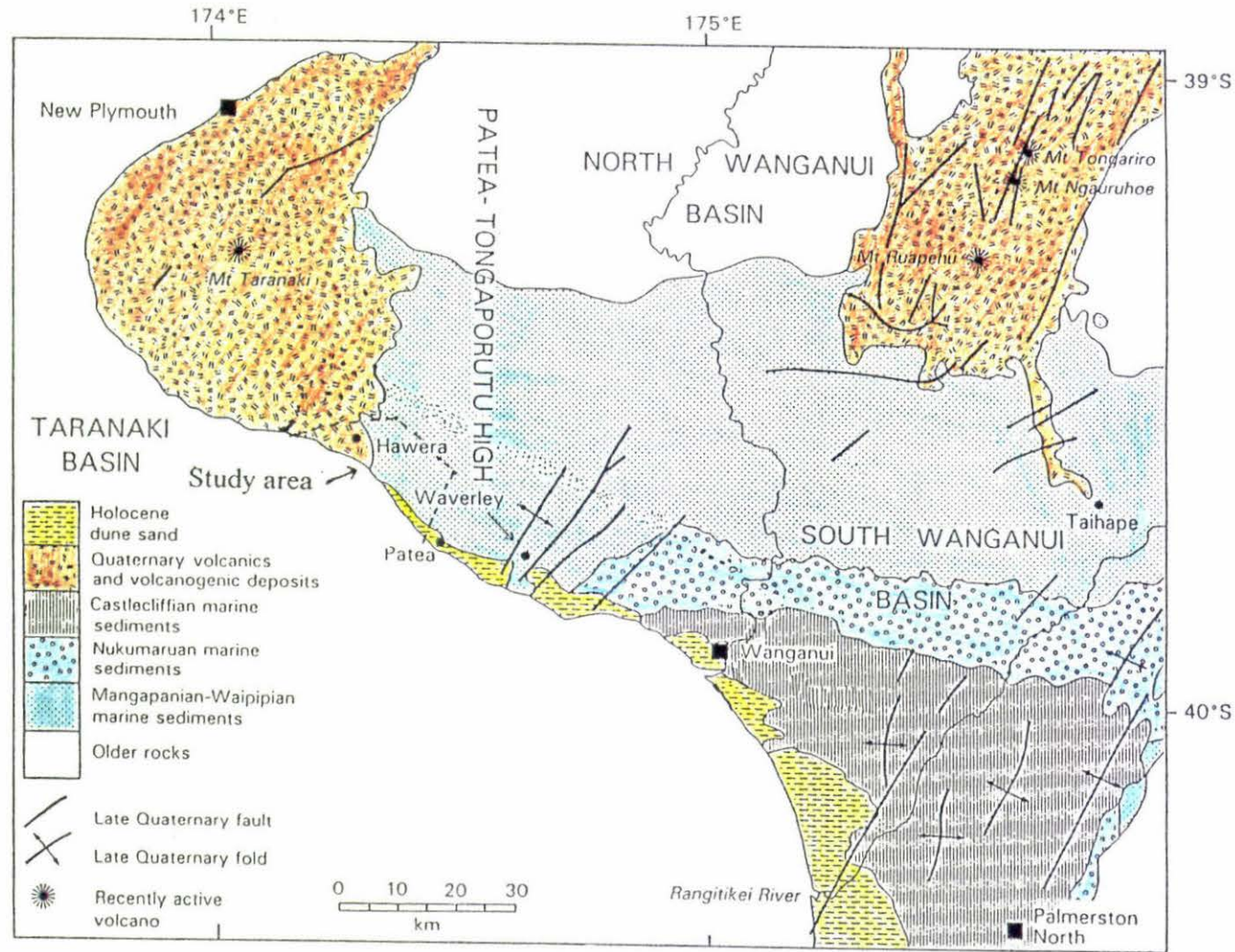


**Figure 1.2** Regional geology and study area location in relation to the South Wanganui Basin, Patea-Tongaporutu High and South Taranaki Basin to the west. Northeast-trending faults east of Patea mark the Nukumarau Fault Zone along the eastern margin of the Patea-Tongaporutu High. The Taranaki Fault Zone (a series of high angle reverse faults) marks the eastern margin of the South Taranaki Basin and is interpreted to underlie the study area. Quaternary volcanoclastics from the Taranaki Volcanic succession have infilled the South Taranaki Basin, forming the Taranaki Peninsula (after Pillans, 1990).

### **1.3 Geological setting**

#### **1.3.1 Subsurface geology**

The study area lies directly above a basement horst called the Patea-Tongaporutu High (Figure 1.2). This structural high separates the Taranaki Basin to the west from the South Wanganui Basin to the east. The study area lies on the boundary of these two basins. Therefore to provide a suitable geologic background to the study area, a brief history of each basin follows.

#### **The South Taranaki Basin**

The South Taranaki Basin (STB), has an extensive distribution offshore and onshore is now deeply buried beneath Quaternary volcanics and volcanoclastics. Its history as an independent geological province began approximately 80 ma (Haskell and Palmer, 1984). The eastern margin of the STB is bounded by the Taranaki Fault Zone (Figure 1.2) which may be a splay of the Alpine Fault (Knox, 1982). The Taranaki Fault Zone is interpreted as a 50 km-wide zone of stacked thrusts (Haskell and Palmer, 1984). Immediately adjacent to the east is the Patea-Tongaporutu High (Figure 1.2), which separates the STB from the South-Wanganui Basin (SWB).

The STB is comprised of two major structural blocks, the western platform to the west and the Taranaki graben to the east (Pilaar and Wakefield, 1978). The western platform is bounded to the east by the Cape Egmont Fault Zone which separates it from the Taranaki graben (Haskell and Palmer, 1984). The Taranaki graben is estimated to be 7 km thick (McBeath, 1977) and contains a sequence of Late Cretaceous (80 ma) to Recent sedimentary rocks. These sediments overlie basement rocks of Paleozoic and

early Mesozoic age (120-240 mya). Within the study area only the Pliocene and Pleistocene sediments are exposed above sea level.

### **The South Wanganui Basin**

The South-Wanganui Basin is an elliptical-shaped basin that contains approximately 4 km of shallow water marine sediments. Development of the SWB took place largely during the Pliocene and Pleistocene with regional tilting causing submergence to the south and uplift to the north (Anderton, 1981). The SWB is bounded to the west by a series of en echelon oriented basement highs (eg. the Patea-Tongaporutu High). The margin of the high is marked by the Nukumaru Fault Zone (Figure 1.2). The eastern basin margin is marked by the southern North Island axial ranges.

To the north is the North Wanganui Basin (NWB). The boundary between the two is taken as a line between Mt. Egmont in the west and Mt. Ruapehu in the east. Basin growth has been from north to south and since the early Pliocene the SWB depocentre has migrated in a southeastwards and then southwestwards direction (Figure 1.3). The Late Pleistocene depocentre of the SWB is located 50 km south of Wanganui (Anderton, 1981) and coincides with the greatest negative gravity anomaly (-165 milligals) in the New Zealand region. Sediments were laid down in a shallow marine environment as sedimentation kept pace with subsidence. Subsidence alone however cannot explain the large thickness of sediments in the Basin. Watts *et al.*, (1982) state that on isostatic grounds the greatest thickness of sediment that can accumulate in a basin is unlikely to exceed 2.5 times the original water depth. As the large thickness of shallow water sediments in the Basin were deposited in approximately 100 m of water,

the sediments in the SWB cannot be attributed to sediment loading alone, and an additional driving force for the formation of the SWB must be proposed (Stern *et al.*, 1993). The Basin is now thought to be related to lithospheric downwarping (Stern *et al.*, 1993) proceeding in a southwards direction (Figure 1.4) with sediments younging towards the south. Within the Nukumaru Fault Zone faults offset the sediments (Figure 1.2). The majority of these faults are reverse faults that strike northeast, and show a small downthrow to the east. However normal faults have also been reported (Fleming, 1953; Whitten, 1973; Pillans, 1993) which are related to surface stretching associated with the growth of young anticlines (Pillans, 1990).

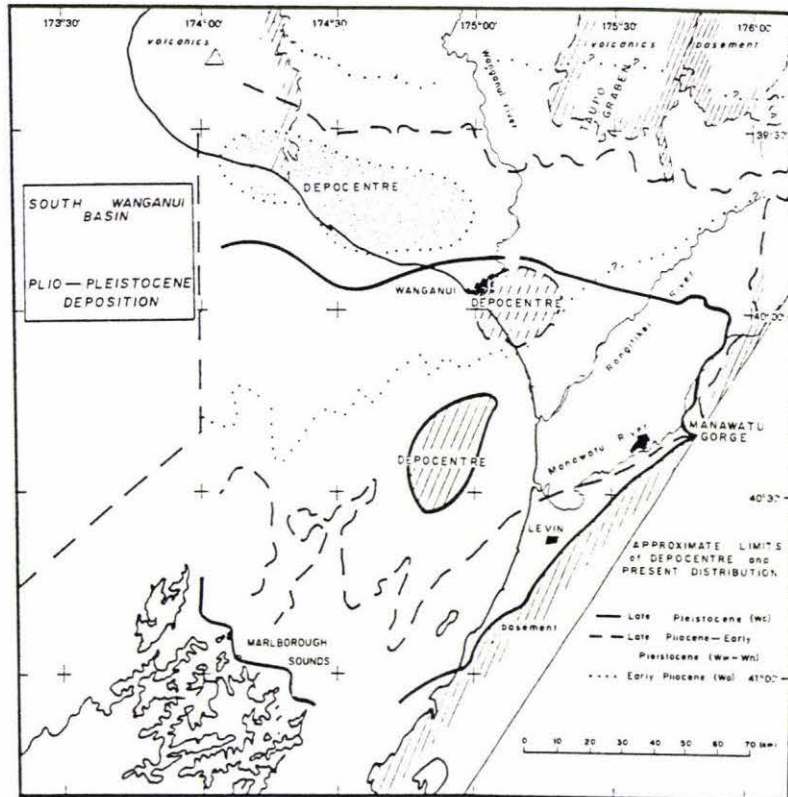


**Figure 1.3** Southeastery migration of South Wanganui Basin depocentre from Early Pliocene to Late Pleistocene and southward younging of uplifted marine sediments (Anderton, 1981).

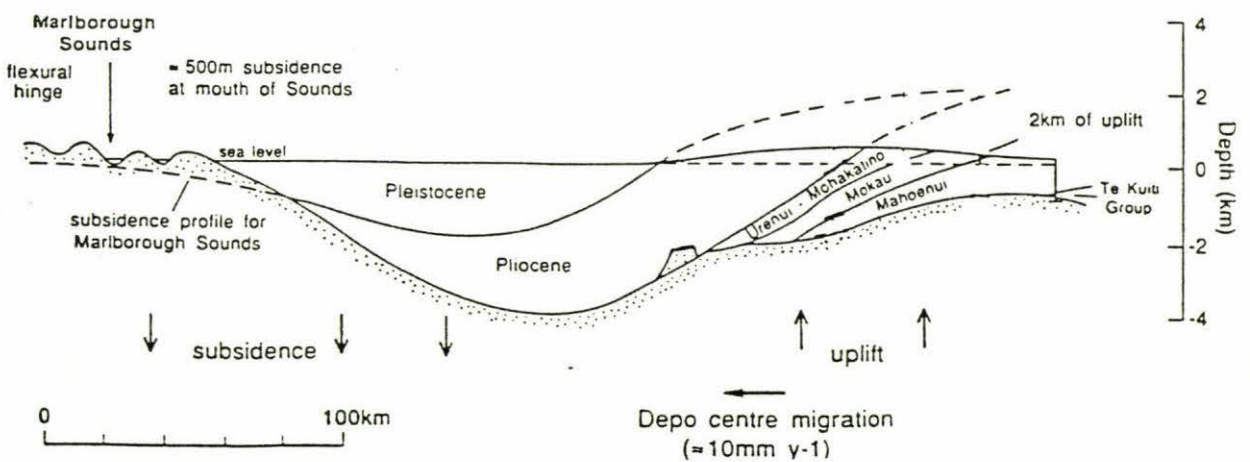


**Figure 1.4** SSE - NNW cross section of South Wanganui Basin showing depocentre migration progressing as a lithospheric downwarp with subsidence occurring in the south and uplift in the north (after Stern *et al.*, 1993).

### 1.3.2 Surface geology

The Taranaki Peninsula is constructed mainly of materials derived from the chain of andesitic stratovolcanoes, extending north-northwest from Mt. Egmont. In order of decreasing age they are Paritutu and Sugar Loaf Islands (1.75 ma) in the north, then Kaitake (0.5 ma), Pouakai (0.25 ma) and Egmont to the south, the latter classed as an active volcano formed during the last 0.13 ma (Smith *et al.*, 1994). These volcanoes are of a high K calc-alkaline type characterised by hornblende-andesite lavas (Smith *et al.*, 1994).

Andesitic stratovolcanoes are potentially unstable landforms and they tend to quickly build up thick sequences of detrital volcanoclastics to form ring plains which surround the mountain. The extensive ring plain comprises coalescing aprons of reworked volcanoclastic deposits forming a relatively undissected sloping surface that grades away from the edifice (Palmer and Neall, 1991). These ring plain deposits are then capped with a variable thickness of tephra and loess. Tephra deposits generally decrease in thickness with increasing distance from source while volcanic loess deposits increase in relative thickness away from the edifice, at least out to 100 km from source.

To the south, Quaternary airfall deposits cover the marine terrace surfaces. The coverbeds are usually composed of materials derived from the volcanic chain to the northwest that has been reworked to leave a complex array of marine, littoral, and dune-sand sediments interbedded with tephra. The inland margin of the study area is dissected Tertiary hill country where volcanic airfall material is restricted to a thin veneer on the steep mudstone landscape and thus often prone to shallow landsliding.

The northwestern part of the study area is situated on the southeastern margin of the Egmont ring plain. The ring plain has a radial drainage pattern with a high density of

stream channels close to source, the density decreasing with increasing distance from the mountain. The central and southern parts of the study area are situated on coastal marine terraces. The terraces are probably present closer to the mountain but have been deeply buried beneath the volcanic deposits. On the marine terraces the drainage pattern is denedritic with streams and rivers flowing normal to the coast. All watercourses in the study area, except the Waingongoro and Patea Rivers (which are sourced on Mt. Egmont), drain the inland mudstone hill country which has a high potential for erosion. These rivers therefore tend to carry a much larger amount of suspended sediment (Taranaki Regional Council, 1991) and this is reflected in the colour and nature of the stream channels and their associated floodplains.

#### **1.4 Present climate**

Rainfall in the area is related to elevation and hence exposure to the predominant rain-bearing westerly winds. Mt. Egmont affects weather both locally and regionally; rainshadow effects caused by the mountain are recorded as far southeast as Waikanae and Levin. The study area receives *c.* 1200 mm rainfall that is distributed evenly throughout the year with the coastal plains receiving less rain than the inland terraces at higher elevations (Figure 1.5).

The coastal regions experience a warm temperate climate with few extremes; the highest and lowest temperature recorded being 30°C and -1.5°C respectively. Annual temperatures in inland areas are cooler than average with common frosts and fogs. The region experiences predominantly west and northwest winds (Thompson, 1981). Relatively strong winds occur in late spring and early summer, mostly from the westerly or southerly quarter.

### 1.5 Past and present vegetation

Very little of the original native forest remains on the ring plain or the coastal terraces. Isolated pockets now remain in gullies and on land too steep to be farmed. The coastal strip was the first area to be cleared by the Maori and by the time of European settlement, it consisted of fern and shrub (Dieffenbach, 1843). Near to the coast the forest contained a low canopy consisting of *Dysoxylum spectabile*, *Beilschmiedia tawa*, *Hedycarya arborea*, *Corynocarpus laevigatus*, *Elaeocarpus dentatus*, *Alectryon excelsus*, *Rhopalostylis sapida* and *Myoporum laetum*. The understorey contained *Dodonaea viscosa*, *Macropiper excelsa*, *Melicytus ramiflorus*, *Cyathea spp.* and *Geniostoma rupestre var. crassa*. Within 4 km of the coast black topsoils are predominant. This is thought to be due to the original native scrub vegetation containing *Phormium tenax* and *Pteridium aquilinum var. esculentum* (Stewart *et al.*, 1977). Farther inland brown topsoils dominate and these were formed under a podocarp-hardwood forest dominated by *Beilschmiedia tawa* and podocarps such as *Dacrydium cupressinum*, *Podocarpus totara* and *Dacrycarpus dacrydioides*. The present landscape is now dominated by pasture with farm or paddock boundaries comprised of boxthorn hedges as well as small stands of *Pinus radiata* and macrocarpa.

### 1.6 Soils

The present day soils in this region are formed largely from Late Quaternary tephra of hornblende-andesite composition derived from Egmont Volcano (Palmer *et al.*, 1981) with the tephra mantle progressively thinning and becoming finer away from source. The soils at the southeastern margin of the Egmont ring plain and the northern

end of the coastal marine terraces belong to the Egmont series (Allophanic Soils) on flat and rolling terrane.

On the flat to rolling ring plain and terrace surfaces the Allophanic Soils generally have a very high amorphous clay (allophane) content with silt loam textures. The subsoils contain fine volcanic ash and volcanic loess, and it is this that gives these subsoils their characteristic waxy feel. The allophane imparts many desirable qualities such as friable consistence, high macroporosity and thus good drainage to the soils, making them some of the most productive or potentially productive soils in the country. High phosphate retention values also characterise these soils; this is overcome by heavy applications of phosphate fertilisers. Often the topsoils close to the coast have a sandy texture derived from wind blown sand imparting a lower phosphate retention.

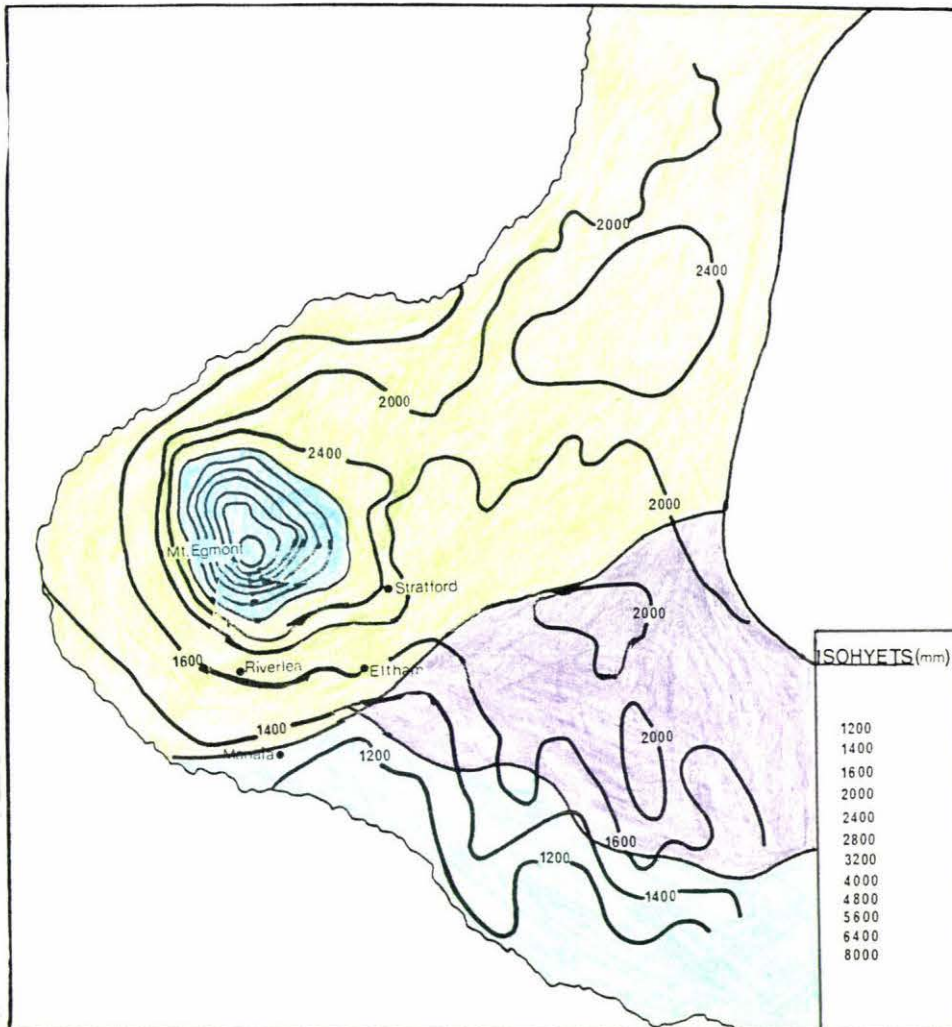
Farther inland and southeastwards on the dissected marine terraces the underlying Tertiary sedimentary strata are often exposed. The landscape becomes progressively more dissected as uplift rates and terrace age both increase inland. In the river valley systems where moderately steep to steep slopes dominate the landscape, the soil pattern is related to the different lithologies exposed to weathering. In places composite soils have formed which have very well developed pedological features and are classed as Granular Soils. In contrast, undissected flat to rolling interfluvial terrace surfaces have a mature and stable landscape history with little or no erosion of covered units. With increasing terrace age the marine sediments on each wave-cut surface (WCS) are mantled by progressively older volcanic ash and volcanic loess deposits.

A narrow coastal strip of Holocene sand dunes, sand plains, peaty swamps and lakes that extend from Wanganui to Cape Egmont, form the sand country of the Wanganui-South Taranaki region (Wilde, 1979). Between Wanganui and Patea, Wilde

(1979) mapped the sand country soils and described eight soil series (3 on the dunes and 5 on the associated sand plains) with differences being mainly attributed to drainage conditions and landform age.

### **1.7 Landuse**

The landuse in the area centres around livestock farming; dairy farming being dominant. Sheep and beef farming is the second largest activity, generally in the hill country. Horticulture in the region is represented by a few orchards and commercial gardens in the vicinity of Hawera and Normanby where up to *c.* 200 ha of asparagus are grown (Water and Soil Misc. Publication No. 110).



| <u>Climatic types</u>   |  |
|---|--|
|  | <b>A2</b> Warm humid summers, mild winters. Annual rainfall 1500 to 2500 mm with a winter maximum. Prevailing wind southwest.  |
|  | <b>C3</b> Warm summers. Very heavy rain at times from south and southeast. Annual rainfall mainly 1500 to 2500 mm.   |
|  | <b>D1</b> West to northwest winds prevail with relatively frequent gales. Annual rainfall 900 to 1300 mm. Rainfall reliable and evenly distributed throughout the year. Warm summers and mild winters. |
|  | <b>M</b> High rainfall mountain climates. Conditions vary greatly with altitude and exposure.  |

**Figure 1.5** Mean annual rainfall isohyets and climatic regions of the Taranaki region (Official New Zealand Meteorological Office data, 1941-1970).

## Chapter Two

### 2.1 Previous work and terminology

Fluctuating sea levels combined with progressive uplift during the Quaternary has preserved a set of well dated marine terraces throughout the south Taranaki-Wanganui area. This work has centred on correlation of terrace covered units and calculation of terrace uplift rates between Kakaramea and Ohawe Beach. Ages of the terraces are based on correlation to the marine oxygen isotope curve and terrace covered units established by previous workers (e.g. Fleming, 1953; Dickson *et al.*, 1974; Chappell, 1975; Pillans, 1981; Bussell, 1988 and Alloway, 1989). Thus it is appropriate to review previous relevant work.

The most comprehensive account of the geology of the South Taranaki-Wanganui region and the first to describe the coastal marine terraces there was that of Fleming (1953). Earlier workers in the region (Hutton, 1886; Park, 1887; Marshall and Murdock, 1920), all cited by Fleming (1953), concentrated on the older pre-Hawera series sediments. Morgan (1920) outlined the geology and stratigraphy of the younger sediments in the Patea district.

Fleming (1953) recognised three major groups of coastal terraces. He named these (from youngest to oldest) the Rapanui, Brunswick and Kaiatea group of terraces. Fleming however noted the polygenetic character of the Rapanui Terrace (Fleming, 1953, p 42.) and named the lowest the sub-Rapanui terrace. Fleming's work concentrated on the older marine sands, gravels and dune sands overlying the wave-cut surfaces and lumped together the upper younger ash and loess units into one unit which he named the Egmont Ash. Grant-Taylor (1964) and Dickson *et al.*, (1974) later redefined Fleming's Rapanui and sub-Rapanui Terraces, confining the name Rapanui Terrace to Fleming's sub-Rapanui Terrace and renaming the older terrace the Ngarino Terrace. Dickson *et al.*, (1974) were unable to establish whether the Ngarino and Rapanui Terraces represented separate interglacial stages.

Chappell (1975) studied coastal marine terraces in North Auckland, Auckland and the Bay of Plenty. Chappell's correlation and dating of the terraces, particularly in

the Bay of Plenty was supported by tephrostratigraphy. The uplift and warping of these terraces in each region was measured and the formation of the terraces related back to dated sea level curves from New Guinea and around the world. Correlation of the terraces with the marine terraces of Taranaki and Wanganui was also attempted.

The most important study of the South Taranaki-Wanganui marine terraces is by Pillans (1981) who named and dated twelve marine terraces (Figure 2.1). The terraces were dated using fission track, radiocarbon and amino acid racemisation techniques. In subsequent papers (Pillans, 1983, 1985, 1988, 1990; Pillans *et al.*, 1988), a comprehensive stratigraphic framework was established for each terrace thereby providing a well dated landform and inferred climatic history of the area. The twelve terraces were all dated at younger than 700 ka, five are of Wanganui Series age and seven belong to the Hawera Series (Figure 2.1). The chronology was then used to construct a deformation model with the following constraints:

1. The Ararata Terrace (Pillans 1983) is interpreted to have formed *c.* 400 ka. This age is based on a fission track date of 370 ka (Pillans and Kohn, 1981; Kohn *et al.*, 1992) obtained for the Omahina Tephra (Pillans, 1981) which overlies the Ararata WCS. Assuming linear accumulation rates of sediments between the tephra and the WCS an age of 400 ka was obtained for the Ararata WCS.

2. Underlying the Omahina Tephra on the older Rangitatau Terrace is the Meremere lignite. An age of 400 ka for the lignite is based on its correlation with the emergence of the Ararata Terrace *c.* 400 ka. The 400 ka age of the lignite was then used as a calibration date for the amino acid racemisation (a.a.r) technique.

3. The strandline at the back of the Rapanui Terrace was last active *c.* 120 ka, during oxygen isotope stage 5e.

Rates of uplift were determined from strandline height and age of the Rapanui and Ararata Terraces. Strandlines were used because they are the last active position of erosion before sea level falls after forming each terrace. Using terrace strandlines allows for better consistency with other similar studies overseas. Sea level highstands have been closely studied and are well dated, whereas the history of intermediate sea levels is less well known. The Rapanui strandline that formed 120 ka, represents a paleosea level of +5m relative to present (Pillans, 1990). Paleosea level which formed the Ararata strandline *c.* 400 ka is assumed to have been similar to present sea level. This paleosea level is based on the similar amplitude of glacial/interglacial cycles identified in oxygen isotope curves in deep sea cores (Pillans, 1990). Based on the hinging uplift model, and uplift rates for the Ararata and Rapanui Terraces, the uplift rates for the Ngarino, Brunswick and Braemore Terraces were calculated. Five stages of terrace development, based on the interaction between tectonic uplift and sea level change, are recognised (Pillans, 1983), summarised in Figure 2.2.

In the study area the Rapanui Terrace was originally interpreted to be preserved along and parallel to the present coastline west to Ohawe Beach where the Inaha Terrace is once again preserved (Pillans, 1981) (Figure 1.1b). Recognition of the marine terraces at Ohawe and inland is difficult because deposition of abundant volcaniclastics has complicated the stratigraphy and obscured any terrace risers. Subsequent studies by Bussell (1988, 1990, 1993), examining pollen assemblages within the coverbeds of the terraces, have resulted in a reinterpretation of the distribution of the Ngarino and Rapanui Terraces west of Patea. Bussell examined two sites, the Ohawe waterfall (Q21/144785) and Ohawe east sections (Q21/147783) in the coastal cliffs west of Hawera. Based on an interpretation of the pollen in the organic deposits preserved interbedded with laharic breccias and alluvium, the marine platform previously assigned to oxygen isotope stage 5e was placed in stage 7. Interpretation of the marine terrace along the coast from a point *c.* 1.5 km southeast of the Manawapou River, to Ohawe as being the Ngarino Terrace implies the loss of the 120 ka Rapanui and the 100 ka Inaha Terraces (Figure 1.1a).

|             |          | MARINE TERRACE                     | ESTIMATED STRANDLINE AGE                          | ISOTOPE STAGE |  |
|-------------|----------|------------------------------------|---|---------------|--|
| PLEISTOCENE | HAWERA   | * Rakaupiko                        | 60,000  | 3             |  |
|             |          | ph Hauriri                         | 80,000  | 5a            |  |
|             |          | pi Inaha                           | 100,000   | 5c            |  |
|             |          | pr Rapanui                         | 120,000   | 5e            |  |
|             |          | pn Ngarino                         | 210,000   | 7a            |  |
|             |          | pb Brunswick                       | 310,000   | 9             |  |
|             |          | pe Braemore                        | 340,000   | 9             |  |
|             | WANGANUI | pa Ararata                         | 400,000   | 11            |  |
|             |          | pt Rangitatau                      | 450,000   | 11            |  |
|             |          | pl Ball                            | 520,000   | 13            |  |
|             |          | pp Piri                            | 600,000   | 15            |  |
|             |          | pu Undifferentiated older terraces |   |               |  |
|             |          | *                                  | Known at only one locality with no surface extent |               |  |

**Figure 2.1** South Taranaki-Wanganui Pleistocene marine terrace chronology and correlation to the marine isotope record (after Pillans, 1990).

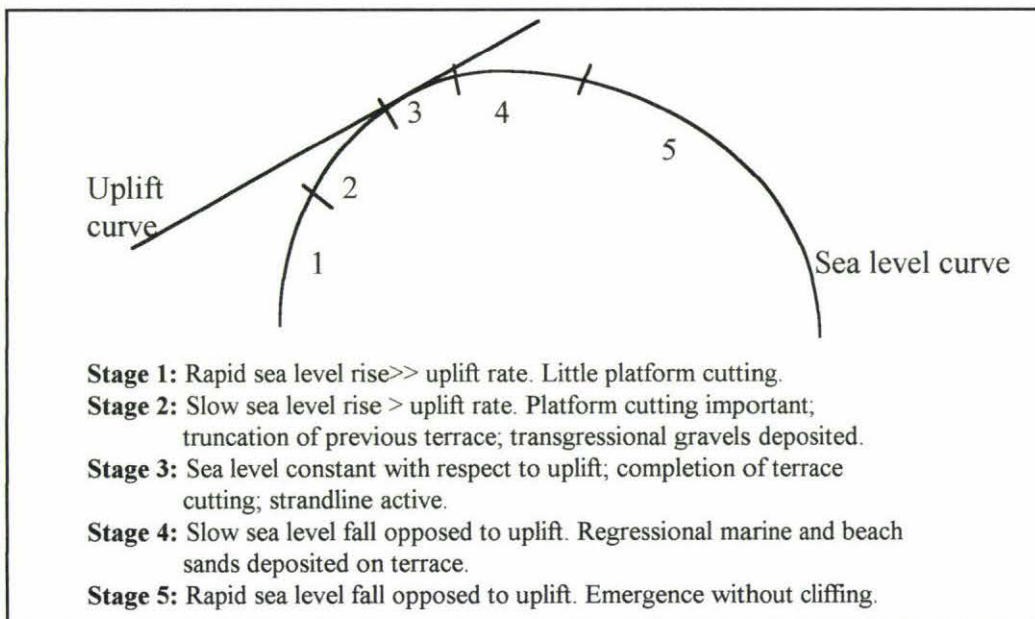


**Figure 2.2** The five stages of marine terrace development as expressed by the relationship between rate of sea level rise and fall and terrace uplift rate (after Pillans, 1981).

The terrace covered units described in this study are dated on the basis of interbedded tephra (Alloway, 1989) and correlation to sea level curves (Chappell, 1982; Pillans, 1987) ( Figures 2.3a and 2.3b), oxygen isotope curves (Martinson *et al.*, 1987) (Figure 2.3c), and corresponding dated coverbeds elsewhere in the Wanganui region (based on stratigraphic position and important physical criteria (Wilde, 1979; Wilde *et al.*, 1988 and Pillans, 1985, 1990). Table 2.1 summarises the height of relative sea level during stages 5a to 9 used in the calculation of terrace uplift and the subsequent tectonic deformation (Chapter 5).

| Age (ka) | Terrace   | Stage | Rel. sea level | Reference                   |
|----------|-----------|-------|----------------|-----------------------------|
| 80       | Hauriri   | 5a    | -12m           | Chappell, 1983              |
| 100      | Inaha     | 5c    | -12m           | “                           |
| 120      | Rapanui   | 5e    | +5m            | “                           |
| 210      | Ngarino   | 7a    | c.0m           | Pillans <i>et al</i> , 1987 |
| 230      |           | 7b    | >-32m          | “                           |
| 240      |           | 7c    | c. -10m        | “                           |
| 310      | Brunswick | 9     | c.0m           | “                           |

**Table 2.1** Marine terrace chronology and oxygen isotope stage correlation (after Pillans, 1990) with paleosea level data used in this study.

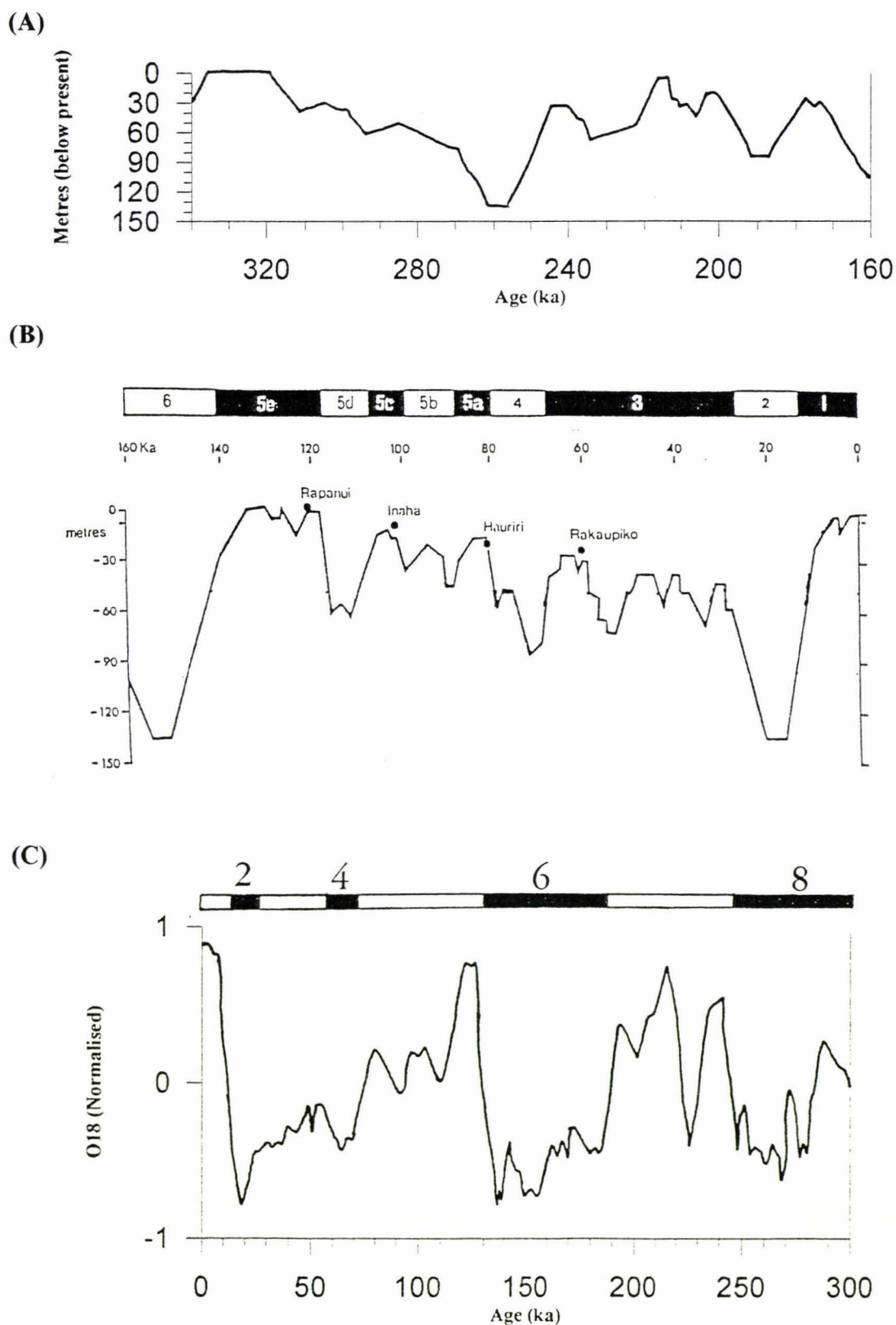


**Figure 2.3** Sea level and oxygen isotope curves to which marine terrace covered beds in this study are correlated. **(A)** Sea level 340-160 ka (after Chappell, 1975). **(B)** Sea level 160 ka to present (after Pillans, 1985). **(C)** Oxygen isotope curve (after Martinson *et al.*, 1987).

## **2.2 Marine terrace terminology**

The terrace nomenclature adopted in this study follows that of Pillans (1981, 1990) (Figure 2.4). As studies of the genesis and deformation of the marine terraces become more detailed it is important that the terms used are adequate and allow for ease of correlation between studies. The following are the terms employed and their definitions (after Pillans 1990).

### **Marine terrace**

A gently sloping sub-planar landform which is bounded at its outer edge (seaward margin) by a steep descending slope and along the inner margin by a similar ascending slope. Accompanying such landforms is evidence of a marine origin such as the presence of marine sediments and/or a wave-cut surface (WCS). The term marine terrace is applied to present day topographic expression of a WCS and its overlying coverbeds.

### **Wave-cut surface (WCS)**

A sub-horizontal marine surface of erosional origin that truncates older sediments. This surface often shows signs of boring by marine organisms such as *Barnea similis* and is overlain by marine sediments and/or fossils. This surface is bounded at its inner edge by a fossil sea cliff (Figure 2.4).

### **Strandline**

The terrace strandline is a wave erosional feature found at the intersection of the wave cut surface and the base of the fossil sea cliff at the terrace's inner margin (also known as the nick point ). A marine terrace strandline marks the position of the fossil cliff when active erosion of the terrace by the sea ceased as relative sea level began to fall (Figure 2.2) and is the most accurate height to obtain for terrace correlations, uplift and deformation studies.

### **Terrace coverbeds**

A collective term referring to all sediments and deposits above the WCS and terminating at the terrace surface. Coverbed sequences in the area generally include marine sands and gravels immediately overlying the WCS grading into alluvial floodplain deposits, including silts and lignites, with terrestrial deposits such as dune sands, tephra and loess.

### **Terrace riser**

Surface expression of a terrace strandline, often deeply buried beneath coverbed deposits, representing the intersection of a wave-cut surface with the base of a fossil sea cliff.

## **2.3 Lahar and debris-avalanche deposits**

A ring plain depositional system is an assemblage of debris-flow, debris-avalanche and fluvial deposits that form genetic lithostratigraphic units (Palmer *et al.*, 1991). The term lahar has come to refer to a rapidly flowing mixture of volcanic debris intimately mixed with water (excluding streamflow) from a volcano (Smith and Fritz, 1989). Debris avalanches are rapidly moving, incoherent masses of unsorted rock and soil mobilized by gravity (Schuster and Crandell, 1984). Debris-avalanche deposits contain deposits derived both from the source area and from debris eroded during flow (Neall, 1979; Crandell *et al.*, 1984; Glicken, 1986; Palmer and Neall, 1989; Palmer *et al.*, 1991). Sediment eroded during flow includes rip-up clasts of stratified gravel and sand, diamicton, tephra and lignite.

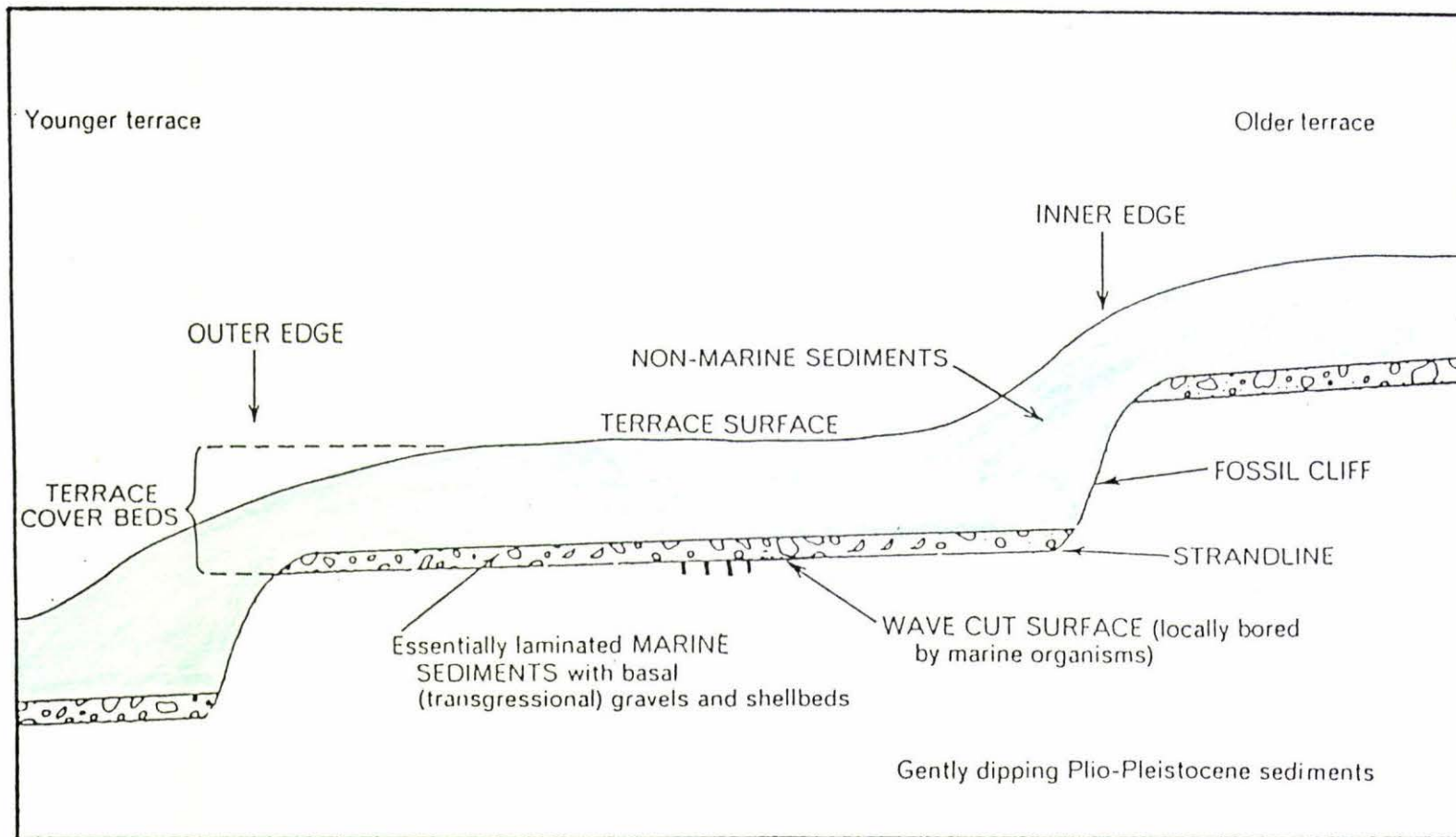


**Figure 2.4** Generalised marine terrace cross section and nomenclature (after Pillans, 1990).

## Chapter Three

### Terrace covered stratigraphy and physiography

#### 3.1 Introduction

This chapter establishes the covered stratigraphy of the Rapanui and Ngarino Terraces between Hawera and Kakaramea. Correlation of the coverbeds with previous workers' chronologies (Fleming, 1953; Dickson *et al.*, 1974; Wilde, 1979; Pillans, 1988, 1990, 1991; Wilde and Vucetich, 1988; Alloway, 1988, 1989; Bussell, 1990, 1993) is based on descriptions of physical characteristics such as colour, structure, and the nature of contacts. The distribution of key stratigraphic units, age correlations and inferred depositional environments are combined to provide a landscape history of the South Taranaki marine terrace sequence.

This work involved closely examining and describing over fifty sections. The location of type and reference sections described in this study are shown in Figure 3.1 with section descriptions collated in the appendix. A composite stratigraphy of the coastal marine terraces is presented in Figure 3.2. Coverbeds overlying the terrace WCS comprise up to six Late Pleistocene volcanic loess units, eight aeolian sand units and abundant interbedded tephras, lignites and west of the Tangahoe River towards Hawera, volcanic debris flow deposits. The Tangahoe River marks the southeastern limit of the Egmont ring plain and its associated volcanoclastic flow deposits. The ring plain is here referred to as the northwest sector and the coastal marine terraces southeast of the Tangahoe River as the southeast sector (Figure 3.1).

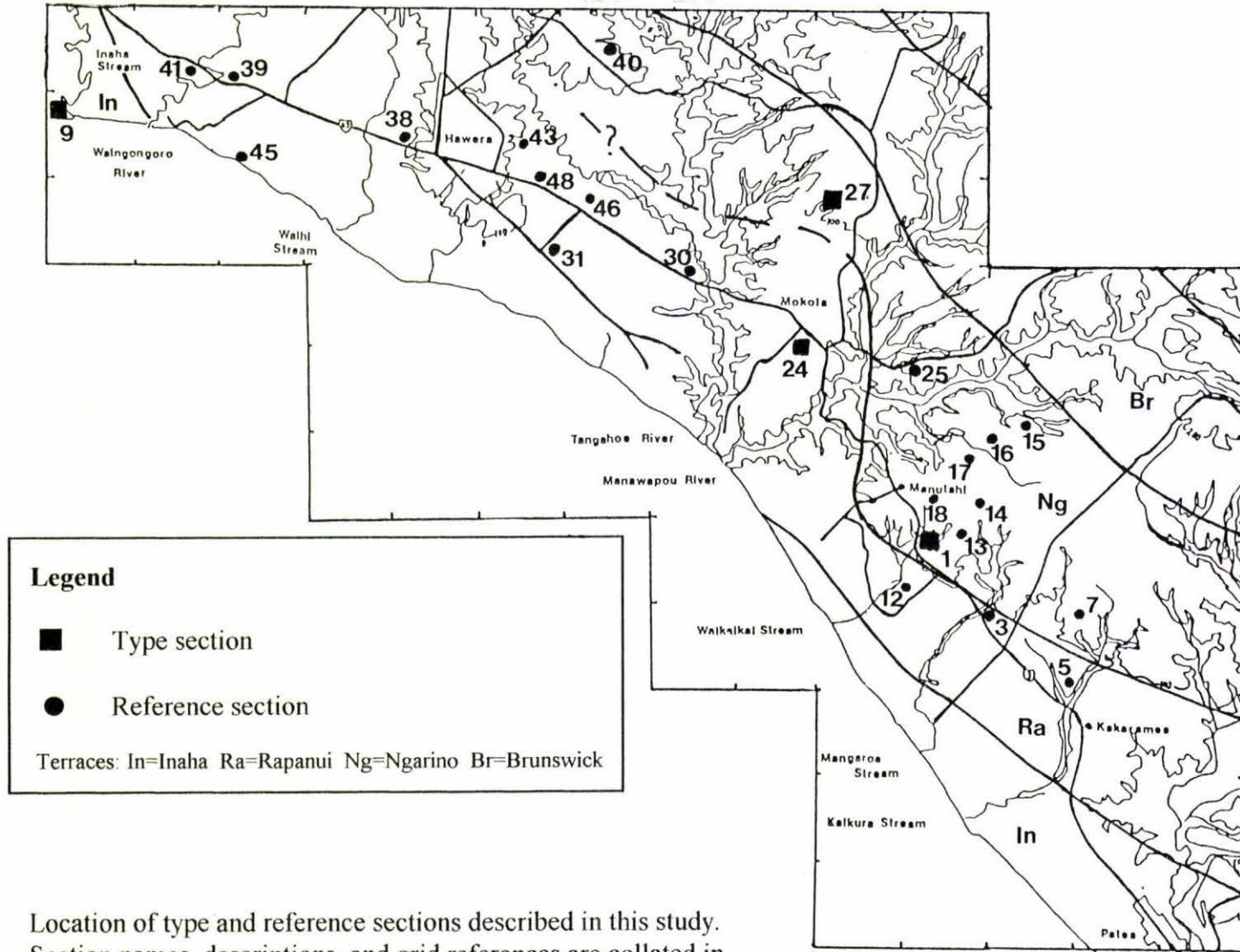


**Figure 3.1** Location of type and reference sections described in this study. Section names, descriptions, and grid references are collated in appendix A.

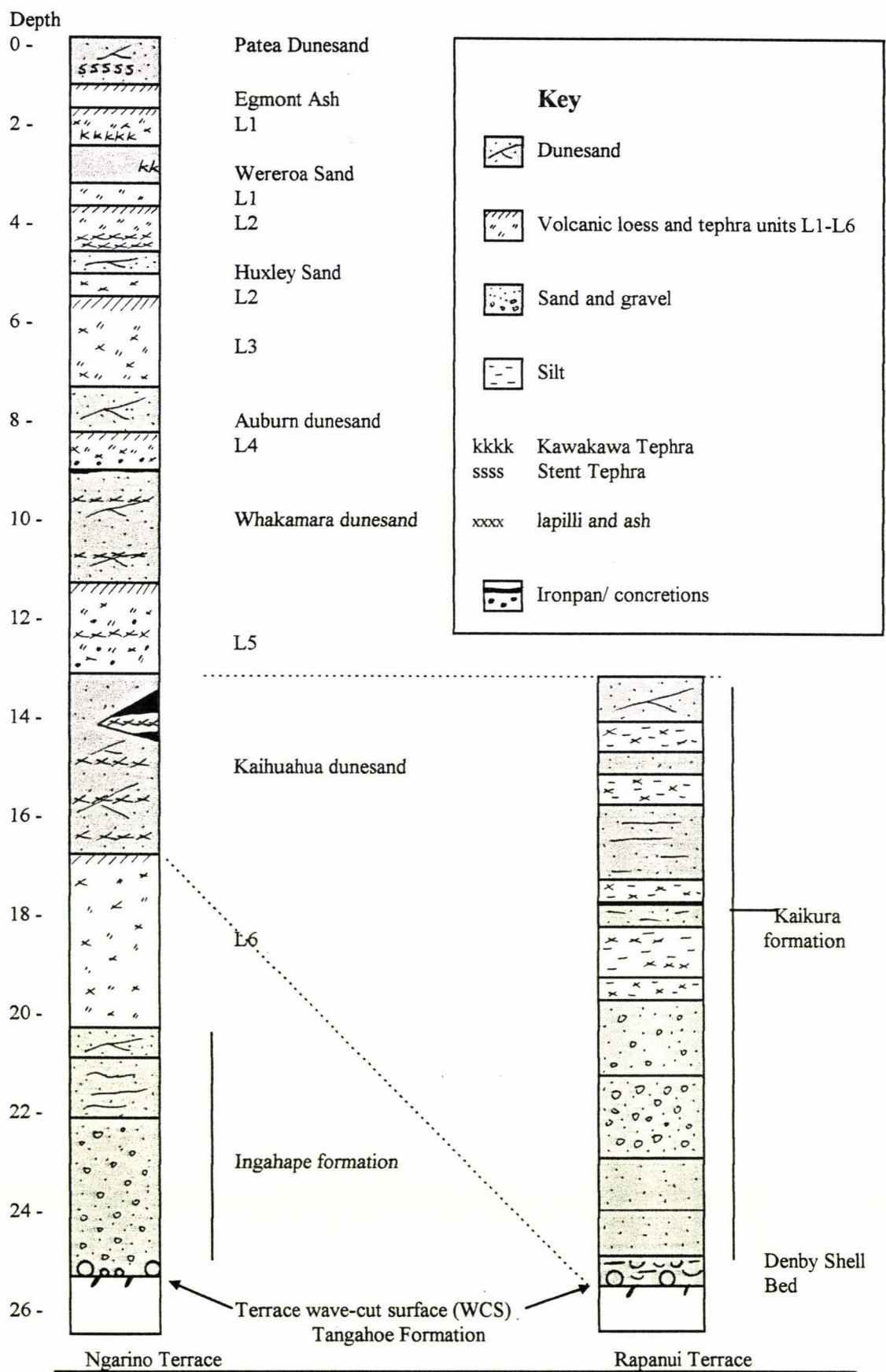


**Figure 3.2** Composite stratigraphic columns of aeolian and marine coverbeds overlying the Rapanui and Ngarino Terraces in the southeast sector.

In this thesis the marine terrace covered units are discussed in order from youngest to oldest. The youngest unit referred to is the Patea Dunesand dated *c.* 6 ka, while the oldest unit, the Ingahape formation (Figure 3.2) is *c.* 210 ka.

Loess 5 (L5) is the oldest terrestrial unit found on the Rapanui Terrace (Pillans, 1985, 1990), and therefore the distribution of older covered units provides a picture of the distribution of the Ngarino Terrace in the study area. This chapter attempts to ascertain the current evidence for the mapped distribution and age of the Ngarino and Rapanui Terraces between Kakaramea and Ohawe Beach.

### **3.1.1 Southeast sector**

The Tangahoe River has served as the boundary to volcanoclastic flows originating from Egmont Volcano, *c.* 45 km to the northwest. The terrace stratigraphy to the southeast of the Tangahoe River is dominated by aeolian deposits (volcanic loess and dunesands) compared with the fluvially dominated sands, gravels and interbedded silts and lignites of the northwestern sector. Streams and rivers in the southeast sector are confined within narrow valleys and, as a result fluvial deposits are rare within the terrace covered sequence.

Inferred distribution of the Inaha, Rapanui and Ngarino Terraces southeast of the study area as mapped by Pillans (1983, 1990) is accepted here, however, mapping and correlation of the older covered units becomes difficult towards Hawera due to a lack of exposures and increasing volumes of volcanoclastics complicating the stratigraphy.

The Rapanui Terrace (as mapped by Pillans, 1986) is separated from the younger Inaha Terrace by an obvious riser in the vicinity of Kakaramea. This riser intersects the

coast approximately 1.5 km southeast of the Manawapou River at Q21/345543. The difference in height between the Rapanui and Inaha Terrace WCS ranges from 18 m at the coast to *c.* 20 m where the riser crosses the Hawera-Wanganui highway south of Kakaramea (Q21/667876). The inner margin of the Rapanui Terrace however is less defined, particularly northwest of Kakaramea where either the riser separating the Ngarino Terrace from the Rapanui Terrace has little relief, and/or the riser has been obscured by terrestrial deposits such as advancing dune sands ramping up and over it.

### **3.1.2 Northwest sector**

The northwestern part of the study area constitutes the southeastern sector of the Egmont ring plain. The ring plain records volcanoclastic accumulation over the last 100 ka (Neall *et al.*, 1986) and comprises a coalescing apron of reworked and *in situ* volcanoclastic sediments derived from both periods of edifice construction (tephras) and destruction (debris flows and debris avalanches) (Neall, 1976; Neall *et al.*, 1986; Alloway, 1989). Within the northwest sector chronological control is facilitated by the presence of a marine terrace WCS cut into Pliocene mudstone and sandstones, however inland of the coast the WCS is deeply buried. Identification of marine terraces northwest of the Tangahoe River and inland from the coastal cliffs has remained difficult, complicated by low uplift rates, high sedimentation and lack of exposures of older covered units.

### **3.1.3 Method of study**

During preliminary fieldwork a number of important and readily accessible road sections were examined. These provided excellent lateral and vertical exposure, from which a preliminary stratigraphic framework was compiled. Later field work concentrated on obtaining height data of the WCS for structural analysis (chapter 5). It was at this time that other important sections were found. The most useful sections included track cuttings, silage pits, slips and the coastal sea cliffs, while numerous smaller sections providing limited exposure were also examined. Facies changes between the northwest and southeast sectors, the similar appearance of dune and marine sands and various aged volcanic loess units has in the past led to difficult correlations and explains the poor understanding of the distribution of the marine terraces in this area.

The next section is my attempt to correlate the volcanoclastic deposits found in the area west of the Tangahoe River with deposits found on the coastal marine terraces in the southeast of the study area. In doing so comments will be made on lahar stratigraphy and implications to the terrace chronology discussed.

## **3.2 Holocene deposits**

Two Holocene deposits are mapped in the study area, the coastal Patea Dunesand and the more widespread Egmont Ash (Figure 3.3).

### **3.2.1 Patea Dunesand (Fleming, 1953)**

**Type section:** Pickwick Road, Wanganui, at R22/823429

**Reference sections:** Manawapou Road at Q21/264711, Geary Road at Q21/295681

#### **Previous references**

Fleming first described this unit as Holocene dunesands overlying both coastal and river terraces in the Wanganui Subdivision. Based on geographical distribution he recognised and named six dunesand complexes, namely the Kaitoke, Westmere, Kairari, Okehu, Nukumaru and Waverley dune complexes. These were correlated with the Foxton, Motuiti and Waitarere dune building phases of Cowie (1963). Wilde (1979) mapped eight soil series on the coastal sand country between Wanganui and Patea. He recognised three series on the dunes and five series on the associated sand plains.

The Patea Dunesand is the youngest covered within the study area, and is the parent material of the present day soil along the coast.

#### **Nature and distribution**

The Patea Dunesand reaches thicknesses >20 m and consists of structureless to loose, dark brown to very dark greyish brown, medium to fine andesitic sand. Once exposed, they are very prone to deflation (Plate 3.1) by the strong prevailing (in order of

frequency) northwest, west and southerly gales experienced along the coast. Soils on the Patea Dunesand are frequently thin (<15 cm) and consist of a very friable to friable dark grey to black A horizon overlying greyish brown to dark greyish brown loose sand. The dark colours exhibited by these sands reflect the high content of magnetite, derived from the erosion of andesitic volcanoclastics and transported by longshore drift in a southeasterly direction.

Along a section exposed by the Waikaikai Stream at Q21/287676, a light brown to dark brown buried soil with root channels and iron staining is present within the Patea Dunesand up to 5 m below the land surface. Here Patea Dunesand exhibits steep dune and tabular bedding sometimes containing interbedded fine granular, pale white to yellow andesitic tephra up to 5 mm thick. In places, where the buried soil is peaty, a fine pink/grey to white/grey glassy ash up to 10 mm thick is preserved. Stewart *et al.*, (1977); Neall and Alloway, (1986); Alloway, (1989) identified a minor rhyolitic glass peak or bed intercalated with Late Holocene distal andesitic tephra from Egmont Volcano which was tentatively correlated to the Taupo-sourced *c.* 3.2 ka Waimihia Tephra. Subsequent work (Alloway *et al.*, 1994) has shown the silicic ash to be the Stent tephra, which appears to be more widespread in Taranaki than the younger Waimahia Tephra. The pale glassy ash found within the buried soil is here correlated with the Taupo-sourced Stent tephra, dated by Alloway *et al.*, (1994) at *c.* 3.9 ka. The occurrence of Stent tephra *c.* 160 km upwind from source represents a moderately large (possibly westward-directed) plinian eruption.

The Patea Dunesand is unweathered and may be found overlying Egmont Ash with a distinct contact. Towards Wanganui Egmont Ash thins becoming increasingly diluted with quartzofeldspatic loess and is absent at the type section. At the type

section (Pickwick Road, Wanganui, after Wilde (1979)), Patea Dunesand overlies Rangititau loess (L1) with an indistinct contact.

Figure 3.3 shows the distribution of the Patea Dunesand along the South Taranaki coast. As the Dunesand advanced inland a number of streams flowing to the coast had their drainage impeded or blocked. This led to numerous small lakes and swamps forming adjacent to the advancing dune margin (Figure 3.3). One such swamp formed when the Waikaikai Stream was blocked. Larger water courses such as the Manawapou and Tangahoe Rivers had sufficiently large flows to keep their channels free of sand and hence were not impeded by the advancing dune-sands. Figure 3.3 also shows the dune shadow zones (where the Patea Dunesand is thin or absent) in the lee of larger watercourses and lakes. The dune shadow zones are found along the southeast margins of these water bodies which implies a dominant wind direction from the west and northwest quadrants. As dune-sands advance by way of saltation, the grains of sand are only able to cross the smallest of stream channels.

### **Environment of deposition**

Present day dune advancement in the Wanganui district is to the northeast as a result of southwest winds and is shown by the presence of northeast-trending, steep slip faces of the active transverse dunes (Wilde, 1979). As in the Wanganui district, northeast-trending transverse dunes are present in the study area; these are largest along the inner margin of the dunes. Wind directions from the west and south are generally the strongest and occur in late spring and early summer (Robertson, 1953). The dune shadow zones shown in Figure 3.3 are more evident on the southeastern and eastern sides of watercourses and lakes and have resulted from the more persistent northwest

and west winds rather than the less frequent southerly gales: the largest dunes result from the integrated wind directions.

The presence of buried peaty soils exposed along the course of the Waikaikai Stream shows that drainage was frequently impeded by the advancing dunes. The presence of the rhyolitic ash on the buried soil indicates dune stability and soil formation on the Patea Dunesand *c.* 4 ka. Following deposition of the ash, active dunes then covered the soil. Whether deposition of the Stent tephra led to destabilization of the dunes or not is beyond the scope of this study.

### **Inferred age**

A dune impounded swamp on the Waikaikai Stream at Q21/295682 was cored with the help of Assoc. Prof. V.E. Neall. The core revealed approximately 6m of organic material (including large trees) and carbonaceous mud above andesitic marine sand. Typical accumulation rates for peat are in the order of 1m/ ka, therefore the 6 m of peat cored suggests that the advancing Patea Dunesand first impeded the drainage of the Waikaikai Stream and many of the other streams in this area *c.* 6 ka. It is interpreted that advancement of the Patea Dunesand began *c.* 6 ka in response to the maximum sea level rise of the post-glacial transgression.

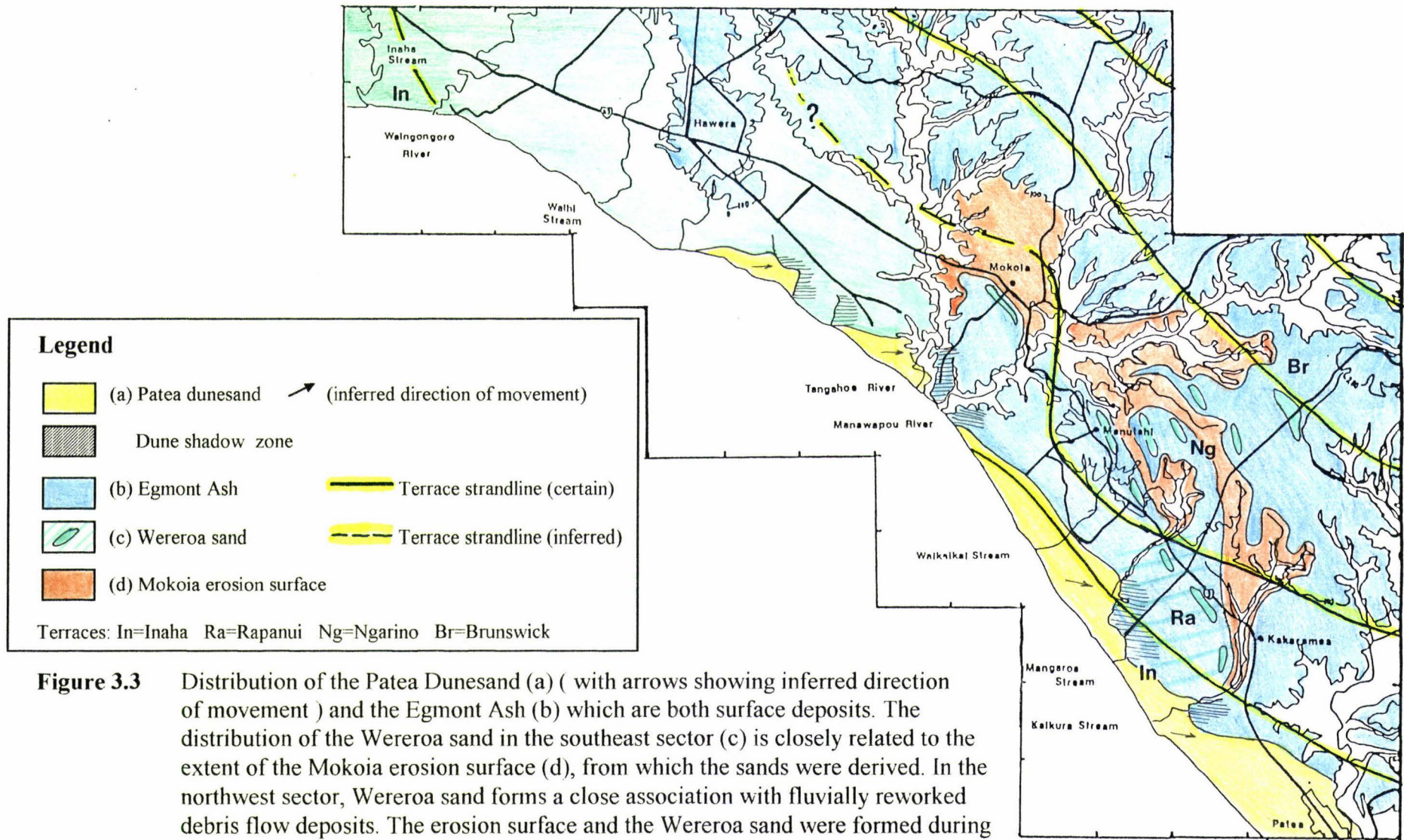


**Figure 3.3** Distribution of the Patea Dunesand (a) ( with arrows showing inferred direction of movement ) and the Egmont Ash (b) which are both surface deposits. The distribution of the Wereroa sand in the southeast sector (c) is closely related to the extent of the Mokoia erosion surface (d), from which the sands were derived. In the northwest sector, Wereroa sand forms a close association with fluviually reworked debris flow deposits. The erosion surface and the Wereroa sand were formed during a period of widespread covered erosion in oxygen isotope stage 2.



**Plate 3.1** Wind erosion of the Patea Dunesand which has infilled the Waikaikai Stream valley at Q21/290680. Note deflation of dunes down to the watertable and the subsequent formation of a small pond.

### 3.2.2 Egmont Ash (Fleming, 1953)

**Type section:** Omahina Road, Waverley, at R21/528626 (after Wilde, 1978)

**Best section:** Manutahi section (#1) at Q21/304693

**Reference sections:** Hawkin's section (#24) at Q21/275733; Sturgeon's section (#27) at Q21/276771; Passing lane, SH3 (#30) at Q21/252757; Mokoia section (#32) at Q21/269752; Subway section (#48) at Q21/220777

#### **Previous references**

Fleming (1953) referred to surficial terrace coverbeds that consisted of andesitic ash containing augite, hornblende and magnetite as the 'Egmont Ash'. The term 'Egmont Ash' referred to all sub-aerial beds except dunesands that were younger than the Brunswick Dunesand. More recently the name 'Yellow-Brown Ash' has been introduced by Wilde (1979) and refers to friable yellow-brown sub-aerial deposits that lie above well structured volcanic loess. The term Egmont Ash is employed here and therefore departs from the terminology used by Wilde (1979).

#### **Nature and distribution**

Inland of the Patea Dunesand complex the present day soil is developed in Egmont Ash and is best observed on the gentle to flat terrace surfaces. The Egmont Ash ranges in thickness from <0.5 m to 1 m. At the best section Egmont Ash is the present soil-forming deposit and is 0.8 m thick. Plate 3.2 shows a typical Egmont Ash profile where a 10-12 cm black A horizon is developed on Egmont Ash. The ash overlies Loess

1 (L1), distinguished by a marked change in structure from friable ash above to a well structured volcanic loess below, separated by a distinct contact. In some cases Egmont Ash unconformably overlies older dunesand and loess units, where erosion of terrace coverbeds occurred during the Ohakean, a factor explained more fully in section 3.3.3. The fine friable allophanic nature of the Egmont Ash and the desirable properties this imparts (porosity, drainage water holding capacity) is ideal for intensive dairying, the main form of landuse in South Taranaki.

The Egmont Ash covers all but the youngest surfaces in the study area. Young surfaces such as Late Holocene river terraces and floodplains are devoid of Egmont Ash (Figure 3.3). To date little work has been carried out on differentiating and correlating separate tephra falls comprising the Egmont Ash southeast of Hawera. It is known that all the major post-glacial tephtras from Egmont Volcano were erupted to the east and southeast, these being preserved in the Eltham and Ngaere swamps, *c.* 20 km north of Hawera (Stewart *et al.*, 1977; McGlone and Neall, 1994). The Egmont Ash contains a number of very fine andesitic tephtras but at present it remains undifferentiated in this area. No macroscopically visible tephtras have been observed within the Egmont Ash southeast of Hawera. Of the andesitic tephtras described by Neall (1972), two units the Oakura Tephra (*c.* 0.5- 7 ka) and the Okato Tephra (*c.* 7-16 ka) were erupted during the period Egmont Ash is thought to have accumulated. Of the Holocene tephtra units mapped by Alloway (1986), distribution patterns (Figure 3.4) suggest that likely contributors to the Egmont Ash profile in the study area are the Mahoe (11 - 11.4 ka) and Konini (10.1 ka) Tephtras, with thin accretions of the Kaponga (5.3 - 10.4 ka), Waipuku (5.2 ka), Korito (3.5 - 4.1 ka) and Inglewood Tephtras (3.6 ka). Wilde (1979) reports that the Egmont Ash, thins towards the southeast and is absent southeast of the

Wanganui River. Figure 3.3 shows the distribution of Egmont Ash is throughout the study area.

On the steeper parts of the landscape, along margins of interfluves, a strong paleosol may be preserved. Here soils have remained at the surface for prolonged periods because they have not been buried by subsequent younger deposits or the latter have been slowly removed. These relict soils have been present on or near the land surface long enough to have acquired characteristics which are the outcome of a former pedological cycle (Ruhe, 1965). On flatter parts of the terrace surface deposition of tephric material gradually removes the underlying units from the active weathering regime. However on some gently undulating areas of the terrace surfaces where cold climate dunesands are present the Egmont Ash is thin. This suggests that the underlying sands continued to accumulate and are coeval with the lower Egmont Ash (Plate 3.7). Once the Egmont Ash began to accumulate there are no further significant erosion breaks or influxes of dune sand.

### **Environment of deposition**

The sand fraction of the Egmont Ash has been analysed by a number of authors (New Zealand Soil Bureau, 1968; Wilde, 1974; Stewart *et al.*, 1977 and Fieldes *et al.*, 1966) who have found that in places it has been contaminated by accretions of windblown minerals such as quartz, acid feldspar, mica, epidote, zircon, tourmaline and garnet (Wilde, 1979). These accretions of wind blown material of non-andesitic origin are microscopic and probably represent local wind deflation during climatic extremes. With increasing distance from Egmont Volcano the relative abundance of wind-blown

detrital minerals increases (Wilde, 1979) and is directly related to the thinning of tephric material from Egmont Volcano.

### **Inferred age**

Stewart *et al.*, (1977) estimate an age of 10-11 ka for the base of the Egmont Ash at a road cutting *c.* 1 km northwest of Mokoia (Q21/269752, section #32) on State Highway 3 (Plate 3.3). At this site the base of the Egmont Ash lies directly upon mixed andesitic tephra (L1) and aeolian and fluviually reworked andesitic sands and gravels. Thin accretions of fine grained tephra to the Egmont Ash profile southeast of Hawera are likely to have ceased *c.* 3.6 ka, after eruption of the Inglewood Tephra. The fine-grained nature of the Egmont Ash and the inability to differentiate separate eruptive deposits in this area makes age determination difficult. However the likely tephra contributions to the Egmont Ash profile in this area based on the distribution of the Toko Tephra Sub-group (Alloway, 1989) (Figure 3.4) and the degree of soil development, suggests Egmont Ash in this area has a likely age range of 11-3 ka. The Egmont Ash profile contains no significant erosion breaks or influxes of sand and it is inferred that after the Last Glacial Maximum *c.* 18 ka the climate ameliorated and covered erosion became much less widespread by 12 ka.

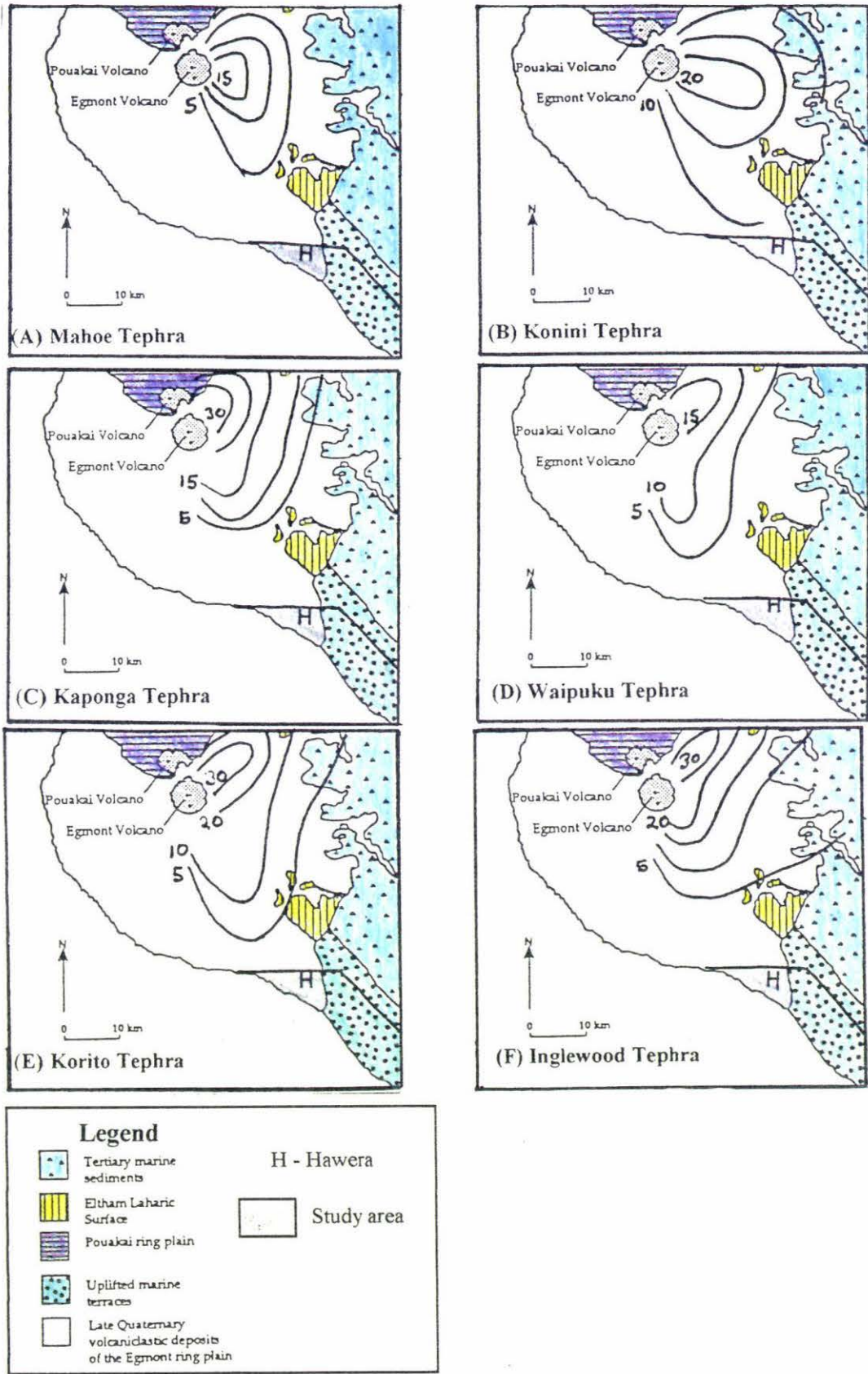


**Figure 3.4** Distribution of Toko Sub-Group Tephra (after Alloway, 1989) showing likely contributions to the Egmont Ash profile in the study area (shaded). These are the Mahoe (A), and Konini (B) Tephra with thin accretions of the Kaponga (C), Waipuku (D), Korito (E) and Inglewood (F) Tephra. Isopachs are in cm.

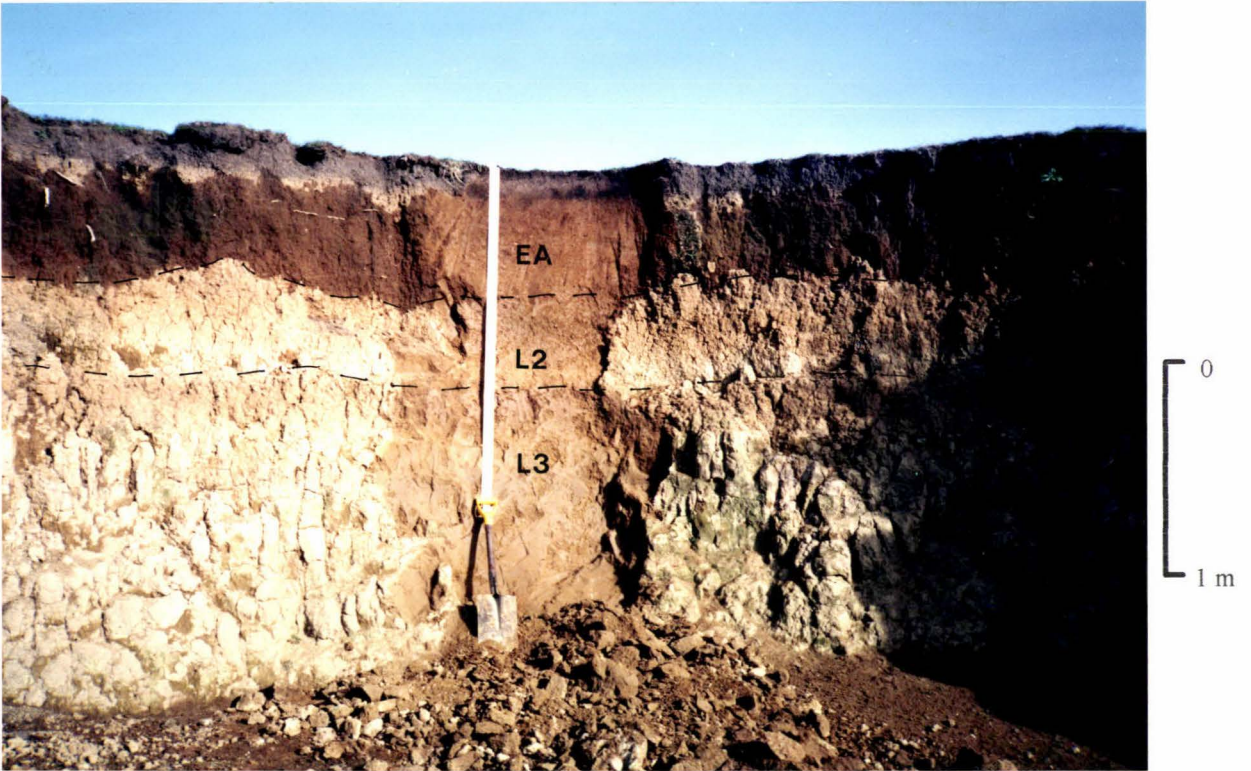


**Plate 3.2** (above) Egmont Ash profile (EA, moist horizon) which overlies partially stripped L2. Tape is 2 m long. Section 21 at Q21/277718.



**Plate 3.3** (left) Egmont Ash overlying L1 and fluvially reworked andesitic sands and gravels. Tape is 2 m long. Section 32 at Q21/269752.

### 3.3 Ohakean substage deposits

Two sedimentary stratigraphic units deposited in the Ohakean Substage are mapped in the study area. The first is Loess 1 (L1), a volcanic loess containing interbedded andesitic tephra, and the rhyolitic chronohorizon the Kawakawa Tephra (Vucetich and Howorth, 1976) erupted from the Taupo Volcanic Centre about 22.5 ka. The second is Wereroa sand (Wilde, 1979) often seen interbedded within L1, representing the deposits from covered erosion during the Last Glacial Maximum.

#### 3.3.1 Loess 1 (L1)

**Type section:** Manutahi section (#1), SH3 at Q21/315693

**Reference sections:** Buhler's section (#13), at Q21/313694; Hawkin's section (#24), at Q21/275734; Mokoia section (#32), at Q21/269752; Passing lane (#30), at Q21/252757; Subway section (#46), at Q21/213779

#### Nature and distribution

##### (a) Southeast sector

L1 is widespread in the study area and underlies friable Egmont Ash, separated in most cases by a weak paleosol (Plate 3.2), identified by moderately to well developed structure, finer texture and firm consistence. At the type section L1 is 0.7m thick, the upper contact with Egmont Ash being at 0.8m depth. Where Wereroa sand is not present (Figure 3.3), L1 consists of brown or yellowish brown silt loam, or silty clay loam that exhibits a fine blocky structure.

The presence of the Kawakawa Tephra in the lower part of L1 aids in identification, but it is macroscopically visible at only a few sites in the southeast sector. These sites are generally where depositional rates are high, resulting in overthickening of the loess (Plate 3.4) or deposition of dunesands (Plate 3.5). The Kawakawa Tephra is often seen in sections as a pale band within L1 and below the Egmont Ash. At these sites mixing by soil organisms resulted in it being mixed into the enclosing volcanic loess.

Localised erosion during the Ohakean substage, adjacent to watercourses (Figure 3.3) removed many older covered units (sections 14, 16, 34, 4 for example), although in some places only partially stripped L2.

#### **(b) Northwest sector**

The thickness of L1 decreases steadily with increasing distance from Egmont Volcano. Near Hawera it is *c.* 1 m thick and decreases to *c.* 0.5 m thickness in the southeast sector, except where it is overthickened by interstratified Wereroa sand. L1 exhibits a weakly developed coarse blocky structure. In comparison to the southeast sector, tephra and lapilli units have larger grain sizes and are thicker.

In the northwest sector the nature of the coverbeds changes significantly. Here large broad and flat river valleys have been infilled with volcanoclastics. Figure 3.5 shows the inferred distribution of these deposits on the southeastern margin of the Egmont ring plain. Sediments here are dominated by fluvially reworked volcanoclastic deposits associated with debris flows and/or debris-avalanches channelled down the broad river floodplains. The stratigraphic columns in Figure 3.6 show the upper coverbeds in this

area, where tephric lignites and fluviually reworked andesitic sands and gravels are widespread.

### 3.3.2 Wereroa sand (Wilde, 1979)

**Type section:** Rangikura Road, 5 km WSW of the Waverley Post Office  
at Q22/453573 (after Wilde, 1979)

**Best section:** Mangaroa Stream (#3) at Q21/ 314685

**Reference sections:** Hawkin's section (#24) at Q21/275733; Buhler's  
section at Q21/313694; Kiwi track (#46) at Q21/227775;  
Subway section (#48) at Q21/220777

#### Nature and distribution

##### (a) Southeast sector

In the southeast sector, Wereroa sand ranges in thickness from <0.4 m to over 2 m. The contact between L1 and Wereroa sand is sharp where the sand is unmixed with L1, however often L1 is thoroughly mixed with the Wereroa sand in this area resulting in an indistinct contact, with the colour of the sands ranging from grey/black to grey/brown depending upon the amount of mixing. At the best section the sand is well mixed with L1 and overlies L2, separated by a distinct contact.

The distribution of Wereroa sand in the southeast sector is patchy but it is generally found inland of the Rapanui strandline (Figure 3.3). It is best preserved on terrace interfluves in close proximity to the Mokoia erosion surface (further discussed in section 3.3.3) from which it is derived. In places the Kawakawa Tephra has been identified within Wereroa sand as a thin (<0.5 cm) fine pale ash.

### **(b) Northwest sector**

Wereroa sand is up to 8 m thick in the northwest sector and in places is reworked fluvially as indicated by fine ripple bedding (Plate 3.6) and thin gravel lenses.

At reference section #48 (Q21/220777) (Figure 3.6) *c.* 400 m southeast of the Hawera subway, the upper 8 m of deposits are interpreted to have been deposited in Ohakean and Holocene time. Here Egmont Ash is *c.* 1 m thick and overlies 7 m of Wereroa sand. In the upper part the sand is orange-brown in colour and 2 m thick which overlies 5 m of grey/black sands. The Kawakawa Tephra (22.5 ka) and 4 andesitic ash beds are found in the upper part of the Wereroa sand. Andesitic tephra within the sand are thicker and better preserved in the northwest sector and thin rapidly to the southeast.

Wereroa sand is widespread in this sector (Figure 3.3). However a lack of exposures inland from the coast, makes it difficult to determine the extent of the sand. To date Wereroa sand has not been observed north of Tawhiti Stream on surfaces here interpreted as the Ngarino Terrace, but is mapped to the west on younger surfaces.

## **Environment of deposition**

### **(a) Southeast sector**

Three distinct phases of L1 are recognised in the southeast sector (Figure 3.7), these being distinguished by the presence and nature of dunesands interbedded within L1. The Wereroa sand is commonly seen thinly interbedded within L1 (Plate 3.7) seaward of the Brunswick Terrace riser. In places the presence of the Kawakawa Tephra (Vucetich and Howorth, 1976) within the Wereroa sand, indicates active covered erosion during the Last Glacial Maximum *c.* 22.5 ka.

L1 and Wereroa sand sometimes rest upon a widespread unconformity separated from older underlying units by a sharp to indistinct contact. The unconformity signifies erosion during the Ohakean within the study area. The intensity of the water and wind erosion varies between locations, often being related to proximity to watercourses or depth to the watertable. In places L1 is thin as a result of minor erosion, in other places L1 and Wereroa sand are missing (Plate 3.2) with Egmont Ash unconformably overlying much older covered units. In the vicinity of Mokoia, fluvial erosion during pre-early Ohakean time has removed all but the marine sediments above the Rapanui and Ngarino WCS's. Here Egmont Ash and thin L1 overlie fluvially reworked andesitic sands and gravels (Plate 3.3).

The Wereroa sand in the southeast sector is interpreted to represent redeposition of locally eroded sediments and/or distal deposits of remobilized dune sands from the exposed continental shelf.

#### **(b) Northwest sector**

Wereroa sand thickens to over 5 m in this sector and contains 4 discrete interbedded andesitic ash and lapilli beds up to 0.1 m thick. These are important markers and useful in this sector for correlation of the Wereroa sand.

West of the Tangahoe River, Wereroa sand is closely associated with fluvial reworking and subsequent aeolian redeposition of volcanoclastic deposits from the broad floodplains of the Egmont ring plain. In close proximity to present watercourses, alluvial reworking of Wereroa sand is indicated by the presence of rare, thin gravel lenses and fine ripple-bedding e.g at Section 46 (Plate 3.6) which is situated close to Tawhiti Stream, a major conduit for floods and/or debris flows in the past 25 ka (Figure

3.5). The Wereroa sand here is interpreted to represent distal resorting of a debris avalanche that originated from Egmont Volcano *c.* 23 ka (Ngaere Formation (Alloway, 1989)) that probably made its way into the upper headwaters of Tawhiti Stream. Here the Wereroa sand abruptly overlies Ratan-aged carbonaceous silts and tephric lignite (sections 30, 45, 46). The sharp lower contact, >5 m thickness and the well preserved tephra in the Wereroa sand, suggest that in this sector it accumulated at a greater rate than in the southeast, due to proximity to a greater supply of andesitic sand.

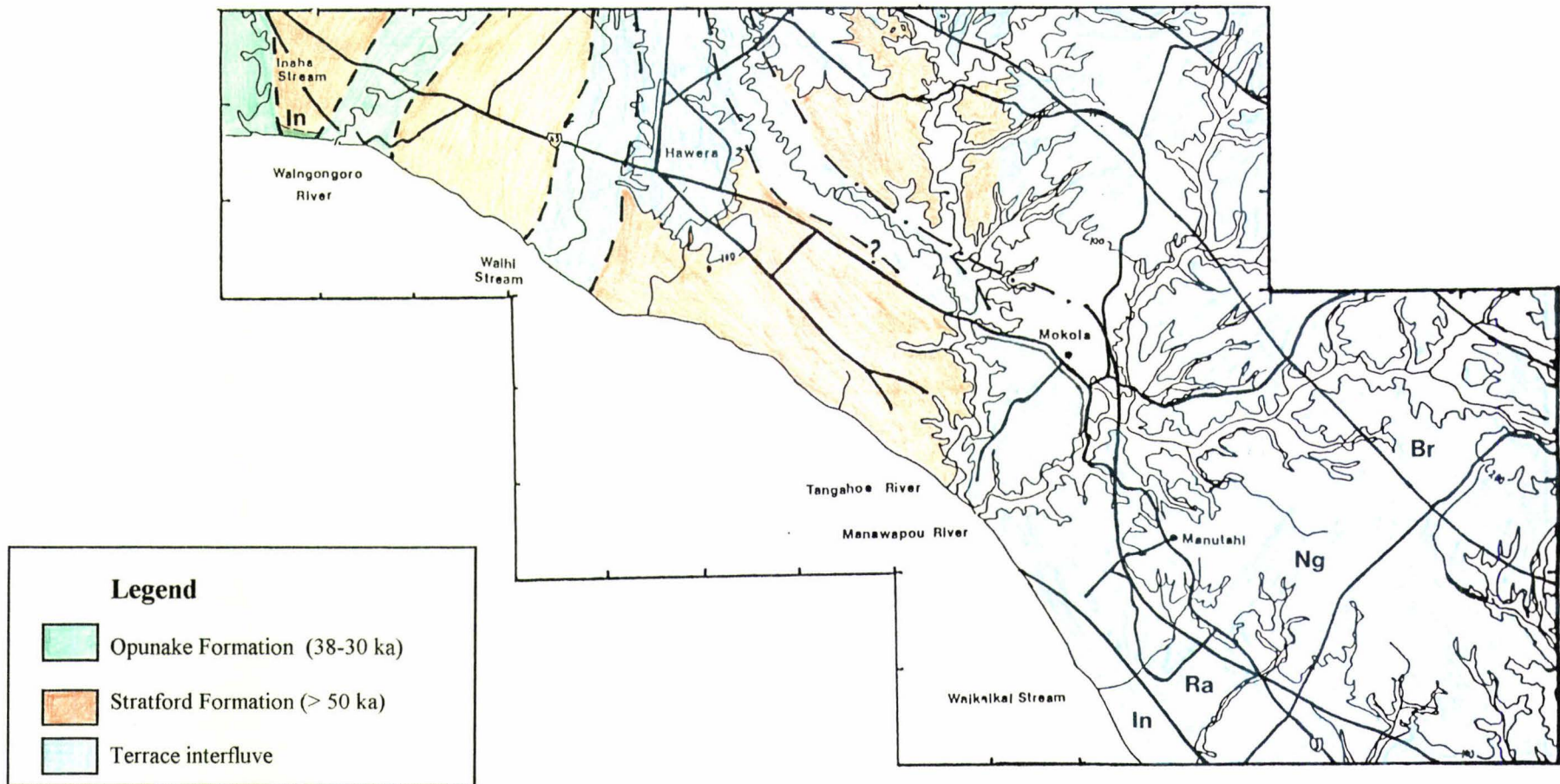


**Figure 3.5** Distribution of the Stratford (> 50 ka) and Opunake Formations (38-30 ka). The map shows inferred paleovalleys cut into the Stratford Formation down which the Opunake Formation was deposited during Ratan time. Within the paleovalleys, channel deposits such as gravelly sands commonly represent the Opunake Formation whereas on floodplains interbedded sands, carbonaceous silts and lignites are more widespread. On terrace interfluvial areas above the floodplain volcanic loess units dominate the stratigraphy.

### Northwest sector correlation diagram: units L1-L3

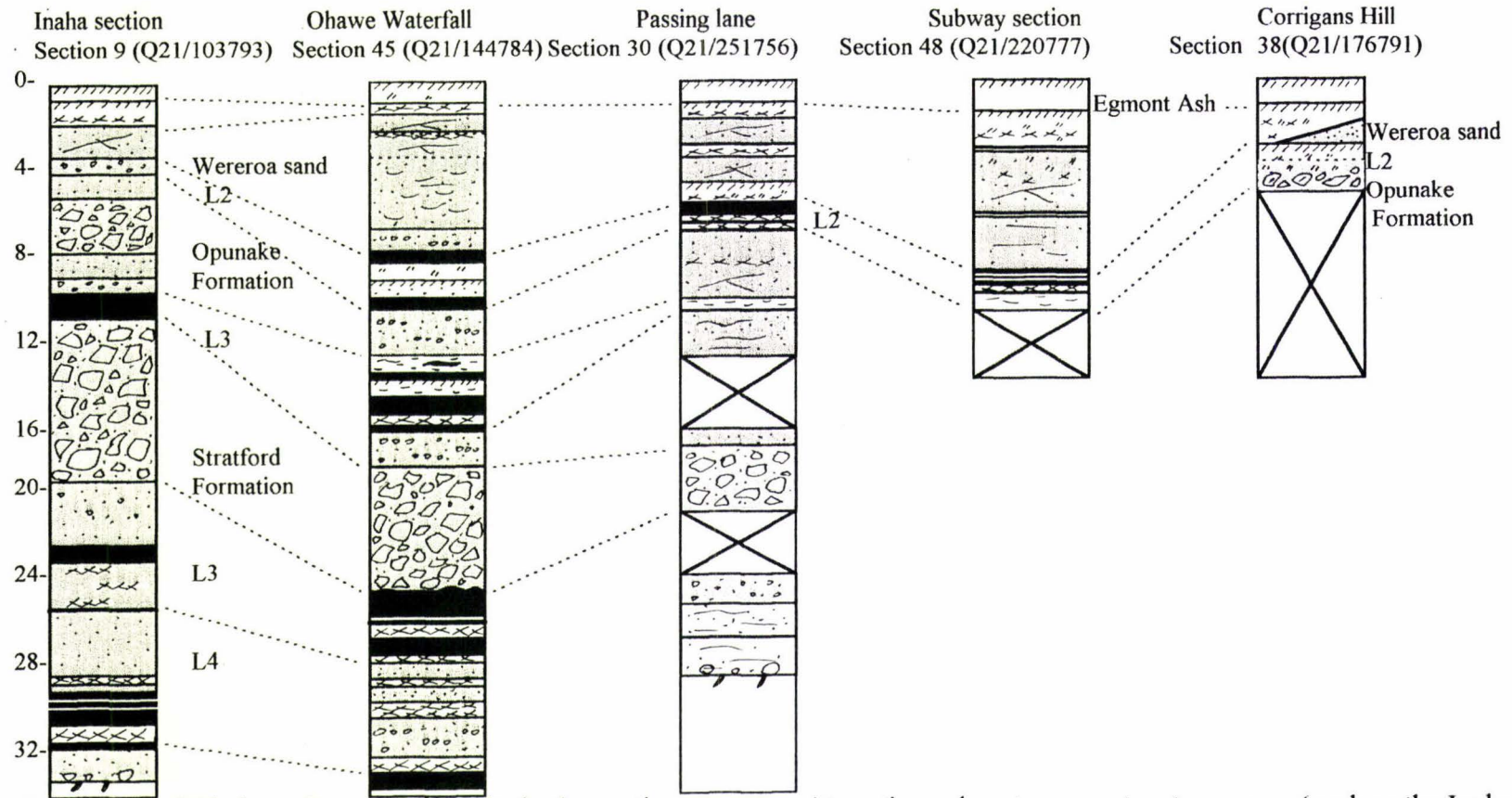


**Figure 3.6** Correlation of Ohakean-Porewan deposits in the northwest sector. At sections close to present watercourses (such as the Inaha and Waihi Streams (sections 9 and 38)) the Opunake Formation has flowed down paleovalleys cut into the older Stratford Formation. Marginal to the paleovalleys the Opunake Formation is represented by fine fluviually reworked pumiceous sands and gravels. Distal deposits are represented by fine grained overbank flood deposits. Inaha section after McGlone *et al.*, 1984; Waterfall section after Bussell 1990.

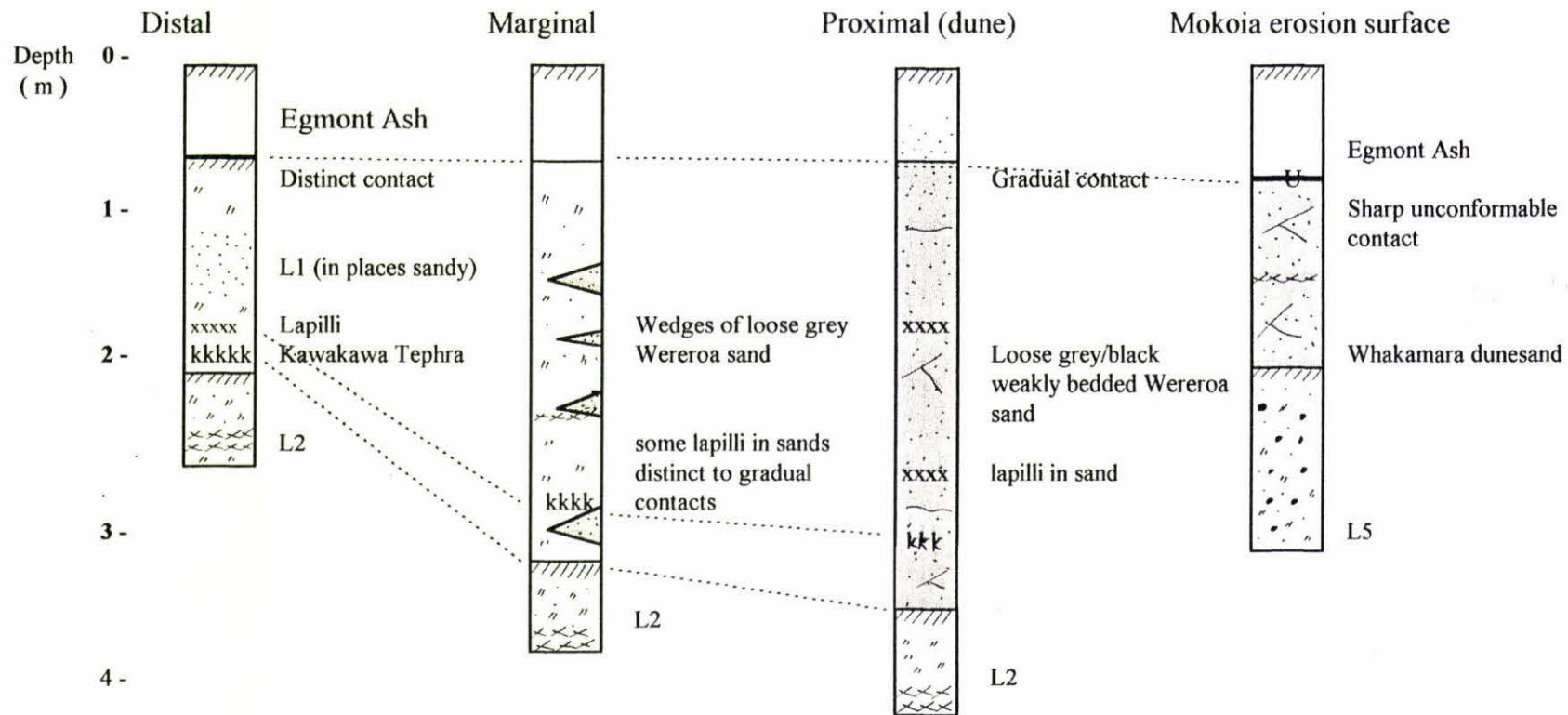


**Figure 3.7** Generalised stratigraphy of L1 and interbedded Wereroa sand in the southeast sector. During the Ohakean, L1 and Wereroa sand were deposited and have resulted in varying amounts of Wereroa sand being mixed with L1 depending upon site proximity to active dunes. In places the lower contact of L1 and/or Wereroa sand is unconformable with L2. However on the Mokoia erosion surface in the southeast sector, L1 and Wereroa sand are missing and Egmont Ash unconformably overlies older covered units.



**Plate 3.4** Overthickened sandy L1 with prominent layer of Kawakawa Tephra (kk). Exposure is close to erosion scarp between Ngarino Terrace remnant and Mokoia erosion surface at end of Lysaght Road (Q21/274774). Note the unconformity (-u-) between L1 and L6 at the base of the spade.



**Plate 3.5** Kawakawa Tephra (kk) within sandy volcanic loess (L1) below Egmont Ash (EA) and above thick Wereroa sand (ws). Section 48, SH3 c. 400 m southeast of the Hawera subway (Q21/220777).

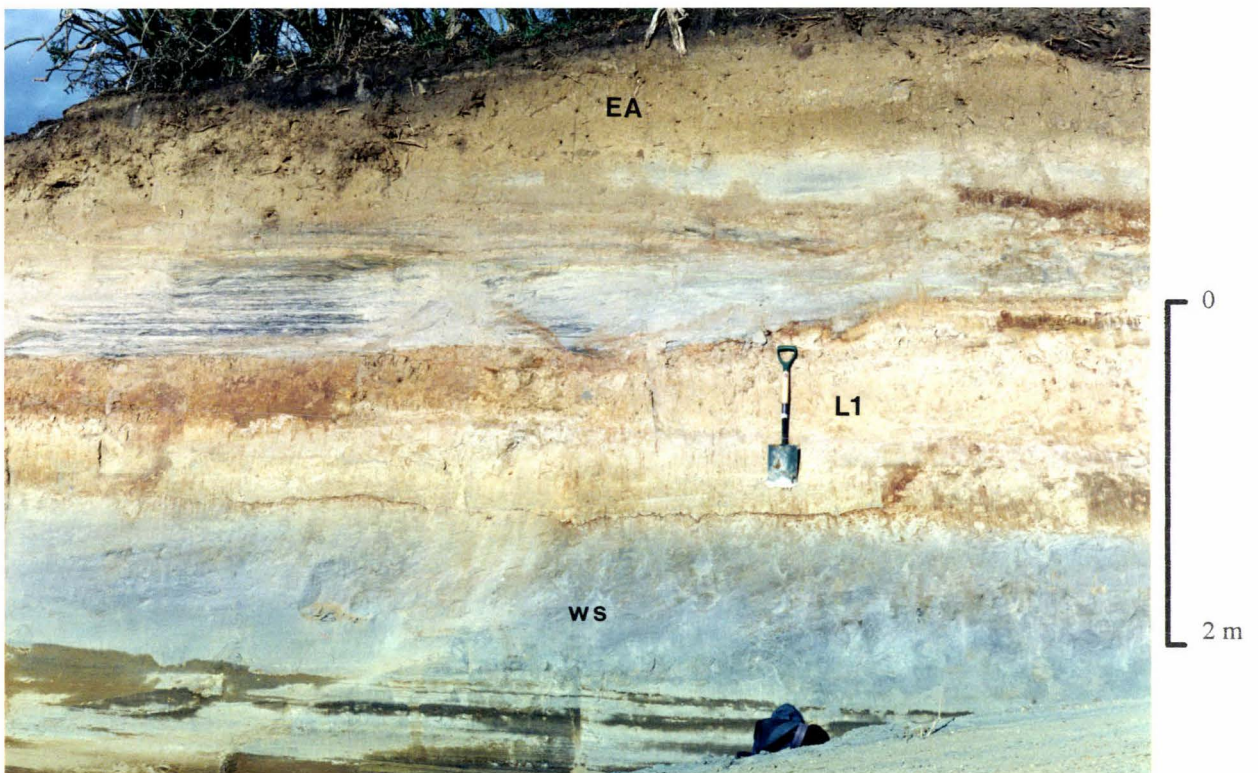


**Plate 3.6** Ripple bedded Wereroa sand below Egmont Ash (EA) in the northwest sector, associated with deposition of a distal debris flow down the Tawhiti Stream (*c.* 600 m to the left of the section) overlying volcanic loess (L1). Below L1 more steeply steeply inclined laminae of Wereroa sand (ws) dip to the north-northeast. Section 46 (Kiwi track) at Q21/227775.

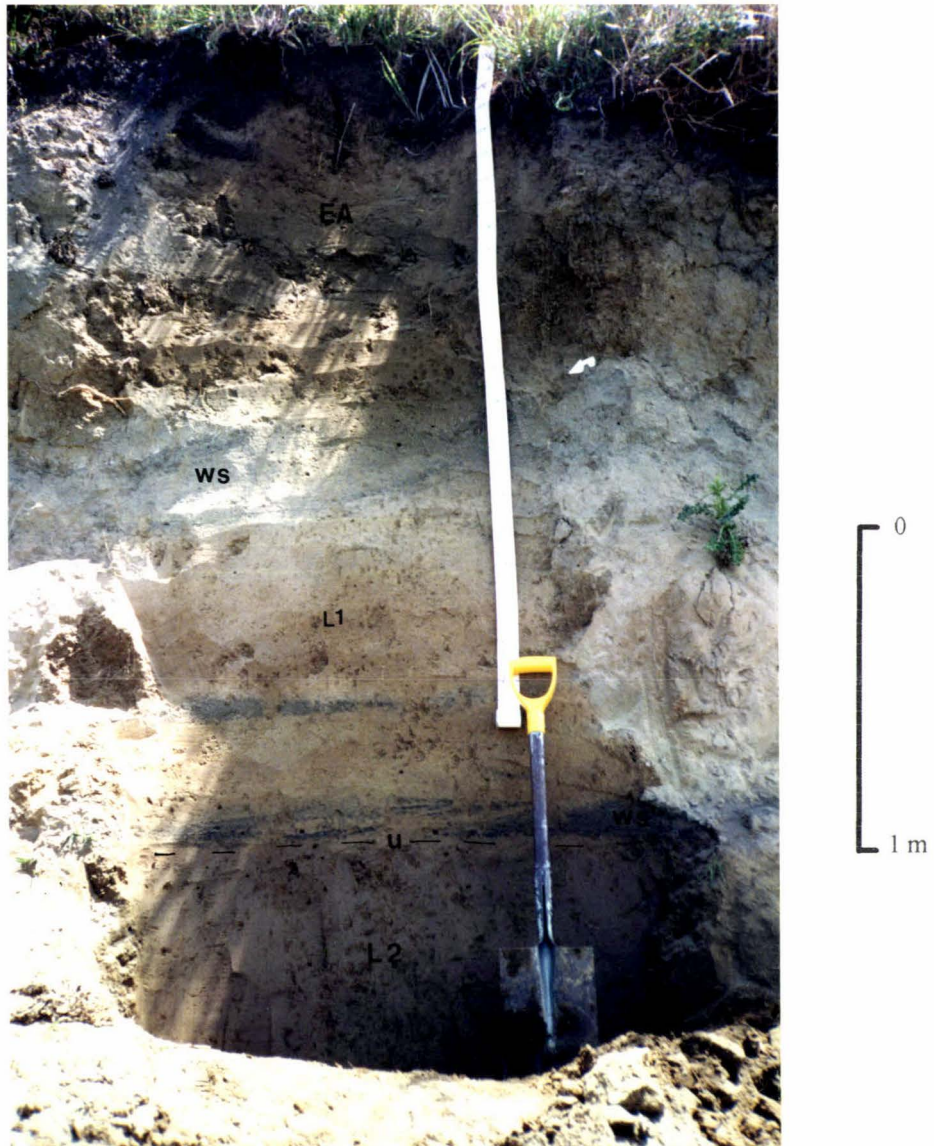


**Plate 3.7**

Wereroa sand (ws) in the southeast sector interbedded within L1 and overlying L2. Egmont Ash thins towards the southeast and here overlies Wereroa sand separated by an indistinct contact (white arrow). A sharp erosional contact (-u-) on L2 indicates covered erosion prior to and during the Ohakean. Section 13 (Bulhers section) at Q21/313694).

### 3.3.3 Landscape erosion during the Ohakean substage

During the Ohakean, sea level was *c.* 120 m below present, resulting in the coastline shifting *c.* 50 km to the southwest. Figure 1.2 shows the 100 m isobath offshore of the study area giving an indication of the paleoshoreline *c.* 20 ka, during which time large areas of continental shelf were exposed to terrestrial processes. In the Ohakean, erosion of coverbeds in the study area was widespread. A coeval erosion surface is extensively preserved in the vicinity of Mokoia *c.* 7 km southeast of Hawera (Figure 3.3). The Mokoia erosion surface is introduced here to refer to this surface. It is most widespread between the Manawapou and Tangahoe Rivers where only a few isolated terrace coverbed remnants are preserved as rounded conical hills. In this area Egmont Ash directly overlies Ohakean age L1 or fluvially reworked andesitic gravelly sands (Plates 3.3, 3.9) which appear to be the reworked uppermost marine sediments on the Rapanui or Ngarino WCS.

The Mokoia erosion surface is characteristically an unconformity which underlies Egmont Ash and/or Wereroa sand. The Wereroa sand is a combination of remobilized coastal sand and the erosional products derived from localised stripping of coverbeds during this period. In the southeast sector Wereroa sand is thickest along the margins of the Mokoia erosion surface indicating proximity to its source area. It is here interpreted to be the result of localised erosion from a landscape devoid of continuous vegetative cover.

Many of the stream valleys aggraded to the changing baselevel during the Ohakean. In addition, to the west of the Tangahoe River, inundation by lahars supplied large quantities of andesitic volcanoclastics, that inundated rivers with high bed loads which were transported to the distant coast. Southeast of the Tangahoe River, the

resulting aggradational surfaces adjoin many of the smaller present streams, such as the upper reaches of the Mangaroa Stream.

Little stream incision has occurred on the Mokoia erosion surface between the Manawapou and Tangahoe Rivers. Here streams are characterised by *c.* 8 m deep narrow steep v-shaped gullies which have cut into the reworked marine gravelly sands. In most cases streams have incised only 2-3m into the mudstone below the WCS. This is possibly due to the youthfulness of the stream incision which presumably began at the end of Ohakean time. In close proximity to these streams, the fluviially reworked andesitic gravelly sands thicken markedly (Plate 3.10).

The stratigraphy on the terrace interfluves between the active areas of erosion is more complete and in places records all the influxes of windblown Wereroa sand and L1 (Plate 3.7). Stratigraphic columns shown in Figure 3.8 clearly show an erosional unconformity below the Egmont Ash, overlying older volcanic loess or dunesand units. Along terrace interfluve margins the Mokoia erosion surface is an angular unconformity and towards stream channels progressively truncates older covered units (Plate 3.8).

In northern and western Taranaki, aeolian sand named the Katikara Formation (Neall, 1972; Alloway, 1986) , accumulated in the interval 23-13 ka (Alloway, 1989). The Katikara Formation is most widespread on the Pouakai ring plain between 200-600 m and is thought to represent a period of intense but localised wind deflation of older andesitic tephra sequences and exposed fluvial deposits (Alloway, 1989).

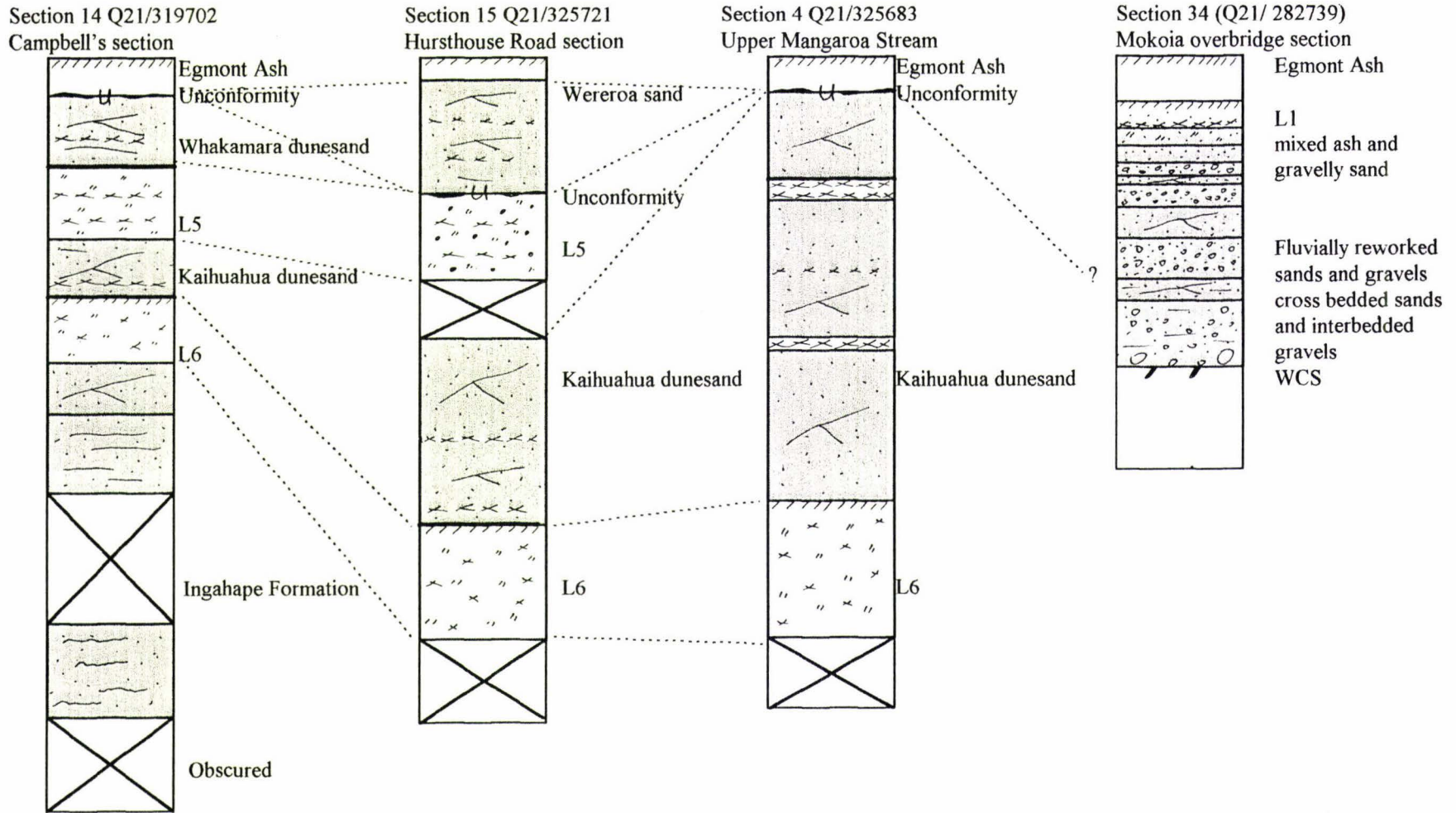


**Figure 3.8** Southeastern sector correlation columns showing erosional unconformity (Mokoia erosion surface) below Egmont Ash and overlying older units. Sand units truncated by the unconformity have provided material that has subsequently been redistributed forming the Wereroa sand.

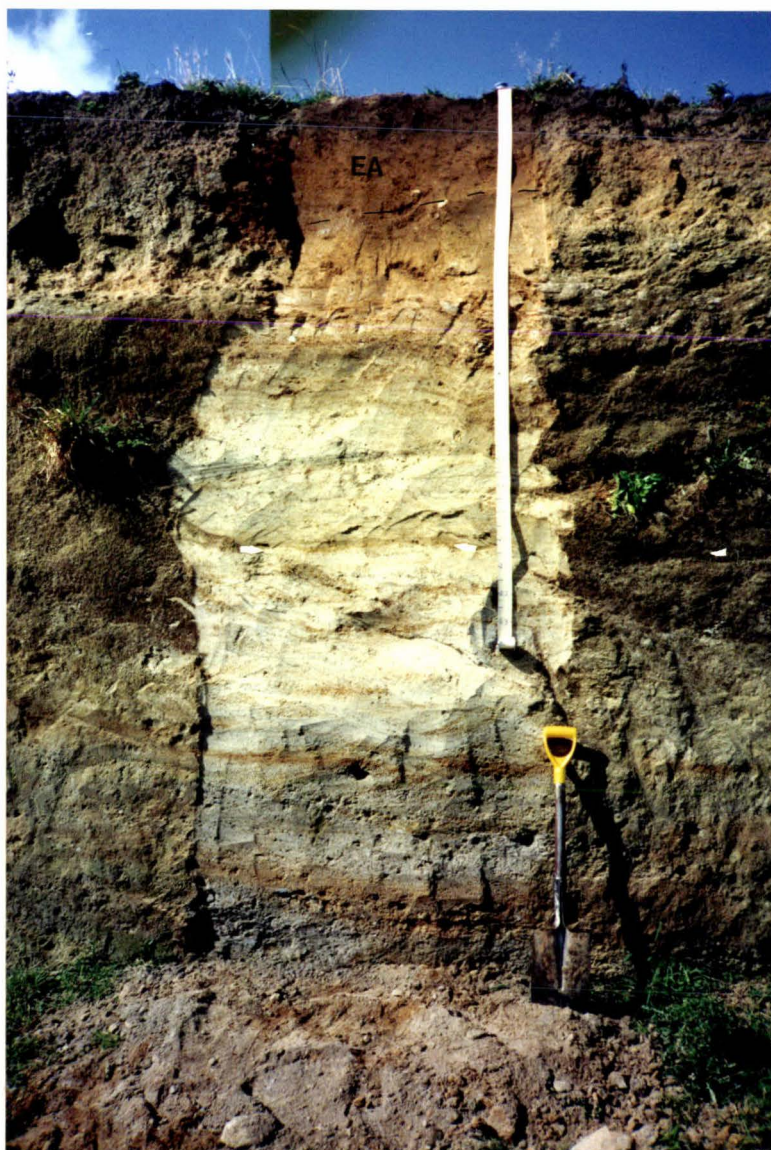


**Plate 3.8** (above) Angular unconformity (-u-) on edge of Ngarino Terrace inter-fluve with L1 overlying L4 and Whakamara dunesand (Wk). Note the Kawakawa Tephra (arrows) above the unconformity. Section 16 at Q21/318718.

**Plate 3.9** (left) Mokoia erosion surface at Q21/273774, showing fluviually reworked andesitic marine sands and gravels capped with Egmont Ash. Ngarino WCS is *c.* 7 m below the base of the section. Tape is 2.3 m long.



**Plate 3.10** Fluvial andesitic sands and gravels on the Mokoia erosion surface *c.* 400 m northwest of Mokoia on SH3 (Q21/274748). To the left of the section fluvial gravelly sands thicken towards a present day stream. Streams on this surface since the end of the Ohakean have entrenched by only 2-3 m into the underlying WCS (cut in Tangahoe Formation mudstone).

### 3.3.4 Interbedded andesitic tephra

#### Introduction

Egmont Volcano lies *c.* 40 km to the north-northwest of Hawera township. It last erupted between 200-250 years ago. Numerous eruptions occurred during the Ohakean Substage (Figure 3.9), with a recurrence interval of 1 every 250 years (Alloway, 1989). Andesitic lapilli sourced from Egmont Volcano are abundant throughout the volcanic loess coverbeds overlying the marine terraces in south Taranaki. Lapilli are also found interbedded in other deposits such as lignite, dunesands and lake sediments.

A large proportion of the lapilli have been preserved within loess at a comparatively constant rate. During periods of increased volcanic loess deposition (glacial or stadial climatic episodes) andesitic minerals are diluted within the volcanic loess. In interglacial/interstadial times volcanic loess deposition rates decreased, leading to concentrations of andesitic minerals in paleosols. The volcanic loess coverbed sequence described in this work contains a number of discrete tephra horizons. Identification of individual tephras relies heavily upon the distinguishing characteristics of the enclosing volcanic loess and dunesand units because many distal andesitic tephras lack unique identifying characteristics.

#### Tuna Tephra Sub-group

Figure 3.9 shows the tephras known to have been erupted between *c.* 13 ka and 28 ka. These comprise the Tuna Sub-group of Alloway (1989) which is subdivided into the Upper and Lower Tuna Sub-groups. Southeast of Hawera many of these tephras are not identifiable as discrete lapilli units within volcanic loess due to post-depositional mixing. They appear as fine lapilli within very fine to fine medial material of tephric

origin. Here only the most prominent tephra beds can be identified and correlated. West of the Tangahoe River many of the older tephra units are best preserved in lignite and carbonaceous fine-grained sediments, commonly found associated with fluvial volcanoclastic sediments. However in this area a lack of exposures in the older covered units means that only tentative correlations can be attempted.

Based on the description and distribution (Figure 3.10) of Alloway (1989), four Tuna Sub-group tephra have been identified within L1 southeast of Hawera. These are the Upper Tuna Sub-group Kaihourī, Paetahi and Poto Tephra and one Lower Tuna Sub-group tephra, the Tuikonga Tephra (Alloway, 1989).

#### **Upper Tuna Tephra Sub-group (post-Kawakawa Tephra)**

The Upper Tuna Tephra Sub-group are comprised of a number of discrete tephra eruptions younger than the Kawakawa Tephra. Of the named tephra shown in Figure 3.9 only a few are preserved macroscopically in the covered sequence southeast of Hawera township. Section 48 at Q21/220777 *c.* 500 m southeast of Hawera on SH3, is the designated reference section for the three Upper Tuna Sub-group tephra identified in the study area and described below (after Alloway, 1989).

#### **Kaihourī Tephra (Alloway, 1989)**

The Kaihourī Tephra comprises a set of at least 8 lapilli beds (Kai.a - Kai.h). Southeast and east of Egmont Volcano the uppermost unit of the Kaihourī Tephra (Kai.h) comprises two distinct layers. The other units of the Kaihourī Tephra are much less widespread and hence less useful for correlative purposes. Kai.h comprises variable proportions of yellowish/red and reddish/yellow pumiceous fine lapilli, with an upper

layer of firm, massive to normally graded, well sorted grey coarse ash. Within the study area the Kaihouri Tephra is rarely seen as a discrete unit, but more often as scattered lapilli (in a fine ash) (Plate 3.11). At some sections lapilli scattered throughout the upper part of Wereroa sand are possible correlatives of Kaihouri Tephra.

Alloway (1989) estimated an age of between 12.9 and 18.5 ka for the Kaihouri Tephra based on assumed constant accumulation rates of medial material between the *c.* 10.1 ka Konini Tephra above and the *c.* 22.5 ka Kawakawa Tephra below.

### **Paetahi Tephra** (Alloway, 1989)

Paetahi Tephra comprises 6 lapilli beds of which the lowermost bed Pae.a is a widespread marker throughout eastern Taranaki (Alloway, 1989). Pae.a near Stratford is *c.* 0.2 m thick and consists of yellowish/red (5YR 4/6) friable moderately-well developed lapilli with a reddish/yellow (2.5YR 6/8) basal pumicious lapilli bed. In the vicinity of Manutahi, Pae.a is *c.* 1 cm thick and found interbedded within L1 and Wereroa sand, distinguishable by its basal lapilli and stratigraphic position above the Kawakawa Tephra. It is usually found in conjunction with Kaihouri, Poto and the Kawakawa Tephra inland of SH3 between Manutahi and Kakaramea. Southeast of Manutahi Pae.a thins and its usefulness in correlation is limited to locations which had favourable conditions for deposition and preservation. Areas with high rates of deposition include a belt of cold climate Wereroa sand active at the time Pae.a was erupted. The age of Paetahi Tephra is estimated to be between 19-19.9 ka (Alloway, 1989).

### **Poto Tephra** (Alloway, 1989)

Close to source Poto Tephra comprises at least 15 units, Pot.a-Pot.e occurring immediately below the Kawakawa Tephra and Pot.f to Pot.o above. Towards the southeast many units thin and become indistinguishable. Figure 3.10 shows that Pot.e, Pot.f and Pot.g are recognisable within the field area. Field identification of Poto Tephra which often occurs in pockets as grey/black sandy lapilli is facilitated by the presence of the underlying Kawakawa Tephra (Plate 3.12). Alloway (1989) estimated the age range of the Poto Tephra to be between *c.* 20.7 and *c.* 23.0 ka, based on accumulation rates of medial material and the age of the Kawakawa Tephra.

### **Lower Tuna Tephra Sub-group** (pre-Kawakawa Tephra)

#### **Tuikonga Tephra** (Alloway, 1989)

The Tuikonga Tephra to the northeast of Egmont Volcano, is represented by a set of four closely spaced coarse ash and lapilli beds informally named in order of decreasing age, Tui.a to Tui.d (Alloway, 1989). Unit Tui.a has a limited distribution and is of limited correlative usage. Tui.b, Tui.c and Tui.d are widely distributed with Tui.b and Tui.d distinctive chronohorizons along the north Taranaki coastline (Alloway, 1989). Tui.d comprises profuse, moderately well sorted, reddish/yellow pumiceous lapilli and a few grey lapilli. Tui.c is characterised by massive to very firm, moderately well to well sorted, grey to dark grey and greyish/brown, coarse ash and lapilli which along the north Taranaki coastline often forms distinctive but discontinuous 'creamcakes' (Plate 3.12). Tui.b is shower-bedded with dark grey to very dark grey, coarse ash and lapilli within layers of profuse, moderately well to well sorted reddish-yellow pumiceous lapilli. Along the North Taranaki coastline it has a similar

appearance to Tui.d. Figure 3.10 shows the distribution of Tui.b and Tui.d, after Alloway (1989). It has since become apparent that Tuikonga Tephra is also particularly widespread towards the southeast and is an important marker bed within L1 in the South Taranaki-Wanganui district (B.V. Alloway, *pers. comm.*). Alloway (1989) assigned an age range of 23.4 to 24.1 ka for the Tuikonga Tephra based on its stratigraphic position below the overlying Kawakawa Tephra.

### **Correlation of the Tuna Sub-group**

Correlation of L1 is facilitated by the presence of the rhyolitic Kawakawa Tephra and andesitic tephra and lapilli units. Alloway (1989) subdivided L1 into 2 sub-units, L1.1 and L1.2, based on variations in texture, structure and firmness. L1.1, the upper unit is distinguished from the the lower L1.2 unit by a weakly developed coarse blocky structure compared to the very firm, massive structure of L1.2. Both units exhibit similar brownish yellow (10YR 6/8) colours. Recognition of these sub-units close to Egmont Volcano is helped by the presence of discrete interbedded tephtras. Unit L1.1 contains Kaihouru, Paetahi and Poto Tephtras of the Upper Tuna Sub-group, with the rhyolitic Kawakawa Tephra present near the base. L1.2 contains tephtras of the Lower Tuna Sub-group, the Tuikonga, Koru, Pukeiti and Waitepuku Tephtras. The latter marks the lower boundary of L1.2 (Alloway, 1989). Towards the southeast the decreasing thickness of L1 and the interbedded tephtras makes sub-division of the volcanic loess unit more difficult.

### **Age range of the Tuna Sub-group**

In Taranaki L1 ceased to accumulate soon after the eruption of the Kaihouru Tephra dated at 12.9 ka (Alloway, 1989). L1 and the interbedded Wereroa sand are both correlated to Onaero volcanic loess of North Taranaki (Alloway, 1988), Rangititau Loess (L1), Manawapou Sand, Wereroa sand (Wilde, 1979) and Ohakea loess (Pillans, 1988) in the Wanganui District. Milne and Smalley (1979) estimated that the Ohakea loess accumulated between 12 and 25 ka during oxygen isotope stage 2 which is accepted here on the basis of the position of the Kawakawa Tephra and the estimated age for the base of the Egmont Ash.

### Ohakean and Holocene Egmont Volcano tephra stratigraphy (after Alloway, 1989)

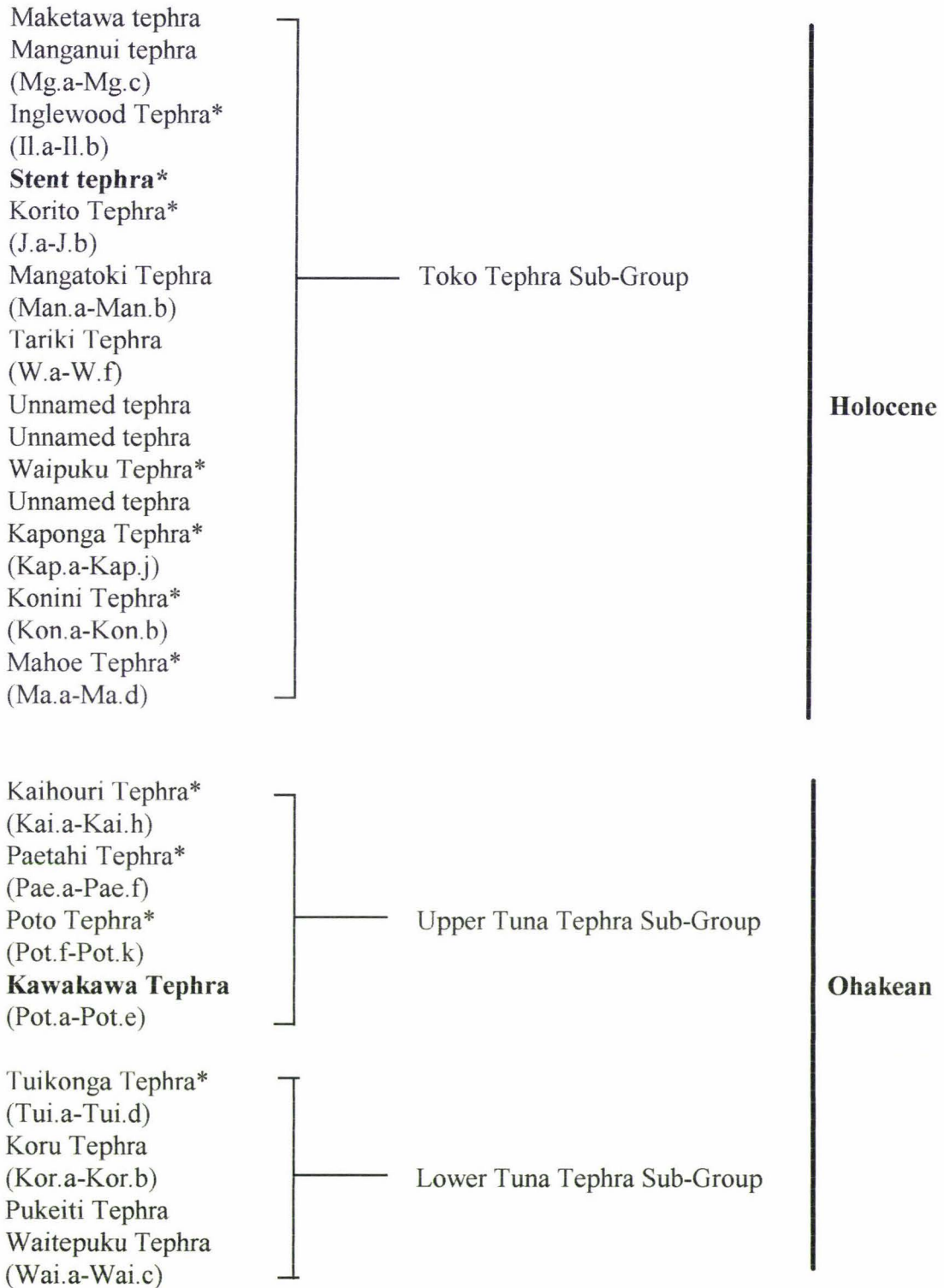


**Figure 3.9** Stratigraphy of the Egmont-sourced Toko and Tuna Sub-Group tephras (after Alloway, 1989). Widespread members of the Toko and Tuna Sub-Groups are identified with an asterisk (\*) and contribute to the Egmont Ash and L1 in the study area. Two rhyolitic tephras sourced from the Taupo Volcanic Centre found in the study area are shown in bold.

### Tuna Sub-Group tephra (Alloway, 1989): distribution and thickness isopachs

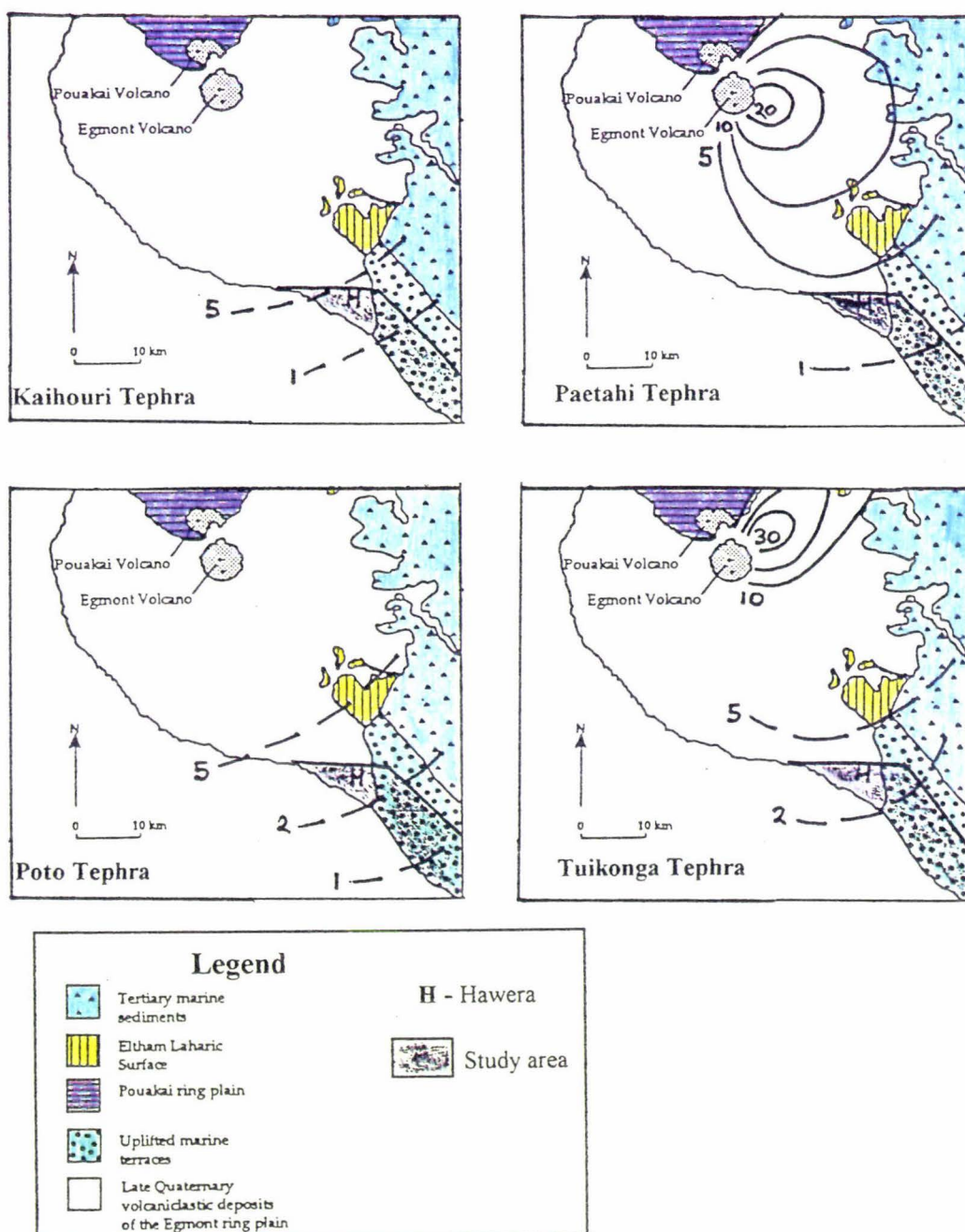


**Figure 3.10** Distribution of Tuna Sub-Group Tephra (after Alloway, 1989) showing tephra thickness in the study area. Upper Tuna Tephra Sub-Group tephra, Kaihouri and Paetahi Tephra occur as scattered lapilli in L1 and Wereroa sand, and rapidly thin southeast of Hawera. Poto Tephra is between 1 and 2 cm thick in the study area and is generally found in 'pockets' overlying the Kawakawa Tephra. The Lower Tuna Sub-Group Tephra, the Tuikonga Tephra, is generally c. 2 cm thick and forms discontinuous grey 'creamcakes' below the Kawakawa Tephra. Isopach thickness is in cm.



**Plate 3.11** Medium to coarse grey and yellow/red lapilli of the Kaihouri Tephra (Kai) overlying medium yellow/red lapilli of the Paetahi Tephra (Pae). Fine grey/brown ash of the Poto Tephra (Pot) immediately overlies pale massive fine ash of the Kawakawa Tephra (KKT) sourced in the Taupo Volcanic Zone. Section 47 (Smillie section) at Q21/217778).



**Plate 3.12** Pocketed grey sandy ash of the Poto Tephra (Pot) immediately above pale Kawakawa Tephra (KKT), here forming small 'creamcakes'. Tuikonga Tephra (Tui) forms small grey 'creamcakes' within strong brown medial material which immediately overlies an unconformity (-u-) formed by hillslope erosion during oxygen isotope stage 2. Section 16 (Ruttens section) at Q21/318718).

### 3.4 Ratan substage deposits

Four lithologic units mapped in the study area are interpreted to have been deposited during the Ratan substage between 32 and 40 ka. In the southeast sector volcanic loess unit L2 and Huxley sand (Wilde, 1979) were deposited. In the northwest sector a tephric lignite and the Opunake Formation debris flow (Grant-Taylor and Kear, 1970) are also present (Figure 3.2).

#### 3.4.1 Loess 2 (L2)

**Type section:** Manutahi section (#1) at Q21/304693

**Reference sections:** Brewer's section (#17) at Q21/310713; Hawkin's pond (#24) at Q21/275733; Mangaroa Stream (#3) at Q21/318678; Sturgeon's section (#27) at Q21/276771; Kiwi track (#46) at Q21/227775; Passing lane (#30) at Q21/ 252757

#### **Nature and distribution**

##### **(a) Southeast sector**

L2 is a relatively thin unit, ranging from <0.6 m to 1 m in thickness. The upper contact at reference section 17 is *c.* 3.2 m below the terrace surface and is overlain by intermixed L1 and Wereroa sand. A moderately well developed paleosol is formed within the upper 0.2 m of L2 (Plate 3.13). L2 overlies a pronounced paleosol on L3 at *c.* 4 m depth. Two pale andesitic tephras are seen within L2. Towards the southeast near Kakaramea, Huxley sand (Wilde, 1979), is interbedded within L2 but where the sand is thin, L2 appears sandy in nature.

L2 is widespread on terrace interfluves in the southeast sector but is absent from the Mokoia erosion surface and on nearby partially stripped surfaces. L2 thins towards the southeast where its thickness is  $<0.8$  m. With increasing distance from Egmont Volcano the two pale andesitic tephra seen towards the north thin and become well mixed into the enclosing fine medial material.

#### **(b) Northwest sector**

On terrace interfluves inland a chocolate brown-coloured volcanic loess (L2) c. 1 m thick is correlated with the Ratan Substage. Here L2 is thickest and overlies L3. On the Egmont ringplain L2 is generally thinner ( $< 1$  m) and overlies a lignite (containing prominent bedded pale andesitic tephra) and grey Huxley sand also of Ratan age.

L2 comprises abundant sandy ash and coarse lapilli within fine brown medial material with many rhizomorphs present. L2 is separated from L1 above by a dark brown moderately developed paleosol. On the ring plain where Wereroa sand is more widespread, a distinct contact separates L2 from the overlying sands.

Towards the margin of paleovalley interfluves, L2 was deposited on the Opunake Formation inferred to be between 23-40 ka (McGlone *et al.*, 1984). At section 38 (Corrigan's Hill at Q21/176791) near the western outskirts of Hawera township, L2 overlies the Opunake Formation which here is characterised by 0.1- 0.3 m angular andesitic cobbles within a fine allophanic matrix.

### 3.4.2 Ratan lignite and Huxley sand

**Type section:** Passing lane (#30) at Q21/ 252757

**Reference sections:** Kiwi track (#46) at Q21/ 227775; Tokora Hill (#39) at Q21/145802; Opie's section (#7) at Q21/344685

#### **Nature and distribution**

##### **(a) Southeast sector**

The Huxley sand has a limited distribution but is present in the vicinity of Kakaramea northwest to the Mangaroa Stream where it is up to 2 m thick. Here it is characterised by grey parallel bedded loose andesitic sand. In places pale andesitic tephra are seen interdigitating with the sands. Inland they thin rapidly and are seen mixed with L2 or are absent.

##### **(b) Northwest sector**

Huxley sand often overlies grey carbonaceous tephric silt (Porewan Substage) separated by a sharp contact. The Huxley sand is light-grey to grey, medium to coarse sand up to 4 m thick that in places exhibits steep dune bedding. Light grey pumicious pebbly sand in a similar stratigraphic position throughout the northwest sector is inferred to represent distal fluvial reworking of the Opunake Formation (Section 3.4.3). Two 1 cm thick pale andesitic lapilli beds occur within the upper section of the sand. In places the lowermost lapilli bed is overlain by a thin (< 1 cm) discontinuous ironpan.

A sharp contact separates Huxley sand from an overlying lignite. The 1-1.5 m thick lignite contains numerous fine to coarse ash and lapilli layers (Plate 3.14). The upper tephra beds comprise grey-white to grey-brown ashes between 1-2 cm thick

spaced at 5-10cm intervals throughout the lignite. Immediately above the base of the lignite, two prominent 2 cm thick yellow to yellowish/red pumiceous lapilli layers with minor grey lapilli are present.

The lignite is separated from the overlying volcanic loess unit L2 by an indistinct to distinct contact. The thickness of the lignite is variable, particularly close to paleovalleys on the ring plain (Figure 3.5 ) where it overlies Huxley sand. Farther inland on the terrace interfluves, Huxley sand and the lignite are missing. Here L2 is generally up to 1 m thick and is separated from unit L3 below by a distinct contact.

In the northwest sector the lignite is thickest where the ring plain was inundated with fine-grained volcaniclastics intermittently (Figure 3.5). The lignite is probably limited to the west of Tawhiti Stream where it varies in thickness from <0.5 to *c.* 1.5 m. Closer to paleochannels the lignite is thinner and is interbedded with light grey pumiceous pebbly sands which represent more frequent volcaniclastic flows down channels. Figure 3.5 shows the inferred distribution of paleovalleys where fluvial and debris flow deposits are thickest.

### 3.4.3 Opunake Formation (Grant-Taylor and Kear, 1970)

**Type section:** Inaha section (#9) at Q21/103793 (after McGlone *et al.*, 1984)

**Reference sections:** Tokora Hill (#39) at Q21/145802; Tokora Quarry (#41) at Q21/139805; Corrigan's Hill (#38) at Q21/176791; Ohawe waterfall (#45) at Q21/144785.

#### **Nature and distribution**

The Opunake Formation is mapped in the west of the study area where debris flows travelled down paleovalleys cut into the older Stratford Formation (Figure 3.5). The main channel facies of the Opunake Formation has been directed down the Waihi and Tawhiti Streams (Figure 3.5). Subsequent fluvial erosion by the present day streams has cut down through the volcanic coverbeds exposing and leaving large (>1 m) andesite boulders on the floodplain. The main channel facies is infrequently exposed due to subsequent fluvial erosion; however at section 38 on the western outskirts of Hawera township it is well exposed. Here it is characterised by 0.1 -0.3 m angular andesitic cobbles within a fine allophanic matrix. The upper part of the formation grades up into L2 which in turn is overlain by Wereroa sand. Away from the main channel areas the Opunake Formation grades into distal sandy debris flow deposits which are generally tabular in nature and often fine upwards. Redistribution of these fine sands has formed dunes (Huxley sand).

### **3.4.4 Environment of deposition**

#### **(a) Southeast sector**

In the southeast sector L2 ranges from <0.5 m to 1 m in thickness. Towards the northwest sector, input of tephra contributes to a thickening of L2. The presence of Huxley sand in places indicates that climate during this period was harsh enough to redistribute and/or erode sand deposits. In the southeast sector deposition of L2 predates Huxley sand and there is little evidence of covered erosion prior to deposition of the Huxley sand or L2, inferring that climate was not as harsh as during the Ohakean Substage. It is inferred that an increased supply of andesitic sands to the southeast sector coastline following deposition of the Opunake Formation, may have led to large quantities of sand advancing inland from the coast.

#### **(b) Northwest sector**

Extensive interbedded lignite with volcanoclastic deposits west of Tawhiti Stream indicate high fluvial sedimentation rates and a constantly changing low-lying landscape. Deposition of the Opunake Formation to the west of Hawera (Figure 3.5) and subsequent fluvial reworking resulted in andesitic sands and gravels being deposited over much of the ring plain to the west and south of Hawera. Southeast of Hawera the Huxley sand represents dunesand that covered parts of the area as wind redistributed fine sands from fluvial deposits. The deposition of the Opunake Formation blocked drainage in many places forming swamps with the subsequent formation of lignite and carbonaceous silt. It is apparent that site proximity to paleochannels has a large influence on the genesis of lignites in this area. Egmont Volcano was clearly active at this time with deposition of andesitic tephra and lapilli within the lignite. Development

of the swamp deposits continued for perhaps 3-6 ka during which up to 2 m of lignite formed. The formation of swamp deposits then ceased, perhaps as a result of water courses entrenching as a result of a change in relative sea level or a blockage removed by stream erosion. This led to deposition of unit L2 upon the now drained or semi-drained lignite. Climate at this time probably warmed slightly and was accompanied by a rise in sea level. Weathering of L2 is evidenced by the presence of rhizomorphs and in the west at the Ohawe waterfall section, iron cemented layers above the lignite and pebbly sands represent a period of weathering and soil formation.

In this sector deposition of lignite between the Huxley sand and L2 indicates that Huxley sand predated the start of L2 deposition in the west. Huxley sand here is directly associated with distal fluvial deposition of the Opunake Formation.

West of the study area Palmer and Neall (1991) recognised three unconformity-bound sequences within the Opunake Formation which show progressive onlap towards the southeast. Within the western part of the study area it is probable that the youngest of the 3 sequences is present. Palmer and Neall (1991) showed that deposition of the Opunake Formation was related to edifice construction during a period of relatively frequent tephra eruptions.

### **Inferred age**

The prominent pale yellow tephra observed within L2 (Plate 3.13) in the southeast and the lignite in the northwest (Plate 3.14) are correlated with the Mangapotoa Tephra dated by Alloway (1989) to be between 28 and 50 ka. This tephra comprises two units, Mp.a (the oldest) and Mp.b. both characterised by yellow to

yellowish red fine to medium pumiceous lapilli with minor grey to light grey fine lapilli (Plates 3.13 and 3.14).

L2, Huxley sand and the lignite are inferred to have been deposited during oxygen isotope stage 3, based on the correlation of the Mangapotoa Tephra. Deposition of L2 is interpreted to have begun *c.* 50 ka as sea level dropped and the climate cooled. Rising sea level late in stage 3 led to channels beginning to entrench, lignite deposition ceasing and pebbly sands and sands being restricted to the main channels. During oxygen isotope stage three (Figure 2.3), three minor sea level rises and falls occurred which resulted in contraction and expansion of the broad floodplains. At the Ohawe waterfall site, which is close to the Waiongongoro River valley, deposition of pebbly sands occurred during low sea level as rivers aggraded, whereas lignite deposition and/or soil formation occurred as sea level rose and river channels became entrenched. L2 ceased to accumulate in early stage two *c.* 32 ka, and was followed by a 2-3 ka period of weathering before sea level dropped and deposition of the Wereroa sand and L1 commenced *c.* 28 ka.

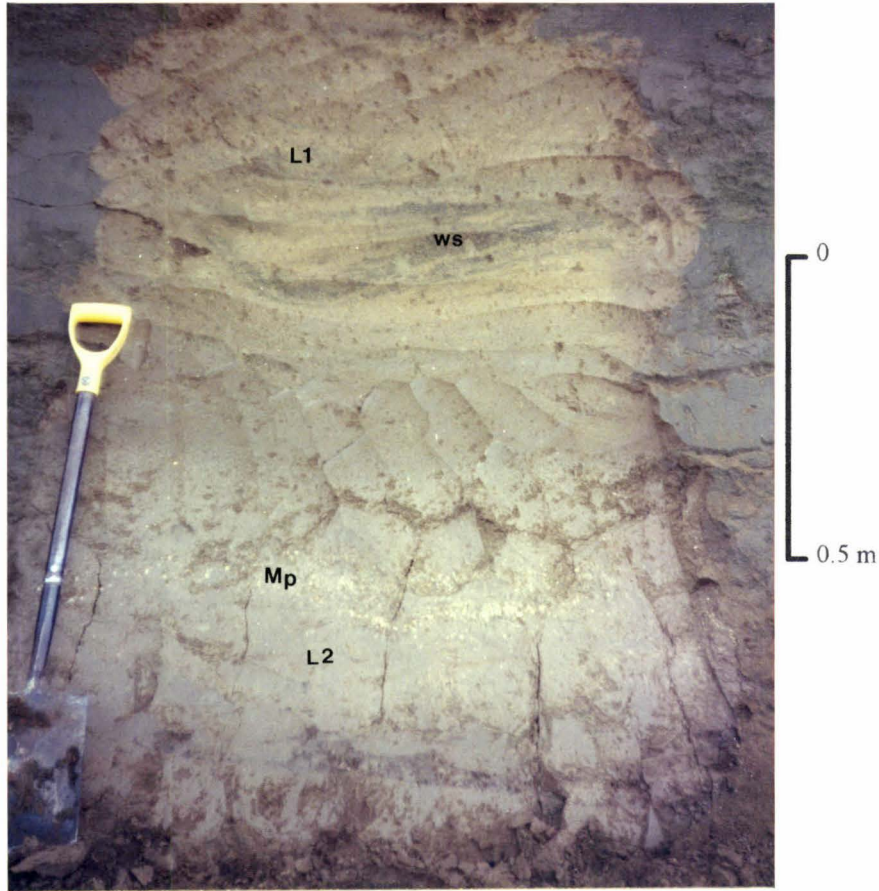


**Plate 3.13** Interbedded Wereroa sand (ws) within L1 and overlying a moderately well developed paleosol (p) on L2 in the southeast sector. Pale coarsed lapilli (Mp) within L2 are correlated with the Mangapotoa Tephra (Alloway, 1989) thought to have been erupted between 28 and 50 ka. Section17 (Runoff section) at Q21/310713.



**Plate 3.14** Mangapotoa Tephra (Mp) within Ratan lignite in the northwest sector. The lignite overlies Huxley sand which is interpreted to represent redistributed andesitic fluvial volcanoclastics associated with the Opunake Formation debris flow deposit.

### 3.5 Porewan substage deposits

In the southeast sector and on terrace interfluves in the northwest sector only one unit (L3) is interpreted to have accumulated during the Porewan substage. In the northwest sector on the Egmont ring plain, this unit is missing and is replaced by interbedded light-grey pumiceous pebbly sands, carbonaceous muds and a 1-2 m thick lignite which has been truncated by a very large debris avalanche. The large debris-avalanche deposit is extensive and important in interpreting and correlating the stratigraphic record in the northwest sector and will be discussed separately in section 3.5.2. Correlation of the coverbeds in the northwest sector is based largely on the interpretation of pollen diagrams (Chapter 4) and debris flow stratigraphy (Section 3.5.2) at two sites along the coastline west of Hawera (Figure 3.1), the Inaha section (after McGlone *et al.*, 1984) and the Ohawe waterfall section (after Bussell, 1988).

#### 3.5.1 Loess 3 (L3)

**Type section:** Manutahi section (#1) at Q21/304693

**Reference sections:** Mangaroa stream section (#3) at Q21/318678; House cutting (#12) at Q21/304685; Upper Taumaha Road cutting (#18) at Q21/308708; Sturgeon's section (#27) at Q21/276771; Ngaumai Park (#43) at Q21/213785

#### **Nature and distribution**

##### **(a) Southeast sector**

L3 is chiefly recognised by its orange/brown colour, the prominent dark chocolate coloured paleosol developed within it (Plate 3.15), and its stratigraphic

position above Last Interglacial deposits the Auburn dunesand and L4 (Figure 3.2). The upper contact is with L2 at the type section at 3.5 m below the terrace surface. The prominent paleosol on L3 is *c.* 0.2 m thick and has a distinctive dark chocolate colour a moderately well developed structure, a greasy feel and abundant rhizomorphs. Below the paleosol, L3 exhibits a moderately well developed structure with rhizomorphs and iron/manganese staining present throughout. Frequent accumulations of fine-grained andesitic ash and abundant fine lapilli give this unit its orange/brown colour and greasy feel. Below L3, is L4 or Auburn dunesand (section 3.6) sometimes marked by a zone of concretions. In comparison to L2 and L4, L3 is relatively thick, varying between 1 and 1.5 m (Plate 3.15).

L3 is found as a volcanic loess on all terrace surfaces southeast of the Tangahoe River and only on the Ngarino and older terraces in the northwest sector. On the terrace surfaces away from the ring plain fluvial system, L3 has been deposited on elevated surfaces which were well drained and did not experience frequent inundation by volcanic flow deposits. Throughout the southeast sector L3 is generally 1-1.5 m in thickness and does not appear to thin noticeably towards the southeast. Ash and lapilli are abundant throughout the medial ash profile, but no discrete identifiable units are present. No sand units have been identified within L3.

#### **(b) Northwest sector**

At the Ohawe waterfall section a 1 m thick blue-grey to medium brown carbonaceous mud represents the base of the Porewan (Figure 3.6). It underlies a black woody tephric lignite *c.* 1.5 m thick. The lignite is unconformably overlain by the extensive Stratford Formation debris-avalanche, which here here is *c.* 10 m thick. Above

the Stratford Formation 1.5 m of light grey pumiceous pebbly sand is overlain by *c.* 1.2 m of light brown interbedded mud and lignaceous horizons. A iron cemented layer *c.* 0.1 m thick at the top of this unit is interpreted to represent the top of the Porewan.

## **Environment of deposition**

### **(a) Southeast sector**

In Porewan time, two contrasting depositional environments existed northwest and southeast of the Tangahoe River. On the terrace surfaces in the southeast sector the abundance of rhizomorphs throughout L3 indicate that soil processes influenced the profile throughout its depositional history. The deposition rate of fine ash and lapilli was low compared to the accumulation rate of volcanic loess. As a result lapilli and fine medial material are well dispersed with no well defined stratigraphic units. This is probably due to the climate during oxygen isotope stage 4 being much cooler and with less forest vegetation volcanic loess accumulation rates were higher. During stage 4, sea level was between 90 and 30 m below present sea level, at these times large areas of the continental shelf were exposed, providing large source areas of fine silt sized material able to be redistributed as volcanic loess.

The absence of cold climate sands implies that climate during this period was not as harsh as during the Last Glacial Maximum and did not result in coverbed erosion and the subsequent redistribution of sand. The well developed dark chocolate paleosol in the upper 0.2 m suggests that the climate subsequently warmed with subsequent increased rates of weathering and accretions of redistributed fine andic material slowed.

**(b) Northwest sector**

During this period 2.5 m of lignite and fine grained sediment accumulated at the Ohawe waterfall section. Watercourses at this time may have entrenched to some degree due to rising sea level which subsequently led to a restriction in the extent of coarse fluvial sediments. Deposition of the lignite persisted for perhaps 10 ka, during which time additions of tephra from Egmont Volcano were frequent. A large scale gravitational collapse of Egmont Volcano led to the mass emplacement of the Stratford Formation debris-avalanche. This event created a new landscape upon which streams became established. The pebbly sands above the formation represent fluvial reworked of the deposit. With time the new streams and rivers established new channels and deposition at the Ohawe waterfall section slowed and led once again to the accumulation of fine grained overbank deposits.



**Plate 3.15** Section through coverbeds of the Rapanui Terrace. This site is on the edge of scarp between the Rapanui Terrace and the Mokoia erosion surface. An erosional unconformity (-u-) on L2 is immediately overlain by Wereroa sand (Ws). A band of pale andesitic tephra within L2 is correlated with the Mangapotoa Tephra (Mp) (Alloway, 1989) aged between 28 and 50 ka. A prominent paleosol (p) is developed on L3, a relatively thick unit in this area.

### 3.5.2 Stratford Formation (Grant-Taylor and Kear, 1970)

#### Introduction

The southeastern part of the Egmont ring plain has been inundated by at least two large lahar and debris-avalanche events over the last 100 ka. Grant-Taylor and Kear (1970) mapped the geology of Waimate West County immediately west of the study area and recognised two lahar formations. The older and larger they named the Stratford Formation, which was believed to be greater than 50 ka. The younger they named the Opunake Formation which was thought to be between 30 and 38 ka. Both formations were believed to represent remnants of ring plains formed during the Last Glaciation. The older Stratford Formation in the west of the study area is deeply buried beneath the Opunake Formation. McGlone *et al.*, (1983) described a coastal cliff section *c.* 200 m west of Inaha Stream (Q21/103793) (Figure 3.11), which exposes the coverbeds of the 100 ka Inaha Terrace. Two laharic intervals were described and correlated with the Stratford and Opunake Formations (Figure 3.6). A lignite above the Stratford Formation gave a radiocarbon age of 33.3 +/- 1.1 ka (A.N.U. 1887) providing a minimum age for the Stratford Formation.

Bussell (1988) described the stratigraphy and interpreted the pollen assemblages of two sites along the coastal cliffs *c.* 3 km to the southeast of the Inaha section. Two sites, the Ohawe waterfall and Ohawe east sections (Figure 3.1), provide the complete stratigraphy overlying a marine terrace in a volcanic ring plain environment. The Ohawe waterfall section contains a prominent debris avalanche deposit which can be mapped laterally for over 3 km to the Inaha section which is interpreted by McGlone *et al.*, (1984) to contain both the Stratford and Opunake Formations.

### **Nature and distribution**

The coastline provides the best sections for determining the stratigraphy of the Stratford Formation and its enclosing coverbeds. The base of the Formation occurs at *c.* 40 m above the high water mark. The basal contact is with lignite and is wavy and erosional in nature, with fallen blocks exposing lignite incorporated rip-up clasts (Plate 3.17).

Two facies of the Stratford Formation are observed in the study area; these are related to paleotopography. The former topography influenced both the flow direction of lahars and debris avalanches, particularly along stream and river valleys, and their ultimate thickness. The facies observed are:

1: A tabular sheet, up to 10 m thick, that consists of a clast-supported base of angular andesitic clasts that range from 0.3 m to 2 m in diameter. The lithology grades up into matrix-supported clasts of smaller size (Plate 3.16). Here the matrix is allophanic and of a sandy silt texture, possibly derived from the incorporation of volcanic ash material into the flow (Palmer *et al.*, 1991).

2: The second facies is restricted to thin veneers of laharic material deposited on valley sides. Here the Stratford Formation has infilled valleys with the central part of the flow subsequently draining away leaving thin remanent deposits on the flows margins. This facies is characterised by a yellow-brown silty sand to mud matrix that supports rounded to angular clasts, ranging in size from small pebbles to cobbles up to 0.3 m diameter (Plate 3.18). Where exposed the lower contact is wavy and erosional. In places the weight of large boulders in the flow may have deformed the underlying soft silts and lignites also leading to the wavy form of the basal

contact. The base of valley fill deposits are always unconformities and can be seen to lie on a number of varying aged stratigraphic units. Examples of this are easily observed in the coastal cliffs (Plate 3.16) but inland along river valleys the base is seldom exposed, but where found lies unconformably upon units such as Quaternary marine sand, and Pliocene mudstone.

The Stratford Formation is stratigraphically distinctive and appears to be either the result of two separate events or two phases of a single event. Plate 3.16 shows one of the best exposures of the two units within the Stratford Formation at the Ohawe waterfall section (Q21/ 445433). At the base, interbedded sands and muds have been eroded and incorporated into the Stratford Formation. The basal unit (S1a) consists of clast-supported angular andesitic cobbles and boulders up to 0.75 m in diameter. This coarse unit ranges in thickness from 1 to 2 m and grades up into an increasingly matrix-rich middle unit (S1b) (Plate 3.16). Clast size here is smaller than that of the basal unit. The middle unit has an average thickness of 6 m and generally makes up the largest proportion of the volume of the Stratford Formation. In places the top of the middle unit has been reworked by fluvial processes (Plate 3.16). This reworked unit ranges in thickness from 0.5 m to 3.5 m.

Above the reworked horizon, unit S2 contains smaller clasts than the units beneath, although a few larger cobbles and boulders are present. The matrix content is less than the units beneath, probably because the surface over which this flow crossed would have been devoid of any significant tephra or swamp deposits. The upper unit is reversely graded with the top 1-2 m having a larger clast size and decreased matrix content.

The Stratford Formation is exposed continuously along the coastal cliffs for over 7 km from west of Ohawe Beach to approximately 1.5 km northwest of the Tangahoe River, where subsequent erosion during oxygen isotope stage 2 removed it. Along the coast the Formation ranges from <3 m to over 10 m in thickness. A minimum volume estimate of 1.3 km<sup>3</sup> is calculated for the Stratford Formation in the area between Egmont volcano and the eastern margin of the deposit within the study area. Its volume suggests that a very large sector collapse of a former Egmont edifice was responsible for such a large deposit. The distance from Egmont Volcano to the distal margin of the Formation near the Tangahoe River mouth, is approximately 45 km where large andesitic boulders up to 2 m in diameter were transported (Plate 3.19). The Formation thickness is dependent upon the former topography. On gently sloping surfaces it maintains a relatively uniform thickness whereas locally it infills depressions to >10 m.

Megaclasts are seen in large exposures within the Formation, (Plate 3.20). After initiation of the original debris avalanche, large blocks must have been transported intact but as the avalanche gained momentum these blocks become shattered yet coherent, supported by the matrix. Some large scale normal grading is apparent in the Stratford Formation (Plate 3.16).

Along the coastal cliffs fallen blocks of the Formation exposed to wave action show distinctive fine parallel laminations (Plate 3.21) which is not visible in cuttings and fresh exposures. It is possible these laminae record the mixture flowing in a laminar fashion (Fisher *et al.*, 1984).

### **Environment of deposition**

Two distinct depositional environments are observed. The first, northwest of the Tangahoe River, is dominated by volcanic deposits of flow and airfall origin. In contrast

the second occurs southeast of the Tangahoe River where the stratigraphy does not include large volumes of volcanoclastics. In fact the Tangahoe River may mark the eastern limit of the large volcanic debris flows and avalanches originating from Egmont Volcano. To the west of the river drainage channels originate on volcano or the ring plain and act as conduits for volcanic flows and avalanches. However the Tangahoe River flows perpendicular to the direction of such flows and avalanches and has impeded their progress further towards the southeast. In only one place found in this study has the Stratford Formation been observed to have crossed the Tangahoe River. A section at Q21/256804 exposed where Ohangai road crosses the Tangahoe River shows the Formation approximately 10-12 m above the wave cut surface of the Ngarino Terrace.

Eruptive episodes are represented in many of the silt and lignite units as thin horizons of sandy andesitic tephra. Such tephra immediately underlie the Stratford Formation at the Ohawe waterfall section, suggesting that the initiation of the avalanche responsible for the emplacement of the Formation was related to increased volcanic activity at Egmont Volcano. The zone of reworking between the middle and upper units of the Stratford Formation (Plate 3.16) appears to be relatively widespread, particularly close to watercourses as streams became established on the new unvegetated surface. On state highway 43, *c.*150 m west of the Tokora quarry (Q21/133808), reworked rounded gravels and sands occur within the Waingongoro River valley. It is here considered that the amount of time represented by the reworked horizon is relatively short ( $< 1$  ka) because no soil or other sediments are seen beneath the upper unit. The reworked unit represents a period of time that possibly separates two phases of the one episode. Subsequent to its deposition paleovalleys were cut into the Stratford Formation

(Figure 3.5). West of Hawera the younger Opunake Formation has flowed down these paleovalleys.

### **Inferred age**

In the southeast sector deposition of L3 began *c.* 75 ka as sea level dropped during the Porewan (Figure 2.3). During this time Egmont Volcano was relatively active, providing a frequent source of fine grained andic material. Deposition of L3 continued for *c.* 15 ka. At *c.* 60 ka the climate warmed with marked soil formation. This relatively short period (*c.* 7-10 ka, Figure 2.3) resulted in the pronounced paleosol on L3. The paleosol ceased forming *c.* 50 ka as the climate deteriorated leading to the beginning of deposition of L2.

In the northwest sector Bussell (1989) radiocarbon dated a sample from a thin lignite 2 m above the top of the Stratford Formation at the Ohawe east section (Q21/144783) (Figure 3.11) (thought to be a correlative to the unit at the Inaha section) and obtained a date of *c.* 35.3 ka (ANU-5211) (Figure 3.11). This age was obtained from the holocellulose fraction of the sample but was believed to be contaminated with young radiocarbon. Analysis of different cellulose fractions led to the confirmation that contamination by younger radiocarbon was giving low ages and in fact the real age was beyond the radiocarbon dating range (Bussell, 1989). If this is the case and the radiocarbon age is in fact greater than 40 ka, the established debris avalanche chronology of Neall (1979), and Grant-Taylor and Kear (1970) is valid.

Bussell (1989) suggests that the age of the lignite above the Stratford Formation is much greater than 50 ka and correlates the lignite to oxygen isotope stage 5e, the Last Interglacial maximum dated at 120 ka, based on the full forest pollen assemblage of the

overlying lignite (discussed further in Chapter four). An age of 120 ka for the lignite implies the WCS below to be older than the Last Interglacial, *i.e.* the terrace is the Ngarino Terrace.

The coverbeds above the Stratford Formation are here correlated with deposits representing the Ohakean, Ratan and Late Porewan substages, suggesting an age of 55-65 ka for the emplacement of the Stratford Formation. Further, if the lignite above the Stratford Formation is correlated with early oxygen isotope stage 3 (Figure 3.13) then an age of *c.* 55-65 ka for the Stratford Formation is further supported. The tephra and lapilli below the Stratford Formation, are here correlated to the Ninia and Epiha Tephra, estimated to be *c.* 100-115 ka and 80-100 ka respectively (Alloway, 1989).

The conclusion reached by Bussell (1988) that the terrace at the Ohawe waterfall site is the Ngarino Terrace has led to a major revision in the terrace mapping in this area. Previously this terrace was mapped as Rapanui terrace by Lensen (1959), Grant-Taylor (1978), Pillans (1981, 1983), and McGlone *et al.* (1984). Bussell's conclusions are solely based on palynology and no stratigraphic evidence is used to support the revision of the terrace identification. In my interpretation, the non-polleniferous marine sediments below zone OH1 at the Ohawe waterfall site represent stage 5e.



**Plate 3.16** (left) Stratford Formation exposed in coastal cliffs at the Ohawe waterfall section (section 45 at Q21/144785). The debris avalanche unconformably overlies tephric silts and lignite (ts), and gravelly sands correlated with oxygen isotope stage 4. Note the coarse basal unit (S1a) and the reworked horizon (rw) between the middle (S1b) and upper (S2) units in the Stratford Formation.

**Plate 3.17** (below) Fallen block of the Stratford Formation southeast of the Ohawe waterfall section showing basal unconformity (-u-) with tephric silts (ts) that contain large pieces of wood (arrow). *In situ* rip-up clasts within the debris avalanche are largely derived from the underlying tephric silts.





**Plate 3.18** Stratford Formation valley-fill facies, with a higher proportion of yellow/brown silty sand-textured matrix derived from the surface over which the debris avalanche travelled.



**Plate 3.19** One of a number of large andesitic boulders (c. 2 m diameter) derived from the Stratford Formation, exposed as slope erosion has removed the finer overlying sand and volcanic loess coverbeds near watercourses. Site is near end of Hicks Road c. 45 km from Egmont Volcano, 2 km north-northwest of the Tangahoe River mouth.



**Plate 3.20** (left) Large megaclast exposed within the Stratford Formation c. 1 km southeast of the Ohawe waterfall section. At initiation of the debris avalanche this large block is interpreted to have been relatively intact, but as the flow gained momentum it became shattered yet coherent as it was supported by the surrounding matrix.

**Plate 3.21** (below) Fine parallel laminations exposed in fallen blocks of the Stratford Formation along the coastal cliffs southeast of the Ohawe waterfall section (Q21/144785). Constant action by waves has removed fine material revealing the wavy but parallel bedding characteristic of laminar flow. Hammer for scale is 0.35 m high.



### 3.6 Oxygen isotope stage five terrestrial deposits

In the southeast sector five covered units are correlated with oxygen isotope stage 5. Volcanic loess units L4 and L5 are interpreted to have been deposited during substages 5b and 5d respectively. During the intervening periods 5a, 5c and 5e, three dunesand units were deposited. In order of increasing age these are the Auburn, Whakamara and Kaihuahua dunesands (Figure 3.2).

In the northwest sector, ringplain accumulation resulted in the deposition of interbedded volcanoclastic sands and gravels, tuffs, lignites and fine-grained silts. Descriptions here are from two coastal sections, the Ohawe waterfall section (section 45 at Q21/144785) and the Inaha section (section 9, Q21/103793) (Figure 3.6). At only a few inland localities are these units exposed and correlation to coeval units in the southeast sector is tentative.

#### 3.6.1 Auburn dunesand

**Type section:** Manutahi (#1) at Q21/304693

**Reference sections:** Mangaroa Stream (#3) at Q21/318678; Ohawe waterfall section (#45) at Q21/144785; Runoff section (#10) at Q21/313717

#### **Nature and distribution**

##### **(a) Southeast sector**

The Auburn dunesand consists of unconsolidated to consolidated grey to dark grey, medium andesitic sands (Plate 3.22). The dunesand ranges from <1 m to *c.* 5 m in thickness and underlies L3, separated by a distinct contact. The contact is often marked by a 0.2 m thick zone of concretions or less commonly, an ironpan. At the type section,

impressions of roots can be seen within and along the upper surface of the sand *c.* 4 m below the terrace surface. Here the dunesand is *c.* 2 m thick. It overlies L4 (section 3.6.2), separated by a distinct or sharp contact. In places yellow/white pumiceous sands are finely interbedded within the Auburn dunesands as thin (< 2 cm) beds or are well mixed in the sands.

In the southeast sector the Auburn dunesand has a patchy distribution. On the Rapanui Terrace the dunesands are more widespread, generally less than 2 m thick and dune forms are relatively uncommon. Inland of the Rapanui strandline, they have ramped up on to the Ngarino Terrace and have advanced inland by up to 4 km (Figure 3.11). Here dune forms are commonly preserved on the terrace interfluves (Plate 3.22).

**(b) Northwest sector**

At the Ohawe waterfall section the following units are considered to be coeval with the Auburn dunesand.

A 0.5 m thick blue-grey carbonaceous mud unit that contains *in situ* fossil reeds marks the base of this time period. The mud unit grades up into a pink-grey silt and grey sand unit *c.* 0.3 m thick, above which is a 1 m thick light-grey pumiceous pebbly sand unit. A thin (*c.* 0.20 m thick) andesitic tuff separates the underlying pebbly sand from a 0.5 m thick tephric lignite unit. The tephric lignite grades up into a medium brown to blue-grey carbonaceous mud *c.* 1.2 m thick, that also contains *in situ* reeds. Above this, a tephric lignite *c.* 1 m thick is unconformably overlain by the Stratford Formation debris-avalanche deposit. The unconformity is marked by a sharp wavy contact.

## **Environment of deposition**

### **(a) Southeast sector**

The Auburn dunesands are rarely seen interbedded with L4 below; usually both are separated by sharp to distinct contacts. It is inferred that the sands accumulated relatively quickly during a period when the climate was mild. There appears to have been little covered erosion at the time. The presence of concretions at the upper contact with L3 suggests that a fluctuating watertable has subsequently influenced the profile. At the type section, root impressions along the upper surface, suggest that vegetation was able to grow on the sands at or soon after the dunes ceased accumulating.

The extent, thickness and form of the Auburn dunesand suggests that the sands accumulated during a period of warm climate and high sea level, similar to the present day Patea Dunesand.

### **(b) Northwest sector**

At the base, fine grained overbank sediments are overlain by coarse fluvially deposited volcanoclastics. These coarse pumiceous deposits are interpreted to represent the distal lithofacies of debris flows and avalanches that originated from an ancestral Egmont Volcano. Tephra within lignite below these deposits (section 3.6.2) suggest that initiation of these events is related to an earlier period of volcanic activity.

Overlying the fluvial deposits, the fine-grained carbonaceous mud represents a period during which the ringplain in this area received little coarse sediment before again being inundated by volcanoclastic sediment.

A relatively prolonged period of ringplain stability then followed, during which a 2.5 m thick tephric lignite was deposited. Tephra within the lignite demonstrate that Egmont Volcano continued to be relatively active at this time and possibly led to the initiation of the debris-avalanche that emplaced the Stratford Formation.

### 3.6.2 Loess 4 (L4)

**Type section:** Manutahi (#1) at Q21/304693

**Reference sections:** Hawkin's pond (#24) at Q21/275733; Sturgeon's section (#27) at Q21/276771; Garsed Road (#5) at Q21/227775; Mangaroa Stream (#3) at Q21/318678; Symes track (#27) at Q21/276771

#### **Previous references**

The first reference to L4 was by Fleming (1953) who referred to it as pale loess-like silts and included it in his Egmont Ash. Wilde (1978) redefined and named L4 and L5 as the Parao loess, described from a section in the coverbeds of the Brunswick Terrace. Towards the southeast of the study area units L4 and L5 merge to become one unit and form a distinctive marker throughout the south Taranaki-Wanganui region.

#### **Nature and distribution**

##### **(a) Southeast sector**

L4 has undergone considerably more weathering than L3. Although thin, often less than 0.5 m, its weathered nature with well a developed paleosol, concretions and/or ironpan indicate relatively strong weathering. Generally Fe/Mn staining, and distinctive

concretions increase in size and abundance with depth but where the overlying Auburn dunesand is thin or absent, L4 is separated from L3 above by a thick (*c.* 0.2 m) ironpan or zone of concretions.

North of the Manawapou River and Tawhiti Stream, L4 is approximately 0.5 m thick. Here it consists of tephric loess and lapilli and is distinguished by its brighter yellow-brown colour compared to the overlying dark chocolate brown-coloured L3. Tephra within L4 and Auburn dunesand are correlated with the Epiha Tephra (Alloway, 1989). The Epiha Tephra comprises at least seven coarse ash and lapilli beds (Epi.a - Epi.g), the most widespread of these being Epi.c, Epi.d and Epi.e. These beds show a broad eastward distribution which combined make them a potentially important marker horizon in the south Taranaki-Wanganui district (Alloway, 1989). The Epiha Tephra is correlated with a closely spaced set of tephra beds in lignite at the Ararata Road section (#40) at Q21/160823, and the Ohawe waterfall section (#45) at Q21/144785.

L4 is present only on the Inaha and older terraces. On the Rapanui and Ngarino Terraces, L4 lies above the Whakamara dunesand (section 3.6.3) but on the Inaha Terrace it lies above marine sand (Inaha Formation). L4 is distinguished from both L3 and L5 (section 3.6.4) by its bright yellow-brown colour, interbedded pale tephra, and sandy texture. This is thought to be due to the tephric nature of L4 and the mixing in of aeolian sand, particularly near the coast where volcanic loess and tephra deposition occurred contemporaneously with the advancing sand (Plate 3.22). Figure 3.11 shows the distribution of L4 in the study area is much greater than the Auburn dunesand.

### **(b) Northwest sector**

At the Ohawe waterfall section a black tephric lignite *c.* 1.2 m thick marks the base of deposits interpreted to be coeval with L4 in the southeast sector. The lignite contains abundant flattened wood, white sandy andesitic tephra beds and fossil rootlets at the base (Bussell, 1990). Above the lignite a 0.8 m thick carbonaceous grey/brown andesitic tuff is sharply overlain by a light grey pumiceous andesitic conglomerate *c.* 2 m thick. Above is a purple/brown carbonaceous tuff and mud unit *c.* 1 m thick cemented by iron along the upper surface where it is in contact with another pumiceous conglomerate. This overlying conglomerate is *c.* 2 m thick and is overlain by a blue/grey mud unit that is interpreted to be coeval with the Auburn dunesand unit found in the southeast sector.

### **Environment of deposition**

#### **(a) Southeast sector**

The weathered nature of L4 and the surface of the Auburn dunesand, indicates strong weathering conditions found during the latter warm periods of the Last Interglacial-oxygen isotope stage 5. L4 is notably thin compared to L3 above and reflects the less severe climate and the reduced amounts of fine-grained volcanic loess added to the profile. During stage 5, Egmont Volcano was active providing frequent additions of ash and lapilli to L4 (Epiha Tephra).

#### **(b) Northwest sector**

The thick lignite that marks the base of this time period shows that a peat-forming environment existed at this site and that additions of tephra were frequent. The

tephra beds within the lignite are correlated with Epiha Tephra. Flattened wood is abundant within this lignite and its presence may be related to volcanic activity and the deposition of significant ash in this area at that time. The deposition rate of tephra was high enough to disrupt the peat-forming environment and resulted in the formation of the carbonaceous andesitic tuff. The site is interpreted to have been a low-lying, poorly drained floodplain close to a watercourse down which volcanic debris-flows travelled. The pumiceous conglomerate above the tuff represents fluvial reworking of pumice-rich tephra or pyroclastic flow deposits. Following deposition of the fluvial deposits the floodplain once again stabilised and resulted in the deposition of fine-grained overbank silt units.

### **Inferred age**

During stage 5a, rising sea level led to a small sand advance, the deposits of which are patchy. These sands, the Auburn dunesands are here assigned an age of *c.* 85-80 ka. In areas where the sands are not present, a paleosol developed in L4, representing stages 5a. L4 is correlated to oxygen isotope stage 5b having been deposited *c.* 95-85 ka. This correlation is based on the maximum age of L3, the presence of the Epiha Tephra and features associated with strong weathering and soil formation. Tephra and lapilli within L4 and the Auburn dunesand are correlated with the younger representatives of the widespread Epiha Tephra, erupted from Egmont Volcano between 80-100 ka. The age of the Tephra is based on its position within L4 and uppermost L5 in North Taranaki (Alloway, 1986).

In the northwest sector polleniferous sediment within coeval units has been interpreted to represent the transition from oxygen isotope stage 5b to 5a and from 5a to early stage 4 (see Chapter four).

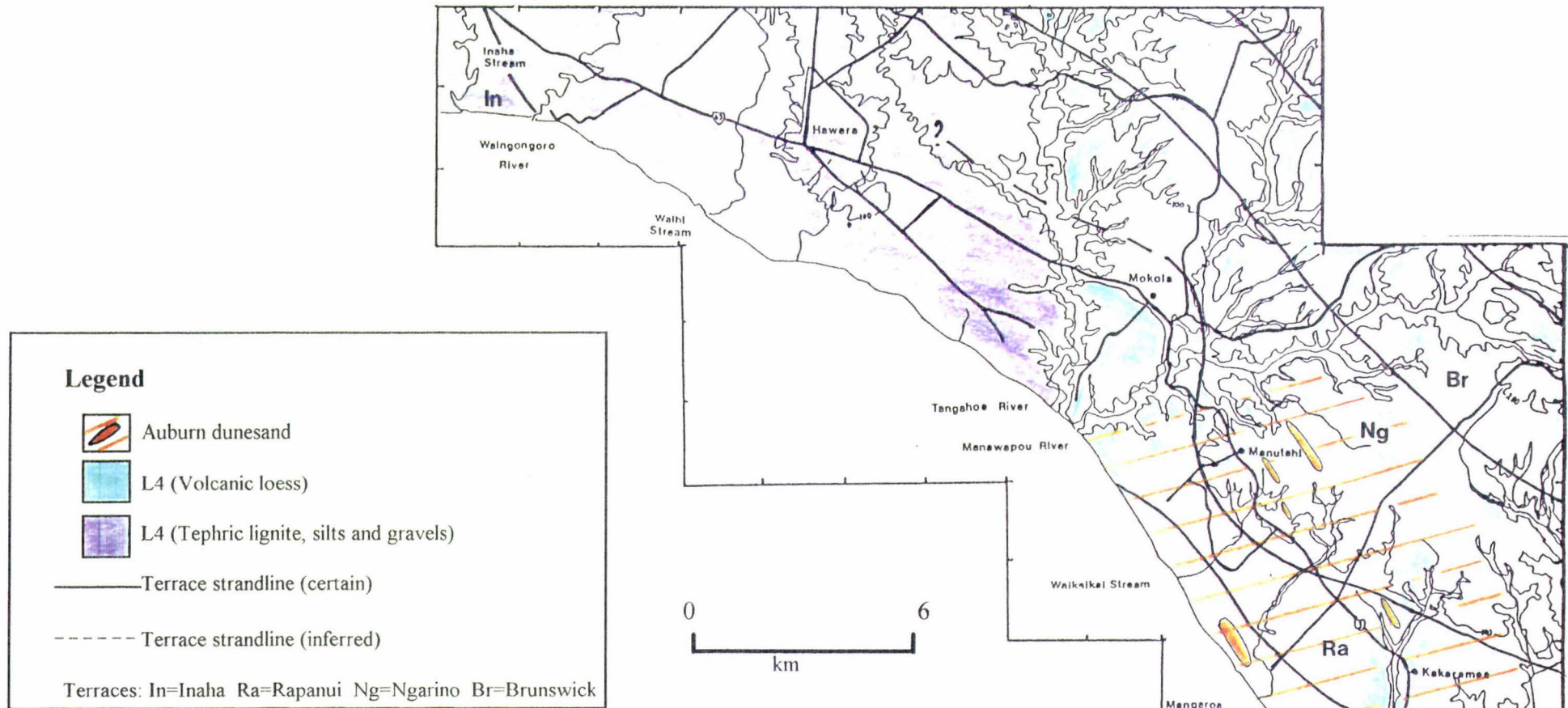


**Figure 3.11** Distribution of the Auburn dunesand (oxygen isotope stage 5a) and L4 (oxygen isotope stage 5b). In the northwest sector the Auburn dunesand and L4 are absent with stage 5a deposits represented by silts, carbonaceous muds and dark grey sands. Stage 5b deposits are represented by tephric lignite, andesitic tuffs and pumiceous pebbly sands. In the southeast sector L4 is represented by a yellow/brown tephric-rich volcanic loess unit. Tephra within L4 and coeval deposits in the northwest sector are correlated with the Epiha Tephra, thought to have been erupted between 80 and 100 ka (Alloway, 1986).



**Plate 3.22** (above) Section through Auburn dunesand which underlies L3 on the Ngarino Terrace at section 10 (Q21/313717). At well drained sites such as here, the boundary between L3 and the Auburn dunesand lacks a zone of iron concretions. The Auburn dunesand is interpreted to have been deposited during a period of high sea level *c.* 80 ka (oxygen isotope stage 5a). Spade for scale is 1 m long.



**Plate 3.23** (left) Thin Auburn dunesand overlying yellow/brown L4 which was deposited during oxygen isotope stage 5b. Here L4 is sandy as volcanic loess and tephra deposition occurred contemporaneously with sand deposition. Within L4, pale andesitic lapilli are correlated with the Epiha Tephra, erupted between 80 and 100 ka (Alloway, 1986). Section 12 at Q21/304685. Spade for scale is 1 m long.

### 3.6.3 Whakamara dunesand

**Type section:** Manutahi section (#1), SH3 at Q21/304693

**Reference sections:** Upper Taumaha Road (#17) at Q21/310713; Mangaroa

Stream (#3) at Q21/318678; Ohawe waterfall section (#45) at

Q21/144785

#### Nature and Distribution

##### (a) Southeast sector

The Whakamara dunesand is widespread in the study area. It overlies L5, the contact usually being distinct to sharp. The dunesand ranges from 1 m to >6 m thick, and consists of grey to brown-grey, consolidated magnetite-rich sand. A feature of this unit is the steep dune bedding and erosional unconformities, best seen where steeply bedded foredune units are unconformably overlain by parallel-bedded sand-plain units (Plate 3.24). Interbedded within the Whakamara dunesand are a number of thin (<2 cm) tephra horizons, indicating active volcanism at the time this unit was deposited. At the Manutahi section (#1) the Whakamara dunesand contains pumiceous andesitic dunesands up to 2 m thick which are enclosed by two thin (<0.1 m) fine silty ash beds. At some sites deposition may have ceased for short periods of time and small accretions of loess, tephra or alluvium interrupted the deposition of sand. Where this occurred, the sands are discoloured brown and have a silty sand to sandy silt texture with thin ironpans at the contacts.

The upper contact of the Whakamara dunesand is weathered to varying degrees due to the thickness of the overlying dunesands and loess units. Where the younger

Auburn dunesand is thin, soil formation has developed within L4 and the upper part of the Whakamara dunesand. Where there is a high water table a dark brown ironpan often separates the Whakamara dunesand from L4 above.

The Whakamara dunesand is thickest on the Ngarino Terrace, south of the Manawapou River, but thins appreciably towards the back of the Terrace (Figure 3.12). It may also be found on older terraces not included in this work. Along with the younger Auburn dunesands, the Whakamara dunesand is responsible for the large dune forms found along the outer margin of the Ngarino Terrace close to the Rapanui strandline (Plates 3.22 and 3.25). It seems that the riser separating these two terraces is relatively low (less than 6 m, see chapter 5) in the vicinity of Manutahi, and can be explained by the dunes sands being able to ramp up and onto the Ngarino Terrace.

#### **(b) Northwest sector**

At the Ohawe waterfall section the base of this time period is marked by a medium grey cross-bedded pebbly conglomerate with a coarse sandy matrix. This unit is *c.* 1.5 m thick and andesitic pumice clasts are common. Above is an 0.2 m-thick purple brown andesitic tuff which becomes increasingly carbonaceous upwards. Overlying the tuff is a 1 m-thick dark grey fine-grained laminated sand unit. The top of this zone is marked by a 0.2 m-thick grey brown tuff and a 1 m-thick tephric lignite which contains abundant white sandy tephra layers and is correlated with unit L4.

## **Environment of deposition**

### **(a) Southeast sector**

Brown colours and the presence of concretions and iron pans are evidence of a high watertable following deposition of the Whakamara dunesand. Thin iron pans form either under a high ground water or a perched water table where marked textural changes occur, in this case resulting from either loess and/or thin tephra deposition. Egmont Volcano continued to be active at the time the Whakamara dunesand accumulated. In one instance pumiceous tephra have been reworked and incorporated into the dunesand as a discrete marker bed. Where the reworked yellow/white tephra is thick, dunes formed adjacent to watercourses.

The Whakamara dunesand is inferred to have accumulated quickly during a period of warm climate and high sea level, similar to the present day Patea Dunesand. It is contemporaneous with the cutting of the Inaha Terrace during stage 5c.

### **(b) Northwest sector**

Deposition at the Ohawe waterfall site at this time was largely related to continuing volcanic activity at Egmont Volcano. The activity resulted in deposition of pebbly sands (and pumice clasts) most probably from debris-flows and their subsequent reworking. During periods of slow sedimentation on the ring plain, fine-grained mud units and lignites formed. Thin tuff units and lapilli layers within the lignite show that eruptions from Egmont were frequent.

### 3.6.4 Loess 5 (L5)

**Type section:** Manutahi (#1) at Q21/304693

**Reference sections:** Hursthouse Road (#15) at Q21/325721, Manutahi Marae (#16) at Q21/318718; Campbells section (#14) at Q21/319702; Sturgeon's section (#27) at Q21/276771; Ohawe waterfall (#45) at Q21/144785

#### Previous references

The first reference to L5 was by Fleming (1953) who referred to it as pale loess-like silts and included it in his Egmont Ash. Here L5 is interpreted to be part of the Paroa loess described by Wilde (1979).

#### Nature and distribution

##### (a) Southeast sector

L5 is an extensive volcanic loess with an average thickness of 1 m showing bright yellow/brown to orange colours and abundant fine ash and lapilli. Particularly noticeable is the silty clay texture imparting a smooth feel to this unit. In the southeast sector, L5 is fine grained and exhibits fine bedding (Plate 3.26). It is separated from L4 above by an 0.2 m thick paleosol, which exhibits grey/brown colours and rhizomorphs (Plate 3.27). At the type section the upper contact with the overlying Whakamara dunesand is sharp and *c.* 12 m below the terrace surface. L5 commonly directly overlies the Kaihuahua dunesand (Plates 3.24, 3.29 and 3.30) and in other places a tephric lignite (Plate 3.28) (Section 3.6.5). At sites subjected to water table fluctuations, L5 shows

small, well formed, round concretions throughout, and has a silty clay texture (Plate 3.27). In contrast at sites with better drainage, L5 contains no concretions and has a silt loam texture (Plate 3.26).

L5 is found on the Rapanui and older terraces (Figure 3.12). It thins towards the southeast like many of the younger volcanic loess units. At section #27 (Q21/276771), it is *c.* 1.2 m thick while southeast towards Kakaramea L5 is *c.* 0.8 m thick.

In the vicinity of Manutahi and Kakaramea, L5 is enclosed by thick Last Interglacial Whakamara and Kaihuahua dunesands (Plate 3.28). West of the Manawapou River towards the back of the Ngarino Terrace e.g. at section #27 (Q21/276771), the dunesands are absent. Their absence has affected the morphology and texture of L5 because it has been influenced by weathering processes for longer resulting in a more pronounced paleosol and well developed structure.

#### **(b) Northwest sector**

At the Ohawe waterfall section L5 is absent. Instead *c.* 7 m of thin interbedded sands and laminated mud units are preserved. They overlie andesitic sands and gravel units of marine origin. The non-marine sand units generally range from grey and well laminated to orange brown muddy sand. Fine mud units are light grey to pink and some exhibit fine laminations with thin iron pans often forming above them. Thin lignaceous laminae, some of which contain *in situ* fossil reeds are also present. At the top of this zone medium grey mafic and pumiceous pebbly sands underlie a purple brown carbonaceous tuff.

## **Environment of deposition**

### **(a) Southeast sector**

Differences in the morphology of L5 are probably due to drainage conditions affecting the site both during and after deposition. In the southeast near Manutahi and Kakaramea, L5 is gleyed, contains concretions and its association with silts and lignites suggest that deposition occurred in poorly drained sites. The advancing (Last Interglacial) dunesands at times blocked the drainage and caused the watertable to rise locally for intermittent periods of time.

### **(b) Northwest sector**

The thin interbedded sand and mud units are interpreted to have been deposited on a low coastal plain that was actively aggrading during a period of relatively low sea-level. Throughout much of this period conditions did not stabilise enough to lead to the deposition of subaerial volcanic loess deposits. At the top of the zone however a purple brown carbonaceous tuff was deposited and is interpreted to represent the Ninia Tephra (Alloway, 1989).

## **Inferred age**

The Ninia Tephra is assigned an age of between 100 and 115 ka (Alloway, 1989). Based on the presence of the Ninia Tephra within the lower Whakamara dunesand, the dunesand is here correlated with oxygen isotope stage 5c, dated at *c.*100 ka. Between 105-100 ka the Inaha Terrace was being cut, and its strandline is less than 5

km from the farthest inland extent of the Whakamara dunesand (Figure 3.12). The Whakamara dunesand ceased accumulating during the transition from stage 5c to 5b.

L5 is correlated with oxygen isotope stage 5d and therefore immediately post-dates the cutting of the Rapanui Terrace (Figure 3.19). During this period (115-105 ka) Egmont Volcano was active and lapilli within L5 and coeval deposits in the northwest sector are here correlated with the Ninia Tephra. Deposition of L5 continued until *c.* 105 ka when the climate began to warm and sea level rose.

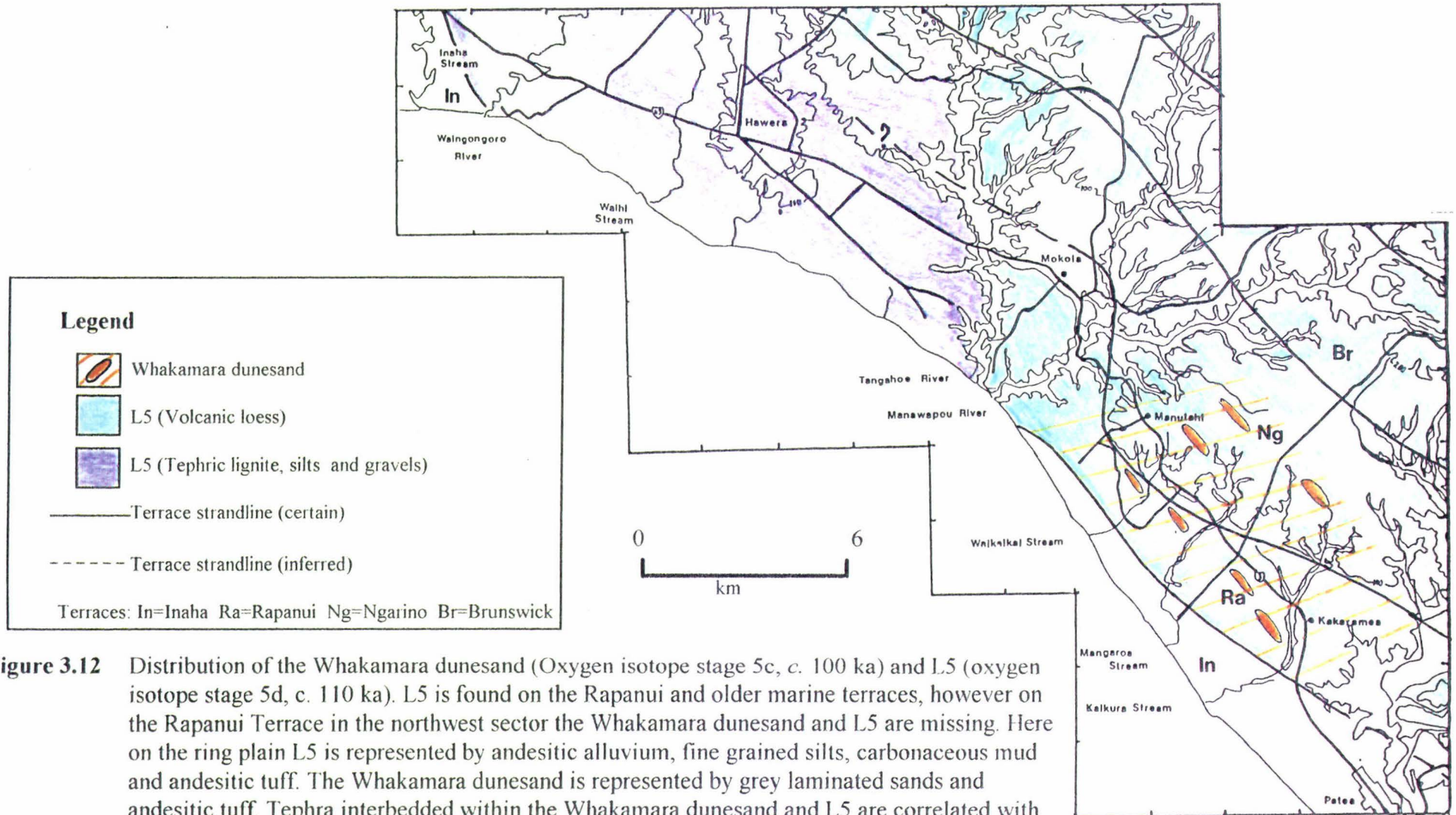


**Figure 3.12** Distribution of the Whakamara dunesand (Oxygen isotope stage 5c, c. 100 ka) and L5 (oxygen isotope stage 5d, c. 110 ka). L5 is found on the Rapanui and older marine terraces, however on the Rapanui Terrace in the northwest sector the Whakamara dunesand and L5 are missing. Here on the ring plain L5 is represented by andesitic alluvium, fine grained silts, carbonaceous mud and andesitic tuff. The Whakamara dunesand is represented by grey laminated sands and andesitic tuff. Tephra interbedded within the Whakamara dunesand and L5 are correlated with the Ninia Tephra, thought to have been erupted from Egmont Volcano between 100 and 115 ka (Alloway, 1986).



**Plate 3.24** Steeply dipping cross-bedded foresets of the 100 ka Whakamara dunesand (Wk) overlying L5. Thin pale brown tephra within the flat lying parallel-bedded sand-plain units are correlated with the younger representatives of the Ninia Tephra (c. 100 - 115 ka, Alloway, 1986). At this site Egmont Ash (EA) unconformably overlies Whakamara dunesand. Section 18 (Upper Taumaha Road) at Q21/308708.



**Plate 3.25** Whakamara dunes (oxygen isotope stage 5c) near the outer margin of the Ngarino Terrace. The size of the dunes is enhanced because of widespread covered erosion during oxygen isotope stage 2 forming the Mokoia erosion surface (ms). The photo looks south from Q21/325721 towards section 13 (Bulhers section) on dune in centre of photo.

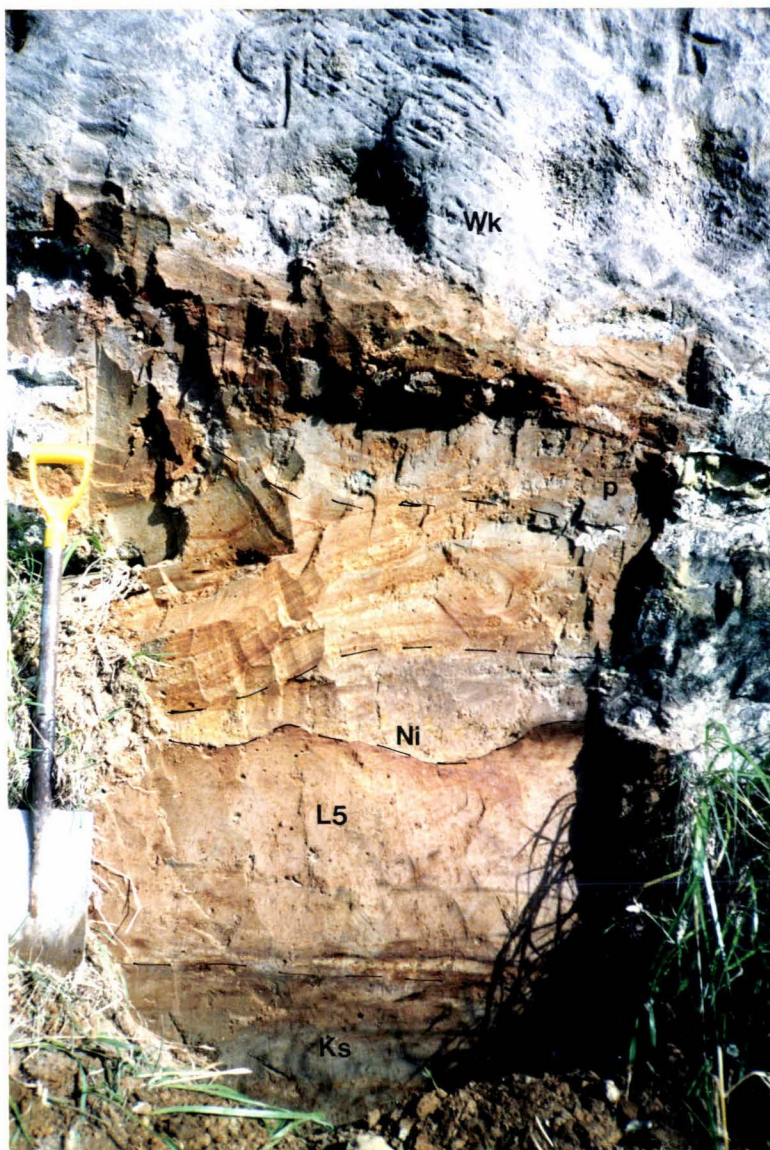


**Plate 3.26** (left) L5 below the Whakamara dunesand (Wk) separated by a grey/brown paleosol (p). At the base of the spade an indistinct contact separates L5 from the Kaihuahua dunesand (Ks) beneath, the upper part of which is stained brown due to mixing of tephra and sand. The purple/brown tephra within L5 is correlated with the Ninia Tephra (Alloway, 1986) thought to be between 100 and 115 ka. Section 18 (Upper Taumaha Road) at Q21/308708. Spade for scale is 1 m long.

**Plate 3.27** (below) L5 showing bright yellow/brown colours, concretions and a grey/brown paleosol (p). The upper contact with Wereroa sand is sharp and marked by an erosional unconformity (-u-), representing the Mokoia erosion surface. Section 15 Hursthouse Road at Q21/325721.



### 3.6.5 Kaihuahua dunesand

**Type section:** Manutahi section (#1) at Q21/304693

**Reference sections:** Mangaroa Stream (#3) at Q21/318718; Campbell's section (#14) at Q21/304685; Manutahi Marae (#16) at Q21/318718; Sturgeon's section (#27) at Q21/276771; Ohawe waterfall (#45) at Q21/144785

#### Previous references

Fleming (1953) first described and named a magnetite-rich sand unit that overlies the marine bench of the Rapanui Terrace, as the Rapanui Dunesand. Wilde (1978) assigned a type section and described it below the Karahaki loess (L3) and assigned it to the Oturian Interglacial stage. Wilde however could not correlate the loess units below the Rapanui Dunesand. Subsequently Wilde and Vucetich (1988) redefined the Rapanui Dunesand as occurring between the Parao loess (L4) and Omahina loess (L5).

#### Nature and distribution

##### (a) Southeast sector

The Kaihuahua dunesand consists of medium- to fine-textured, grey to brown sand that exhibits steep cross bedding (Plate 3.29). The upper contact is usually a thin ironpan, below which is *c.* 1 m of weathered brown sand over grey unweathered sand. A 0.4 m thick tephric lignite is sometimes present within the upper parts of this unit (e.g. Manutahi section (#1), (Plate 3.28)). At the Mangaroa Stream section (#3, Q21/318678),

a dune-impounded diatomaceous earth occurs and is here considered to be a correlative of the lignite. Lignite and dune-impounded lake sediments within the Kaihuahua dunesand are often found at sections close to present day streams, such as the Waikaikai and Mangaroa Streams, indicating the influence that relatively small watercourses had on covered deposition.

Two thin discrete tephra layers are seen within the Kaihuahua dunesand. At the upper Managroa Stream section (#4), the lower tephra is *c.* 3 cm thick and is enclosed by thin discontinuous ironpans above and below. The upper tephra is *c.* 1 cm thick. The tephrae are correlated to the Ninia Tephra erupted *c.* 100-115 ka from Egmont Volcano (Alloway, 1989).

The Kaihuahua dunesand is directly overlain by L5 and often the contact is marked by a thin (1-3 cm), often discontinuous ironpan. The lower contact of the Kaihuahua dunesand is with L6 (Plates 3.34 and 3.35). The sands appear to have accumulated quickly as they directly overlie tephric silts and loess units with sharp to distinct contacts and little evidence of mixing.

The Kaihuahua dunesand is found on the Ngarino Terrace and is best preserved between the Manawapou River and the southeast boundary of the study area. Figure 3.13 shows locations where the Kaihuahua dunesand has been identified and the inferred distribution of the sand in the study area.

The thickness of the sand varies between 2 and 12 m. Fluvial erosion between the Manawapou and Tangahoe Rivers has removed all of the terrestrial coverbeds above the WCS (Figure 3.3, Mokoia erosion surface), but the Kaihuahua dunesand is found on the Ngarino Terrace remnant in the vicinity of Lysaght Road at section #27

(Q21/276771). No positive correlation of the sand unit was possible farther northwestwards towards Hawera due to a lack of exposures.

### **(b) Northwest sector**

In this area, deposits considered coeval with the Kaihuahua dunesand are represented by the Kaikura formation marine units which are discussed in section 3.7.

## **Environment of deposition**

### **(a) Southeast sector**

The Kaihuahua dunesand advanced landwards after the deposition of L6. The unweathered nature of the lower parts of this unit, the steep dune-bedding and the sharp lower contact suggests rapid uninterrupted deposition. The overlying L5 began to be deposited as the sand became more stable and a component of tephric loess has been incorporated into the upper part of the dunesand. This is most evident at sites close to the coast. However at other sites, such as the Manutahi section, an ironpan is present at the top above a thin weathered horizon, suggesting the sand dunes were stabilized for a short time period before L5 was deposited.

The association of lignite and diatomaceous earth within the dunesand suggest that advancing dunes temporarily blocked streams draining the terrace surface, leading to the formation of swamps and lakes, just as the Patea Dunesand has done in the Holocene (Plate 3.1)

### **Inferred age**

The Kaihuahua dunesand represents deposits of oxygen isotope stage 5e when a rising sea level led to dune advancement inland between *c.* 120 and 115 ka. Weathering of the upper surface of the dunesand is interpreted to have occurred during a period of warm climate and high sea level *c.* 120 ka. In places the sand remained unstabilised for a longer period of time so lacks a weathered upper horizon where the sand grades up into L5.

The Kaihuahua dunesand ceased accumulating as sea level dropped *c.* 120 ka and ceased being weathered when L5 began accumulating *c.* 115 ka. At this time Egmont Volcano was active and tephras within the Kaihuahua dunesand are correlated to the Ninia Tephra, assigned an age of 100-115 ka by Alloway (1989). The Kaikura sand (section 3.7) overlying the marine sediments on the Rapanui Terrace is contemporaneous with Kaihuahua dunesand, both having formed during the Last Interglacial.

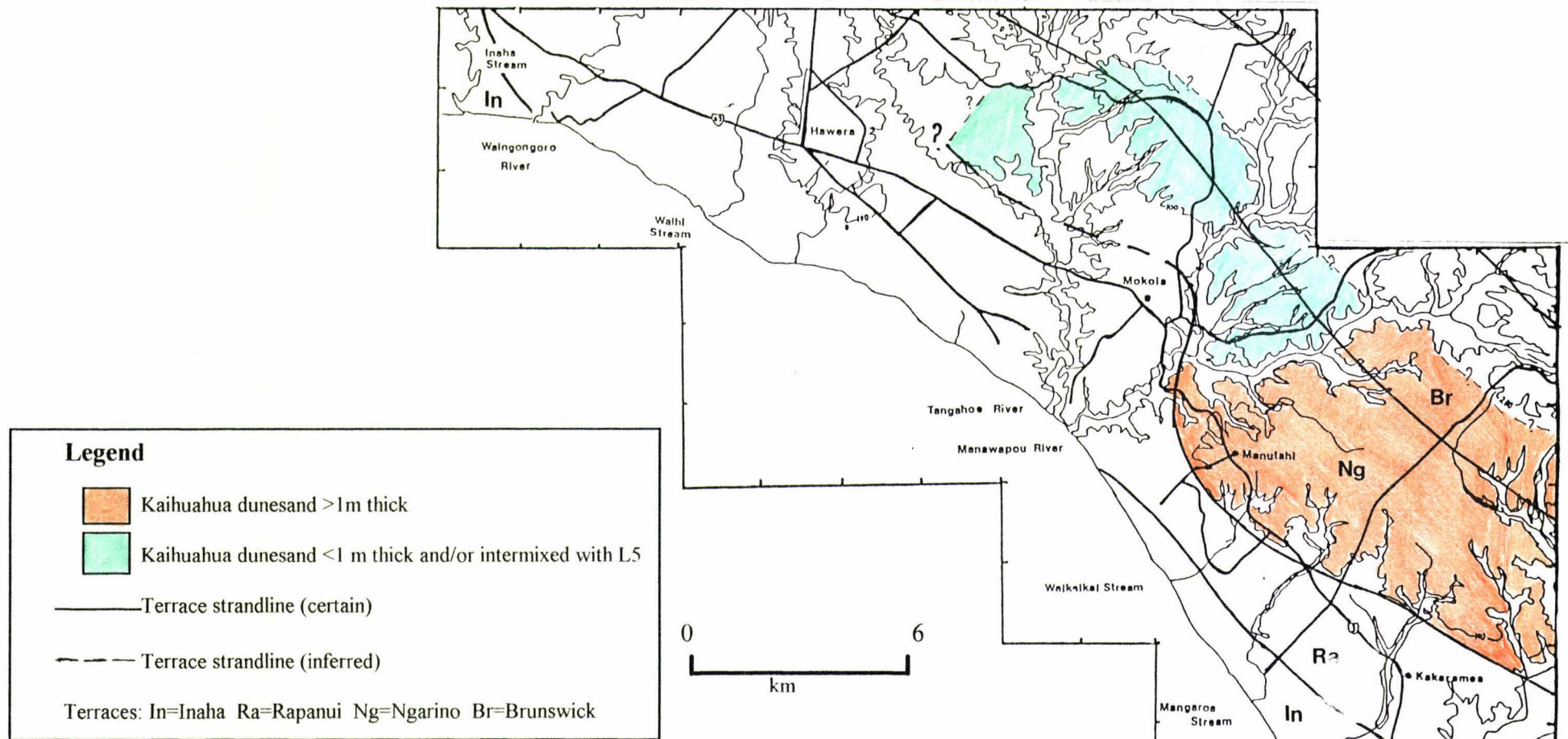


**Figure 3.13** Distribution of the Last Interglacial Kaihuahua dunesand (oxygen isotope stage 5e, *c.* 120 ka). The dunesand is present on terraces older than the Rapanui and is thickest east of the Manawapou River. On the Ngarino Terrace west of the Tangahoe River, the Kaihuahua dunesand thins to < 1 m, is intermixed within lower L5 or is absent. On the Rapanui Terrace, stage 5e deposits are represented by the Kaikura sand which immediately overlies marine sands and silts of the Kaikura formation.



**Plate 3.28** (left) L5 above the Kaihuahua dunesand (Ks). Lignite within the upper part of the dunesand contains tephras correlated with the older representatives of the Ninia Tephra, dated at between *c.* 100 and 115 ka (Alloway 1986). Section 1 (Manutahi section) at Q21/304693.

0  
0.5 m

**Plate 3.29** (below) Steeply dipping foreset beds of the Kaihuahua dunesand (Ks) below L5. Section 1 (Manutahi section) at Q21/304693.



0  
5 m

### 3.7 Oxygen isotope stage five marine deposits

#### Introduction

Marine sediments on the Rapanui Terrace, here named the Kaikura formation are subdivided into five members. The youngest of these, the Kaikura silt and fine sand member, represents emergence of the terrace.

Figure 3.14 shows a simplified stratigraphic column of the units encountered on the Rapanui Terrace and their inferred depositional environments as a result of sea level rise and fall. Relative changes in sea level (transgressions and regressions) and sediment deposition result from the interaction of tectonism and eustatic changes. The depositional sequences resulting from rising, constant and falling relative sea levels are comprised of systems tracts, with the depositional system of each tract linked by changes in sedimentary facies. There are four systems tracts: lowstand, transgressive (retrograding highstand), highstand (prograding highstand) and shelf margin (Vail *et al.*, 1991). Figure 3.15 shows the distribution of depositional environments during sea level high stand. The lowstand and shelf margin systems tracts are preserved below the datum of sea level lows and due to uplift and coastal erosion are not preserved in the sediments above the terrace WCS's in this area. Only the transgressive and highstand systems tracts are preserved in the study area. The highstand systems tract (HST) comprises three parts-

1. Early highstand
  2. Late highstand prograding complex
- and
3. Late highstand subaerial complex.

The late highstand prograding complex and subaerial complex may be deposited contemporaneously. Following descriptions of the Kaikura formation members an attempt is made to infer the depositional environments of the marine sediments by relating them to the types of deposits known to be indicative of early and late highstand nearshore environments.

### **3.7.1 Kaikura formation**

- **Kaikura sand member**
- **Kaikura silt and fine sand member**
- **Kaikura gravelly sand member**
- **Kaikura fine sand member**
- **Denby shell bed member** (informal name, Grace, 1976)

#### **Nature and distribution**

##### **Kaikura sand member**

The Kaikura sand member at its type section, immediately overlies marine sediments of the Rapanui Terrace. It is separated from the Kaikura silt and fine sand member by a distinct wavy contact. The Kaikura sand member is separated from L5 above by a 0.1 m thick zone of iron concretions formed on the upper surface of the coversand. At the type section the unit comprises semi-consolidated to consolidated grey to dark grey, medium andesitic sands and reaches a maximum thickness of *c.* 1 m.

A lack of sections exposing this unit and the similar nature to the younger Whakamara and Auburn dunesands has meant that little is known of the Kaikura coversand's nature and distribution. A thin and patchy distribution seems likely, in

contrast with the widespread distribution of the Last Interglacial dunesands (Figure 3.12 and 3.13).

### **Kaikura silt and fine sand member**

A striking feature of the Kaikura silt and fine sand member is the well defined trough and/or planar bedded cross stratification which consists of very dark grey, greyish brown or brown, fine-grained sands up to 10 m thick (Plates 3.31 and 3.32). The brown sand beds contain abundant small soft black manganese concretions. Within this unit are thin silt beds which often coincide with thin discontinuous iron pans. Changes in the colour of the sands result from variations in the sand mineralogy and water table effects. The latter effect results in strong gleying where water perches upon the thin silt beds. The contacts between the individual sand beds are generally sharp, indicating sudden influxes of sediment following partial or total erosion of the underlying beds. A number of the silt beds near the top of the member contain tephras derived from either erosion of older tephric coverbeds or influxes of contemporaneous eruption products from Egmont Volcano.

Intertidal silts and fine sands of the silt and fine sand member are thicker in the northwest (Figure 3.17) and progressively thin to the southeast. This accompanies a progressive increase in uplift rates and a decrease in sediment supply southeastwards toward Manutahi. In the vicinity of Manutahi the marine sediments are dominated by near shore andesitic sands and gravels of the gravelly sand member.

### **Kaikura gravelly sand member**

This member comprises two units. The first consists of dark brown pebbly marine sand with little bedding and contains a few rounded, andesitic pebbles up to 30 mm diameter. The second consists of a gravelly unit containing abundant small rounded andesitic pebbles in a grey/black sandy matrix. This member has a variable thickness ranging from 1 to over 5 m. Where both the Kaikura fine sand and the gravelly sand members are both present, the gravelly sand member always lies stratigraphically above the fine sand member. The gravel and sands are andesitic erosional products derived from Egmont Volcano to the northwest and differ from the quartzofeldspathic composition of cobbles occurring immediately above the WCS. The action of the sea eroding lahars and other volcanoclastic sediments and subsequent longshore drift have moved the sands and gravels southeastwards along the Taranaki coastline at this time.

### **Kaikura fine sand member**

The Kaikura fine sand member lies immediately above the WCS except where underlain by the Denby shell bed, and is characterised by its very fine micaceous nature. The fine sand is derived from the underlying Tangahoe Formation muddy sandstones. The high proportion of mica leads to the sand's characteristic smooth feel and sparkling reflection. This unit is not particularly widespread (even though its thickness varies from 2 to 4 m) and is best observed along the present coastline between the Tangahoe River and Ohawe Beach (Figure 3.16). The action of wind and spray enhances the parallel bedding of the unit in coastal exposures which often cannot be seen in sections farther inland. In places, small lenses of quartzofeldspathic gravel occur, similar in appearance to the gravels found on the WCS in this area. The gravels are dominantly

small (less than 2 cm dia.) and well rounded. The lithologies of these cobbles are similar to rock types found in the northwest Nelson region. Many are metamorphic in origin and consist of sandstones and quartz. The sand colour varies between grey/brown and yellow/brown depending upon water content and the degree of post-depositional weathering. The Kaikura fine sand is missing from inland and southeastern sections but is present in sections farther west and northwest. It has probably been derived from a 5 m-thick mica-rich fine sand unit within the Tangahoe Formation which dips to the southeast. At some localities the WCS unconformably cuts across this fine sand unit (Plate 3.30), whereas inland and to the southeast the WCS truncates blue/grey mudstone.

#### **Denby shell bed member**

This unit lies unconformably on the WCS cut into the Tangahoe Formation (Fleming, 1953). It lies below the Kaikura fine sand member. The shell bed contains numerous warm water mollusc valves of *Leucotina ambigua* (Fleming, 1953) which are thought to be Last Interglacial in age and now known not to be living south of Auckland (Pillans, 1985). The shell bed is generally between 0.5 and 2 m thick and best seen along the coastline between the Tangahoe River and Ohawe Beach. To date the shell bed has not been observed farther inland (Figure 3.16). The shells are contained in a sandy matrix with thin interbeds of grey mud (Bussell, 1988) and appear to have been deposited in a quiet near-shore coastal environment perhaps in sheltered embayments or an estuary.

## **Environment of deposition**

### **Kaikura sand member**

The Kaikura sand member accumulated as sea level dropped and the surface of the emerging marine terrace became influenced by subaerial agents such as wind. Wind deflation of the exposed marine sands and interbedded silts resulted in small dunes migrating over the surface. The wavy lower contact (Plate 3.15) has resulted from fluvial dissection of the unconsolidated marine sands prior to deposition of the coversand. The thin coversand represents an increasing rate of relative sea level fall and emergence of the Rapanui Terrace surface. Deposition of L5 commenced shortly after deposition of the coversand.

### **Kaikura silt and fine sand member**

The Kaikura silt and fine sands display bedding structures typical of intertidal nearshore deposits, such as thin tabular and convolute bedding. The decreasing relative rise of sea level during the late high stand has resulted in thin bedding. Within the upper horizons of the cross-bedded sands are pale silt beds and rip-up clasts of tephric origin up to 0.3 m in diameter (Plate 3.31 and 3.32). These have been derived from two possible sources. One is shoreline erosion of the coverbeds of the Ngarino Terrace. The second is streams and rivers in the area draining Egmont Volcano carrying fine grained sediment out to sea. At times cohesive tephric silts (such as fine ash from eruptions at Egmont Volcano and silts deposited as overbank deposits) were eroded and transported downstream, possibly by floods, and deposited within the upper part of the member (Plate 3.32). It is apparent that volcanic activity at this time was high with deposition of fine grained andesitic ash which has subsequently been deposited on the emergent

terrace platform. The upper boundary of these intertidal deposits is marked in most places by a thin discontinuous iron pan forming above the fine grained silts.

#### **Kaikura gravelly sand member**

The Kaikura gravelly sand member represents an early highstand system tract. The gravelly sands do not show cross bedding which may be explained by the grain size, since ripple bedding only occurs in sands finer than 0.7 mm (Leeder, 1982). Andesitic sediment input from Egmont Volcano increased at this time, with active andesitic volcanism evidenced by tephra units within coeval eolian coverbeds (Kaihuahua dunesand) of the Ngarino Terrace.

#### **Kaikura fine sand member**

Initially derived from the Tangahoe Formation below, the sediment of the fine mica-rich sand member is interpreted to represent the approach of sea level to a still stand. With little sediment input, particularly from the andesitic provenance to the northwest, the fine sand unit is dominantly quartzo-feldspathic.

#### **Denby shell bed member**

This assemblage was interpreted by Dr A. Beu (in Bussell, 1986) to be a beach accumulation, an estuarine environment or a quiet, sheltered embayment with common *Austrovenus* and *Paphies australe* and the warm water mollusc *Leucotina ambigua*. The underlying unconformity cut into the Tangahoe Formation represents transgressive erosion as the shoreline was displaced landward, cutting the Rapanui WCS. Above this surface the Denby shell bed is interpreted to represent a condensed section caused by

very low sedimentation rates. Seaward of the zone of storm wave action, the sedimentation rate may decline to very low values during transgression and the approach to sea level highstand (Einsele and Bayer, 1991). Because of low sedimentation rates, condensed sections usually coincide with zones of maximum fossil diversity and abundance (Vail *et al.*, 1991). The Denby shell bed is therefore here interpreted to have been deposited during the early part of the Last Interglacial as sea level approached a stillstand (Figure 3.14).

### **Inferred age**

Based on the inferred age of the overlying L5 (115-105 ka) the Kaikura Formation at its type section, is correlated with emergence of the Rapanui WCS as sea level dropped during the transition from oxygen isotope substage 5e to 5d *c.* 120-115 ka.

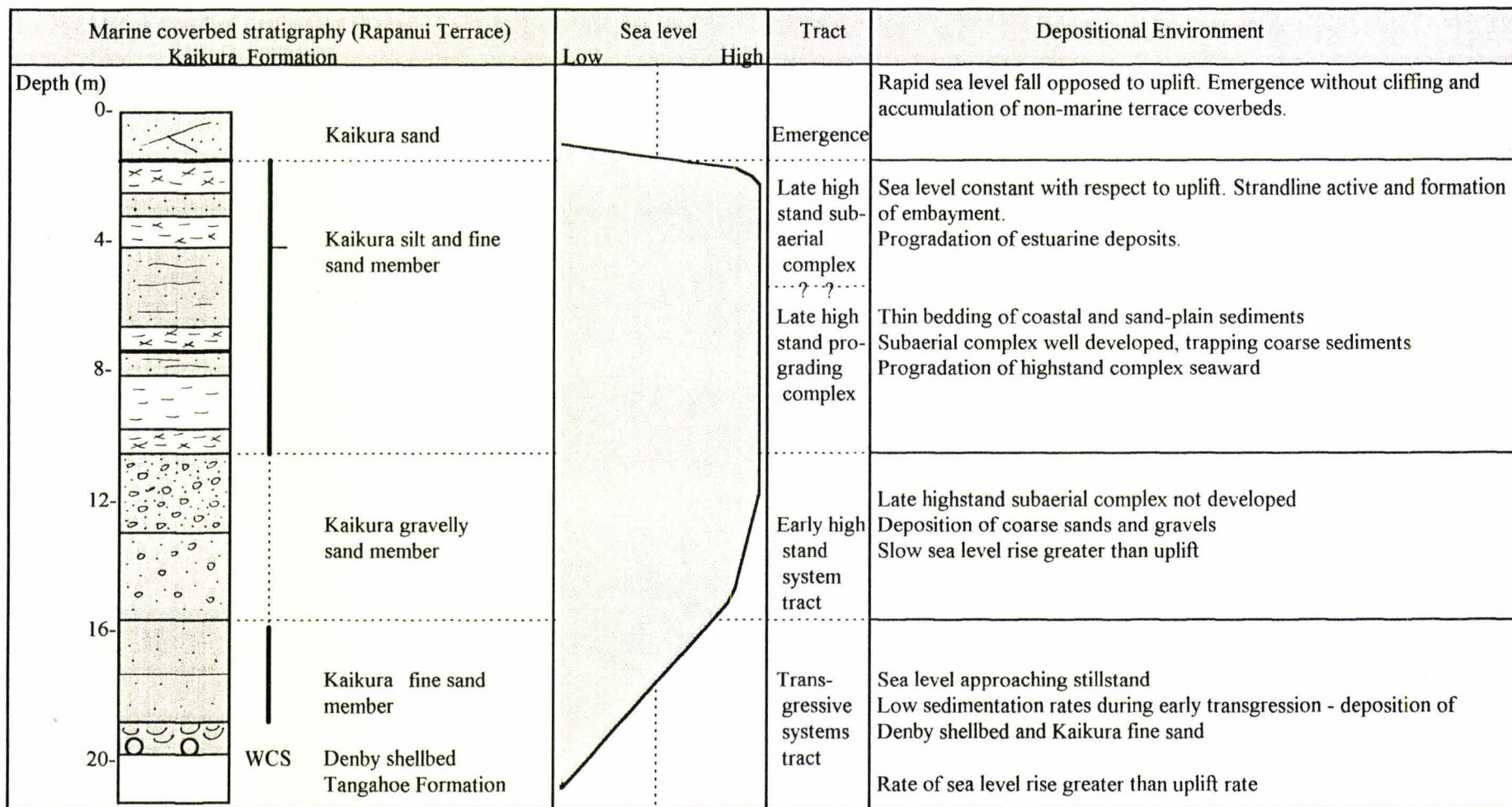


**Figure 3.14** Generalised stratigraphy, depositional environments and the relationship between sea level rise and fall for the Kaikura formation overlying the Rapanui WCS.

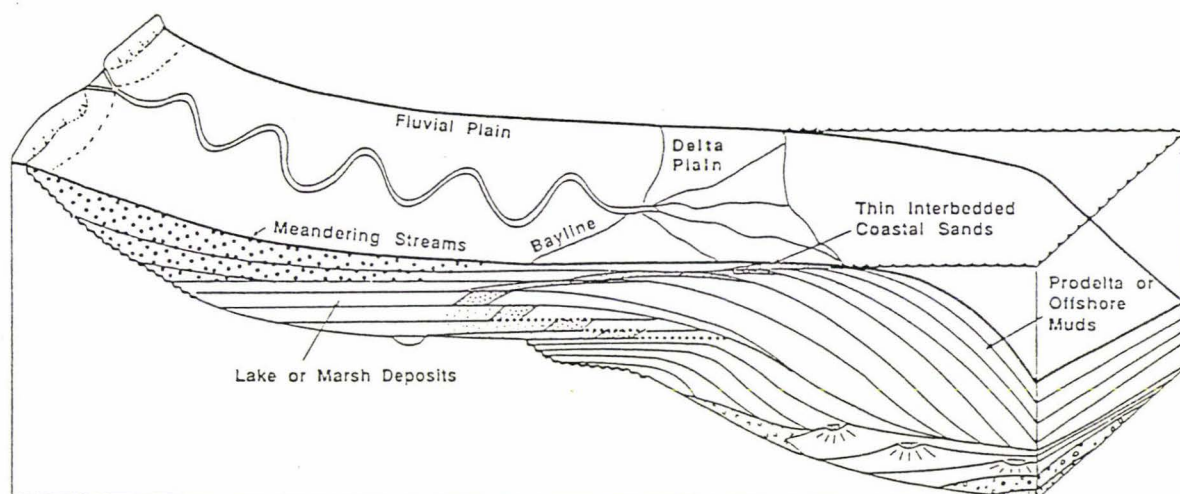


**Figure 3.15** High stand system tract showing the depositional environments present and the resulting deposits. The formation of coarse fluvial deposits inland on the fluvial plain results in fine thin interbedded coastal sands. After Vail *et al.*, (1991).

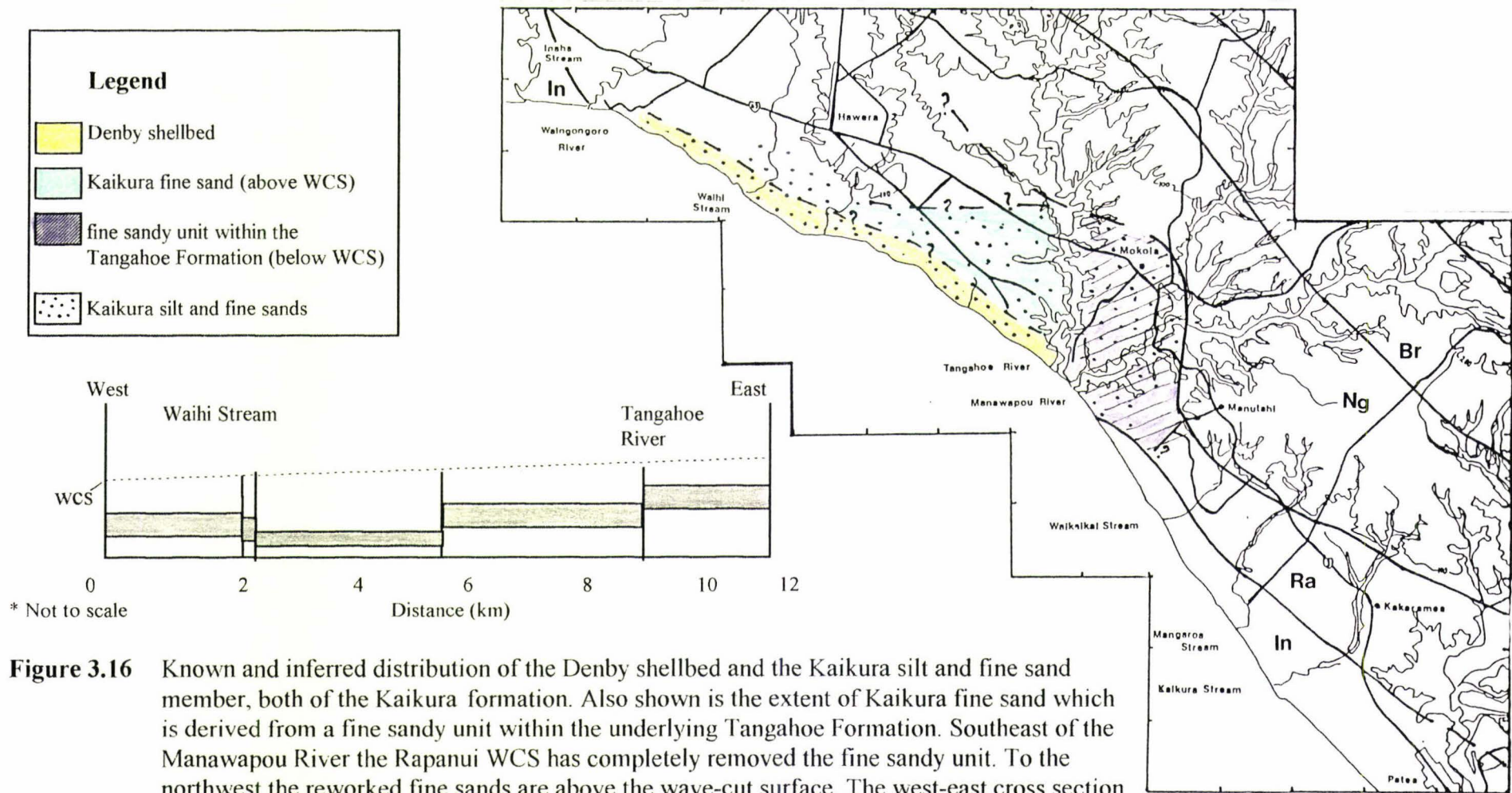


**Figure 3.16** Known and inferred distribution of the Denby shellbed and the Kaikura silt and fine sand member, both of the Kaikura formation. Also shown is the extent of Kaikura fine sand which is derived from a fine sandy unit within the underlying Tangahoe Formation. Southeast of the Manawapou River the Rapanui WCS has completely removed the fine sandy unit. To the northwest the reworked fine sands are above the wave-cut surface. The west-east cross section shows normal faults that offset the Tangahoe Formation between Waihi Stream and Tangahoe River. (Faults after Whitten, 1973).

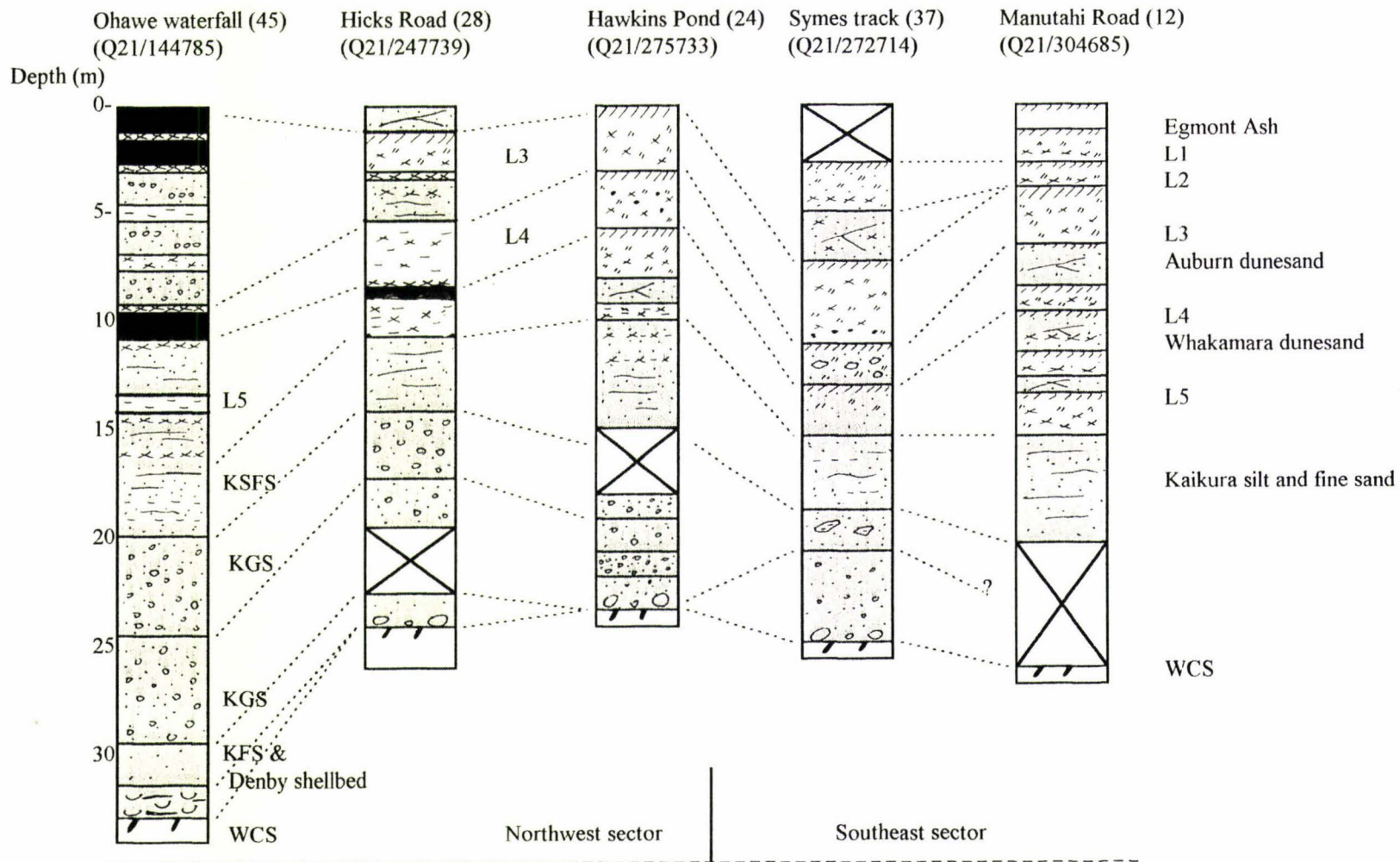


**Figure 3.17** Facies changes from northwest to southeast within the Kaikura formation above the Rapanui WCS. In the northwest sector, silts are extensive (Kaikura silt and fine sand member (KSFS)) and thin to the southeast.

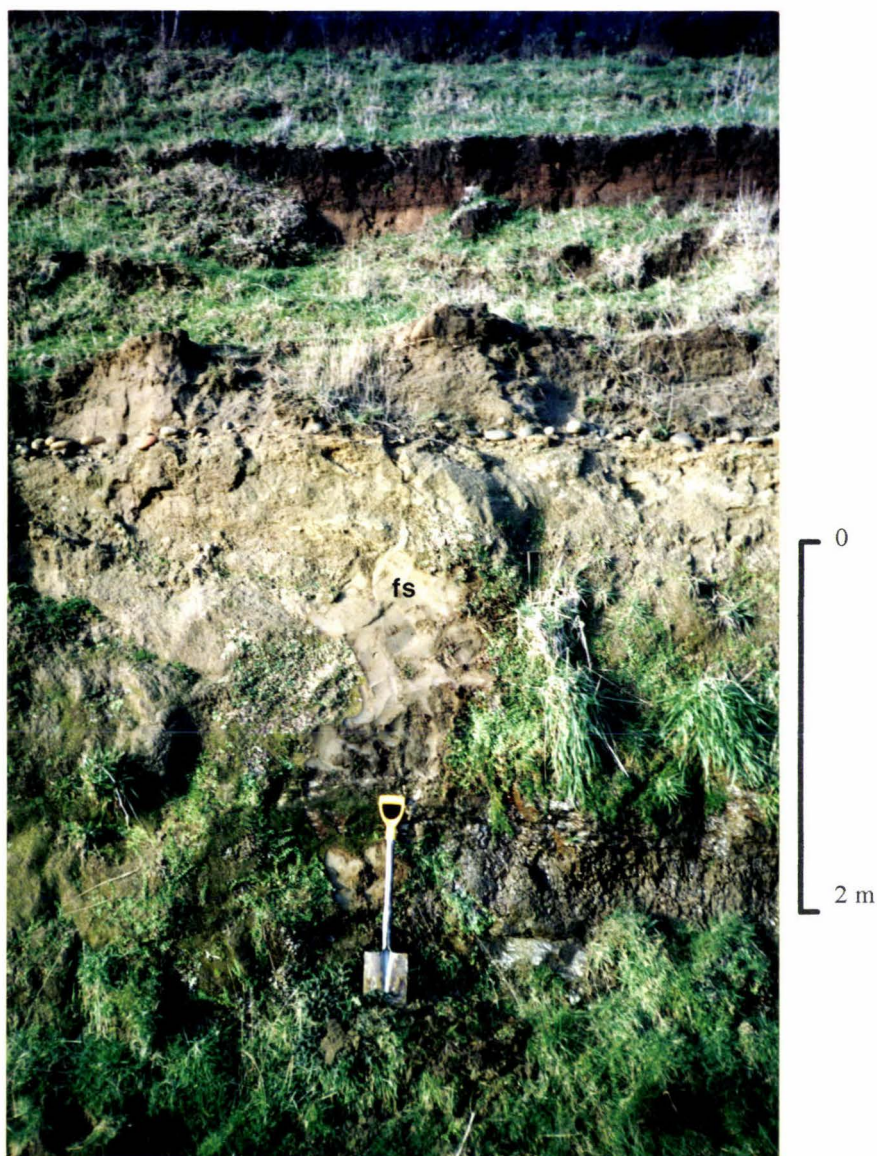


**Plate 3.30** The fine mica-rich sand unit (fs) within the Tangahoe Formation (3.1-3.6 ma) from which the Kaikura fine sand member (*c.* 120 ka) is derived. The unconformity representing the Rapanui WCS is marked by a basal layer of smooth well rounded quartz cobbles. Section 37 (Symes track 2) at Q21/272714.



**Plate 3.31** (above) Tabular cross-bedding within the Kaikura silt and fine sand member. Flow direction is from left to right. Note water escape structures at base of section and silt rip-up clasts (s). Section 24 (Hawkin's section) at Q21/275733.

**Plate 3.32** (left) Trough cross-bedding within sand of the Kaikura silt and fine sand member on the Rapanui Terrace. Silt rip-up clasts (s) within the sands contain abundant tephra. They have probably been derived from redeposition of volcanic river floodplain sediment and direct airfall. Another possible source is fallen debris eroded from the Ngarino riser nearby and incorporated into the thinly bedded near-shore sands. Section 24 (Hawkin's section) at Q21/275733.

### 3.8 Oxygen isotope stage six deposits

One unit, L6 is interpreted to have been deposited during oxygen isotope stage 6. L6 is the thickest volcanic loess unit described in this study and contains abundant ash and lapilli. It is an important unit that occurs on terraces older than the Rapanui Terrace.

#### 3.8.1 Loess 6 (L6)

**Type section:** Manutahi section ( #1 ) at Q21/304693

**Reference sections:** Mangaroa Stream ( #3 ) at Q21/318678; Sturgeon's section ( #27 ) at Q21/276771; Rutten's section ( #16 ) at Q21/318718

#### Previous references

Fleming (1953) referred to andesitic ash and pale silts occurring together and beneath the Brunswick dunesand as Fordell Ash. Wilde (1978) described Waitahinga loess (L6), in the same stratigraphic position as Fleming's Fordell Ash. At its type section 2 km southeast of Maxwell (R22/703521), Waitahinga loess is interbedded between Brunswick beachsand below and Brunswick dunesand above, separated from both by sharp contacts marked by thin ironpans. Wilde (1978) described it as massive yellowish brown or greyish brown beds with either silt loam or clay loam texture, that contained distinct mottles and abundant rhizomorphs. At Omahina Road (R21/528627) Pillans (1985) recognised fluvial micaceous fine sands and silts beneath the Omahina loess (L5) as being a correlative of the Waitahinga loess (L6). The Omahina loess immediately postdates the cutting of the Rapanui Terrace *c.* 120 ka (Pillans, 1988). Milne and Smalley (1979) estimate it was deposited 130-140 ka ago, therefore putting it

in oxygen isotope stage 6. The Waitahinga loess once thought to be present on only the Brunswick and older terraces (Wilde, 1978) has since been mapped on the Ngarino Terrace (Pillans, 1990).

### **Nature and distribution**

The thickness of L6 ranges from 1.5 m to >3 m, but a lack of sections exposing both upper and lower contacts means the maximum thickness of L6 may be greater. Two L6 facies are commonly seen; a gley and a well drained facies. The gley facies exhibits a wide range of colours from pale orange/brown to pale blue/grey tephric-rich volcanic loess of silt loam to clay loam texture (Plate 3.33). Rhizomorphs are sometimes present, often associated with carbonaceous laminae, and layers of lapilli up to 5 cm thick are common in the L6 gley facies. The well drained facies exhibits grey to yellowish brown colours with abundant yellow and yellow red lapilli throughout the profile (Plate 3.34). In this facies lapilli are well mixed into the enclosing medial material.

L6 is found to directly overlie the Ingahape formation (section 3.10) and is generally separated from the underlying units by a thin 1-2 cm ironpan. In the gley facies the upper contact with the Kaihuahua dunesand is sharp (Plate 3.35) with a thin discontinuous ironpan often present. In the well drained facies the overlying dunesand is separated by a distinct contact.

L6 occurs on the Ngarino and older marine terraces (Figure 3.18). It has not been identified on the younger Rapanui Terrace, indicating that it was deposited before the cutting of the Rapanui Terrace. Towards the strandline of the Ngarino Terrace, L6 has

been subjected to weathering processes in a better drained environment compared to the loess at sites nearer the coast.

### **Environment of deposition**

The nature and appearance of the gley facies indicates aeolian deposition of volcanic loess and lapilli into wet sites or sites subsequently subjected to a high watertable. A high water table (caused by dunes or volcanoclastics impounding waterways) may be responsible for the parallel bedding and the associated carbonaceous silts and lignite. The tephric nature of the loess indicates regular volcanic activity occurring from the volcanic chain to the northwest. At the time of formation of L6, Pouakai Volcano or possibly a very young Egmont Volcano may have been responsible for the tephra additions.

### **Inferred age**

L6 was deposited after the cutting of the Ngarino WCS *c.* 210 ka. Deposition of L6 continued until sand dune advancement began with the rising sea level *c.* 120 ka. As loess deposition ceased Kaihuahua dunes continued to advance inland with the warmer climate. Thus L6 is here interpreted as having accumulated between 200 and 130 ka, during oxygen isotope stage 6.

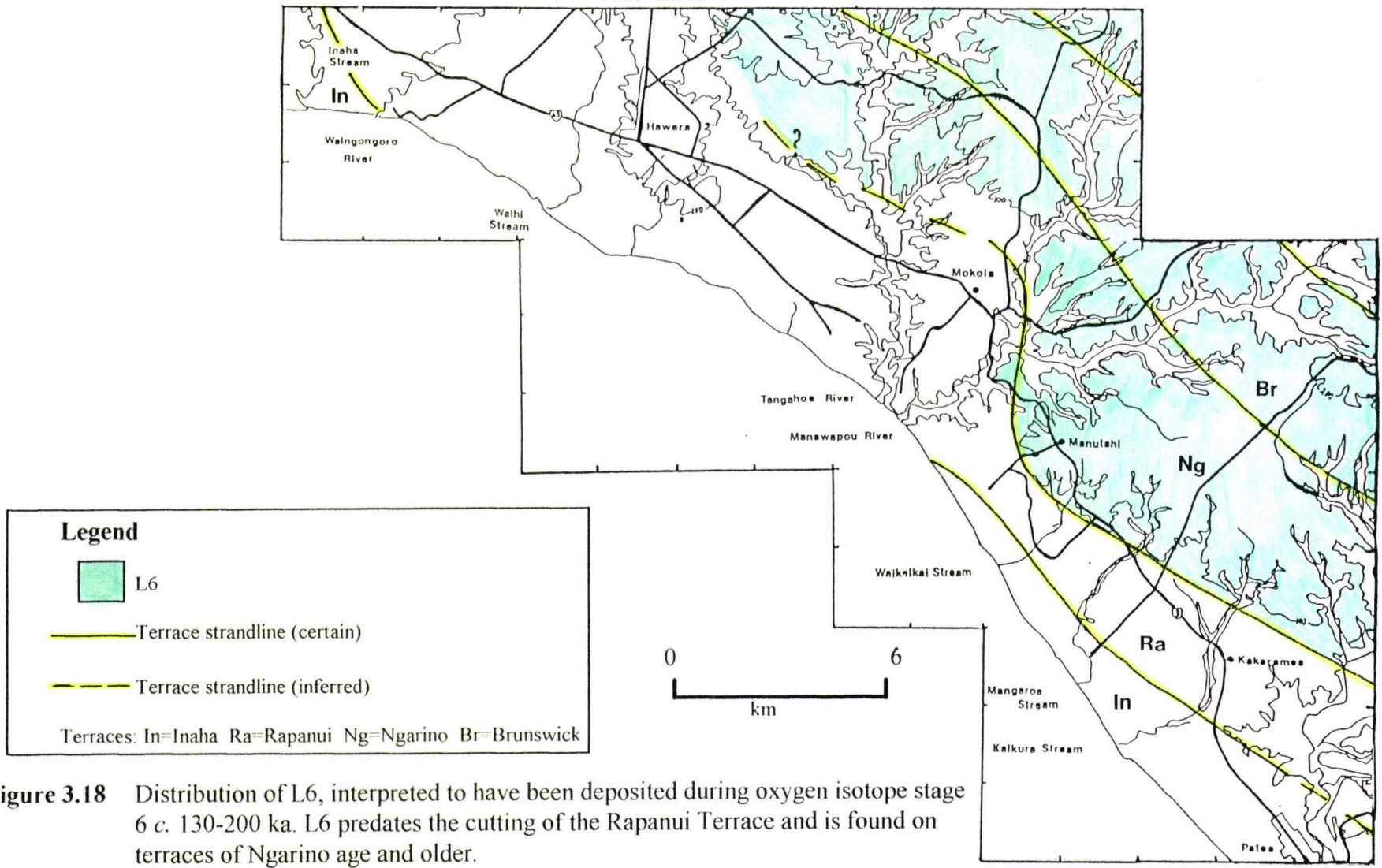


**Figure 3.18** Distribution of L6, interpreted to have been deposited during oxygen isotope stage 6 c. 130-200 ka. L6 predates the cutting of the Rapanui Terrace and is found on terraces of Ngarino age and older.

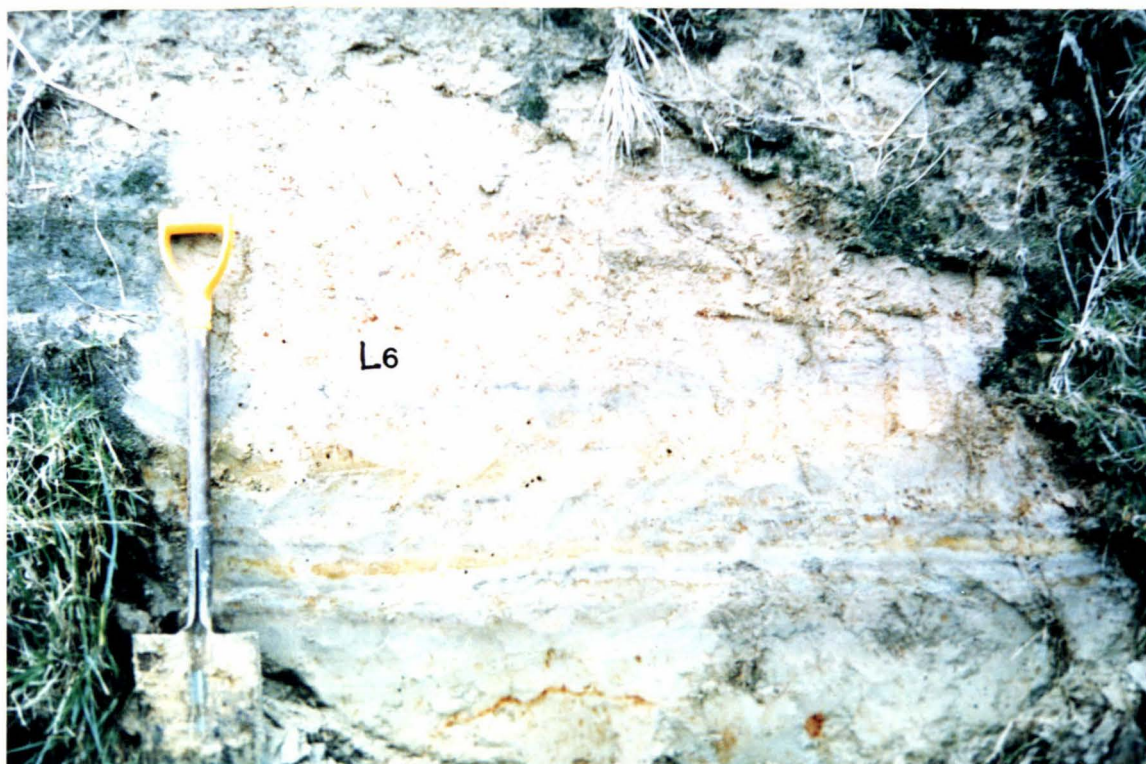


**Plate 3.33** (above) L6 near the outer margin of the Ngarino Terrace showing interbedded andesitic lapilli and fine silt texture. This unit represents the gley facies, a high watertable being responsible for the pronounced bedding of the lapilli. The Ngarino WCS is *c.* 6 m below section. Section 3 (Mangaroo Stream) at Q21/318678. Spade for scale is 1 m long.

**Plate 3.34** (left) Sharp lower contact of the Kaihuahua dunesand (ks) with L6, towards the inner margin of the Ngarino Terrace. Here L6 was well drained and lapilli are dispersed throughout the unit. Section 15 (Hursthouse section) at Q21/325721. Spade for scale is 1 m long.



**Plate 3.35** Sharp contact between L6 and the Kaihuahua dunesand (ks) which is *c.* 2 m thick, and is overlain by L5. Section 3 (Mangaroa Stream) at Q21/318678. Spade for scale is 1 m long.

### 3.9 Oxygen isotope stage seven deposits

One formation mapped on the Ngarino Terrace, the Ingahape formation is interpreted to have been deposited during oxygen isotope stage 7. It comprises two members, the younger, Ingahape sand (Figure 3.2) represents the transition from marine sedimentation to subaerial deposition as the Ngarino Terrace was uplifted from a lowering sea level, the older, Ingahape gravel represents transgressional deposition.

#### 3.9.1 Ingahape formation

**Type section:** Sturgeon's section (# 27) at Q21/ 276771

**Reference sections:** Campbell's section (#14) at Q21/318703, Mangaroa Stream section (# 3) at Q21/318678; Symes quarry (#11) at Q21/289727; Sturgeon's #2 (#33) at Q21/273768; Ingahape Road (#25) at Q21/296736

#### **Previous references**

Fleming (1953) first defined and named this unit the Brunswick dunesand which he believed was present on the Brunswick Terrace. Fleming also included the Brunswick Dunesand on the older Kaiatea terraces but mentioned they may be an older unit. Milne (1973) redefined the Brunswick Dunesand as overlying the Mt Curl tephra dated at 230 ka (Milne, 1973b) and therefore could not be present on the Brunswick Terrace thought to be 310 ka (Milne, 1973; Wilde and Vucetich, 1988).

## **Nature and distribution**

### **Ingahape sand member**

The Ingahape sand overlies the Ingahape gravel member. The sand exhibits low angle cross bedding and is of a fine to medium texture, with dark orange/brown colouring, resulting from weathering of the magnetite minerals present. The upper part of this member in places comprises a thin dunesand which originated after emergence of the Ngarino Terrace. In places the dunesand is missing and the Ingahape sand member directly underlies L6. With the limited exposures of the dunesand and the difficulty of separate identification from the marine sand, inferences on distribution and environments of deposition cannot be accurately determined for most of the study area.

### **Ingahape gravel member**

The Ingahape gravel member consists of rounded andesitic pebbles (Plate 3.36) with a few cobbles (>64 mm) and interbedded cross-bedded tabular sands that occur directly above the Ngarino WCS. Ingahape gravel is distinguished from gravel units found on the Rapanui Terrace because it is generally more cemented, exhibits orange staining (Plate 3.36) and smaller pebbles are easily crushed (i.e. are grussified), indicative of a longer period of weathering. Bedding is pronounced where the gravels are interbedded with orange, dark grey or black, andesitic medium to fine sands, but where the sands are absent bedding appears weakly developed. A feature of them is their darker colour to those on the Rapanui Terrace attributable to the high percentage of ferromagnesian minerals derived from an andesitic provenance. In some sections weathering has translocated iron from the sands and gravels partially cementing them.

In sections located between interfluves where fluvial erosion and slope processes have removed overlying deposits, tephra-rich colluvium overlies the marine sediments. In these cases allophane appears to have been translocated downwards and is seen coating the gravels and filling voids (Plate 3.37).

The Ngarino WCS cuts into blue/grey Tangahoe Formation mudstone and marks the lower contact of the Ingahape formation at the type locality (Q21/276770). A thin dunesand unit below a pale tephric loess unit (L6) marks the upper contact of the Ingahape formation.

### **Environment of deposition**

The Ingahape gravel member gravels and tabular cross-bedded sands are interpreted as being deposited in the surf zone. These sediments are thinner towards the back of the Ngarino Terrace where their thickness reaches 4-5 m. Towards the outer margin of the terrace they thicken up to 6 m. Immediately above the WCS the gravel and sands represent transgression and early highstand systems tract deposits (Figure 2.3). Many of the sections are thought to represent the transgression phase which then grades up into fine sands represented by the Ingahape sand member deposited as the rate of relative sea level rise slowed. The absence of relatively thick deposits of fine sands and only thin gravelly units (<6 m) suggest that the sea level high that formed the Ngarino WCS was relatively short in duration in comparison to the high stand that formed the Rapanui WCS.

### **Inferred age**

The sand and gravel units of the Ingahape formation represent deposition during the cutting of the Ngarino Terrace *c.* 210 ka (Pillans, 1983, 1988) and immediately following retreat of the sea from the terrace. The age of the Ingahape formation is therefore thought to range between 210 and *c.* 205 ka.



**Plate 3.36** Small rounded orange stained andesitic gravels of the Ingahape formation on the Ngarino Terrace. Section 27 (Sturgeon's section) at Q21/276771. Spade for scale is 1 m long.



**Plate 3.37** Rounded andesitic gravels towards the inner margin of the Ngarino Terrace. Note clay coatings infilling voids. Exposure at Q21/276778.

## Summary

Sea level during the Last Glacial Maximum dropped by *c.* 120 m and exposed large areas of the continental shelf. At this time the study area would have been over 50 km from the coast separated by a low lying coastal plain. Dry winds blowing across the plain probably dried out vegetation and surficial deposits ultimately leading to wind deflation of the coverbeds. Erosion of older andesitic dunesand units provided plentiful andesitic material for remobilisation and deposition as the Wereroa sand. Winds during this time were mainly from the southwest and west with the thickest Wereroa sand deposits being found leewards of watercourses, often forming transverse dunes trending northwest-southeast. Another feature of wind deflation was the formation of the Mokoia erosion surface. This surface is most widespread between the Manawapou and Tangahoe Rivers. In the southwest sector the Mokoia surface occurs close to and along watercourses on the Ngarino Terrace (Figure 3.3). On the ring plain in the northwest sector however it seems that during oxygen isotope stage 2 the high input of volcanoclastic sediments meant that the ring plain was able to maintain equilibrium river gradients, forming a low gently seaward sloping land surface. With the high input of volcanoclastics in the northwest sector it seems unlikely that erosion of older covered units was widespread during oxygen isotope stage 2.

Egmont Volcano was frequently active during the Ohakean with seven eruptive episodes being recognised by Alloway (1989) (Figure 3.9). Within the study area four eruptive episodes are tentatively correlated to the Kaihouri, Paetahi, Poto and Tuikonga Tephtras. Of these the Poto and Tuikonga Tephtras are the most widespread. Near Manutahi the Poto Tephtra is *c.* 1 cm thick and occurs in pockets above the Kawakawa Tephtra. The Tuikonga Tephtra is distinctive as discontinuous grey ‘creamcakes’.

During the Ratan substage climate did not deteriorate to the same extent as during the later Ohakean substage. Covered erosion was not so widespread in the southeast sector but widespread deposition of the Huxley sand in the northwest sector implies that the climate was sufficiently dry and windy to redistribute andesitic sands. These sands are sourced from the Opunake Formation debris flows which inundated large areas of the northwest sector. The presence of unit L2 on the Opunake Formation confirms an age of  $< 40$  ka for this deposit.

In the northwest sector repeated inundation and subsequent changes to drainage patterns resulted in the formation of lignite deposits. Correlation of tephra within the Ratan lignite as the Mangapotoa Tephra (28-50 ka) shows that volcanic activity at this time was frequent and was related to the earlier deposition of the Opunake debris-flow.

Lignite deposits in this area therefore cannot be seen as warm climate indicators, but are instead a reflection of the landscape response to repeated inundation by volcanoclastics. The genesis of peat deposits in the Taranaki region is influenced more by the deposition of volcanoclastic detritus transported by lahars than by any other eruptive event (Alloway, 1992).

During the Porewan, continuing tephra deposition coupled with a cool but warming climate resulted in the deposition of volcanic loess unit L3. A pronounced paleosol on L3 records the climatic warming *c.* 60 ka. A warming climate is also suggested by the absence of cold climate sands within this unit in the southeast sector. Continuing volcanic activity culminated in the emplacement of the Stratford Formation in the northwest sector.

During the Last Interglacial the climate was warmer and wetter than present, with soil-forming processes affecting surficial deposits at a faster rate than during the preceding glacial period (stage 6). Northwest of the Manawapou River on remnants of the Ngarino and Rapanui Terraces, the only Last Interglacial deposits found are those representing stages 5d and 5b. In this area, dunesands representing stages 5c and 5a are missing, and paleosols on L4 and L5 represent the periods when climate warmed during stages 5c and 5a as loess deposition slowed down or ceased (Plate 3.15). Interpretation of these paleosols is based on soil structure, colour, clay coatings and rhizomorph abundance. At the Manutahi section (#1) after deposition of the Whakamara dunesand during stage 5c, the climate cooled and deposition of L4 commenced. Because L4 is only thin, the top of the Whakamara dunesand has been affected by weathering processes, indicated by the orange colours and structure. The grey Auburn dunesand overlying L4, accumulated during oxygen isotope stage 5a. Wilde (1978) stated that Holocene dunes near Waverley advanced north-northwest. However the Pleistocene dunes mapped in the study area appear to have advanced in a north-northeast direction, possibly indicating different wind patterns than during the Holocene. The Pleistocene dunes are only preserved southeast of the Tangahoe River, which appears to be a major boundary between two different depositional environments. In the past dunes may have been deposited northwest of the Manawapou River but now have little or no topographic expression due to fluvial erosion, deflation by wind (Fleming's ventiplanation) and/or burial by volcanoclastic deposits.

The distribution of different facies within marine sediments on the Rapanui WCS shows the influence of high sediment supply from Egmont Volcano. Towards Ohawe in the northwest, volcanoclastics and associated fluvial deposits increase in

thickness towards their source, the Egmont ring plain, and maintain a relatively constant terrace surface height.

Towards the west the increasing thickness of fluvial deposits (gravels and fine sands with or without silts) has resulted from the interaction of low uplift rates, sea level highstand and high sediment input. The fluvial deposits to the northwest are characteristic of sediments deposited during sea level stillstands (Vail *et al.*, 1991). In the southeast, fluvial deposits have not been observed, this being attributed to higher uplift rates and lower sediment input compared to the northwest.

The lithology and location of the marine units may be related to the positions of former rivers. The Kaikura fine sand member is the erosional product derived from the underlying Tangahoe Formation whereas the Kaikura gravelly sand member is derived from erosion of volcanoclastic sediments brought down rivers and along the coast as well as erosion of the andesitic gravels present in the coverbeds of older terraces. The Rapanui marine deposits are much thicker and widespread north of the Tangahoe River which does coincide with the southeastern extent of the lahars from Egmont Volcano.

The Kaikura formation in the northwest sector seems to merge into fluvial sediments associated with broad floodplains that were inundated with lahars which choked channels and led to frequent flooding and deposition of overbank deposits. The present day floodplains on the terrace surfaces are in contrast small and confined within v-shaped valleys. The former floodplains were broad and formed on the gently sloping surface associated with the dropping relative sea level that was abandoning the continental shelf. To the south of the Tangahoe River the marine sediments grade up into terrestrial dunesands, lignites and volcanic loess units.

Volcanic loess unit L6 was deposited during oxygen isotope stage 6. This is a relatively thick unit (up to 3 m thick) and immediately predates the cutting of the Rapanui Terrace. The distribution of L6 is important because due to its absence along the coastline it confirms the Rapanui Terrace is preserved west of the Manawapou River. L6 immediately overlies the Ngarino Terrace's Ingahape formation. Sands and gravels of the Ingahape formation are stained orange and weathered to a much greater extent than similar units found on the younger Rapanui Terrace.

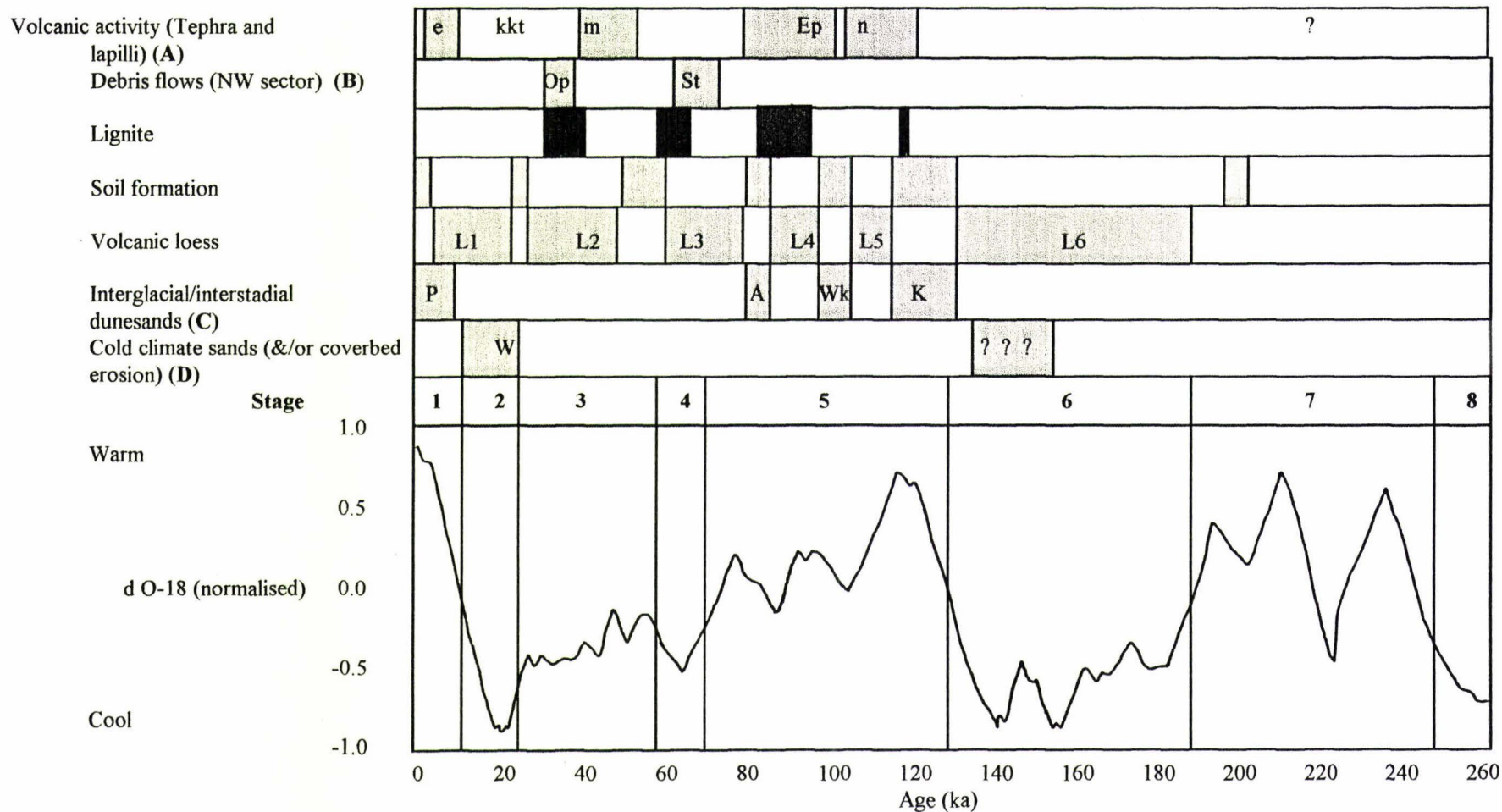


**Figure 3.19** South Taranaki terrace coveredbed units and their correlation to the oxygen isotope curve (after Martinson *et al.*, 1987). (A) Egmont Ash=e, Kawakawa Tephra=kkt, Mangapotoa Tephra=m, Epiha Tephra=Ep, Ninia Tephra=n; (B) Opunake Formation=Op, Stratford Formation=St; (C) Patea Dunesand=P, Auburn dunesand=A, Whakamara dunesand=Wk, Kaihuahua dunesand=K; (D) Wereroa sand=W

## Chapter four

### Palynological interpretation and correlation of the Ohawe Waterfall section to the Inaha and Ararata Road sections

#### 4.0 Introduction

Early studies near Hawera mapped the coastal marine terrace as the Rapanui Terrace (Hay, 1967; Pillans, 1981; McGlone *et al.*, 1984). McGlone *et al.*, (1984) studied the stratigraphy and pollen from a coastal marine terrace west of Waingongoro River. This site (Inaha section) was interpreted to overlie the 100 ka Inaha WCS. Bussell (1988) subsequently assigned an age of 210 ka for the marine terrace exposed along the coastal cliffs southeast of the Waingongoro River. This was based on the interpretation of Last Interglacial pollen (stage 5e) within the subaerial coverbeds of the marine terrace at two sites along the coastal cliffs. These sites, the Ohawe Waterfall and Ohawe East Sections (Figure 4.1) described in detail by Bussell (1988) provide a relatively complete stratigraphic sequence above a well exposed marine WCS. In this study the upper 11 m exposed at the Ohawe East Section is similar to sections 30, 46, 47 and 48 near Hawera, where units representing the Holocene to the Porewan are described in the previous section (Figure 3.6). Also section 3.7 describes and correlates marine sediments of the terrace sequence from the southeast sector to the Ohawe Waterfall Section, providing evidence that a redefinition of the marine terrace southwest of Hawera may be required.

Figure 4.2 shows the combined coverbed stratigraphy, pollen zones and the inferred ages of the zones assigned by Bussell (1988) to the Ohawe Waterfall and Ohawe East Sections. This section provides an alternative correlation of the pollen zones by Bussell (1988) based on stratigraphic correlation to the Inaha site of McGlone

*et al.*, (1984). The following section summarises the stratigraphy and pollen zones of the Ohawe waterfall, Inaha and Ararata Road sections and concludes with a revised interpretation and age of the Ohawe waterfall section.

#### **4.1 Ohawe Waterfall and Ohawe East Sections (Bussell, 1988)**

Bussell divided the stratigraphic sequence exposed at the Ohawe Waterfall and Ohawe East Sections into five pollen zones, in the order oldest to youngest OH1-OH5 (Figure 4.1). The stratigraphy of zones OH1-OH4 are described from the Ohawe Waterfall site with zone OH5 described from the Ohawe east site located *c.* 300 m to the southeast.

##### **Stratigraphy**

The 60 m-thick stratigraphic sequence exposed at the Ohawe waterfall section (Figure 4.1) can be interpreted as recording a range of depositional environments. Immediately above the wave cut surface, 10 m of pebbly marine sand was deposited. Above this, the sequence grades into interbedded sands and silts that contain *in situ* fossil reeds and lignaceous laminae (Bussell, 1988). Within these units are thin cross-bedded gravels interbedded with sands and silts that represent alluvial floodplain deposits. These are largely resorted volcanoclastic sediments which interdigitate with backswamp lignites and carbonaceous silts. Large sections of the stratigraphy at Ohawe contain little or no pollen. For example, in zone OH1 the pollen spectra are derived from quite widely spaced spot samples of lignaceous horizons with many of the samples containing too few pollen to provide an ecologically meaningful count (Bussell, 1988). During OH1 time there was rapid aggradation of alluvium, deposited during overbank

flooding events with intermittent ponds represented by finer grained sediments in the sequence. The lignaceous horizons represent quite brief periods of relative local stability when swamp communities were able to establish, but each time the site was soon covered over by alluvium.

A thin lignite layer at the base of zone OH2 is overlain by a 1.5 m-thick dark grey laminated mud unit that shows evidence of bioturbation. Overlying the laminated mud unit is an andesitic tuff which becomes increasingly carbonaceous upwards (and immediately underlies a 1m-thick black woody lignite of zone OH3). Pollen samples were obtained from the basal lignite, and the andesitic tuff at the top of the zone.

A laterally extensive *c.* 1 m-thick lignite unit occurs at the base of zone OH3 which gives way to alluvial aggradation deposits. The lignite unit contains fossil rootlets at the base, white sandy andesitic tephra and poorly preserved flattened wood. Wood samples were identified by R. Patel (in Bussell, 1988) as *Podocarpus hallii/totara* or *Dacrydium cupressinum*, *Halocarpus* and *Dracophyllum*. A brown carbonaceous tuff overlies the lignite. The middle and upper parts of the zone comprise interbedded pumiceous conglomerates and carbonaceous, tephric and diatomaceous muds.

A barren section at the base of zone OH4 consists of light grey pumiceous pebbly sand. Above this is andesitic tuff in turn overlain by a tephric woody lignite *c.* 0.5 m thick. This grades into *c.* 1 m of brown to blue/grey carbonaceous mud. Above, a black woody lignite is unconformably truncated the Stratford Formation debris-avalanche. The lignite is *c.* 1 m thick and contains numerous layers of coarse andesitic ash.

Zone OH5 overlies pumiceous alluvium associated with reworking of the Stratford Formation. Pollen samples were obtained from a thin lignite horizon within a

light brown carbonaceous mud (Figure 4.2). An iron-cemented layer overlies the lignite. Pollen samples were also obtained above the cemented layer from carbonaceous laminae within grey mud. A barren section of alluvium overlies this and samples at the top of the zone were obtained from two thin (<15 cm) lignaceous horizons. The lowermost and thicker horizon is within the alluvium and the topmost sampled is a thin lignite directly overlying an iron-cemented layer and a *c.* 0.75 m thick tephra-rich loess unit containing fossil rootlets.

**Pollen Zone summary** (after Bussell, 1990)

**Zone OH1** (41.75-35.0 m)

This zone is characterised by abundant grass pollen which shows a general decline through the zone from a maximum of 90% at the base. Asteraceae (Tubuliflorae) shows a general upward decline, whilst *Coprosma* increases upward. Fern spore abundance fluctuates markedly from sample to sample. Pollen of many small tree and shrub taxa display a rise at the top of the zone, particularly *Leptospermum* type. Arboreal pollen is sparse (<5%) except for *Nothofagus fusca* type.

**Zone OH2** ( 35.0-33.5m)

Grass and shrub pollen are common with grass pollen rising to *c.* 40%, followed by a decline and then a marked rise at the top of the zone. An increase in arboreal pollen values occurs during this time with *Prumnopitys taxifolia*, *Dacrydium cupressinum*, and *Nothofagus menziesii* pollen more common than before. *Myrsine*, *Dracophyllum* type, and *Halocarpus* pollen, which show an upward increase, become common for the first time.

**Zone OH3 (33.5-27.5m)**

Grass pollen remains common and increases to a maximum of 90% then declines to <5% at the top of the zone. Shrub pollen remains common but arboreal pollen values are low.

**Zone OH4 (27.5-23.5m)**

Grass pollen are low at the base of this zone but dominate in the upper part, with shrub pollen remaining common. Asteraceae (Tubuliflorae) is low at the base but rises to become common at the top, whilst *Halocarpus* is common at the bottom and top of the zone.

**Zone OH5 (11.75-7.25m)**

This zone is characterised by high levels of arboreal, particularly podocarp pollen. *Dacrydium cupressinum* and *Metrosideros* pollen are the dominant types in the lower and middle parts of the zone. In the upper part of the zone above the barren section, *Prumnopitys taxifolia* is dominant. Pollen of *Ascarina lucida*, *Coriaria*, and *Dodonea viscosa* are represented where they were previously rare or absent.

#### 4.2 Inaha section (after McGlone *et al.*, 1984)

McGlone *et al.*, (1984) described a coastal section *c.* 0.2 km west of the mouth of the Inaha Stream at grid reference Q21/103793 (Figure 3.1). The 38 m-thick sequence (Figure 4.1) records ring-plain accumulation superimposed on a marine wave-cut platform. Based on the pollen within these units McGlone *et al.*, (1984) subdivided the stratigraphic column into five zones, Inaha zones A to F. The pollen diagram and pollen zones are shown in Figure 4.2. This work resulted in correlation of the WCS (Inaha marine terrace) to oxygen isotope stage 5c, *c.* 100 ka. A summary of the covered stratigraphy and pollen assemblages at this site follows.

##### Stratigraphy

A linear rise that extends inland northwest from the Waingongoro River is interpreted to represent the buried riser between the Inaha and Rapanui Terraces (McGlone *et al.*, 1984). Further to the west the riser is deeply buried beneath the Opunake Formation. Present coastal erosion has removed the Inaha strandline southeast of the Waingongoro River for *c.* 15 km to a point *c.* 1.5 km southeast of the Manawapou River where the Inaha strandline once again intersects the coast. The WCS at the base of the section is an angular unconformity underlain by the Pliocene Riverdale Formation, a sandy mudstone (McKee, 1984) that dips at *c.* 3° to the WSW. Above the unconformity lies a 0.3 m-thick gravel unit consisting of rounded to subrounded Pliocene sandstone and andesitic boulders up to 0.74 m in diameter, the softer sandstone cobbles being extensively bored by worms and molluscs. Marine fossils within the bored boulders, identified by Dr A.G. Beu (in McGlone *et al.*, 1984) as the mussel *Lithophaga (Zelithophaga) truncata*, confirm the marine origin for this surface. Above,

1.9 m of weakly cross-laminated andesitic sand with minor pebbles and cobbles overlies the basal gravel. This entire unit which fines upwards was formally named by McGlone *et al.*, (1984) the Inaha Formation. Immediately above lies a thin (<0.3 m) lignite, informally named Inaha zone A, (Figure 4.2), which passes sharply upwards into 0.3 m of andesitic gravel. A 0.4 m-thick grey carbonaceous tuff designated Inaha zone B (McGlone *et al.*, 1984) sharply overlies these gravels, and near its top, thin sand lenses intercalate. A prominent tephric lignite *c.* 1.2 m thick formally named the Manaia Lignite by McGlone *et al.*, (1984), overlies the tuff. The Manaia Lignite forms a protruding ledge, and contains wedges of sand up to 0.14 m thick. McGlone *et al.*, (1984) referred to this lignite as Inaha zone C. Above the lignite, 3.5 m of coarse grey and yellow-brown sands grade up to 1.6 m of bedded tephric lignite. This lignite represents Inaha zone D and also contains thin sand lenses. It is overlain by 1.8 m of laminated silts and sands which contain thin allophanic tephtras (McGlone *et al.*, 1984). Above lies an 0.8 m-thick lignite and blocky tuff, containing numerous thin pumiceous tephra and sand beds which is assigned to Inaha zone E. Grey andesitic sands and gravels 3.35 m thick lie above which are in turn buried by a 10 m-thick debris avalanche deposit correlated to the Stratford Formation (McGlone *et al.*, 1984) (section 3.5.2). Above the Stratford Formation a tephric lignite *c.* 1.2 m-thick is referred to as Inaha zone F. The lignite contains pumiceous sand lenses and is overlain by a 9.1 m-thick sequence of andesitic sands and gravels that are in places channelled and show weak cross laminations. McGlone *et al.*, (1984) correlated these sediments with distal highly aqueous deposits of the Opunake Formation (Figure 4.1). Capping the terrace at the Inaha site is 1.5 m of volcanic loess and ash.

### **Pollen zone summary (after McGlone *et al.*, 1984)**

#### **Inaha zone A**

Levels of Gramineae are around 39-52% and shrubland pollen is moderately high, comprising Compositae, *Dacrydium bidwillii* type and *Coprosma*. Levels of tree pollen, mainly *Nothofagus fusca* type, are low at 2-3%. McGlone *et al.*, (1984) interpret that the regional vegetation at this time was predominantly grassland, with a considerable shrub component. Forest was very restricted, most probably confined to sheltered areas inland. Inaha zone A is correlated with the early part of oxygen isotope stage 5b (McGlone *et al.*, 1984).

#### **Inaha zone B**

Zone B is similar to zone A in that grassland and shrubland, with areas of open ground were dominant. Forest during this period was restricted to inland areas. Inaha zone B is also correlated to oxygen isotope stage 5b.

#### **Inaha zone C**

The most detailed pollen sequence at the Inaha section is obtained from the Manaia Lignite which is subdivided into 4 subzones, C1-C4 (Figure 4.2). Subzone C1 is defined by initially high but rapidly dropping Gramineae percentages, and by very low levels of tree pollen. However in subzone C2, tree pollen values increase from previous levels of 3% to over 60%. The common tree types at this time were *Dacrycarpus dacrydiodes* and *Podocarpus spicatus*. Also present in the area at low levels were *Dacrydium cupressinum*, *Elaeocarpus*, *Nothofagus*, and *Libocedrus*. Throughout the subzone Gramineae percentages drop from 10% to negligible levels. Shrubland pollen

was much reduced in comparison to subzone C1, but still comprised similar vegetation types.

During subzone C3, *Dacrycarpus* undergoes a steady decline falling to levels as low as 1-2%; however *Plagianthus* and *Dacrydium cupressinum* remain unchanged with *Libocedrus* and *Nothofagus menziesii* consistently present. Shrubland pollen increases slightly and mire herb pollen recovers to be abundant in this subzone.

Gramineae increases up to 40% at the top of subzone C4, with levels of *Podocarpus spicatus* dropping steadily from 13 to 3% and *Dacrycarpus* falling to trace amounts. During subzone C4, grassland spread and forest became restricted.

McGlone *et al.*, (1984) correlated zones C1-C4 with oxygen isotope stage 5a (Figure 4.1).

#### **Inaha zone D**

Inaha zone D is similar to subzone C4 where the main vegetation was shrubland with fluctuating amounts of grasses. Some forest was present, probably in the hilly interior of the area and consisted of *Podocarpus spicatus* with small patches of *Nothofagus* and *Dacrydium cupressinum* trees. McGlone *et al.*, (1984) correlated Inaha zone D with oxygen isotope stage 4 (Figure 4.1).

#### **Inaha zone E**

Gramineae percentages are high in the lower part of zone E but fall quickly to 4%, then slowly rise to *c.* 50% at the top of the zone. *Dacrydium bidwillii* type pollen becomes common in the upper part of the zone and is the first substantial appearance of this taxon since subzone C1 (stage 5a). In the lower half of zone E, mire herbs are

dominated by Cyperaceae and *Leptocarpus*, and in the upper part by *Phormium*, *Leptocarpus* and Cyperaceae. The shrubland pollen is dominated by *Coprosma* and *Myrsine*. There was no podocarp-hardwood forest near the site at this time, however *Nothofagus menziesii* may have been present in pockets inland. McGlone *et al.*, (1984) tentatively correlated zone E with the early part of oxygen isotope stage 3 (Figure 4.1).

### **Inaha zone F**

This zone was subdivided into 3 subzones (F1-F3). The 1.2 m-thick tephric lignite from which the pollen sequence was obtained directly overlies the Stratford Formation debris-avalanche deposit (Figure 4.2). Subzone F1 is dominated by shrubland/grassland type pollen. It has moderately high Gramineae (21%), high Compositae (60%) and very low tree pollen values. The mire herb assemblage is completely dominated by *Leptocarpus*.

Subzone F2 is characterised by very high percentages of *Dacrydium bidwillii* type shrubs and significant amounts of Compositae and *Coprosma* pollen. *Nothofagus* and *Libocedrus* make up the low tree pollen values. *Leptocarpus* falls from 60% to 4%, while throughout the subzone, Cyperaceae and Gramineae values are moderate. During subzone F2 the landscape was still treeless being dominated by shrubland and grassland. The subzone is distinguished by the presence of *Dacrydium bidwillii*.

Throughout subzone F3 *Dacrydium bidwillii*-type shrub pollen drops from high values to an average of 4%. Tree pollen values rise to become relatively common, represented by *Libocedrus*, *Nothofagus fusca* type, *N. menziesii*, *Podocarpus spicatus*, and *Dacrydium cupressinum*. McGlone *et al.*, (1984) suggested that during this period *Dacrydium bidwillii* group shrubs may have been excluded from the local vegetation by

the development of a mire into an extensive, raised bog. The immediate area was still dominated by shrubland/grassland, but there is a noticeable increase in trees which grew in sheltered areas inland. Zone F was correlated with the later part of oxygen isotope stage 3 (McGlone *et al.*, 1984).

### **4.3 Ararata Road Section** (after Bussell, 1993)

The Ararata Road section (section #40, Figure 3.1) is situated on the Ngarino Terrace *c.* 4 km inland from Hawera at grid reference Q21/229189 (Bussell, 1993). A prominent road cutting exposes a polleniferous tephric lignite *c.* 5.2 m thick. The lignite overlies a sequence *c.* 30 m thick, consisting of basal pebbly marine sand, interbedded andesitic debris flow, tephra, tuff and alluvium (Figure 4.2). A distinctive tephra sequence within the lignite is considered by Alloway (1989) to be 70-110 ka and is correlated with the Epiha Tephra. This age range is in broad agreement with an amino acid racemisation date of a wood sample from the lignite which yielded an age estimate of 80 +/- 20 ka (Bussell, 1993). Subsequent palynological interpretation of the lignite by Bussell (1988, 1993) concluded that the pollen sequence displayed vegetation patterns consistent with oxygen isotope stage 5. Based on the age constraints and the dominance of forest taxa he correlated the lignite with oxygen isotope stages 5d, 5c and 5b (Figure 4.1).

A summary of the covered stratigraphy and pollen zones at the Ararata Road section follow.

## Stratigraphy

At the base of the section an angular unconformity at 67 m a.s.l. is cut into Pliocene mudstone of the Tangahoe Formation and is inferred to represent the Ngarino WCS. 1.5 m of dark grey andesitic pebbly marine sand overlies the WCS (Figure 4.1). The marine sand is overlain by a 1.2 m-thick grey/brown andesitic tuff. A sharp contact above separates a light grey pumiceous pebbly sand unit which may be up to 10 m thick, but is not exposed. Further up in the sequence another grey/brown andesitic tuff *c.* 1.5 m thick is unconformably overlain by light grey laharic breccia. The upper contact of the breccia is not exposed but has a maximum possible thickness of *c.* 3.5 m. A medium brown andesitic tuff *c.* 2 m thick is exposed between two obscured sections. At 12 m depth a 0.5 m thick pink and white mud unit is overlain by 1.5 m of light grey, cross-bedded, pumiceous, pebbly sand (Bussell, 1993). Overlying the sand, yellow/brown andesitic tephra grades upward into light grey andesitic tuff then black lignite from which pollen samples were collected. Above the lignite 3 m of volcanic loess which contains white, bedded andesitic tephra and fossil rootlets caps the sequence.

### **Pollen zone summary** (after Bussell, 1993)

#### **Zone AR1** (9.0-7.8 m)

Shrub pollen is common throughout this zone with *Coprosma* highest at the base (66%) and declining upwards. *Nothofagus*, *Metrosideros* and *Nestegis*, in contrast with other hardwood pollen, is persistent at low values. *Pruminopitys taxifolia* and *Libocedrus* pollen are predominant and show an increase at the top of the zone. *Dacrydium cupressinum* and *Nothofagus fusca*-type pollen are also persistent at values < 10%.

Grass pollen values increase upwards from the base to peak at 28% in the middle of the zone, then decline to low values at the top of the zone. Swamp pollen is dominated by Cyperaceae with Restionaceae becoming abundant towards the top of the zone, with fern spores common throughout.

**Zone AR2 (7.8-6.1 m)**

A sharp increase in *Dacrydium cupressinum* pollen marks the base of this zone. It becomes the dominant tree with common *Prumnopitys taxifolia* with *Libocedrus* declining to become rare at the top of the zone. Grass pollen values decline upwards along with *Coprosma* and *Leptospermum*-type pollen. *Metrosideros* pollen becomes more common than in zone AR1 and *Dracophyllum*-type pollen increases to become common.

**Zone AR3 (6.1-3.8 m)**

The lower part of this zone is marked by the replacement of *Dacrydium cupressinum* by *Prumnopitys taxifolia* as the dominant tree type. *Nothofagus menziesii* pollen is now persistently present at low values. Shrub pollen values rise with an increase in *Coprosma* and the first appearance of *Halocarpus* pollen at the top and bottom of the zone. *Metrosideros* pollen also becomes sparse. Grass pollen values also show a rise in this zone.

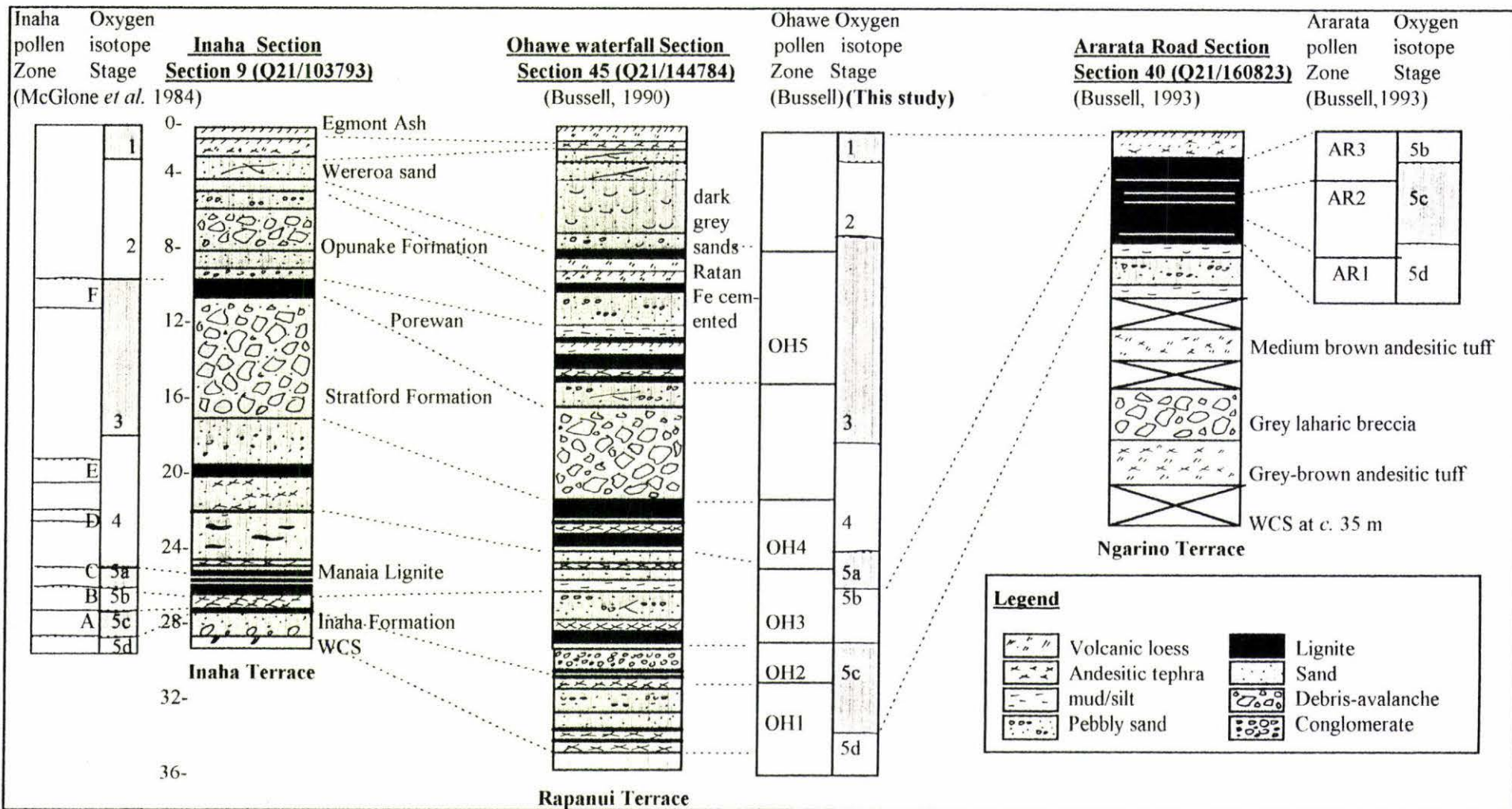


**Figure 4.1** Oxygen isotope stage correlation of the stratigraphy and pollen zones between the Inaha section (after McGlone *et al.*, 1984), Ohawe waterfall and Ararata sections (after Bussell, 1990 and 1993).

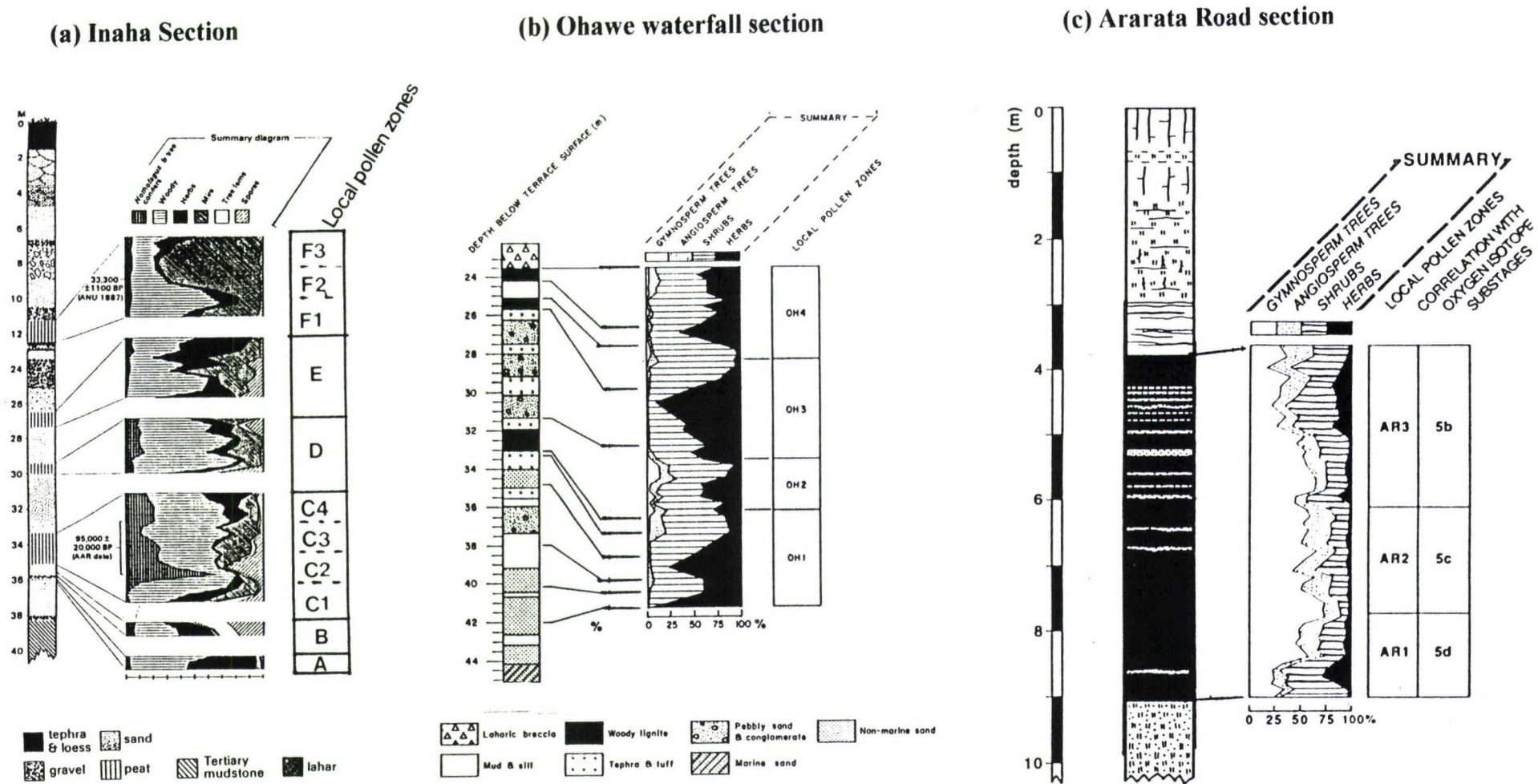


**Figure 4.2** Pollen diagrams and local pollen zones of (a) Inaha section (McGlone *et al.*, 1984) (b) Ohawe waterfall section (Bussell, 1988) and (c) the Ararata Road section (Bussell, 1993).

#### 4.4 Correlation

Figures 4.3 and 4.4 summarise the proposed correlation of the coverbeds and their local pollen zones between the Inaha, Ohawe Waterfall and Ararata Road sites.

At the Ohawe waterfall section, zone OH1 overlies marine sediments *c.* 14 m thick deposited during a period of relatively high sea level and warm climate. The shell bed overlying the WCS below is interpreted to have been deposited in a sheltered embayment or protected waters during the oxygen isotope stage 5e (section 3.7). As relative sea level dropped a broad alluvial plain developed. Sediment supply was high at this time and resulted in conditions unfavourable for deposition of thick fine-grained polleniferous sediment.

Grass pollen is dominant in the lower part of zone OH1 and declines upwards whilst shrub pollen rises during this time representing a general warming. Both pollen zones AR1 and OH1(stage 5d) show that grass pollen values are relatively high and decline upwards (Figure 4.2). During this time shrub and small tree taxa are common being dominated by *Leptospermum* and *Coprosma*, the latter increasing upwards at the Ohawe site and decreasing upwards at the Ararata site. In zone AR1 shrub pollen declines and tree pollen values begin to increase with *Prumnopitys taxifolia* and *Libocedrus* predominant, and *Dacrydium cupressinum* and *Nothofagus fusca* present. Bussell (1993) thus interpreted that zone AR1 represents the later stages of oxygen isotope stage 5d. In contrast at the Ohawe Waterfall site pollen zone OH1 shows tree pollen values are sparse except for *Nothofagus* type. However at the top of the zone, above a barren section, shrub pollen rises to 87% and represents a warming of climate at the beginning of stage 5c.

At this time Egmont Volcano was active resulting in deposition of an andesitic tuff at the top of the zone. The tuff is here correlated to the Ninia Tephra dated at between 100 and 115 ka (Alloway, 1989). On the the basis of pollen trends and the interbedded tephra zone, OH1 is correlated with middle to late oxygen isotope stage 5d, dated at *c.* 115-110 ka (Figure 4.3).

Zone OH2 is characterised by abundant but declining grass and shrub pollen, and tall trees such as *Prumnopitys taxifolia*, *Dacrydium cupressinum*, and *Nothofagus menziesii* are more common than before (Bussell, 1988). Pollen zone OH2 shows similar trends to zone AR2 to which it is correlated and represents the transition to oxygen isotope stage 5c. As the climate warmed, grass pollen values decreased at both sites. The lower part of zone OH2 below the barren zone is here interpreted to represent early to middle oxygen isotope stage 5c (Figure 4.3). The middle of the zone (34.0-34.7 m) containing dark grey laminated fine sands is devoid of pollen. Late in zone OH2 expansion of forest is indicated by the rise in *Dacrydium cupressinum*, *Prumnopitys taxifolia*, and *Nothofagus menziesii* whilst grass pollen values dropped, probably representing middle to late stage 5c. The pollen assemblage suggests that at this time the local vegetation was a mixed shrubland-sedge-*Phormium*-fern community, but identification of fossil wood shows small trees and shrubs such as *Halocarpus*, and *Dracophyllum* were growing locally. During late stage 5c, river channels became entrenched and more restricted than before, with increasing areas stable for longer periods providing shelter and explaining the expansion of forest in protective areas. The carbonaceous andesitic tuff at the top of the zone was probably deposited within fine-grained overbank deposits. The tuff is considered to be a correlative of the older representatives of the Epiha Tephra.

At this time towards the southwest the Inaha Terrace was being cut, the surface expression of which is seen *c.* 2.5 km to the west. Sea level at this time was probably *c.* -15 m below present.

During the transition from zone OH2 to OH3 overbank deposits at the top of Zone OH2 developed into a peat-forming environment, with a laterally continuous lignite layer, that contains frequent additions of andesitic tephra. In this zone grass pollen rises to a maximum of 90% and the local swamp vegetation is interpreted to have contained *Myriophyllum* in open water areas with rush-sedge-*Phormium* dominant around the margins. The lower part of zone OH3 is here correlated with early oxygen isotope stage 5b (Figure 4.4). At the top of zone OH3, grass pollen values drop sharply to <5% whilst shrub pollen remains common throughout the zone. This is here interpreted as the transition from stage 5b to 5a. The Ararata Road and Inaha sites record more completely the vegetation during oxygen isotope stage 5b (Figure 4.2, Inaha zones A and B, zone AR3), with both sites recording increases in grass and shrub pollen. At Ararata Road, *Dacrydium cupressinum* pollen values drop with *Nothofagus menziesii* present at low values, similar to the Inaha site. Zones OH3 and AR3 both show an increase in *Halocarpus* pollen values and in both cases it becomes common for the first time.

As climate cooled and sea level fell, rapid alluvial aggradation of volcanic sediment occurred. Light grey pumiceous pebbly sands representing channel deposits overtop the lignite and andesitic tuff. Sea level rose briefly during stage 5b (Figure 2.3), and rivers once again deposited fine-grained tephric overbank and pond sediments (29.5-30.5 m). A drop in sea level late in stage 5b lead to deposition of another alluvial channel deposit (29.5-28 m).

Grass pollen values are low at the base of zone OH4, but above a barren section become dominant in the upper part of the zone, with shrub pollen remaining common throughout. Zone OH4 is here interpreted as the transition from stage 5a to stage 4 (Figure 4.3). During this time volcanoclastic sedimentation rates decreased and the floodplain became stabilised for a period of time with deposition of *c.* 2.5 m of woody tephric lignites and carbonaceous muds. At the Inaha section, oxygen isotope stage 5a is represented by pollen subzones C1-C4 (Figure 4.3). Throughout these subzones *Gramineae* levels decline, indicating warming climate, followed by an increase representing the transition to oxygen isotope stage 4. Tree pollen values are low, consisting principally of *Dacrydium cupressinum* and *Nothofagus menziesii*. In comparison to zone OH2, correlated with stage 5c, stage 5a did not experience the same degree of forest expansion. The oxygen isotope record (after Martinson *et al.*, 1987) shows that stage 5c lasted longer than stage 5a; perhaps the short period of warming during stage 5a did not allow the forest to expand in Taranaki to the same degree as in stage 5c.

Oxygen isotope stage 4 is represented by Inaha zones D and E, consisting mainly of shrubland with varying amounts of grassland (McGlone *et al.*, 1984). During this time, although tree pollen values remained low, small pockets of forest consisting of *Dacrydium cupressinum* and *Nothofagus* existed in sheltered areas further inland. At the Ohawe waterfall section, stage 4 is represented by zone OH4 which shows grass pollen values increasing to become dominant at the top of the zone. This represents the transition from stage 5a to 4 and a cooling climate. During this period unit L3 was forming in the southeast sector.

The base of zone OH5 overlies the Stratford Formation and is characterised by light grey pumiceous pebbly sands representing fluvial reworking of the debris avalanche. Deposition of carbonaceous mud and a thin lignite followed as the floodplain stabilised. During zone OH5 warming allowed reinvasion of forest to the South Taranaki lowlands (Bussell, 1988). The lower part of zone OH5 is correlated with early stage 3 (Figure 4.4) and represents the time period during which the soil on L3 was forming in the southeast sector. *Dacrydium cupressinum* and *Metrosideros* pollen are common in the lower part with *Ascarina* pollen appearing for the first time in the sequence. At the Inaha site, pollen zone F records moderately high *Gramineae* levels, however there was a noticeable increase in trees such as *Nothofagus menziesii*, *Dacrydium cupressinum* and *Libocedrus*. The immediate area was dominated by shrubland/grassland with the increase in forest again most probably restricted to sheltered areas further inland (McGlone *et al.*, 1984).

The upper part of zone OH5 overlies another pumiceous pebbly sand unit formed as sea level dropped and rivers aggraded *c.* 50 ka (Figure 2.3). This pebbly sand is correlated to the Inaha section (Figure 4.1) and is interpreted to represent distal fluvially reworked deposits of the Opunake Formation. The topmost sample horizon (Figure 4.2) overlies an iron-cemented horizon and a tephric-rich volcanic loess unit. This latter unit is interpreted as representing a period of time during which the terrace surface became stable for a relatively long period of time and climate warmed sufficiently to allow forest to become established in the area. The volcanic loess unit contains fossil rootlets and is lapilli rich and is here correlated to unit L2 in the southeast sector which ceased accumulating *c.* 28 ka, late in stage 3. In the upper part of zone OH5 *Prumnopitys taxifolia* pollen is dominant. Evidence from elsewhere in New Zealand indicates that the period around 30 ka was one of the warmest and wettest of

the Late Otiran. Inaha zone F (McGlone *et al.*, 1984) represents this period of time and is correlated to zone OH5 at the Ohawe Waterfall Section.

| Stage | Inaha section (McGlone <i>et al.</i> , 1984)  | Ohawe waterfall section (Bussell, 1988)  | Ararata Road (Russell, 1993) |
|-------|---|--|------------------------------|
| 4     | <p><b>Inaha zone F1</b><br/>           *Moderately high <i>Gramineae</i> (21%)<br/>           *High <i>compositae</i> (60%)<br/>           *Mire herbs dominated by <i>Leptocarpus</i><br/>           *Low tree pollen</p> <hr/> <p><b>Inaha zone F2</b><br/>           *<i>Gramineae</i> moderate<br/>           *High <i>Dacrydium bidwilli</i>, other shrub include<br/> <i>Coprosma</i> and <i>compositae</i><br/>           *<i>Leptocarpus</i> falls (60-4%)<br/>           *Tree pollen low, mainly <i>Nothofagus</i> and<br/> <i>Libocedrus</i></p> |  |                              |
| 3     | <p><b>Inaha zone F3</b><br/>           *<i>Gramineae</i> generally high but low in middle of zone<br/>           *<i>Leptospermum</i> and <i>D. bidwilli</i> decline, other shrubs<br/>           include <i>Coprosma</i>, <i>Compositae</i> and <i>Myrsine</i><br/>           *<i>Lepocarpus</i> dominant<br/>           *<i>Libocedrus</i>, <i>N. fusca</i>, <i>N. menzeisii</i>, <i>Podocarpus</i><br/> <i>spicatus</i> and <i>Dacrydium cupressinum</i> common<br/>           *Noticable increase in trees</p>  | <p><b>OH5</b><br/>           *Shrub and grass less comon<br/>           *<i>Gunnera</i> and <i>Myrsine</i> common at top of<br/>           zone<br/>           *<i>Ascarina lucida</i> present<br/>           *High values of arboreal pollen esp.<br/> <i>podocarp</i><br/>           *<i>Dacrydium cupressinum</i> and <i>Metrosideros</i><br/>           dominant in lower half of zone<br/>           *<i>Prumnopitys taxifolia</i> dominant at top of<br/>           zone</p> |                              |

**Figure 4.3** Summary diagram showing the correlation of the Ohawe waterfall pollen zones to the pollen zones at Inaha (after McGlone *et al.*, 1984) and Ararata Road (after Bussell, 1988).

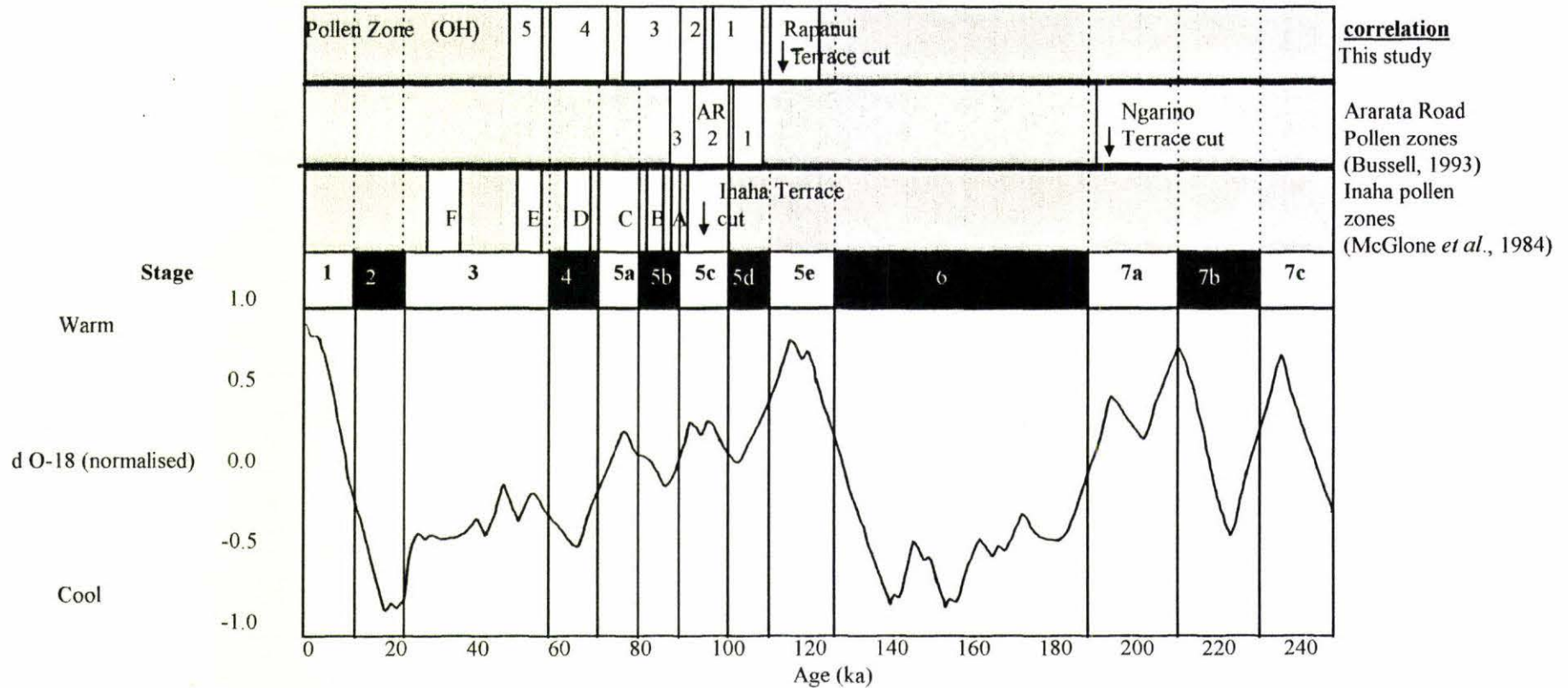


**Figure 4.4** Correlation of Ohawe waterfall pollen zones OH1-OH5 (after Bussell, 1988) to Inaha pollen zones A-F (after McGlone *et al.*, 1984) and Ararata pollen zones AR1-AR3. The Ohawe site, previously mapped as the Ngarino Terrace by Bussell (1988) is now mapped as the Rapanui Terrace based on the new correlation (this study) of the Ohawe pollen zones and the covered stratigraphy.

#### 4.5 Conclusions

The Ohawe Waterfall and Inaha sites are located on the Egmont ring plain and in close proximity to the Waingongoro River (Figure 3.1). Sediments above the WCS at both the Ohawe waterfall and Inaha sites indicate broad flat alluvial floodplains frequently inundated with volcanoclastics, which are subsequently reworked. However, palynological interpretation of the Inaha section by previous workers (eg. McGlone *et al.*, 1984) has been carried out in conjunction with detailed stratigraphic study of the coverbeds. In particular this involved correlation of the Opunake and Stratford Formations, the latter being thickest in the northwest of the study area (Palmer *et al.*, 1991) and mapped to the Ohawe Waterfall site.

In contrast to the Inaha and Ohawe waterfall sections, the Ararata Road section (section 40) *c.* 15 km inland of the Ohawe Waterfall site, provides a well dated and relatively stable depositional environment from which pollen samples were examined by Bussell (1988). The site contains *c.* 5.2 m of continuous tephric woody lignite containing tephra correlated with the Epiha Tephra, considered to have been erupted between 80-100 ka (Alloway, 1989). The Ararata site is located on the 210 ka Ngarino Terrace (Bussell, 1988, 1993) and is further from the coast than the Ohawe site. At the base of the section, light grey pumiceous pebbly sands represent relatively short periods when volcanoclastic deposits filled local river and stream beds. Following this, fluvial reworking of the deposits resulted in deposition of the pumiceous sands across the gently sloping terrace surface. The Ararata site with its infrequent inundation by volcanic debris flows by oxygen isotope stage 5, suggests it was sufficiently distal from Egmont Volcano to support mature forest for long periods of time providing the climate was favourable. During oxygen isotope stage 5e sea level rose to *c.* +5 m relative to

present. Situated on the Ngarino Terrace and influenced less by any rapid aggradation on the Egmont ring plain the pollen preserved in the Ararata lignite clearly records the vegetation present 80-100 ka when on the lower terrace, a high sea level cut the Inaha Terrace. Low rates of fluvial deposition at this site allowed vegetation to respond directly with changing climate during this period without significant volcanic or fluvial disturbance. The Ohawe Waterfall Section by comparison has recorded successive periods of recolonisation by the local vegetation, which consisted mainly of shrubland and bare ground. Bussell (1993) found that in some samples at the Ararata Road section that over representation of local pollen was occurring. It is suggested that this has also occurred at the Ohawe waterfall section resulting in the over representation of grass/shrubland which has masked the presence of forest taxa.

In north Taranaki, Alloway (1989) mapped two formations, the Okawa (debris avalanche deposit *c.* 100 ka) and Motonui (lahar deposit *c.* 115 ka) formations. To date they have not been mapped in south Taranaki. Pollen samples from above and below the Okawa Formation which overlies the NT2 (Rapanui) marine terrace (Alloway, 1989) show the same floristic mixture after the event as that before. However pollen levels were reduced and the forest apparently had an open canopy with areas of grassland/shrubland.

The lignite above the Okawa Formation accumulated quietly over the time period of stage 5*c*. In contrast at the Ohawe Waterfall Section thin pollen-bearing horizons represent relatively short periods of time after the landscape and vegetation in the region was frequently inundated by volcanoclastic and fluvial sediments. Pollen spectra from these lignaceous horizons would contain high levels of rush-sedge swamp type vegetation.

In this area, interpretation of the stratigraphy above the marine sediments records periods of laharic breccia inundation and fluvial reworking followed by volcanic loess and tephra deposition at the top of the section. This shows a progression in the development of depositional environments on the terrace. Deposition initially, is characterised by rapid sedimentation and fluvial reworking followed by a decrease in sedimentation rates as the uplifting terrace is removed from the ring-plain environment. At this stage slowly accumulating lignites and volcanic loess units would have been deposited.

## **Chapter Five**

### **Terrace uplift, deformation and preservation**

#### **5.1.1 Introduction**

Pillans (1983, 1990) demonstrated that the marine terrace sequence between Hawera and Wanganui has undergone variable uplift and deformation. The uplift model he used was based on shore-normal hinging type uplift, with the zero isobase (point of zero uplift) offshore of the present coastline. If uplift is of the hinging type then older surfaces inland would be expected to be tilted more steeply than the younger surfaces closer to the coast. He also studied shore-parallel deformation and produced a model based on a local doming-type uplift. This doming was shown to be greatest in the vicinity of Waverley, close to the Nukumaru Fault Zone.

This section aimed to investigate how uplift and deformation has proceeded with time in the study area. To obtain a greater understanding of the nature of deformation and distribution of the terraces, the Brunswick Terrace (310 ka) was included in this portion of the study. The extent and age of the Brunswick Terrace is also well known (Pillans, 1990) and its inclusion in this chapter provides extra data upon which to compare rates of deformation of the younger Rapanui and Ngarino Terraces. The previous section which outlined the stratigraphy of the marine terraces has been used to provide the chronologic framework upon which the ages of the marine terraces are derived. Once the age of the marine terrace strandline has been established, it is possible to calculate rates of uplift and deformation. The results are then interpreted to show how deformation of the marine terraces is related to the crustal dynamics associated with the South Taranaki Basin (STB), South Wanganui Basin (SWB), Nukumaru Fault Zone (NFZ) and the Taranaki Fault Zone (TFZ).

#### **5.1.2 Methodology**

A structural contour map, of the wave-cut surface (WCS) (Figure 5.1) was constructed using WCS height data, obtained from field observations. Spot heights of

the WCS were particularly important northwest of Manutahi, where previously the location of the Rapanui strandline was uncertain. A large number of spot heights were collected from along the Manawapou River, Tangahoe River, and Tawhiti Stream valleys. Spot heights from Pillans (1990) were also used. The spot heights were obtained using two Paulin surveying barometers. The barometers were calibrated by setting the height at a trigonometric station where the height was accurately known. One of the barometers was then taken as quickly as possible to a home station, and the height accurately recorded. Before each journey into the field both barometers would be set to the known height. While in use the home barometer height was recorded every ten to thirty minutes depending upon the rate of change of atmospheric pressure. When the weather was stable such as in the middle of a large anticyclone, readings were only taken every thirty minutes. By accurately recording such changes, a smooth time versus height curve could be established for the period of observations. When measuring spot heights both the height and the time of the measurement were thus recorded. At the end of the day the changes in height due to weather patterns crossing the study area could be compensated by applying a correction to the field height reading. The accuracy of surveyed WCS heights is estimated to be  $\pm 3$  m. Where evidence for a WCS, such as the presence of rounded cobbles and/or borings on the contact between marine coverbeds and the underlying mudstone could not be seen, the measured height was taken as a minimum value. This was principally due to the observation that along the larger river valleys, erosion of the valley sides and the top of the impermeable mudstone may have lowered the height of the WCS (top of the mudstone).

### **5.2.1 Structural contours**

Using the spot height data a structural contour base map was produced. Figure 5.1 shows the structural contours and the revised distribution of the Rapanui and Ngarino Terraces in this area. The position and orientation of structural contours on the WCS is also determined for the Brunswick, and Inaha Terraces. Generally the structural contour lines parallel both the present coast and probably would have been parallel to

the paleocoastlines (terrace strandlines) at the time they were last active. Between Kakaramea and Manutahi, the structural contour lines swing towards the coast, indicating an area of greater uplift. West of Manutahi towards the Manawapou and Tangahoe Rivers, the contours then swing inland to trend north-northwest (Figure 5.1), indicating lowering uplift rates westwards and a change in the direction of shore-normal deformation.

### 5.2.2 Shore-normal terrace gradients

Gradients on the terraces were accurately determined from the structural contour map by drawing transects extending inland from the coast, normal to the structural contours. Figure 5.1 shows the location of Transects A-A' to D-D'; Table 5.1 shows the terrace gradients. The transects were orientated as best as possible parallel to the dip direction of the terrace treads.

| Terrace   | Transect ( terrace gradient in degrees ) |      |      |      |
|-----------|--|------|------|------|
|           | A-A'                                     | B-B' | C-C' | D-D' |
| Inaha     | ----                                     | ---- | ?    | 0.14 |
| Rapanui   | 0.25                                     | 0.36 | 0.43 | 0.61 |
| Ngarino   | 0.56                                     | 0.44 | 0.27 | 0.66 |
| Brunswick | 0.93                                     | 1.06 | 0.52 | 0.41 |

**Table 5.1** Terrace gradients along Transects A-A' to D-D' (shown in Figure 5.1). Note that the Inaha Terrace is not present on Transects A-A' and B-B', and at C-C' there is insufficient height data on the Inaha WCS.

Generally terrace gradients are lowest to the west of the Tangahoe River (Transect A-A') and increase eastwards. North of the Tangahoe River along Transect A-A' gradients however remain relatively high on the Ngarino (0.56°) and Brunswick Terraces (0.93°) (Figure 5.3). It is interpreted that the two terraces here cross the TFZ. Transect B-B' which also crosses the Tangahoe River shows the largest gradient range

from a low of  $0.36^\circ$  to a high of  $1.06^\circ$  for the Rapanui and Brunswick Terraces respectively. This also coincides with increasing rates of uplift across the TFZ, inland of Mokoia. The river appears to mark the boundary between decreasing uplift rates within the STB, to the west and high uplift rates (block uplift) to the east within the TFZ towards Kakaramea. Across the TFZ, Transect C-C' shows that gradients are relatively high along the coast on the Rapanui Terrace ( $0.43^\circ$ ) and decline inland on the Ngarino Terrace ( $0.27^\circ$ ). Further inland on the Brunswick Terrace, gradients increase slightly to  $0.52^\circ$ . Transect D-D' near Kakaramea shows a similar pattern whereby terrace gradient initially increases rapidly followed by a slow decrease in gradients across the terrace sequence.

### 5.2.3 Positioning of the terrace risers

A number of previous attempts have been made to delineate the position of the Rapanui strandline northwest of Kakaramea, but its position has remained uncertain. The difficulty in mapping the Rapanui strandline in this area, is due to the extensive Mokoia erosion surface, ramping of sands, and abundant volcanoclastics obscuring the Rapanui riser. The final position of the terrace risers in this study are determined from both stratigraphic and structural evidence.

Figure 5.2 shows terrace Transects A-A' to D-D'. From the transects, positions of the strandlines and heights of the terrace risers were plotted. Towards Kakaramea (Transect D-D') fossil cliff heights are *c.* 22 m for the Ngarino riser, 15 m for the Rapanui riser and 8 m for the Inaha riser. These height differences are consistent with the inferred age and height of paleo-eustatic sea level interpreted to have formed each terrace (Chapter 2).

The surface expression of the riser separating the Rapanui and Ngarino Terraces is easily observed southeast of Kakaramea, but northwest towards Hawera at least one of three things occurs.

1. The height of the cliff separating the two terraces lessens, possibly due to lower uplift rates and/or projection of the Rapanui strandline seaward.

2. Dune sands covering the Rapanui Terrace have ramped up onto the Ngarino Terrace therefore obscuring the topographic expression of the riser.
3. The Rapanui Terrace is in fact missing in this region and intersects the younger Inaha Terrace southeast of the Manawapou River as mapped by Pillans (1990).

Shore-normal transects of the WCS show that the height of the Rapanui riser near Kakaramea is approximately 15 m elevation (Figure 5.2d), while farther northwest it is *c.* 5 m (Figure 5.2a). At Manutahi, along Transect C-C', a change in the gradient of the WCS occurs approximately 3-4 km inland from the coastline and is the inferred position of the Rapanui riser. Pillans (1990) however mapped the Ngarino Terrace in the same area and drew the Rapanui riser in a more coastal position. Farther north in the vicinity of Mokoia, Transect B-B' shows a continuation of what is interpreted to be the Rapanui riser (Figure 5.2b), which here is *c.* 10 m high. The interpretation that the riser in the vicinity of Mokoia marks the Rapanui strandline is based on the change in WCS gradient and the covered stratigraphy detailed in chapter three.

### South Taranaki marine terrace distribution and structural contours

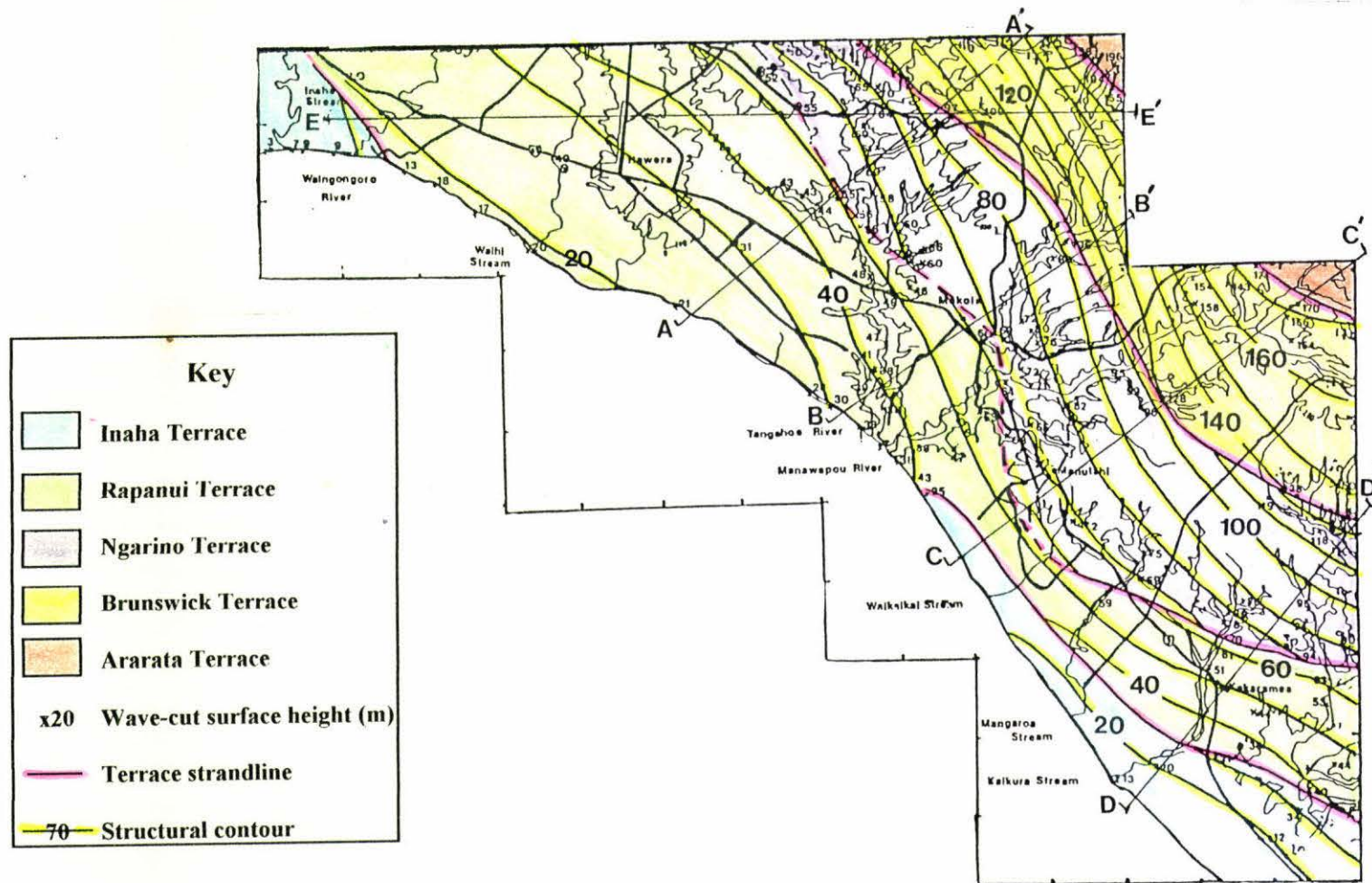


**Figure 5.1** A revised terrace distribution and structural contours of the Inaha, Rapanui, Ngarino and Brunswick WCS between Hawera and Kakaramea. Positions of Transects A-A' to E-E' are shown. Structural contour lines generally parallel the present coastline and the terrace strandlines. West of Kakaramea they swing towards the coast and indicate an area of higher uplift.

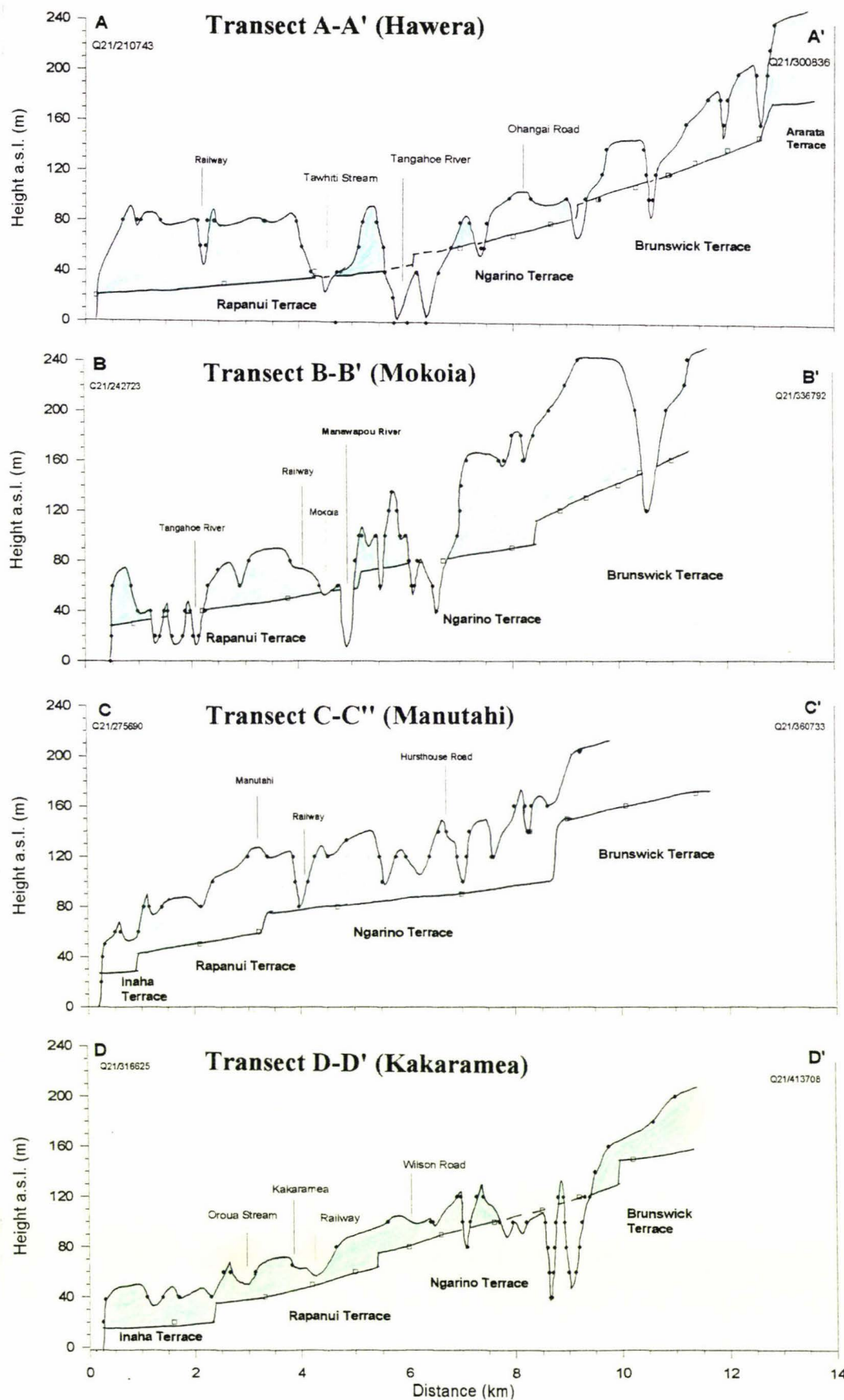


**Figure 5.2** Shore-normal transects A-A' to D-D' showing wave-cut surface heights, position of terrace risers and surface topography. Terrace gradients and risers are highest in the southeast (Transect D-D') and generally decrease westwards towards Hawera (Transect A-A').

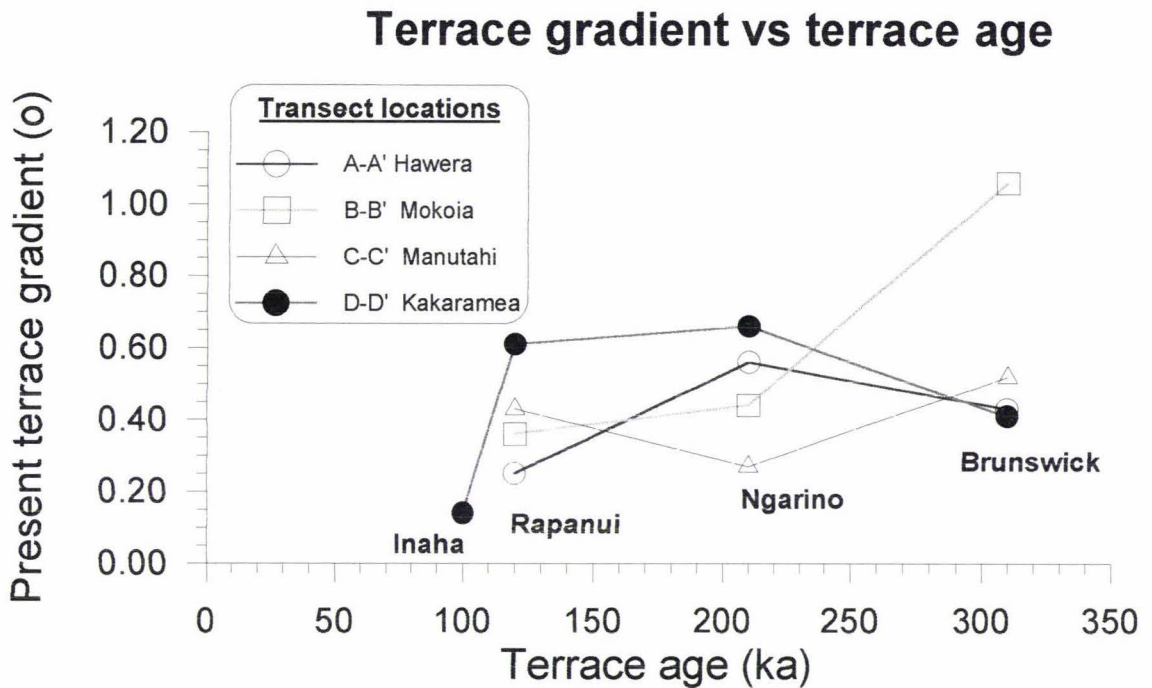


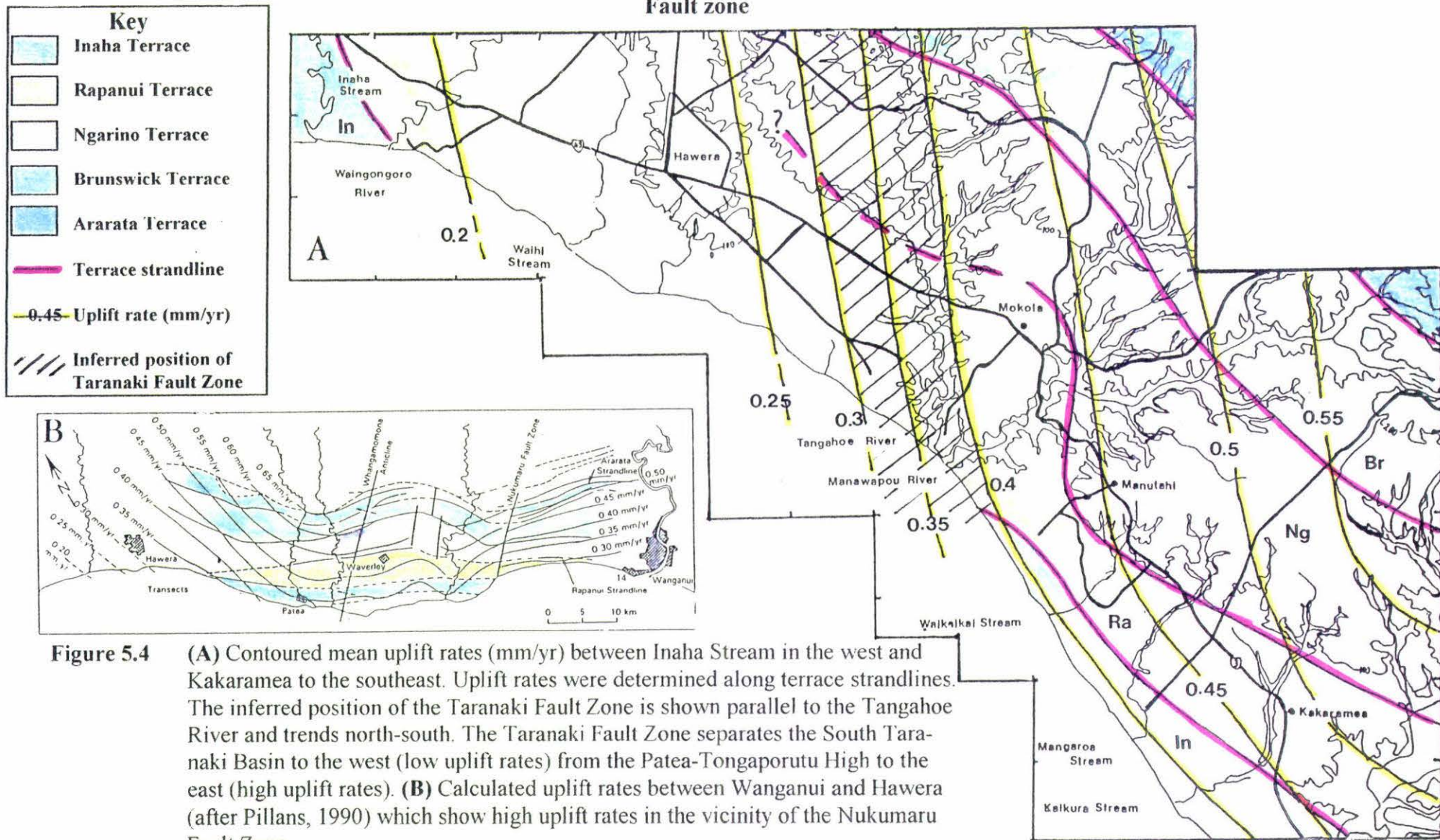
**Figure 5.3** Shore-normal terrace gradient along Transects A-A' to D'D'. The terrace gradients show the influence of the Taranaki Fault Zone to the southeast which is bounded along its western margin by the Taranaki Fault. From southeast to northwest the Transects progressively cross the boundary of the Taranaki Fault Zone. Along Transect D-D' on the Taranaki Fault Zone, gradients are increasing rapidly then subsequently decrease. Farther west at Mokoia, Transect B-B' crosses the Taranaki Fault and shows relatively low terrace gradients to the west and a sharp increase on the Brunswick Terrace as the fault is crossed. Near Hawera, terrace gradients are highest on the Ngarino Terrace which is inferred to overlie the Taranaki Fault.

### 5.3.1 Uplift rates

Uplift rates for the south Taranaki-Wanganui marine terraces were first published by Pillans (1983, 1990). He showed that uplift rates generally increased uniformly inland but in the vicinity of the Nukumaru Fault Zone uplift contour lines are offset along faults, and converge and diverge over structural basement highs. Following Pillans (1990), uplift rates are calculated using the WCS height at the terrace strandlines (Figure 5.1).

Uplift rates calculated for the study area are shown in Figure 5.4a. To the southeast towards Kakaramea uplift rates along Transect D-D' range from 0.4 to 0.55 mm/yr. They follow a similar pattern to Pillans (1990) with uplift greatest to the southeast of Kakaramea. He showed that uplift rates reach a maximum of 0.65 mm/yr inland of Waverley (Figure 5.4b). West of Manutahi however, the uplift contour lines swing further north-northwest than previously thought due to remapping of the Rapanui Terrace farther inland. The remapping has also served to increase the uplift rates immediately west of Manutahi to *c.* 0.45 mm/yr (Figure 5.4a). Towards Hawera the uplift rates quickly decrease and along Transect A-A' near Hawera (Figure 5.5a) they range from 0.25 to 0.45 mm/yr. Farther west at the Waingongoro River mouth where the Inaha strandline intersects the coast, uplift rates decrease to *c.* 0.2 mm/yr (Figure 5.5b) and near Inaha Stream a further 1.2 km west, the Inaha WCS dips westwards below sea level. West of Hawera the uplift pattern cannot be described as shore-normal due to the influence of Egmont Volcano and its associated ringplain deposits. In the absence of these volcanoclastic deposits the Taranaki coastline would presumably parallel the uplift contour lines in a similar fashion to the present coastline southeast of Patea. The south Taranaki marine terraces presumably continue northwestwards beneath the volcanics and subsequently swing northeastwards to meet the north Taranaki terrace sequence.

### South Taranaki marine terrace uplift rates and inferred position of the Taranaki Fault zone



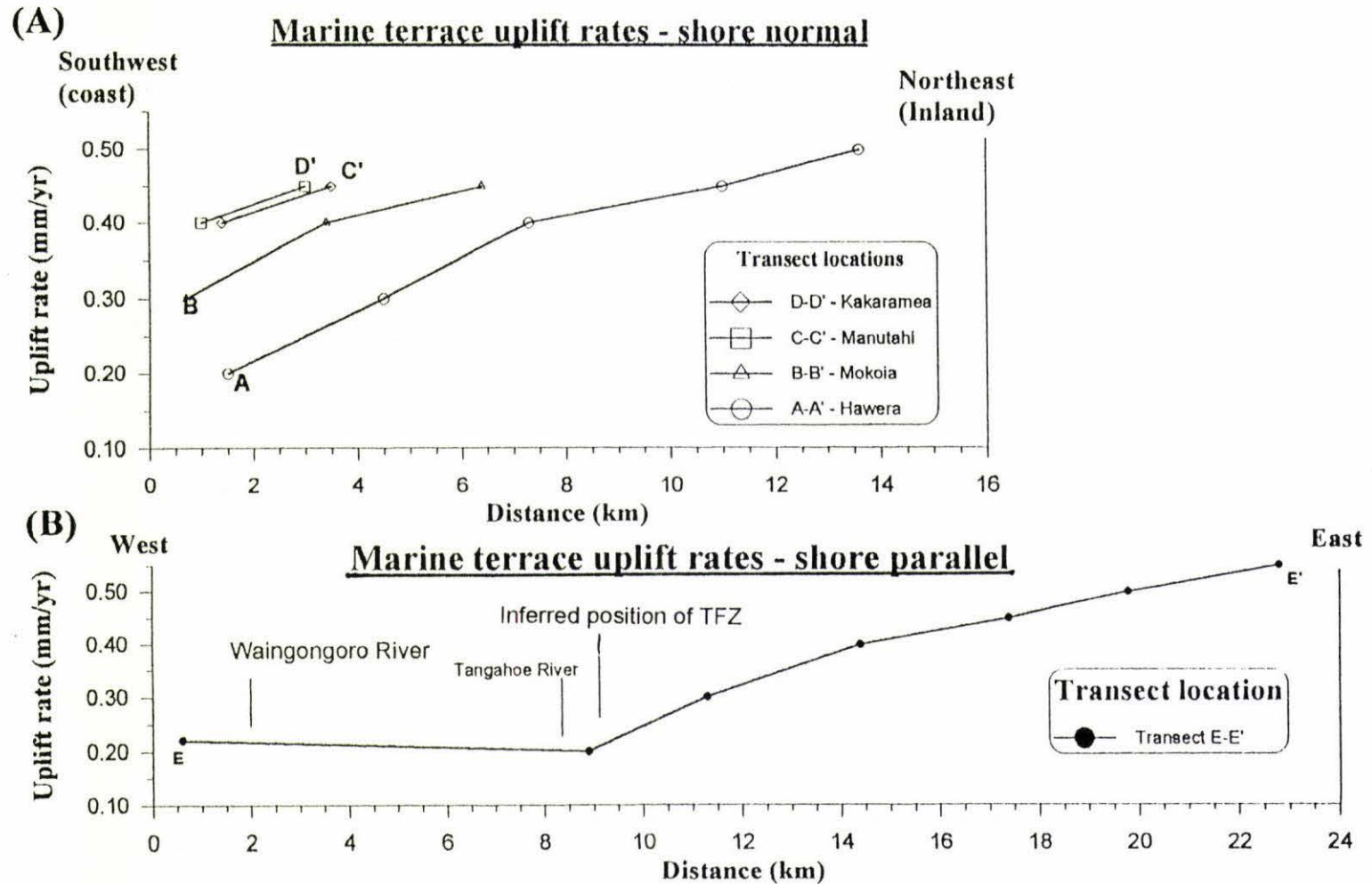


**Figure 5.5** (A) Shore-normal uplift rates along Transects A-A' to D-D'. From southeast (D-D') to northwest (A-A') uplift rates progressively decrease. Along Transect A-A' uplift rates in the vicinity of the Tangahoe River steepen and subsequently level out further inland. This area is interpreted to overlie the Taranaki Fault Zone. The other transects are situated east of this zone and show higher uplift rates that also level out inland. (B) Shore-parallel uplift rates along Transect E-E' show an increase in the vicinity of the Tangahoe River, and also marks the Taranaki Fault Zone.

## 5.4 Uplift rates over time

Strandline uplift rates calculated in the previous section (Figure 5.4) have been averaged over time with strandline ages determined from the covered stratigraphy. However over time, uplift rates may have not remained constant. If uplift rates have varied over time, the cause may be due to tectonic movement within the Taranaki Fault Zone (TFZ). In investigating the changing pattern of shore-normal uplift of the terraces, a model needs to be introduced. As with most models, a number of assumptions need to be made for simplicity. The model used here is based on the linear hinging uplift model introduced by Pillans (1981), in which uplift increases linearly inland from the coast to the c. 400 ka Ararata strandline, while further inland block uplift is assumed. Other assumptions used here are:

1. At  $t=0$  (time when strandline was last occupied for a particular terrace) the gradient on the WCS was zero or such a low gradient to be inconsequential [the initial seaward dip of the WCS surface will depend on rates of uplift and of sea level rise and fall which at the time of formation are unknown].
2. Tilting of the WCS is assumed to be at a constant rate for the period between the formation of successive terraces *i.e* rates in this work are averaged over the periods 310-210 ka, 210-120 ka and 120 ka to present.
3. Tilting is based on linear shore-normal hinging uplift (over short distances).

### 5.4.1 Results

Rates of terrace deformation (expressed as the average increase in terrace gradient with age) are shown in Table 5.2 and Figure 5.6. In the vicinity of Hawera (Transect A-A'), shore-normal deformation rates are highest for the Ngarino Terrace ( $0.27^\circ$  av/100 ka) and are lower for the Rapanui ( $0.21^\circ$  av/100 ka) and Brunswick Terraces ( $0.14^\circ$  av/100 ka). In comparison shore-normal deformation to the east along Transect D-D' has varied widely over time. Here the Inaha Terrace is preserved along

the coast and is included in Transect D-D'. In the southeast of the study area tilting rates increased considerably from 0.31 to 0.51° av/100 ka between the cutting of the Ngarino and Rapanui Terraces. Rates subsequently slowed to 0.14° av/100 ka, between cutting of the Rapanui and Inaha Terraces. Towards the west, rates on the Rapanui Terrace progressively decrease from 0.51°/100 ka at Kakaramea to 0.21°/100 ka at Hawera (Transect A-A'). Inland towards the older Brunswick Terrace, the average increase in terrace gradient per 100 ka, generally decreases.

| Terrace Age ( ka )         | Inaha 100 | Rapanui 120 | Ngarino 210 | Brunswick 310 |
|----------------------------|-----------|-------------|-------------|---------------|
| <b>Transect A-A'</b>       |           |             |             |               |
| Present gradient ( ° )     | --        | 0.25        | 0.56        | 0.93          |
| Gradient ( ° av / 100 ka ) | --        | 0.21        | 0.27        | 0.14          |
| <b>Transect B-B'</b>       |           |             |             |               |
| Present gradient ( ° )     | --        | 0.36        | 0.44        | 1.06          |
| Gradient ( ° av / 100 ka ) | --        | 0.30        | 0.21        | 0.34          |
| <b>Transect C-C'</b>       |           |             |             |               |
| Present gradient ( ° )     | --        | 0.43        | 0.27        | 0.52          |
| Gradient ( ° av / 100 ka ) | --        | 0.36        | 0.13        | 0.17          |
| <b>Transect D-D'</b>       |           |             |             |               |
| Present gradient           | 0.14      | 0.61        | 0.66        | 0.41          |
| Gradient ( ° av / 100 ka ) | 0.14      | 0.51        | 0.31        | 0.13          |

**Table 5.2** Summary of terrace gradients and rates of change of the terrace gradient for Transects A-A' to D-D'. Also shown is the rate of change of terrace gradient expressed in terms of degrees per 100 ka. Note that initial terrace wave cut surfaces are assumed to have been horizontal.

The general trend is that in the southeast of the study area along the coast, rates of shore-normal deformation are highest and progressively decrease inland. Transect B-B' at Mokoia is where relatively high uplift rates to the southeast progressively change to lower rates in the west. At Hawera (A-A') in the west the rate of uplift on the Rapanui Terrace has shown a decrease to 0.21°/100 ka from 0.30°/100 ka at Mokoia.

From the southeast to the west the changing trends in terrace deformation show a close similarity with the strike of the Taranaki Fault Zone. In this area the Tangahoe River appears to be the surface expression of the western margin of the Taranaki Fault Zone. Inland and to the east of the river, rates of uplift are highest and uplift is most similar to the block type uplift inferred by Pillans (1983). Across the inferred position of the fault zone, rates of terrace tilting are highest and progressively decrease away from it.

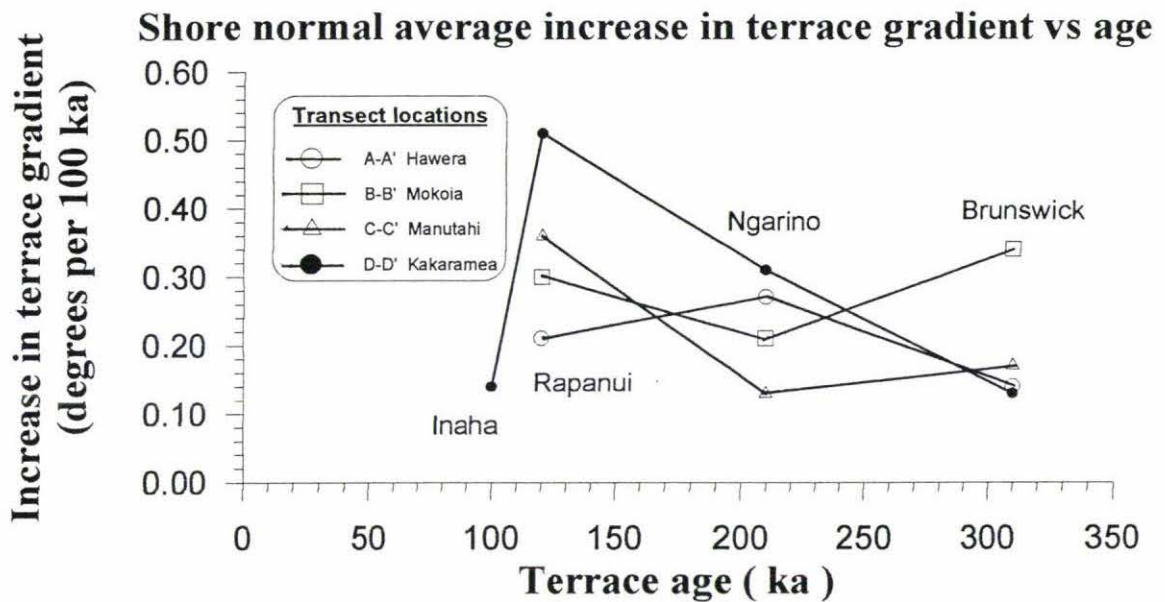


**Figure 5.6.** Average increase in terrace gradient per 100 ka for Transects A-A' to D-D'. Note that with increasing terrace age the rate of gradient change decreases, *i.e.* uplift is not linear. In the southeast close to the coast, rates are highest but decrease westwards towards Manutahi, Mokoia and Hawera.

### 5.5 Shore-parallel terrace deformation

The effect of differential uplift on the terraces is to produce irregularities in the heights of the strandlines. The marine terrace strandlines therefore provide excellent reference horizons once their age and the relative sea level at the time the strandline was last active, are accurately known. When last active, terrace strandlines provide original horizontal chronohorizons which over time have been deformed by differential uplift.

Heights of the terrace strandlines are shown in Figure 5.7 and were drawn by tracing along the terrace strandlines in Figure 5.1 and marking on where the structural contours on each terrace intersect the strandline.

### 5.5.1 Results

The inferred heights of the terrace risers *ie.* the cliffs separating each terrace are shown as the shaded areas on Figure 5.7. Cliff heights are greatest in the vicinity of Kakaramea, the region with the highest uplift rates. The combination of high uplift rates ( $>0.45$  mm/yr) and the length of time the Rapanui strandline was active during stage 5e (chapter 3) has resulted in high risers separating the Ngarino and Rapanui Terraces.

| Transect       | Brunswick | Ngarino | Rapanui |
|----------------|-----------|---------|---------|
| Height at A-A' | 155m      | 83m     | 47m     |
| B-B'           | 165       | 93      | 57      |
| C-C'           | 172       | 92      | 64      |
| D-D'           | 186       | 125     | 64      |
| Difference A-D | 31        | 42      | 17      |

**Table 5.3** Strandline heights on Transects A-A' to D-D'. Figure 5.7 shows the height of the Brunswick, Ngarino and Rapanui strandlines between Hawera and Patea. For the former two terrace strandlines, the area of most rapid uplift is in the vicinity of Kakaramea whereas for the Rapanui Terrace it extends to between Manutahi and Mokoia. Strandline heights are highest along Transect D-D' with heights decreasing towards the west and following the uplift pattern in Figure 5.4.

Northwest of Kakaramea the height of the Rapanui riser decreases from *c.* 15 m to  $<10$  m in the northwest at Mokoia. Uplift rates in this area (Figure 5.4) are lower, between 0.30-0.45 mm/yr. It is interpreted that the low cliff height between the Rapanui and Ngarino Terraces west of Manutahi is the result of rapidly decreasing uplift rates.

The Ngarino riser is shown to be higher than the Rapanui riser west of Mokoia and is generally between 22 and 15m high (Figure 5.7). It also decreases in

height to the west. The greater height of the riser separating the Ngarino and Brunswick Terraces suggests that both terraces were formed during two separate sea level highs a considerable period of time apart.

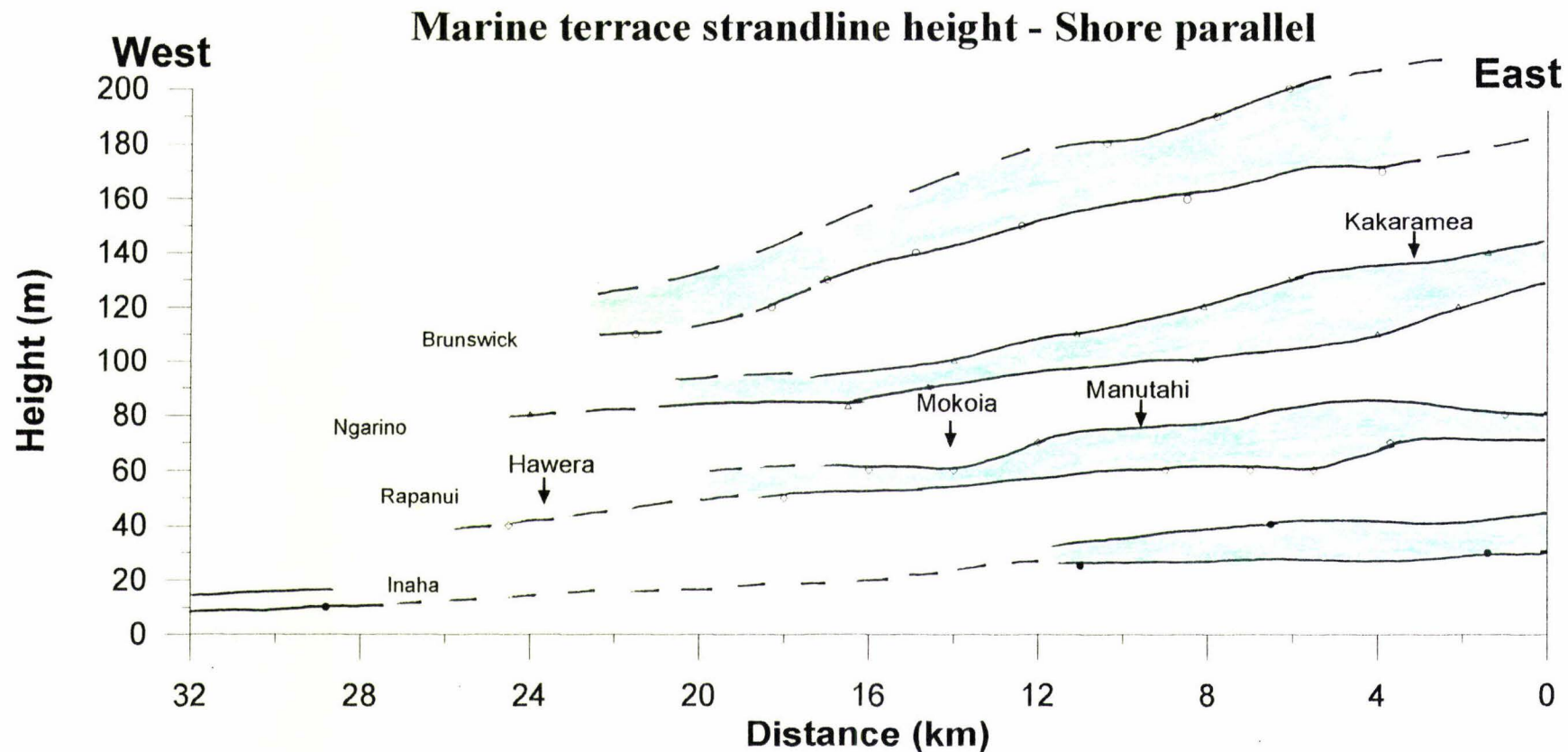


**Figure 5.7** Brunswick, Ngarino, Rapanui and Inaha Terrace strandline heights between Hawera to the west and Kakaramea towards the southeast. Movement of the Taranaki Fault Zone has uplifted the Brunswick and Ngarino Terraces strandlines in the vicinity of Kakaramea. At later stages the focus of uplift has moved towards the west as shown by the increasing height of the Rapanui strandline west of Manutahi. Farther west towards Hawera strandline heights decrease as uplift rates drop and the margin of the South Taranaki Basin is reached. The cliff height to the next terrace tread is shaded and is greatest where uplift is highest.

### 5.5.2 Shore-parallel deformation over time

The assumption for calculating rates of shore-parallel uplift is that at the time a strandline was last active, the strandline would have been undeformed (horizontal). Again by working on a count back basis, uplift rates over time can be examined. Heights of terraces strandlines at specific times are calculated by subtracting the height of younger terrace strandlines. For example the height of the Ngarino strandline 120 ka =  $H_{Ng} - H_{Ra} + 5m$ , where H=height, Ng=Ngarino, Ra=Rapanui, and 5m was the paleosealevel 120 ka. This only approximates to the deformation of the strandlines over time because analysis of the shore-normal component of uplift has shown that differential uplift is occurring, implying that the amount of uplift of one strandline may not equal the uplift of the next older strandline farther inland for a given period of time. Table 5.4 shows the calculated strandline heights at 310, 210 and 120 ka with average shore-parallel uplift rates between the formation of each successive terrace shown in Figure 5.8.

### 5.5.3 Results

Shore-parallel deformation during the period 310-210 ka as with shore-normal uplift was lower than for the period 210-120 ka for Transect D-D'. Rates during this period (Table 5.4, Figure 5.8) for the Brunswick strandline are calculated at 0.61 mm/yr for Transect D-D'. Along Transect A-A' rates during the same period are almost the same at 0.62 mm/yr and decrease over time. In contrast along Transect D-D' uplift of the Brunswick strandline increased between 210 and 120 ka to 0.73 mm/yr. During the same period shore-parallel uplift rates of the Ngarino strandline were greatest along Transect D-D' at 0.73 mm/yr compared with rates of 0.46 mm/yr at A-A'.

Shore-parallel uplift rates for all of the terraces post-120 ka are lower than during the previous periods, with rates at Transect A-A' as low as 0.35 mm/yr.

| Terrace                | Transect A-A'        |                                     | Transect D-D'        |                                     |
|------------------------|----------------------|-------------------------------------|----------------------|-------------------------------------|
|                        | Strandline height    | Uplift rate                         | Strandline height    | Uplift rate                         |
| 310ka Br               | 0m                   |                                     | 0m                   |                                     |
| 210ka Br<br>Ng         | 62m<br>c.0m          | 0.62mm/yr                           | 61m<br>c.0m          | 0.61mm/yr                           |
| 120ka Br<br>Ng<br>Ra   | 113m<br>41m<br>c.+5m | 0.56mm/yr<br>0.46mm/yr              | 127m<br>66m<br>c.+5m | 0.73mm/yr<br>0.73mm/yr              |
| present Br<br>Ng<br>Ra | 155m<br>83m<br>47m   | 0.35mm/yr<br>0.35mm/yr<br>0.35mm/yr | 186m<br>125m<br>64m  | 0.47mm/yr<br>0.47mm/yr<br>0.47mm/yr |

**Table 5.4** Inferred strandline heights and uplift rates, Transects A-A' and D-D' for the period 310ka to present.

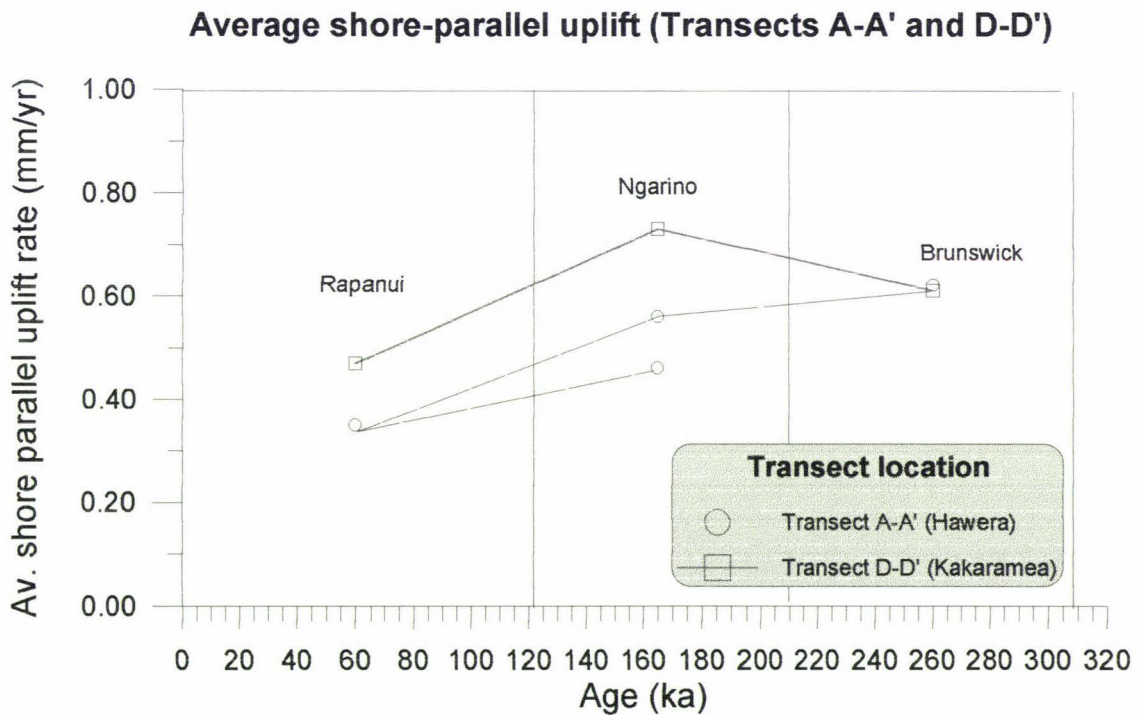


**Figure 5.8** Calculated average rates of shore-parallel uplift for each terrace strandline with data points plotted at the mid point of each period. Uplift rates refer to the average uplift experienced by each strandline along transects A-A' and D-D' for the periods 310-210 ka, 210-120 ka and 120 ka to present.

#### 5.5.4 Shore-parallel tilting

Using the equation  $\text{Tan}^{-1} = \frac{(\text{Hb}-\text{Hd})}{\text{D}}$  the amount of shore-parallel tilting type

uplift can be calculated, where Hb= the height of the terrace strandline at point 'B' near Mokoia, Transect B-B' (Figure 5.9), Hd = the strandline height at the highest point 'D' close to Kakaramea and D= distance between points B and D. Shore-parallel rates of tilt are expressed as degrees of arc per 100 ka.

The amount of shore-parallel tilting between Transects B-B' and D-D' is calculated in the following section and compares the relative amount of tilt along each terrace strandline.

#### 5.5.5 Results

##### **Brunswick strandline**

Hb=165m

Hd=186m

d=17,000m

$$\begin{aligned}\text{Tan}^{-1} &= (186-165)/17000 \\ &= 0.071 \text{ degrees of arc in 310 ka} \\ &= \underline{\underline{0.023 \text{ degrees of arc/ 100 ka}}}\end{aligned}$$

##### **Ngarino strandline**

Hb=93m

Hd=125m

d=18,000m

$$\begin{aligned}\text{Tan}^{-1} &= (125-93)/18,000 \\ &= 0.102 \text{ degrees of arc in 210 ka} \\ &= \underline{\underline{0.049 \text{ degrees of arc/ 100 ka}}}\end{aligned}$$

##### **Rapanui strandline**

Hb=57m

Hd=64m

d=15,000m

$$\begin{aligned}\text{Tan}^{-1} &= (64-57)/15,000 \\ &= 0.027 \text{ degrees of arc in 120 ka} \\ &= \underline{\underline{0.022 \text{ degrees of arc/ 100 ka}}}\end{aligned}$$

Shore-normal and shore-parallel uplift patterns in the study area follow the same pattern where uplift between 310 ka and 210 ka was relatively low. During this period shore-parallel rates of deformation of the Brunswick strandline were *c.* 0.023°/100 ka, whereas between 210 ka and 120 ka this increased to *c.* 0.049°/100 ka along the Ngarino

strandline. Since 120 ka, rates of tilt on the Rapanui strandline have returned to *c.*  $0.022^\circ/100$  ka.

The changing rates of strandline deformation reflect a combination of shore-normal uplift rates which initially increase then slowly decrease coupled with a higher rate of relative uplift of the terrace strandline in the southeast than in the west.

## 5.6 Interpretation

Uplift rates are highest in the vicinity of Kakaramea but decrease westwards towards the Egmont ring plain (Figure 5.4). The zone between Kakaramea and Manutahi is interpreted as overlying the Taranaki Fault Zone (TFZ), a 50 km-wide zone of deep seated thrusts and faults that trend NNW-SSE separating the South Wanganui and South Taranaki Basins (Stern *et al.*, 1990) (Figure 1.2). Stern *et al.*, (1990) suggest that broad bending of the lithosphere has induced westward moving thrust sheets within the TFZ, and this is here implicated as responsible for the uplift pattern shown in Figure 5.4. West of Manutahi the uplift contour lines swing north-northwestwards, parallel to the TFZ. In the region overlying the TFZ (Transect D-D'), rates of shore-normal terrace deformation show differential uplift whereas west and away from the TFZ, uplift is less varied (Figure 5.5). Figure 5.9 shows the Tangahoe Formation from Ohawe Beach to *c.* 2 km southeast of the Manawapou River (after Whitten, 1973). Four faults offset members of the Tangahoe Formation by up to *c.* 30 m. The dip of the Tangahoe Formation is greatest close to the TFZ, and decreases significantly to the northwest.

Along Transect D-D' the trend of uplift rates is one of initially increasing and then decreasing inland. This pattern of uplift is consistent with that predicted by the progressive wave model of Stern *et al.*, (1990) where a lithospheric bulge propagates southeast at approximately 10 mm/yr. The pattern also applies in the past for both Transects A-A' and D-D' where uplift rates appear to have initially increased and then subsequently slowed. Transect D-D' shows much larger rates of terrace uplift in the

vicinity of Kakaramea (Figure 5.6). Here, uplift rates are greatest for the Inaha and Rapanui Terraces whereas farther inland they decrease. This may be explained by a doming effect on the TFZ.

The results above show that during the Pleistocene, tectonic movement associated with the development of the South Taranaki Basin, and depocentre migration of the Wanganui Basin, has resulted in changing uplift rates and deformation of the south Taranaki-Wanganui marine terraces. Figure 1.2 shows the underlying marine sedimentary strata younging towards the southeast consistent with their uplift and tilting as the basin depocentre advanced southeastwards (Stern *et al.*, 1993). Transect D-D' (Figure 5.6a) shows uplift rates on the Inaha Terrace at the coast, which begin to decrease inland on the Brunswick Terrace. Since formation of the Brunswick Terrace *c.* 310 ka the basin depocentre is inferred to have moved *c.* 3.1 km to the southeast. It is apparent from Figure 5.5a that a change in the uplift pattern generally occurs between 3 and 5 km inland from the coast. This pattern resembles the path of a progressive wave with a wavelength of *c.* 300 km (Stern *et al.*, 1993) as shown in Figure 1.4. Over time it would be expected that as the wave front (basin depocentre) propagates further southeastwards, uplift rates would first increase, then decrease as the wave front passes.

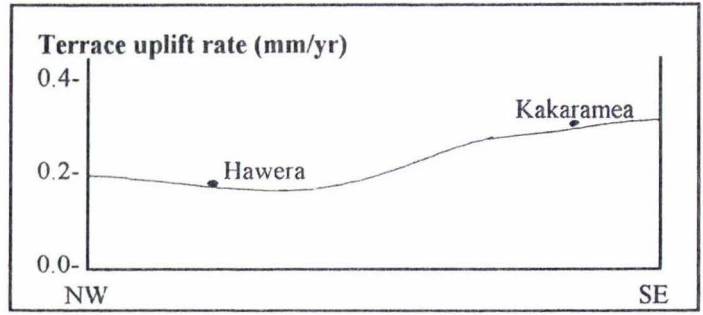
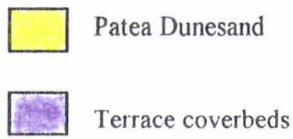
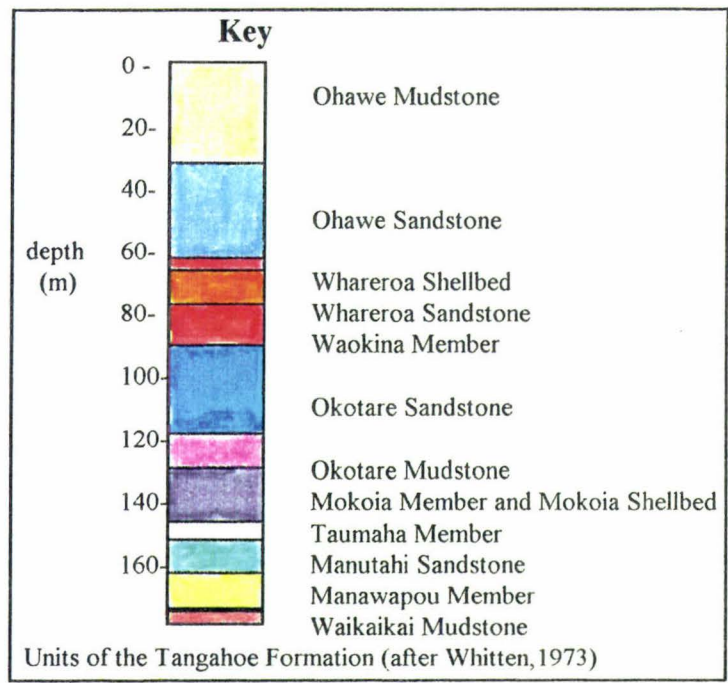
Within the Taranaki Basin, regional compression structures occur in two discrete zones. One is along the southeastern margin of the western platform (outside the area of this study); the other trends north-south between the Manaia and Taranaki Fault Zones (Palmer *et al.*, 1993). The basin is deepest along the eastern basin margin adjacent to the Taranaki Fault Zone. This is consistent with the uplift pattern shown in Figure 5.5b which shows higher uplift of the TFZ to the southeast, and the lower uplift within the STB to the west. The Tangahoe River marks the region of lowest uplift rates which marginally increase towards the west away from the TFZ.

West of the Tangahoe River the height of the Rapanui WCS decreases, reaching *c.* 13 m a.s.l. at Ohawe Beach (Figure 5.9). The ring plain surface however does not follow the underlying dip of the WCS and instead has constructed land to surface heights of 60-70 m a.s.l. along much of the coast. Large volumes of

aggradational volcanoclastics and recent sand dunes are responsible for the progressively thick terrace coverbeds west of Tangahoe River.

A study by Davey and Stern (1988) of a deep seismic cross section of the southern part of the Taranaki Basin resulted in the interpretation that the Taranaki Basin is a retroarc foreland basin. Further studies by Stern, 1989 and Palmer *et al.*, 1993 support this interpretation. Foreland basins form alongside thrust mountain belts in response to flexure of the lithosphere under load. In these settings subsidence is greatest closest to the thrust faults, and further from the load the subsidence rate decreases until uplift occurs some distance away (Palmer *et al.*, 1993) (Figure 5.5b). Primary wedge-shaped thickening of the crust beneath the eastern margin of Taranaki Basin (Stern, 1989), supports greater basin subsidence close to an area of uplift and loading. The westward dip of the Tangahoe Formation and relative movement on faults exposed along the coastal cliffs show that uplift to the east and relative subsidence towards the west has occurred since the Pliocene.

The use of structural contours and transects has proved to be very useful in determining the position of the terrace risers. Although this method relies on accurate height data it has in conjunction with stratigraphic procedures provided an accurate method for discerning patterns of deformation in this region.



\*Not to scale

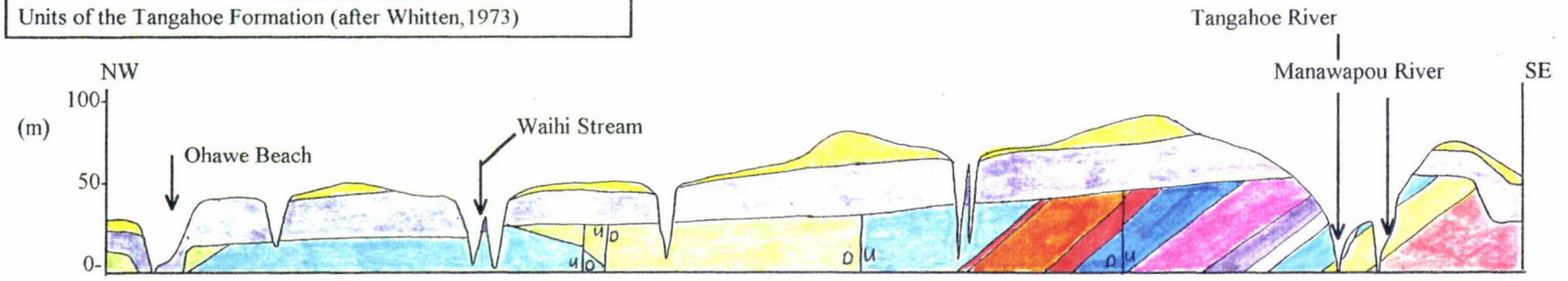


**Figure 5.9** Height of the Rapanui WCS and terrace surface (ring plain) along present coastline between Ohawe Beach and Manawapou River. Four faults offset the Tangahoe Formation with angles of dip increasing to the Southeast towards the Taranaki Fault (after Whitten, 1973). Inset shows generalised uplift pattern from west to east, inferred from terrace deformation data (this study) and offset of units along the coastline (after Whitten, 1973).



**Plate 5.1** Southwestward dipping (*c.* 4-5 degrees) sandstones and mudstones of the Tangahoe Formation looking northwest from *c.* 0.5 km west of the Tangahoe River. A southeast plunging anticline (that marks the western margin of the Patea-Tongaporutu High) *c.* 5 km to the southeast has deformed the Tangahoe Formation. Dip angles are greatest close to the anticline and progressively decrease towards Ohawe Beach in the northwest. The planar erosion surface truncating the Tangahoe Formation (arrow) marks the Rapanui wave-cut surface.

## 5.7 Terrace Preservation

### 5.7.1 Introduction

The combination of uplift rates, paleosea levels and the length of time between successive sea level highs, determines relative differences in height between terraces and ultimately whether terraces are preserved at all. Higher uplift rates and lower paleosea levels accentuate the preservation of terraces, whereas low uplift rates and higher paleosea levels result in terrace retrimming. In areas of higher uplift, terraces are more likely to be uplifted above succeeding sea level and therefore preserved. During a long still stand, landward erosion of the strandline may completely remove evidence of an older marine terrace. An example of this occurs *c.* 1.5 km southeast of the Manawapou River where retreat of the present coastline has completely removed the Inaha Terrace as far west as Ohawe Beach.

### 5.7.2 Results

Based on the paleosea level data provided by Chappell (1983) and Pillans *et al.*, (1987) and the age of marine terraces determined in this study, uplift rates in the study area are sufficient to preserve marine terraces formed 210, 120 and 100 ka. During stage 7, two closely spaced sea level highs were experienced at 240 and 210 ka. Relative sea level at these times were *c.* -10m and *c.* 0m respectively (Pillans *et al.*, 1987). Table 5.5 shows that uplift rates  $>0.4$  mm/yr are required to preserve the 240 ka terrace from the 210 high stand. It is possible that inland of the study area where uplift rates are  $>0.4$  mm/yr the 240 ka terrace is preserved. At one locality (grid reference Q21/323722) near the corner of Hurtshouse and Upper Taumaha Roads, a section is exposed showing L5 above the level of the surrounding terrace surface. However due to a lack of other suitable exposures it cannot be determined whether or not this represents a small remnant of the 240 ka terrace. In the study area the 210 ka transgression has completely

removed all of the 240 ka terrace, an observation confirmed by Pillans *et al.*, (1987) and Pillans (1990) who show no remnants of the terrace further southeast.

Table 5.6 also shows that rates of uplift in the study area are sufficient to preserve both the Rapanui and Inaha Terraces. In the west of the study area low uplift rates  $< 0.2$  mm/yr cause the Inaha WCS to dip below sea level.

| Uplift rate (mm/yr) | Terrace age (ka) | S.L at T=0   | uplift in 30 ka | Height diff. | Result                                      |
|---------------------|------------------|--------------|-----------------|--------------|---|
| 0.2                 | 240<br>210       | -10m<br>c.0m | 6m              | -4m          | 240 Ka terrace<br><b>retrimmed</b>          |
| 0.3                 | 240<br>210       | -10,<br>c.0m | 9m              | -1m          | 240 Ka terrace<br><b>retrimmed</b>          |
| 0.4                 | 240<br>210       | -10m<br>c.0m | 12m             | +2m          | 240 Ka terrace<br>possibly<br>preserved     |
| 0.5                 | 240<br>210       | -10m<br>c.0m | 15m             | +5m          | 240 Ka terrace<br>possibly<br>preserved     |
| 0.6                 | 240<br>210       | -10m<br>c.0m | 18m             | +8m          | 240 Ka terrace<br>likely to be<br>preserved |

**Table 5.5** Uplift rates and preservation of 240ka terrace from 210 ka high stand

| Uplift rate (mm/yr) | Terrace age (ka) | S.L at T=0       | uplift in 90Ka        | Height diff. | Result                          |
|---------------------|------------------|------------------|-----------------------|--------------|---------------------------------|
| 0.1                 | 210<br>120       | c.0m<br>+5m      | 9m                    | +4m          | 210 terrace<br><b>preserved</b> |
| 0.2                 | 210<br>120       | c.0m<br>+5m      | 18m                   | +13m         | 210 terrace<br><b>preserved</b> |
| 0.1                 | 120<br>100       | c.0m<br>c.-12m   | uplift in 20 ka<br>2m | +14m         | 120 terrace<br><b>preserved</b> |
| 0.2                 | 120<br>100       | c.0m<br>c.-12m   | 4m                    | +16m         | 120 terrace<br><b>preserved</b> |
| 0.1                 | 100<br>80        | c.-12m<br>c.-12m | uplift in 20 ka<br>2m | +2m          | 100 terrace<br><b>preserved</b> |
| 0.2                 | 100<br>80        | c.-12m<br>c.-12m | 4m                    | +4m          | 100 terrace<br><b>preserved</b> |
| 0.4                 | 100<br>80        | c.-12m<br>"      | 8m                    | +8m          | 100 terrace<br><b>preserved</b> |

**Table 5.6** Uplift rates and preservation of 210, 120, and 100 ka terraces from subsequent highstands.

**Note.** 60-120 ka sea levels after Chappell (1983)

120-240 ka sea levels after Pillans *et al.*, (1987)

## Chapter six

### Summary

Coverbeds overlying the marine terraces in the southeast sector are dominated by marine sands and gravels, loess, and dune sands. Loess units are characterised by a tephric component, moderate to well developed structure, yellowish brown to dark brown colour and paleosol development on the upper surface of units. Throughout the stratigraphic sequence, accretions of ash and lapilli are abundant, although often thoroughly mixed. Discrete lapilli horizons are common in coverbeds representing oxygen isotope stages 2,3, 5 and 6 and mark periods of increased volcanic activity at Egmont Volcano. During oxygen isotope stage 2, widespread erosion of coverbeds occurred in this sector and resulted in deposition of the Wereroa sand and the formation of a widespread erosional unconformity called the Mokoia erosion surface. The unconformity was formed by base level readjustment of larger streams and rivers during oxygen isotope stage 2 when sea level was *c.* 120 m below present. Kawakawa Tephra (22.6 ka) is found interbedded within both L1 and the Wereroa sand in the southeast sector.

Dunesand units are common southeast of the Tangahoe River and are interbedded within and between loess units. Five interglacial/interstadial dunesand units are recognised, the Kaihuahua, Whakamara, Auburn and Patea Dunesands representing stages 5e,5c,5a and 1. The recognition of the interglacial/interstadial dunesands and interbedded tephra in this area has allowed fine resolution and correlation to the oxygen isotope curve. This area is in close proximity to a large source of andesitic sand and this is reflected in the presence of the warm climate dunesands in particular. The relatively continuous supply of tephra from Egmont Volcano has also served to separate the

dunesand units and paleosols formed on volcanic loess units. This allowed much finer resolution and better correlation of the terrace coverbeds.

The pattern of facies changes within individual coverbed units indicates that in the early stages of terrace emergence coverbeds have been influenced by a high watertable. The emergent units are tephric, gleyed and exhibit pale grey colours and are found near present day streams and rivers. This reflects the early development of watercourses on the emergent terraces. On terrace interfluvies between low lying areas, deposition of volcanic loess occurred where better drainage has resulted in brighter colours, more mixing of tephra layers and increased abundance of rhizomorphs. With steady uplift and entrenching of watercourses the gley facies was restricted to narrow stream valleys with subsequent coverbeds becoming dominated by well drained volcanic loess and dunesand units. The nature of the coverbeds overlying marine terraces to the southeast of the Tangahoe River, allow better chronologic control using volcanic loess, dunesand and tephra chronology. Consequently a better and more accurate record of uplift and terrace distribution has been obtained in this area.

In contrast, in the northwest sector increased volcanoclastic deposits and higher sedimentation rates coupled with lower uplift rates have complicated the stratigraphy in this area. Previously correlation of the Ohawe waterfall section as the Ngarino Terrace was based on the interpretation of forest pollen in lignite overlying the debris avalanche and the lignite was assigned to oxygen isotope stage 5e. The correlation of pollen zones and coverbeds units in this study however suggest a maximum age of 70 ka for the units overlying the prominent debris-avalanche deposit, here interpreted to be the Stratford Formation. The Stratford Formation has also been mapped further west at the Inaha section by McGlone *et al.*, (1984). A wood sample obtained by Pillans (1991) from a

terrace along the Waingongoro River (Q21/138804) gave an a.a.r age of 75 ka and a radiocarbon age >35.2 ka. The author's interpretation of the stratigraphy at this site (section 31) shows the sample is obtained from fine-grained overbank deposits above the Stratford Formation. Reinterpretation of the pollen zones at the Ohawe waterfall site in this study concludes that pollen zones OH1-OH5 represent oxygen isotope stages 5d, 5c, 5b, 5a, 4 and 3 and correlation of the site as overlying the Rapanui Terrace is preferred. The southern margin of the ring plain is characterised by periods of rapid volcanoclastic aggradation followed by fluvial reworking. During the following periods large areas of semi-swamp formed with deposition of silts, carbonaceous muds and lignite, as fluvial channels became established and entrenched. As rivers cut down, volcanic loess units became more widespread as river channels and their floodplains became more restricted. Pollen spectra from sediments in this area are interpreted to represent the vegetation response to both climate and repeated inundation and destruction by volcanoclastic sedimentation. With increasing distance from Egmont Volcano, volcanic loess units on the ring plain become more widespread. Closer to source and to watercourses repeated aggradation and inundation has resulted in alternating sequences of coarse to fine sediment deposition.

North-northwest of the Tangahoe River, the older Ngarino and Brunswick Terraces appear to have been a former ring plain environments. The younger Rapanui Terrace around Hawera is part of the present day Egmont ring plain.

The study area is interpreted to overlie the Taranaki Fault Zone which separates the Patea-Tongaporutu High to the east from the Taranaki Basin towards the west. It is shown that progressive movement within the Taranaki Fault Zone has varied over time. Uplift rates increased after the formation of the Ngarino Terrace. This resulted in high

risers separating the Rapanui and Ngarino Terraces in the vicinity of Kakaramea, a region interpreted to overlie the Patea-Tongaporutu High. Towards Manutahi the riser decreases in height and has resulted from falling uplift rates west towards Mokoia. The decreasing uplift rates west of Manutahi have resulted in the Rapanui strandline cutting further inland forming a large embayment between the Manawapou and Tangahoe Rivers. Here the presence of the warm water mollusc *Leucotina ambigua* which is believed to have lived in sheltered embayments during the Last Interglacial, is consistent with the inferred shape of the Last Interglacial shoreline as shown in Figure 5.1. Low uplift rates west of the Patea-Tongaporutu High and the long duration of the 120 ka high stand have combined to form the large embayment.

The channels of the three main rivers, the Patea, Manawapou and Tangahoe Rivers, may be structurally controlled to some extent by movement associated with the Patea-Tongaporutu High and the Taranaki Fault Zone. Increased uplift rates have led to tributary channels being restricted to the southeast and northwest, flowing away from the apex of the increased uplift towards the Patea and Manawapou Rivers.

## 6.2 Future research

Ample opportunity exists in this area for finer detail studies focussing on the correlation of andesitic tephra beds within the terrace sequence, from closer to source further to the southeast. This will enable future workers to date and correlate with more certainty to covered units in other regions. Detailed mapping and correlation of volcanoclastic deposits in the vicinity of Hawera and further north is bound to provide an interesting picture on evolution of the southern margin of the Egmont ringplain. Palynological interpretation of newly discovered lignite units, in conjunction with

geologic mapping will be important in detailing the paleoclimate record of the region and the response of vegetation in two contrasting but contemporary depositional environments.

Appendix A.

Section locations

| Section number | Name                      | Grid reference    |
|----------------|---------------------------|-------------------|
| 1              | <b>Manutahi section</b>   | <b>Q21/304693</b> |
| 2              | Waikaikai Stream          | Q21/301699        |
| 3              | <b>Mangaroa Stream</b>    | <b>Q21/318678</b> |
| 4              | Upp. Mangaroa Stream      | Q21/325683        |
| 5              | <b>Garsed Road</b>        | <b>Q21/339658</b> |
| 6              | Kaikura Stream            | Q21/339655        |
| 7              | <b>Opie section</b>       | <b>Q21/344685</b> |
| 8              | Ashwood's pond            | Q21/330672        |
| 9              | <b>Inaha section</b>      | <b>Q21/103793</b> |
| 10             | Fishing rock              | Q21/291667        |
| 11             | Symes quarry              | Q21/289727        |
| 12             | <b>House cutting</b>      | <b>Q21/304685</b> |
| 13             | <b>Buhler's section</b>   | <b>Q21/313694</b> |
| 14             | <b>Campbell's section</b> | <b>Q21/319702</b> |
| 15             | <b>Hursthose section</b>  | <b>Q21/325721</b> |
| 16             | <b>Rutten's section</b>   | <b>Q21/318718</b> |
| 17             | <b>Runoff section</b>     | <b>Q21/310713</b> |
| 18             | <b>Upp. Taumaha Road</b>  | <b>Q21/308708</b> |
| 19             | Manawapou Hill            | Q21/283724        |
| 20             | Viaduct section           | Q21/283728        |
| 21             | Symes 's pit              | Q21/277718        |
| 22             | Symes's track I           | Q21/265715        |
| 23             | Manutahi Beach            | Q21/261712        |
| 24             | <b>Hawkin's pond</b>      | <b>Q21/275733</b> |
| 25             | <b>Ingahape Road</b>      | <b>Q21/296736</b> |
| 26             | Turuturu Mokai Pa         | Q21/211811        |
| 27             | <b>Sturgeon's section</b> | <b>Q21/276771</b> |
| 28             | Hicks Road                | Q21/247739        |
| 29             | Phillips race             | Q21/246754        |
| 30             | <b>Passing lane</b>       | <b>Q21/252757</b> |
| 31             | <b>Manawapou Road</b>     | <b>Q21/215764</b> |
| 32             | Waingongoro River         | Q21/138804        |
| 33             | Sturgeon's #2             | Q21/273768        |
| 34             | Mokoia overbridge         | Q21/282739        |
| 35             | Lysaght Road              | Q21/283676        |
| 36             | Luff's section            | Q21/245762        |
| 37             | Syme's track II           | Q21/272714        |
| 38             | <b>Corrigans Hill</b>     | <b>Q21/176791</b> |
| 39             | <b>Tokora hill</b>        | <b>Q21/145802</b> |
| 40             | <b>Ararata Road</b>       | <b>Q21/160823</b> |
| 41             | <b>Tokora quarry</b>      | <b>Q21/139805</b> |
| 42             | Hawera dump               | Q21/215786        |
| 43             | <b>Ngaumai Park</b>       | <b>Q21/213785</b> |

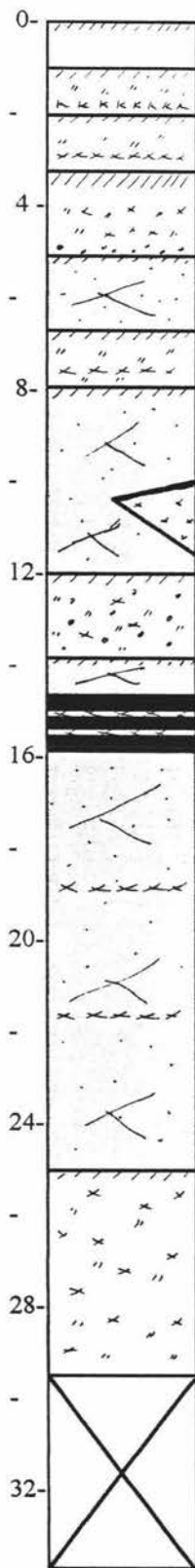
| Section number | Name                   | Grid reference    |
|----------------|------------------------|-------------------|
| 44             | Hawera railbridge      | Q21/213779        |
| <b>45</b>      | <b>Ohawe waterfall</b> | <b>Q21/144785</b> |
| <b>46</b>      | <b>Kiwi track</b>      | <b>Q21/227775</b> |
| 47             | Smillie section        | Q21/217778        |
| <b>48</b>      | <b>Subway section</b>  | <b>Q21/220777</b> |

**Note:** Sections in **bold type** are collated on the following pages.

## SITE DESCRIPTION

Section no. 1    Name. Manutahi section  
 Grid reference. Q21/304693  
 Surface.        Ngarino

Depth (m)



**Egmont Ash**

**(L1)**

Kawakawa Tephra

pale andsitic ash and lapilli in brown volcanic loess **(L2)**

fine tephric rich volcanic loess with pronounced paleosol  
 iron concretions at contact with sand **(L3)**

grey loose to firm sands

**(Auburn dunesand)**

pale volcanic loess and tephra

**(L4)**

firm grey sands with interbedded white pumiceous sands and  
 thin fine ash separated by thin iron pans

**(Whakamara dunesand)**

bright orange silty tephric loess, many concretions

**(L5)**

grey sand

lignite with grey/white lapilli, some large wood  
 thin iron pan

**(Kaihuahua dunesand)**

thin (1-2 cm ) lapilli layers in sand

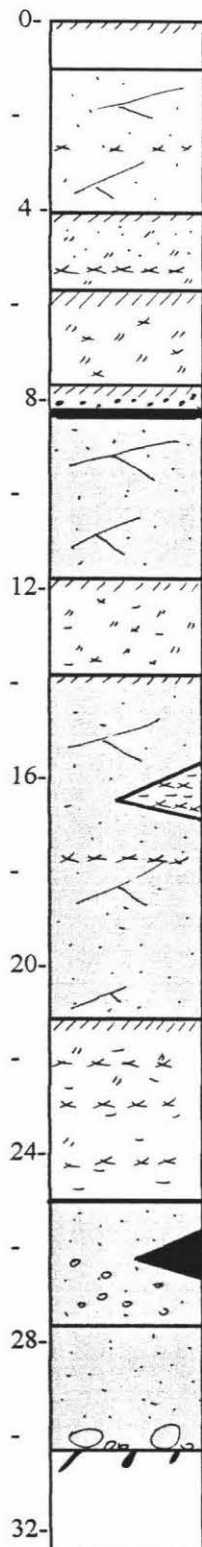
pale grey/brown tephric rich volcanic loess

**(L6)**

## SITE DESCRIPTION

Section no. 3    Name. Mangaroa Stream  
 Grid reference. Q21/318678  
 Surface.        Ngarino

Depth (m)



Egmont Ash

interbedded grey sand and andesitic ash  
 (Wereroa sand and L1)

sandy volcanic loess, many yellow/grey lapilli and lithics  
 (L2)

fine volcanic loess with abundant rhizomorphs and lapilli,  
 (L3)

pale volcanic loess, concretions above ironpan (L4)  
 ironpan

semi-loose grey sands        (Whakamara dunesand)

tephric rich loess        (L5)

(Kaihuahua dunesand)

thin lens of tephric diatomaceous earth

lapilli in sand

tephric rich carbonaceous silts

(L6)

sandy lapilli  
 thin ironpan

thin tephric lignite  
 sands and fine gravels

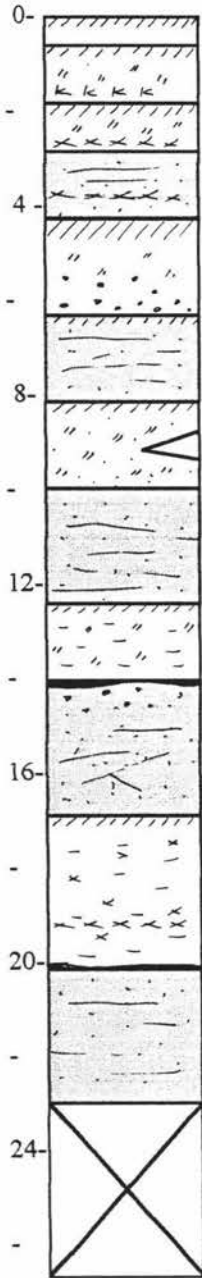
fine andesitic marine sands  
 basal rounded gravels  
 WCS

(Ingahape formation)

## SITE DESCRIPTION

Depth (m)

Section no. 5    Name. Garsed Road  
 Grid reference. Q21/339658  
 Surface.        Ngarino



Egmont Ash  
 (L1)

(L2)  
 grey parallel bedded semi loose sands, sand and tephra  
 interdigitate  
 (Huxley Sand)

pronounced paleosol  
 concretions increasing with depth (L3)

whitish grey parallel bedded sands (Auburn dunesand)  
 paleosol  
 weathered tephra and sand, reddish brown with root channels  
 (L4)

indistinct contact to parallel bedded grey sand  
 (Whakamara dunesand)

silty tephric rich loess with many root channels, iron pan near  
 base (L5)

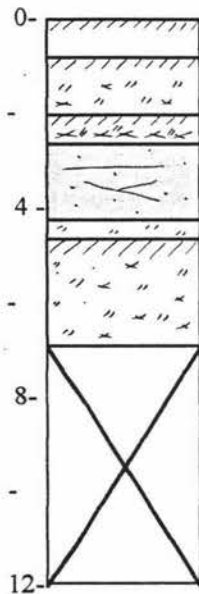
fine reddish sand mixed with ash, few concretions near top  
 sand becomes paler with depth (Kaihuahua dunesand)

silty tephric loess with root channels (L6)  
 andesitic tephra layer  
 thin ironpan

grey sand

## SITE DESCRIPTION

Depth (m)



|                            |                    |
|----------------------------|--------------------|
| Section no. 7              | Name. Opie section |
| Grid reference. Q21/344685 |                    |
| Surface.                   | Ngarino            |

Egmont Ash  
(L1)

(L2)

(Huxley Sand)

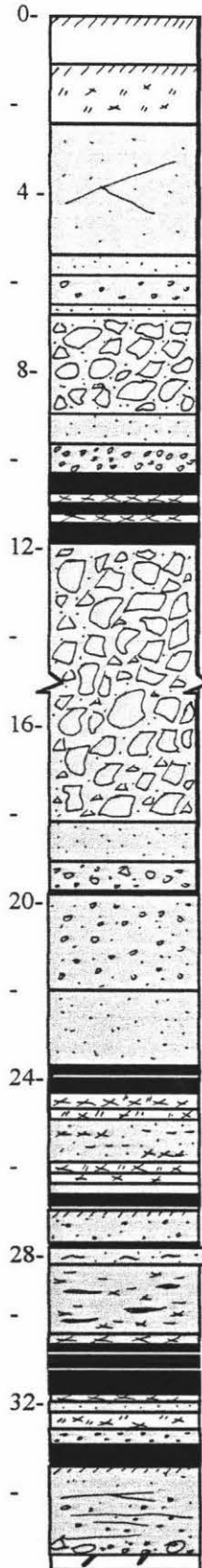
(L2)

pronounced paleosol  
(L3)

## SITE DESCRIPTION

Section no. 9    Name. Inaha  
 Grid reference. Q21/1003793  
 Surface.        Inaha

Depth (m)



Egmont Ash

(L1)

(Wereroa sand)

andesitic gravels and weakly laminated sandstone

(Opunake Formation)

andesitic sand

andesitic gravels

black tephric lignite with thin lenses of pumiceous sand

(Stratford Formation)

andesitic sands and gravels

gravelly sand

andesitic sand

pumiceous coarse sand and carbonaceous tephra

iron stained medium sands with thin tephra and silt bands

andesitic tephra

thin interbedded sand and lignite

organic stained, weathered top

grey carbonaceous tuff with many grass leaves

tephric lignite with some wood fragments and sand lenses

fawn grey lithified carbonaceous tuff with many plant roots

fine andesitic gravel

lignite

weathered and iron stained

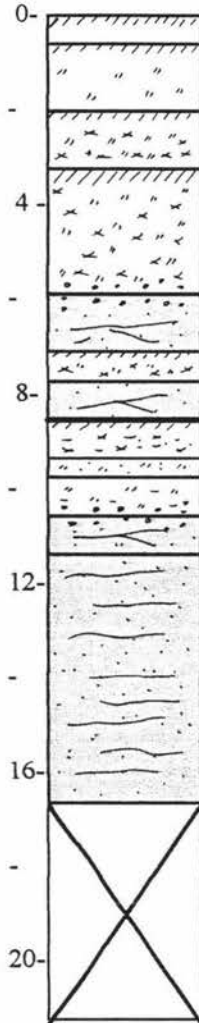
(Inaha Formation)

weakly cross laminated andesitic sand and gravel

basal gravel unit Inaha WCS

## SITE DESCRIPTION

Depth (m)



Section no. 12    Name. House cutting  
 Grid reference. Q21/304685  
 Surface.            Rapanui

Egmont Ash  
(L1)

many rhizomorphs with abundant lapilli (L2)

pronounced paleosol, abundant lapilli (L3)

iron concretions on top of sand  
 grey sand                    (Auburn dunesand)

thin fine tephric loess                    (L4)

(Whakamara dunesand)

thin ironpan  
 silty tephric loess (sandy in places )  
(L5)

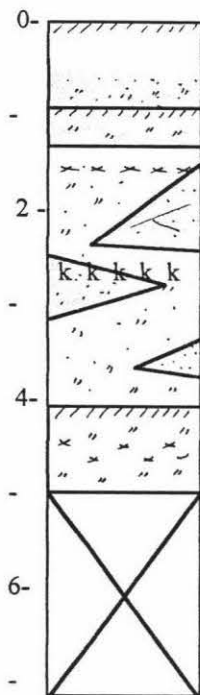
concretions increasing with depth  
 thin grey sand                    (Kaikura sand)

laminated sands  
(Kaikura formation)

## SITE DESCRIPTION

**Section no. 13**    **Name. Bulher's section**  
**Grid reference. Q21/313694**  
**Surface. Ngarino**

Depth (m)



Egmont Ash  
 sandy ash indistinct contact  
 sandy tephric loess (L1)  
 old root channels  
 lapilli

(Wereroa Sand)

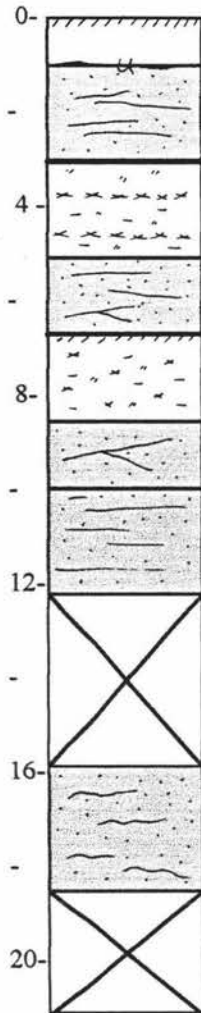
Kawakawa Tephra  
 mixed sand and ash (L1)

sand lenses  
 paleosol  
 large grey and white lapilli  
 fine tephric loess (L2)

## SITE DESCRIPTION

Section no. 14    Name. Campbell's section  
 Grid reference. Q21/319702  
 Surface. Mokoia erosion surface (Ngarino)

Depth (m)



**Egmont Ash**  
 unconformity  
 grey laminated dunesand    (**Whakamara dunesand**)

thin ironpan  
 white lapilli  
 grey and orange tephric silt    (**L5**)

grey cross bedded dunesand    (**Kaihuahua dunesand**)  
 thin ironpan

grey/orange tephric silt    (**L6**)

cross bedded dunesand    (**Ingahape sand**)

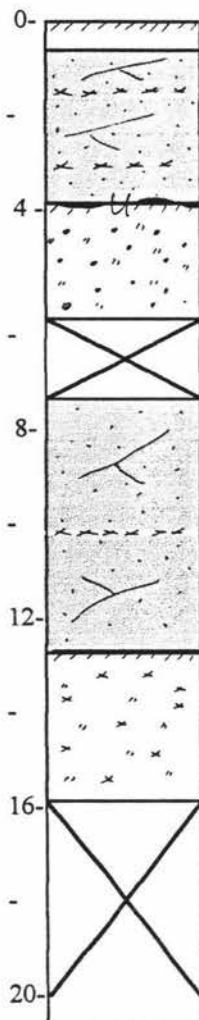
fine laminated sands

ripple bedded sands

## SITE DESCRIPTION

Section no. 15 Name. Hursthouse Road  
 Grid reference. Q21/325721  
 Surface. Mokoia erosion surface (Ngarino)

Depth (m)



thin Egmont Ash

laminated grey dunesand (Wereroa sand)  
 scattered lapilli horizons

unconformity

bright orange tephric loess  
 many concretions (L5)

grey cross bedded dunesand (Kaihuahua dunesand)  
 thin (3cm) grey/white andesitic ash

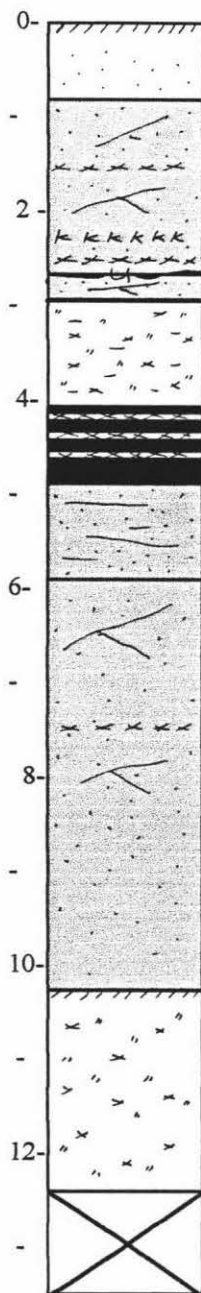
thin ironpan

hard grey tephric loess (L6)

## SITE DESCRIPTION

Section no. 16 Name. Rutton's section  
 Grid reference. Q21/318718  
 Surface. Mokoia erosion surface (Ngarino)

Depth (m)



Egmont Ash (sandy)

grey/black dunesand (Wereroa sand)  
 andesitic lapilli

Kawakawa Tephra  
 unconformity

thin ironpan on orange stained sands  
 brown/grey carbonaceous tephric silts (Whakamara dunesand) (L5)

lignite with interbedded andesitic tephra

planar bedded dunesand

steeply dipping dunesand

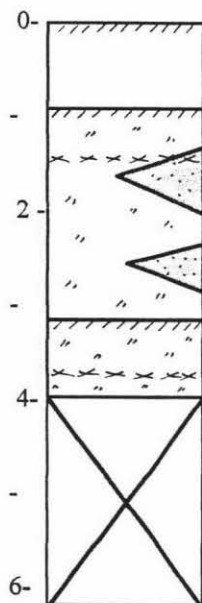
(Kaihuahua dunesand)

hard grey tephric loess (L6)

## SITE DESCRIPTION

Section no. 17 Name. Run off section  
Grid reference. Q21/310713  
Surface. Ngarino

Depth (m)



Egmont Ash

fine ash and lapilli (L1)

interbedded lenses of grey/black sands  
(Wereroa sand)

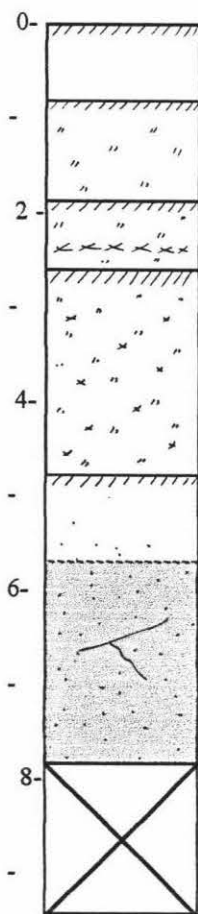
chocolate brown Paleosol (L2)

thick (100mm) white pumiceous lapilli with minor grey  
lithics

## SITE DESCRIPTION

**Section no. 18**    **Name. Upper Taumaha Road**  
**Grid reference. Q21/308708**  
**Surface. Ngarino**

Depth (m)



Egmont Ash

(L1)

paleosol on fine volcanic loess (L2)  
pumiceous lapilli with minor grey lithics

pronounced chocolate brown paleosol (fine ash)  
abundant rhizomorphs and lapilli within fine volcanic loess (L3)

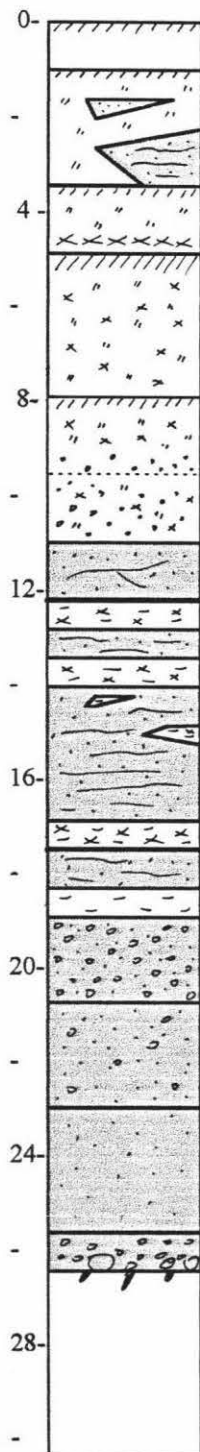
paleosol  
becomes sandier with depth (L4)

grey andesitic dunesand (**Whakamara dunesand**)

## SITE DESCRIPTION

Section no. 24    Name. Hawkin's pond  
 Grid reference. Q21/275733  
 Surface.            Rapanui Terrace

Depth (m)



Egmont Ash

(L1)

lenses of grey sand

(Wereroa sand)

planar bedded grey/brown sand

(L2)

fine volcanic loess

10 cm thick pumiceous andesitic tephra, few grey lapilli  
 pronounced paleosol

abundant lapilli in fine volcanic loess (L3)

paleosol

weathered volcanic loess, concretions increasing with depth

(L4)

fine volcanic loess with many concretions (L5)

thin cross bedded dunesand

(Kaikura sand member)

thin ironpan

tephric rich white silt

planar bedded fine grey grey/black sand

planar bedded fine andesitic sands and silt rip-up clasts

(Kaikura silt and fine sand member)

tephric silts

rounded grey andesitic sandy gravels

(Kaikura gravelly sand member)

grey grey/brown sands with few gravels

fine brown micaceous sands (Kaikura fine sand member)

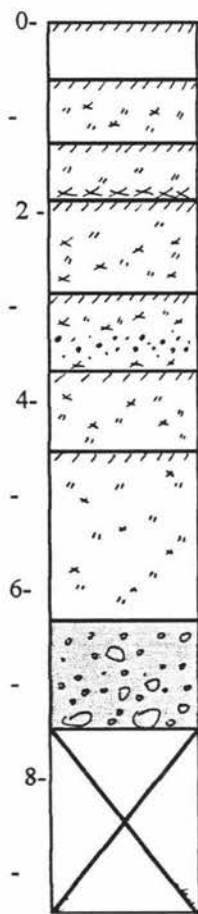
rounded gravels

WCS

## SITE DESCRIPTION

**Section no. 25**    **Name. Ingahape Road**  
**Grid reference. Q21/296736**  
**Surface. Ngarino**

Depth (m)



friable yellow brown andesitic ash                    **(Egmont Ash)**

brown greasy volcanic loess                            **(L1)**

fine volcanic loess and lapilli                        **(L2)**

lapilli layer above paleosol

fine chocolate greasy volcanic loess  
good structure and lapilli throughout                **(L3)**

bright orange volcanic loess and tephra, concretions

forming along sandy horizon                            **(L4)**

bright brown fine volcanic loess with grey sandy ash

iron staining throughout                                **(L5)**

pale fine textured greasy volcanic loess            **(L6)**

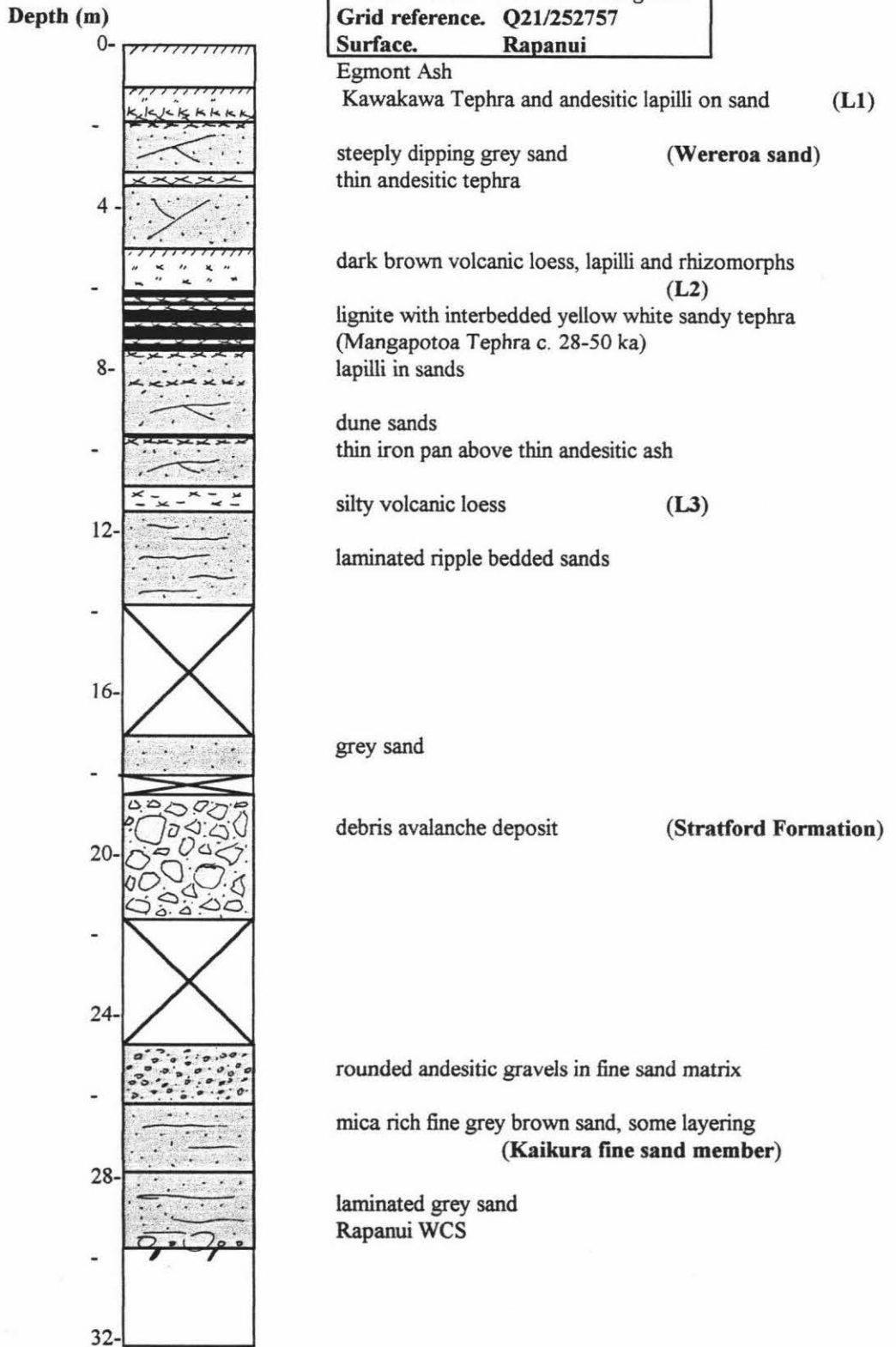
andesitic gravelly sands

obscured



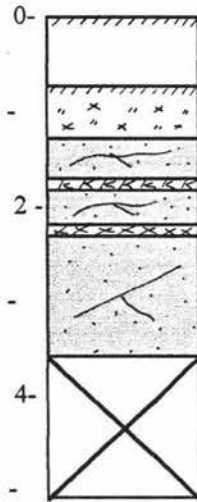
## SITE DESCRIPTION

|                                   |                           |
|-----------------------------------|---------------------------|
| <b>Section no. 30</b>             | <b>Name. Passing lane</b> |
| <b>Grid reference. Q21/252757</b> |                           |
| <b>Surface. Rapanui</b>           |                           |



## SITE DESCRIPTION

Depth (m)



**Section no. 31**    **Name. Manawapou Road**  
**Grid reference. Q21/215764 (after Wilde, 1978)**  
**Surface.            Rapanui**

dark yellowish brown friable andesitic ash    (**Egmont Ash**)

dark yellowish brown greasy volcanic loess and lapilli    (**L1**)

unweathered grey andesitic sand

whitish resorted rhyolitic tephra    (**Kawakawa Tephra**)

yellowish brown fine andesitic tephra

unweathered grey andesitic sand    (**Wereroa sand**)

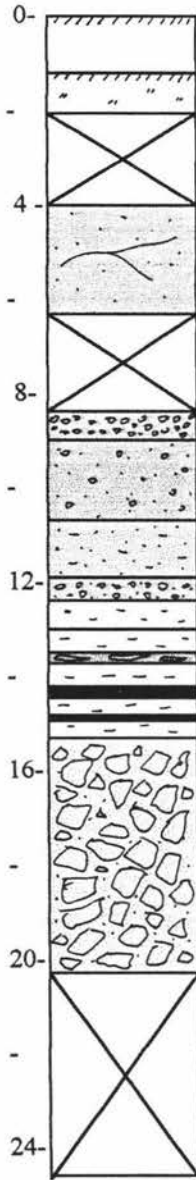
obscured



## SITE DESCRIPTION

**Section no. 39**    **Name. Tokora Hill**  
**Grid reference. Q21/145802**  
**Surface. Rapanui (inferred)**

Depth (m)



friable to loose andesitic tephra    (**Egmont Ash**)

firm volcanic loess    (**L1**)

obscured

grey andesitic sand    (**Wereroa sand**)

obscured

fine rounded brown andesitic gravels

sharp contact

grey andesitic sands with few andesitic gravels

(**Opunake Formation**)

grey sandy silt

gravels and sand

pale silt

(**L3**)

pale tephric silt with layers of lignite and plant material

andesitic volcaniclastic debris

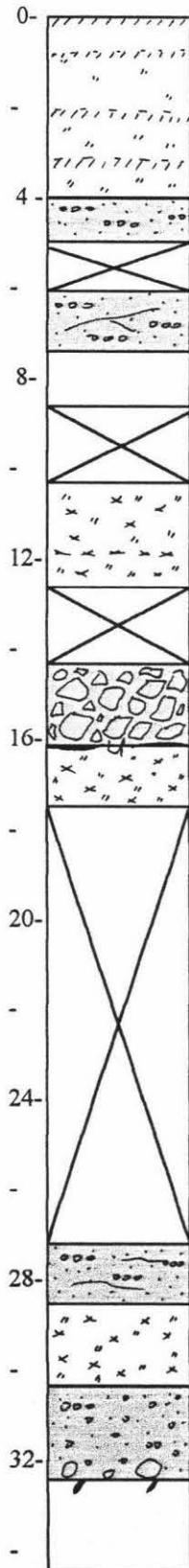
(**Stratford Formation**)

obscured

## SITE DESCRIPTION

Section no. 40    Name. Ararata Road  
 Grid reference. Q21/160823 (Bussell, 1988)  
 Surface.            Ngarino

Depth (m)



yellow brown volcanic loess            (Egmont Ash, L1-L3?)

light grey pumiceous pebbly sand  
obscured

light grey cross bedded pumiceous pebbly sand

pink and white mud

obscured

medium brown andesitic tuff and tephra with lapilli (L4)

obscured

light grey laharc breccia

unconformity  
grey brown andesitic tephra and lapilli            (L5)

obscured

light grey pumiceous pebbly sand

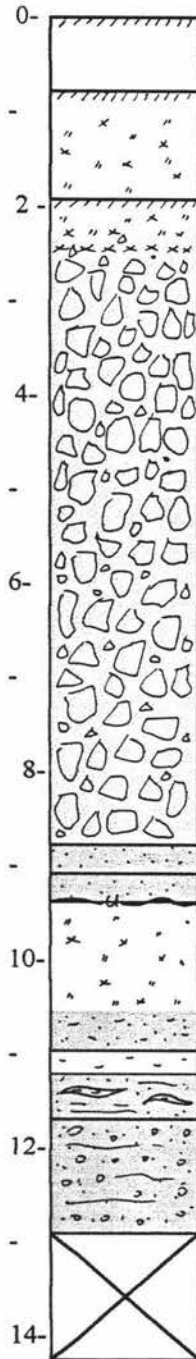
grey brown andesitic tephra and lapilli            (L6)

dark grey marine pebbly sand

Ngarino WCS

## SITE DESCRIPTION

Depth (m)



|                                    |                            |
|------------------------------------|----------------------------|
| <b>Section no. 41</b>              | <b>Name. Tokora Quarry</b> |
| <b>Grid reference. Q21/139805</b>  |                            |
| <b>Surface. Rapanui (inferred)</b> |                            |

friable silt loam (Egmont Ash)

firm volcanic loess (L1)

distinct contact  
yellow brown greasy silt loam paleosol  
lapilli layer  
volcanic loess and lapilli (L2)  
grades into volcaniclastic debris

angular andesitic clasts (Opunake Formation)

sharp contact to fine purple sand  
pale sand with wavy unconformable base

pale orange volcanic loess (mottled) (L3)

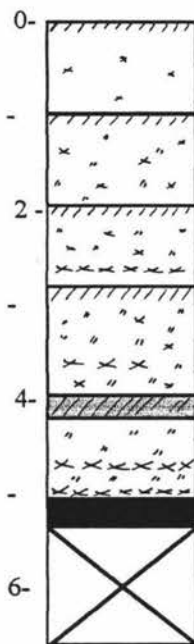
merges into fine sand  
silt  
fine bedded sand with interbedded silt lenses

parallel bedded gravelly sands

## SITE DESCRIPTION

**Section no. 43**    **Name. Ngaumai Park**  
**Grid reference. Q21/213785**  
**Surface. Ngarino**

Depth (m)



friable andesitic tephra and lapilli    (**Egmont Ash**)

volcanic loess and lapilli    (**L1**)

moderately well developed paleosol

fine volcanic loess and lapilli    (**L2**)

purplish lapilli

chocolate brown paleosol

fine volcanic loess with many rhizomorphs and abundant lapilli    (**L3**)

ironpan (20-25 cm thick)

coarse white andesitic tephra with black crystals

orange volcanic loess with basal andesitic lapilli    (**L4**)

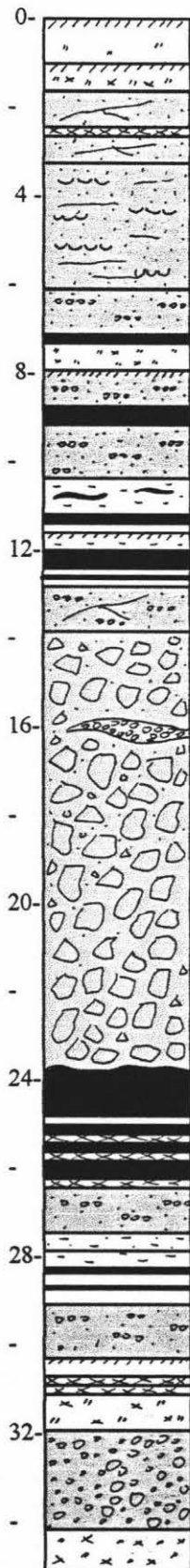
tephric lignite

obscured

## SITE DESCRIPTION

Depth (m)

Section no. 45    Name. Ohawe waterfall  
 Grid reference. Q21/144785  
 Surface.            Rapanui



Egmont Ash  
 volcanic loess (L1)  
 dark grey, well sorted fine grained sand  
 thin tephra and volcanic loess

dark grey laminated sand (Wereroa sand)

light grey pumiceous pebbly sand  
 Fe cemented layer  
 volcanic loess (L2)  
 pumiceous pebbly sand  
 lignite  
 pumiceous pebbly sand  
 medium grey silt with carbonaceous laminae  
 Fe cemented layer  
 light brown carbonaceous silt (L3)  
 lignite  
 light grey pumiceous cross bedded sand

(Stratford Formation)

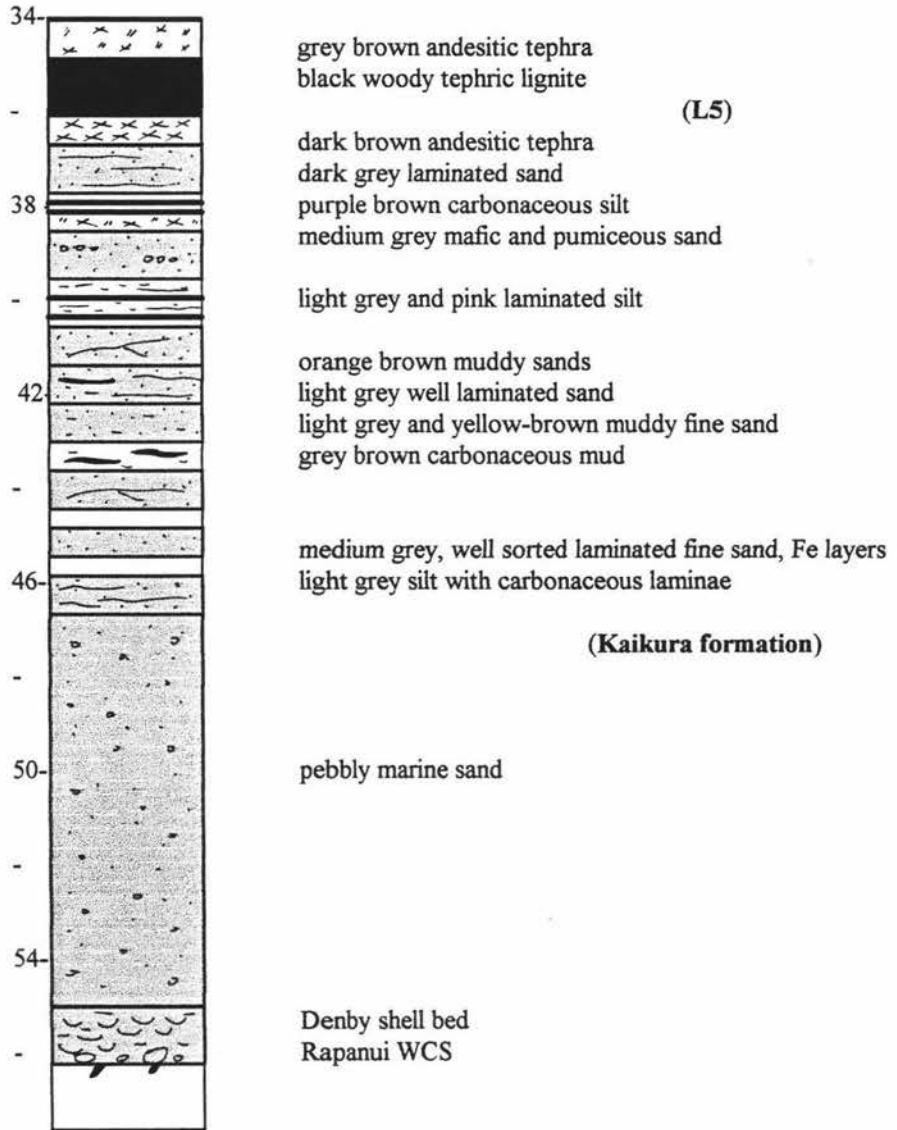
sharp undulating unconformable contact  
 black woody tephric lignite  
 blue grey silt  
 brown carbonaceous silt  
 woody tephric lignite with basal sandy tephra  
 light grey pumiceous pebbly sand  
 pink grey silt and grey sand  
 blue grey carbonaceous silt

light grey pumiceous pebbly sand  
 Fe cemented layer  
 purple brown tephric carbonaceous  
 andesitic tephra/tuff (L4)  
 light grey pumiceous conglomerate

grey brown andesitic tephra/tuff

Ohawe waterfall section continued

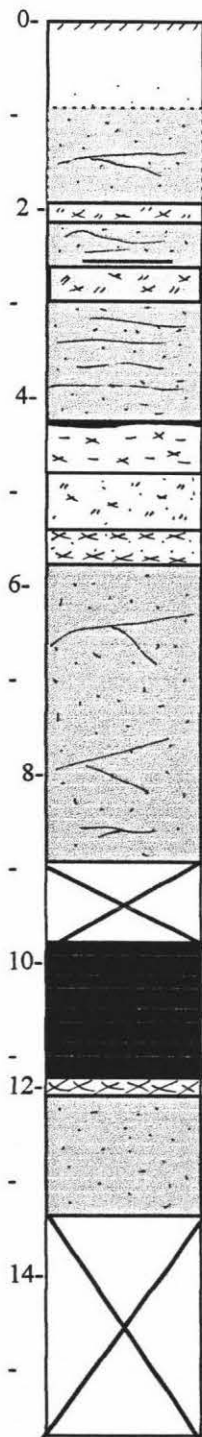
Depth (m)



## SITE DESCRIPTION

**Section no. 46**    **Name. Kiwi track**  
**Grid reference. Q21/227775**  
**Surface. Rapanui**

Depth (m)



Egmont Ash

loose grey sands

brown sandy volcanic loess and lapilli  
 layered grey sand  
 thin discontinuous iron pan  
 sandy loess and tephra

planar bedded sands  
 undulating contact  
 carbonaceous silts and sandy lapilli

(L1)

sandy brown loess  
 sandy lapilli layers  
 indistinct contact (thin iron pan)

grey sands with steep cross bedding

(Wereroa sand)

tabular bedding near base

obscured

tephric rich dark grey brown mud  
 contains large (>30 cm dia.) wood fragments

(L2)

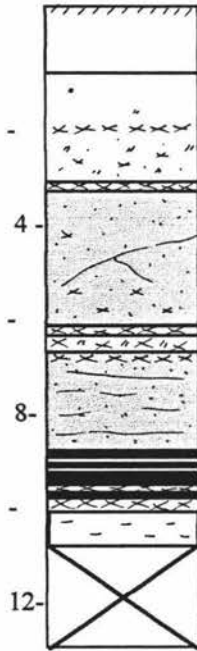
white sandy tephra at the base (3 cm)  
 sharp contact to grey brown sand

obscured

## SITE DESCRIPTION

**Section no. 48**    **Name. Subway section**  
**Grid reference. Q21/220777**  
**Surface. Rapanui**

Depth (m)



Egmont Ash

pale andesitic tephra  
 orange brown tephra and sand    **(L1)**  
 grey/brown fine tephra  
 Kawakawa Tephra

orange tephric sand    **(Wereroa sand)**  
 pale andesitic tephra  
 brown fine tephra over thin yellow/white coarse tephra

grey sand, parallel bedded

tephric lignite  
 grey white fine sandy andesitic tephra  
 brown carbonaceous silts    **(L2)**

## REFERENCES

- Alloway, B.V; Neall, V.E and Vucetich, C.G.** 1988. Localised volcanic loess deposits in North Taranaki, North Island, New Zealand. Loess, Eden and Furkert (eds).
- Alloway, B.,** 1989. The Late Quaternary cover bed stratigraphy and tephrochronology northeastern and central Taranaki, New Zealand. Unpublished PhD thesis, Massey University, Palmerston North.
- Alloway, B.V; Neall, V.E. and Vucetich, C.G.** 1992. Particle size analysis of Late Quaternary allophane-dominated andesitic deposits from New Zealand. Quaternary International, Vol. 13/14, pp. 167-174.
- Alloway, B.V; McGlone, M.S; Neall, V.E. and Vucetich, C.G.** 1992. The role of Egmont-sourced tephra in evaluating the paleoclimatic correspondence between the bio- and soil-stratigraphic records of central Taranaki, New Zealand. Quaternary International, Vol. 13/14, pp. 187-194.
- Alloway, B.V., Stewart, R.B., Neall, V.E. and Vucetich, C.G.** 1992. Climate of the Last Glaciation in New Zealand, based on aerosolic quartz influx in an andesitic terrain. Quaternary Research, Vol. 38, pp. 170-179.
- Alloway, B.V., Lowe, D.J., Chan, R. P. K., Eden, D. and Froggatt, P.** 1994. Stratigraphy and chronology of the Stent tephra, a c. 4000 year old distal silicic tephra from Taupo Volcanic Centre, New Zealand. New Zealand Journal of Geology and Geophysics. Vol. 37. p 37-47.

- Anderton, P.W.** 1981, Structure and evolution of the South Wanganui Basin, New Zealand: New Zealand Journal of Geology and Geophysics, v.24, p 39-63.
- Beu, A.G ; Edwards, A.R.,** 1984. New Zealand Pleistocene and Late Pliocene glacio-eustatic cycles. Paleogeography, Paleoclimatology, Paleoecology, v.46, p 119-142.
- Bussell, M.R.** 1988. Quaternary vegetational and climatic changes recorded in coverbeds of the South Wanganui Basin marine terraces, New Zealand. Ph.D. thesis. Australian National University. Canberra.
- Bussell, M.R.,** 1990. Palynology of oxygen isotope stages 6 and 5e from the coverbeds of a marine terrace, Taranaki, New Zealand. Quaternary Research 34, 86-100.
- Bussell, M.R. and Pillans,B.** 1992. Vegetational and climatic history during oxygen isotope stage 9, Wanganui district, New Zealand, and correlation of the Fordell Ash. Journal of the Royal Society of New Zealand , Vol. 22, No.1. p 41-60.
- Bussell, M.R.,** 1993. A late Pleistocene vegetational and climatic history of part oxygen isotope stage 5, Ararata, South Taranaki, New Zealand. Journal of the Royal Society of New Zealand, v. 23, no. 2.
- Chappell, J.** 1975. Upper Quaternary warping and uplift rates in the Bay of Plenty and West coast, North Island, New Zealand. New Zealand Journal of Geology and Geophysics, vol. 18, p 129-155.
- Cowie, J.D.** 1963. Dune-building phases in the Manawatu district, New Zealand. New Zealand Journal of Geology and Geophysics, vol 6, pp 268-280.

**Grace, A. B.** 1976. The palaeoecology of the Rapanui shellbeds. *Tane* Vol. 20, pp 182-188.

**Crandell, D.R., Miller, C.D., Glicken, H., Christiansen, R.L. and Newhall, C.G.**

1984. Catastrophic debris avalanche from ancestral Mount Shasta Volcano, California. *Geology*, 12: p 143-146.

**Crozier, M. J. and Pillans, B. J.** 1991. Geomorphic events and landform response in southeastern Taranaki, New Zealand. *in* *Catena*

**Davey, F and Stern, T;** 1988. Deep structure of the southern Taranaki Basin. Abstracts, Geological Society of New Zealand Conference, Hamilton 1988.

**Dickson, M.; Fleming, C.A.; Grant-Taylor, T.L.** 1974. Ngarino Terrace: an addition to the Late Pleistocene standard sequence in the Wanganui- Taranaki district. *New Zealand Journal of Geology and Geophysics*, vol. 17, p 789-798.

**Dieffenbach, E.** 1843. *Travels in New Zealand with Contributions to the Geography, Geology, Botany, and Natural History of that Country.* John Murray, London. 2 vols. Vol. 1, 431 pp. Vol. 2, 396 pp.

**Einsele, G and Bayer, U.** 1991. Asymmetry in transgressive-regressive cycles in shallow seas and passive continental margin settings. *in* *Cycles and events in stratigraphy.* Einsele *et al.*, (Eds.)

**Fleming, C.A.** 1953. *The geology of the Wanganui subdivision.* New Zealand Geological Survey Bulletin. 52. 362p. New Zealand Department of Scientific and Industrial Research, Wellington, New Zealand.

- Fieldes, M. and Perrott, K. M.** 1966. The nature of allophane in soils III: Rapid field and laboratory test for allophane. *New Zealand Journal of Science*. Vol. 9. pp 623-629.
- Gage, M.** 1953. The study of Quaternary strandlines in New Zealand. *Transactions of the Royal Society of New Zealand*, 81. p 27-34.
- Geddes, A.M.; Neall, V.E.; Stewart, R.B.** 1981. Recent discovery of the westernmost occurrences of Aokautere Ash and implications for the Late Quaternary in Taranaki. *In* Howarth, R.; Froggatt, P.; Vucetich, C.G.; Collen, J.D. *ed.* Proceedings of tephra workshop. June 30th - July 1st 1980, Victoria University of Wellington. Publication of Geology Department, Victoria University of Wellington no. 20, p 29-32.
- Glicken, H.** 1986. Rockslide-Debris Avalanche of May 1980 Mount St. Helens Volcano, Washington. Ph.D. Dissert., The University of California, Santa Barbara, Calif., 303 p.
- Grant-Taylor, T.L and Kear, D.** 1970. Geology. Land inventory survey, Waimate West County. Wellington, Department of Lands and Survey. p 20-33.
- Haskell, T.R and Palmer, J.A.** 1984. An outline geology of Taranaki. Published by Lands and Survey Department.
- Henderson, J.** 1924. The post Tertiary history of New Zealand. *Transactions of the New Zealand Institute*, 61, p 498-523.
- Hutton, F.W.** 1886. The Wanganui system. *Trans. N.Z. Inst.* 18: p 336-337 ( Abstract in *N.Z.J Sci.* 2: p525 (1885).)

- King, L.C.** 1930. Raised beaches and other features of the south-east coast of the North Island of New Zealand. Transactions of the New Zealand Institute, 61, p 498-523.
- Knox, G.L.** 1982. Taranaki Basin, structural style and tectonic setting. New Zealand Journal of Geology and Geophysics. Vol. 25, p 213-232.
- Kohn, B.P., Pillans, B. and McGlone, M.S.** 1992. Zircon fission track age for middle Pleistocene Rangitawa Tephra, New Zealand: Stratigraphic and Paleoclimatic significance. Palaeogeography, palaeoclimatology, Palaeoecology, 95, 73-94.
- Leeder, M.R.** 1986. Sedimentology: Process and Product.
- Lensen, G. J.** 1959. Sheet 10 - Wanganui Geological map of New Zealand. 1:250000. Department of Scientific and Industrial Research, Wellington, New Zealand.
- Marshall, P. and Murdoch, R.** 1920. The Tertiary Beds near Wanganui. Trans. N.Z. Inst. 52: p 115-28.
- Marshall, P. and Murdoch, R.** 1921. Tertiary Rocks near Hawera. Trans. N.Z. Inst. 53: p 86-96.
- Martinson, D.G., Pisias, N.G., Hays, J.D. Imbrie, J., Moore, T.C. Jr and Shackleton, N.J.** 1987. Age dating and orbital theory of the ice ages: development of a high resolution 0-300,000-year chronostratigraphy. Quaternary Research, Vol. 27. p 1-29.
- McBeath, D.M.** 1977. Gas- condensate fields of the Taranaki Basin, New Zealand. New Zealand Journal of Geology and Geophysics. Vol. 20, p 99-129.

**McGlone, M.S.; Neall, V.E.; Pillans, B.** 1984. Inaha Terrace deposits: a late

Quaternary terrestrial record in south Taranaki, New Zealand. New

Zealand Journal of Geology and Geophysics. Vol. 27, pp 35-49.

**McGlone, M.S. and Neall, V.E.** 1994. The late Pleistocene and Holocene vegetation

history of Taranaki, North Island, New Zealand. New Zealand Journal of

Botany. Vol. 32. p 251-269.

**McKee, J.W.A.** 1994. Geology and Vertebrate Paleontology of the Tangahoe

Formation, South Taranaki Coast, New Zealand. Field Trip Guides.

Geological Society Of New Zealand Miscellaneous Publication 80B, p

53-62.

**Milne, J.D.G.** 1973. Upper Quaternary geology of the Rangitikei Drainage Basin,

North Island, New Zealand. Unpublished Ph.D thesis. Victoria

University, Wellington, New Zealand.

**Milne, J.D.G.** 1973b. Mount Curl Tephra: A 230 000 year old marker bed in New

Zealand, and its implications for Quaternary chronology. New Zealand

Journal of Geology and Geophysics. Vol. 16, p 519-532.

**Morgan, P.G.** 1921. Notes on the Geology of the Patea District. Trans. N.Z. Inst. 53: p

58-64.

**Neall, V.E.** 1972. Tephrochronology and Tephro-stratigraphy of western Taranaki,

New Zealand. New Zealand Journal of Geology and Geophysics. Vol. 15,

p 507-557.

**Neall, V.E.** 1979. Sheets P19, P20 and P21 - New Plymouth, Egmont and Manaia.

Geological map of New Zealand 1:50 000. 3 maps and notes, 36p.

Wellington, New Zealand. Department of Scientific and industrial  
Research.

**Neall, V.E. and Alloway, B.V.** 1986. Quaternary volcanoclastics and volcanic hazards  
of Taranaki. New Zealand Geological Survey record 12. p 101-137.

**New Zealand Meteorological Service.** 1983. Rainfall normals for New Zealand 1941-  
1970. New Zealand Meteorological Service Miscellaneous Publication  
177.

**Palmer, B.A. and Neall, V.E.** 1989. The Murimotu Formation, 9500-year old deposits  
of a debris avalanche and associated lahars, Mount Ruapehu, North  
Island, New Zealand. New Zealand Journal of Geology and Geophysics.  
Vol. 32, p 477-486.

**Palmer, B.A. and Neall, V.E.** 1991. Contrasting lithofacies architecture in ring plain  
deposits related to edifice construction and destruction, the Quaternary  
Stratford and Opunake Formations, Egmont Volcano, New Zealand.  
Sedimentary Geology. vol. 74. p 71-88.

**Palmer, B.A.; Alloway, B.V. and Neall, V.E.** 1991. Volcanic-debris-avalanche  
deposits in New Zealand-lithofacies organisation in unconfined, wet-  
avalanche flows. Sedimentation in Volcanic settings, SEPM Special  
Publication Number 45.

**Palmer, J. A. and Andrews, P. B.** 1993. Cretaceous-Tertiary sedimentation and  
implied tectonic controls on the structural evolution of Taranaki Basin,  
New Zealand. South Pacific sedimentary basins, Sedimentary basins of  
the world, 2. Edited by P. F. Ballance.

- Park, J.** 1887. On the Upper Wanganui and King-Country. N.Z. geol. Surv. Rep. geol. Explor. 1886-1887, 18: p 167-82.
- Pierson, T.C.** 1985. Initiation and flow behavior of the 1980 Pine Creek and Muddy River lahars, Mount St. Helens, Washington. Geological Society of America Bulletin. vol. 96. p 1056-1069.
- Pilaar, W.F.H. and Wakefield, L.L.** 1978. Structural and stratigraphic evolution of the Taranaki Basin, offshore North Island, New Zealand. Australian Petroleum Exploration Association Journal. vol.18. p 93-101.
- Pillans, B.J.** 1981. Upper Quaternary Landscape evolution in South Taranaki, New Zealand. Unpublished Ph.D. thesis, Australian National University.
- Pillans, B.J.** 1983. Upper Quaternary marine terrace chronology and deformation, South Taranaki, New Zealand. Geology. vol. 11. p 292-297.
- Pillans, B.J.** 1985. Southwest North Island paleoenvironments, 150,000 years B.P. to present. *In* B.J. Pillans *ed.* Proc. 2nd CLIMANZ conf. p 37-43. Geology Department Victoria University of Wellington, Publication no. 31.
- Pillans, B.J.**, 1990. Late Quaternary marine terraces, South Taranaki - Wanganui. N.Z. Geological Survey Miscellaneous Map 18.
- Pillans, B.J.** 1991. New Zealand Quaternary stratigraphy, an overview. Quaternary Science Reviews. vol.10.
- Pillans, B.J.; Holgate, G.P. and McGlone, M.S.** 1987. Climate and sea level during oxygen isotope stage 7b, on land evidence from New Zealand. Quaternary Research. vol. 29. p 176-185.

- Pillans, B.J. and Kohn, B.P.** 1981. Rangitawa Pumice: a widespread (?) Quaternary marker bed in Taranaki and Wanganui. Victoria University of Wellington Geol. Dept, Publ., 20: p 94-104.
- Robertson, N. G.** 1953. Climate. In Fleming, C.A., 1953. The Geology of the Wanganui Subdivision. N.Z. Geological Survey Bulletin, vol. 52. pp 2-6.
- Ruhe, R.V.** 1965. The Quaternary of the United States ( Wright Jnr, H.E. and Frye, D.G. Eds). pp 755-764.
- Schuster, R.L. and Crandell, D.R.** 1984. Catastrophic debris avalanches from volcanoes. IV Int. Symp. Landslides, Proc., Toronto, 1: p 567-572.
- Shackleton, M.J. and Opdyke, N.D.** 1973. Oxygen isotope and paleomagnetic stratigraphy of equatorial Pacific core V28-238: oxygen isotope temperature and ice volumes on a  $10^5$  and  $10^6$  year scale. Quaternary Research. Vol. 3. p 39-55.
- Smith, G.A. and Fritz, W.J.** 1989. Penrose Conference Report: Volcanic influences on terrestrial sedimentation: Geology, vol. 17. p 375-376.
- Smith, I.E.M; Price, R.C. and Alloway, B.V.** 1994. Field trip 2, Mount Taranaki. Field Trip Guides. Geological Society Of New Zealand Miscellaneous Publication 80B, p 53-62.
- Stern, T.A; Quinlan, G.M. and Holt, W.E.** 1993. Crustal dynamics associated with the formation of Wanganui Basin, New Zealand. South Pacific Sedimentary Basins. Sedimentary Basins of the World, 2 edited by P.F. Ballance. p 213-223.

**Stern, T.A.; Quinlan, G.M. and Holt, W.E.** 1992. Basins formed behind an active subduction zone: 3D flexural modelling of Wanganui Basin. Basin Research, 4.

**Stewart, R.B.; Neall, V.E.; Pollok, J.A. and Syers, J.K.** 1977. Parent material stratigraphy of an Egmont loam profile, Taranaki, New Zealand. Australian Journal of Soil Research. vol. 15. p 177-190.

**Taranaki Regional Council.** 1991. Patea-Waverly-Waitotara Preliminary groundwater survey.

**Taranaki Regional Council.** 1992. Aggregate extraction in Taranaki. Regional policy statement working paper.

**Thompson, C.S.,** 1981. The climate and weather of the Taranaki region. N.Z. Meteorological Service Miscellaneous Publication 115.

**Vail, P.R; Audemard, F; Bowman, S.A; Eisner, P.N, and Perez-Cruz, C.** 1991. The stratigraphic signatures of tectonics, eustasy and sedimentology - an overview. in Cycles and events in stratigraphy, Einsele *et. al.* (Eds.)

**Watts, A.B., Karner, G.D. and Steckler, M.S.,** 1982. Lithospheric flexure and the evolution of sedimentary basins. Philos. Trans. R. Soc. London, Ser. A, 305: 249-281.

**Whitten, R.F.** 1973. The Waipipian stratigraphy and paleoecology of the South Taranaki coast. Unpublished M.Sc. thesis. University of Auckland, Auckland.

**Wilde, R.H.** 1974. Soils of the Westmere Series in the Wanganui district, New Zealand, and their relationship to adjacent soils. New Zealand Journal of Science. Vol.17. pp 475-492.

**Wilde, R.H.** 1979. Stratigraphy and soils of Late Quaternary terrace coverbeds in the Wanganui and South Taranaki districts, North Island, New Zealand. Unpublished MSc thesis, Victoria University of Wellington.

**Wilde, R.H. and Vucetich, C.G.** 1988. Aeolian coverbeds of marine terraces in the western Wanganui district, North Island, New Zealand. *In* Loess, Eden and Furkert (eds).